

Department of Advanced Energy
Graduate School of Frontier Sciences
The University of Tokyo

2022

Master's Thesis

Development of a Magnesium Wire - Water Thruster for small spacecrafts:
From Proof of Concept to a Breadboard Model

Submitted January 25, 2023

Adviser: Associate Professor Hiroyuki Koizumi

47-216060 章如诚

RuCheng Zhang

Contents

Contents	2
1. Introduction.....	11
1.1 CubeSat industry	11
1.2 Hybrid Thruster.....	14
1.3 1.3 Reaction	14
1.4 Water as Oxidizer	15
1.5 Magnesium as Fuel	15
1.6 Research goals	17
2. Experiment Setup.....	18
2.1 Vacuum Equipment	18
2.2 Power Supply	19
2.3 Thermal Couples.....	19
2.4 Ignition Circuit.....	20
2.5 Combustion Chamber	23
2.5.1 Selection.....	23
2.5.2 Wire guide.....	25
2.5.3 Protection lining.....	27
2.6 Wire feeder.....	29
2.6.1 Previous solution.....	29

2.6.2	Problem	31
2.6.3	Redesign.....	32
2.6.4	Flaws and Rooms for improvements	36
2.7	Automated Program	38
2.7.1	Flame Tracker	38
2.7.2	Feeder control	46
2.7.3	Communication.....	47
2.7.4	Code structure	47
2.8	Water supply	54
2.9	Orifice	55
2.10	Efficiency Measurement	58
2.10.1	Overview.....	58
2.10.2	Device setup.....	60
2.10.3	Assumption	61
2.10.4	Cylinder.....	61
2.10.5	Expected Value	61
2.10.6	Error assessment	62
2.10.7	Deviation cause.....	62
2.10.8	Cooling bath.....	63
2.10.9	Compatibility	64
2.11	Safety	65

2.12	BBM Thruster Design.....	65
2.12.1	Concept	65
2.12.2	Combustion chamber	67
2.12.3	Sensor ports.....	68
2.12.4	Discharge electrode.....	69
2.12.5	Wire inlet and guide.....	69
2.12.6	Nozzle design.....	70
2.12.7	Valve	70
2.12.8	Residue.....	71
2.12.9	Water flow direction	71
2.12.10	Compatibility	71
2.13	Initial BBM Thruster testing.....	71
2.13.1	Parts.....	71
2.13.2	Setup	74
2.13.3	Ignition confirmation	78
3.	Experiment Procedure.....	79
3.1	Wire setup	79
3.2	Leak checks.....	80
3.3	Heater Check.....	80
3.4	Discharge check	81
3.5	Combustion procedure (Air)	81

3.6	Combustion procedure (Water).....	82
4.	Results.....	83
4.1	Sustained Combustion	83
4.2	Varying Pressure.....	83
4.3	Wire combustion under high speed camera	90
4.4	BBM thruster results	126
4.4.1	Closed system	126
4.4.2	Closed then open system.....	131
4.4.3	Open system 35kPa.....	140
4.4.4	Residue.....	141
5.	Analysis.....	143
5.1	Sustained Combustion results	143
5.1.1	Convergence	143
5.1.2	Oscillation Hypothesis	143
5.2	Combustion behavior	145
5.2.1	Ignition.....	145
5.2.2	Flame tracking	147
5.3	Combustion rate and Pressure.....	150
5.3.1	Observations	152
5.4	Combustion Efficiency / Residue	153
5.5	Extinguish case	155

5.5.1	Insufficient wire	155
5.5.2	Wire touching chamber wall	155
5.5.3	Wire leaving guide	156
5.5.4	Hanging on electrode	156
5.5.5	hardware failure	156
5.6	BBM test analysis	156
6.	Conclusion	157
	Appendix A	158
	Appendix B	164
	Appendix C	170
	Conference	172
	Bibliography	173

Figures

FIGURE 1.1 NUMBER OF CUBESATS LAUNCHED PER YEAR FROM 2002 TO MAY 31, 2018.....	11
FIGURE 1.2 APPLICATION OF CUBESATS LAUNCHED PER YEAR FROM 2002 TO MAY 31, 2018.....	12
FIGURE 1.3 EQUULEUS SATELLITE, JAXA.....	13
FIGURE 1.4 WATER METAL HYBRID THRUSTER ILLUSTRATION	14
FIGURE 1.5 HEAT GENERATED FROM COMBUSTION	16
FIGURE 2.1 EXPERIMENTAL SETUP	18
FIGURE 2.2 POWER SUPPLY AND SIGNAL GENERATOR	19
FIGURE 2.3 IGNITION CIRCUIT	20
FIGURE 2.4 DISCHARGE ELECTRODE	21
FIGURE 2.5 ELECTRODE POSITION	22
FIGURE 2.6 MAGNESIUM WIRE AND TUNGSTEN WIRE	22
FIGURE 2.7 IMPROVED DISCHARGE ELECTRODE	23
FIGURE 2.8 DAMAGED NW16 NIPPLE	24
FIGURE 2.9 NW40 NIPPLE	25
FIGURE 2.10 WIRE GUIDE	26
FIGURE 2.11 END OF WIRE GUIDE	26
FIGURE 2.12 WIRE GUIDE AND WIRE IN THE DOWNSTREAM OF COMBUSTION CHAMBER.....	27
FIGURE 2.13 ACRYLIC TUBE	28
FIGURE 2.14 QUARTZ GLASS TUBES USED FOR PROTECTION	29
FIGURE 2.15 WELDING WIRE FEEDER (BACKSIDE).....	30
FIGURE 2.16 WELDING WIRE FEEDER (FRONT SIDE)	30
FIGURE 2.17 PREVIOUS MANUAL CONTROL SYSTEM.....	31
FIGURE 2.18 CONNECTION BELT	33
FIGURE 2.19 CLAMPING MECHANISM.....	34
FIGURE 2.20 INSTALLED WIRE FEEDER ORIGINAL (LEFT) REPAIRED (RIGHT).....	35
FIGURE 2.21 BXM230-A2 MOTOR	36
FIGURE 2.22 WIRE FEEDER MASS	37
FIGURE 2.23 FEEDING SYSTEM ILLUSTRATION	39
FIGURE 2.24 PHOTOVOLTAIC BASED METHOD	40
FIGURE 2.25 CAMERA BASED METHOD.....	41
FIGURE 2.26 EXPERIMENT SETUP	42
FIGURE 2.27 RAW IMAGE FROM VIDEO	43
FIGURE 2.28 TRACKED IMAGE	43
FIGURE 2.29 EFFECTIVENESS OF COLOR CHANNELS	45

FIGURE 2.30 IMAGE PROCESSING.....	46
FIGURE 2.31 FEEDBACK LOOP.....	47
FIGURE 2.32 LABVIEW PI LOOP AND TCP COMMUNICATION	48
FIGURE 2.33 MOTOR DRIVER ENCODER OUTPUT	49
FIGURE 2.34 ENCODER READER.....	50
FIGURE 2.35 LABVIEW OUTPUT CONTROL	51
FIGURE 2.36 USB 6001 DAQ	52
FIGURE 2.37 TARGET AND IGNITION POINT	53
FIGURE 2.38 WATER TANK.....	54
FIGURE 2.39 WATER VAPOR FLOW PATH	55
FIGURE 2.40 ORIFICE LOCATION.....	56
FIGURE 2.41 1 MM ORIFICE PLATE	57
FIGURE 2.42 ORIFICE CLEAN	57
FIGURE 2.43 ORIFICE UPSTREAM SIDE	58
FIGURE 2.44 ORIFICE DOWNSTREAM SIDE.....	58
FIGURE 2.45 MG MEASUREMENT SYSTEM, PURE MG CALIBRATION.....	59
FIGURE 2.46 FUEL EFFICIENCY MEASUREMENT SYSTEM	60
FIGURE 2.47 FUEL EFFICIENCY SYSTEM	60
FIGURE 2.48 CYLINDER 10ML (LEFT) 200 ML (RIGHT)	62
FIGURE 2.49 PH TEST PAPER SHOWING ACIDIC EXHAUST	63
FIGURE 2.50 MG MEASUREMENT WITH COOLING BATH.....	64
FIGURE 2.51 THERMAL IMAGING OF COOLING BATH	64
FIGURE 2.52 BBM MODEL CONCEPT	66
FIGURE 2.53 THRUSTER ILLUSTRATION	67
FIGURE 2.54 COMBUSTION CHAMBER DIMENSIONS.....	68
FIGURE 2.55 CROSS SECTION	69
FIGURE 2.56 NOZZLE CROSS SECTION	70
FIGURE 2.57 ATTACHED NOZZLE	72
FIGURE 2.58 NOZZLE.....	72
FIGURE 2.59 COMBUSTION CHAMBER.....	73
FIGURE 2.60 QUARTZ GLASS.....	73
FIGURE 2.61 SYSTEM OVERVIEW	74
FIGURE 2.62 NOZZLE FROM VIEWPORT	75
FIGURE 2.63 INSTALLED COMBUSTION CHAMBER.....	75
FIGURE 2.64 VACUUM SYSTEM CONNECTIONS.....	76

FIGURE 2.65 DISCHARGE CONFIRMATION	77
FIGURE 2.66 ALTERNATE ELECTRODE CONFIGURATION	77
FIGURE 2.67 WIRE GUIDE EFFECTIVENESS	78
FIGURE 3.1 ROLLED UP WIRES	79
FIGURE 4.1 RESULT SUSTAINED COMBUSTION 280 SECONDS	83
FIGURE 4.2 RESULT 45KPA 1	84
FIGURE 4.3 RESULT 45KPA 2	84
FIGURE 4.4 RESULT 45KPA 3	85
FIGURE 4.5 RESULT 45KPA 4	85
FIGURE 4.6 RESULT 35KPA 1	86
FIGURE 4.7 RESULT 35KPA 2	86
FIGURE 4.8 RESULT 35KPA 3	87
FIGURE 4.9 RESULT 25KPA 1	87
FIGURE 4.10 RESULT 20KPA 1	88
FIGURE 4.11 RESULT 20KPA 2	88
FIGURE 4.12 RESULT 20KPA 3	89
FIGURE 4.13 RESULT 15 KPA (FAILED)	89
FIGURE 4.14 HIGH SPEED CAMERA FOOTAGE FROM PREVIOUS SETUP.....	106
FIGURE 4.15 HIGHSPEED CAMERA FOOTAGE 2	126
FIGURE 4.16 BBM CLOSED SYSTEM COMBUSTION.....	131
FIGURE 4.17 BBM CLOSED TO OPEN SYSTEM COMBUSTION	140
FIGURE 4.18 OPEN SYSTEM FAILED IGNITION	141
FIGURE 4.19 RESIDUE SHAPE EXAMPLE FOR BOTH CASE 1 AND 2	142
FIGURE 5.1 OXIDIZER RELATION STATE 1	144
FIGURE 5.2 OXIDIZER RELATION STATE 2	145
FIGURE 5.3 COMBUSTION CHAMBER BEFORE DISCHARGE	146
FIGURE 5.4 DISCHARGE	146
FIGURE 5.5 JUST BEFORE IGNITION	147
FIGURE 5.6 DIFFERENT EXPERIMENT WITH GREEN LIGHT	147
FIGURE 5.7 WIRE COMBUSTION	149
FIGURE 5.8 COMBUSTION PROFILE SPECULATION ILLUSTRATION	150
FIGURE 5.9 FEED RATE OVER VARIOUS VAPOR PRESSURE	152
FIGURE 5.10 MASS FLOW PRESSURE RELATIONSHIP	153
FIGURE 5.11 MASS FLOW TEMPERATURE RELATIONSHIP	153
FIGURE 5.12 RESIDUE HANGING.....	154

FIGURE 5.13 RESIDUE 35 KPA	154
FIGURE 5.14 RESIDUE 45 KPA	155

1. Introduction

1.1 CubeSat industry

In past decade, the amount of CubeSats, especially the amount of the CubeSats equipped with thrusters launched per year has increased.¹ The mission of CubeSats has also moved from being mostly educational, organized by universities to predominantly commercial by 2014.² Having thrusters enable CubeSats to operate independently in missions with more complex orbit and for longer durations as opposed to traditional missions where CubeSats generally fall to Earth due to the small amount of air resistance at low Earth orbits³.

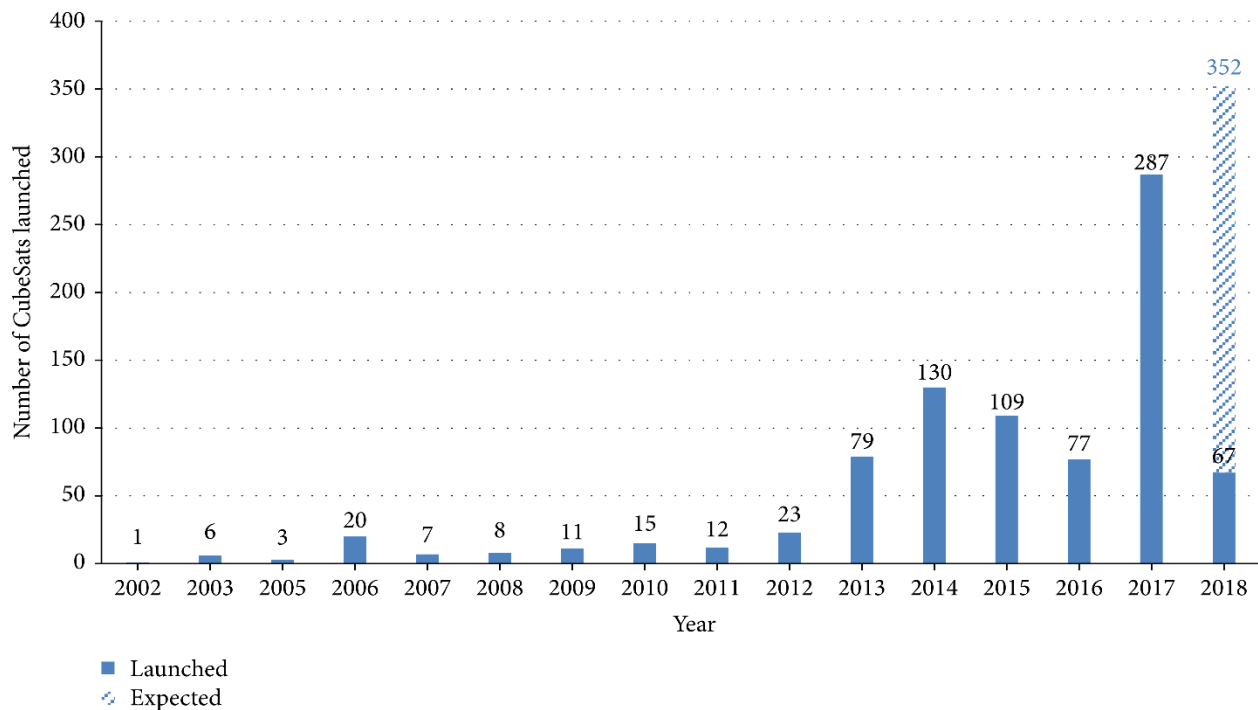


Figure 1.1 Number of CubeSats launched per year from 2002 to May 31, 2018

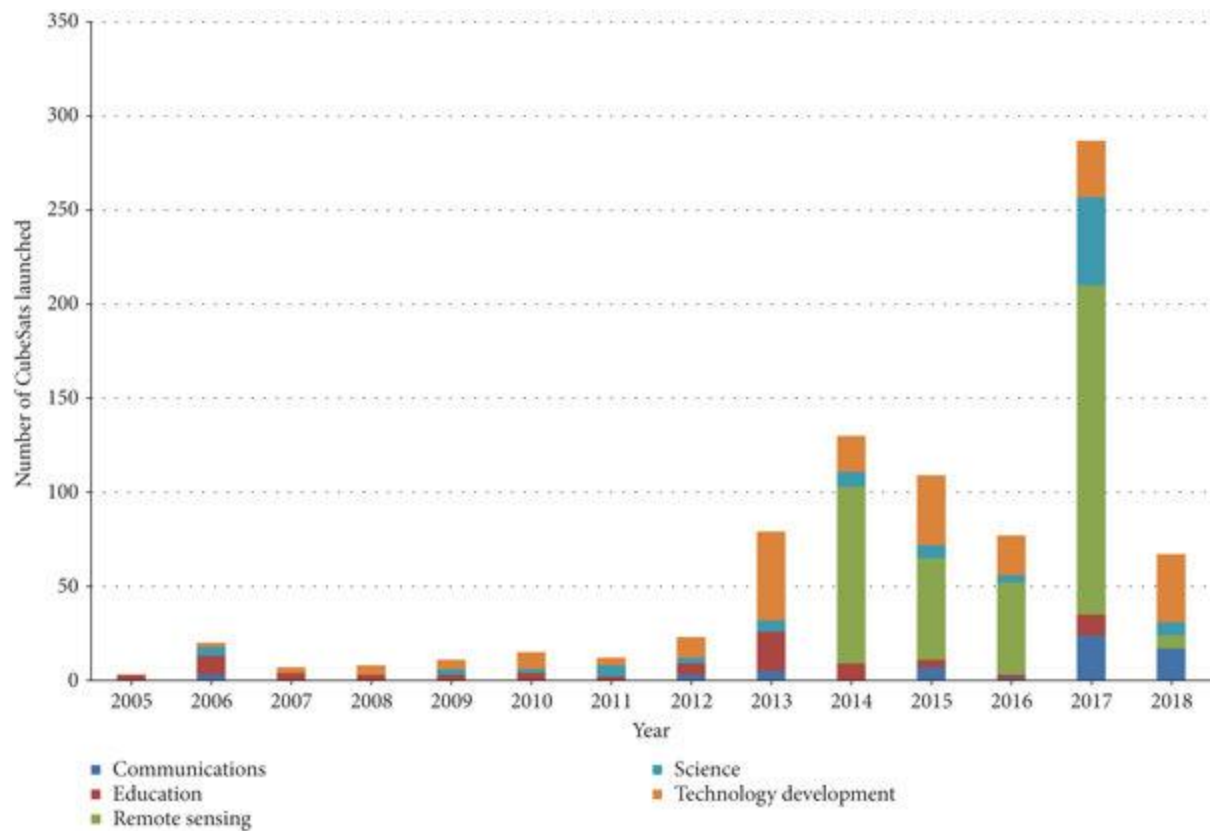


Figure 1.2 Application of CubeSats launched per year from 2002 to May 31, 2018

Towards the Thousandth CubeSat: A Statistical Overview

Safety is paramount in the design of CubeSats as they often must share a ride with larger satellites whose success takes precedence.^{4 5} Water has been proposed as fuel for microsatellite thrusters. Compared to some of the higher performance alternatives such as hypergolic fuels, xenon, argon gas in electrical thrusters, water has the benefit of being safe, cheap, and widely available. Despite the performance deficit, Water is a capable propellant. Equipped with a water resistojet propulsion, EQUULEUS spacecraft is on its way to Earth Moon L2 Point⁶, far beyond just low Earth orbit, for example.



Figure 1.3 EQUULEUS satellite, JAXA

Past research has developed water-based thruster based on design such as ion thrusters, hall thrusters, resistojet, electrolysis-based thrusters, etc.⁷ to tackle various performance needs. However these thrusters are low thruster, some on the scale of a few hundred of μN .⁸⁹¹⁰ Due to the lower thrust of these propulsion systems, a kick motor is sometimes necessary to put spacecraft on a transfer orbit. CubeSats often do not have the luxury of using a kick motor. Kick motor often consists of propellant that is too dangerous to be handled without specialized facilities. Almost all hypergolic fuel that can be used is toxic. The main benefit of them being able to react spontaneously is a drawback in the safety of CubeSats.¹¹ CubeSats are therefore forbidden to use these higher thrust assists. By utilizing propulsion system with higher thrust that is designed for CubeSats that is safe to use, they too can execute the transfer independently.

To produce high thrust that would enable a variety of missions, this research proposes a chemical-based thruster that utilizes water as a propellant and solid metal as fuel¹². Magnesium wires are used in this thruster design to form a combustion in which energy released from the chemical reaction between magnesium and water vapor can be used to produce thrust.

1.2 Hybrid Thruster

Hybrid Thruster, or hybrid Propellant Thruster is here defined as a Thruster that uses propellants that exist in different states. In our concept, Magnesium is the solid fuel and water is the liquid propellant. These two propellants can react and produce Thrust using the chemical energy. Hybrid Thruster is unique in that two different types of propellant delivery mechanisms are required, complicating the controls. While the delivery of liquid is matured technology, the delivery of solid is not as simple. In many cases, the solid portion of the propellant are built into the combustion chamber where reaction would occur. The reaction rate would then be controlled primarily by the flow rate of the liquid propellant and interaction between liquid and solid propellants. In this research, storage of both liquid and solid propellants exists outside of the combustion chamber. Separate control mechanism designs are required for each propellant.

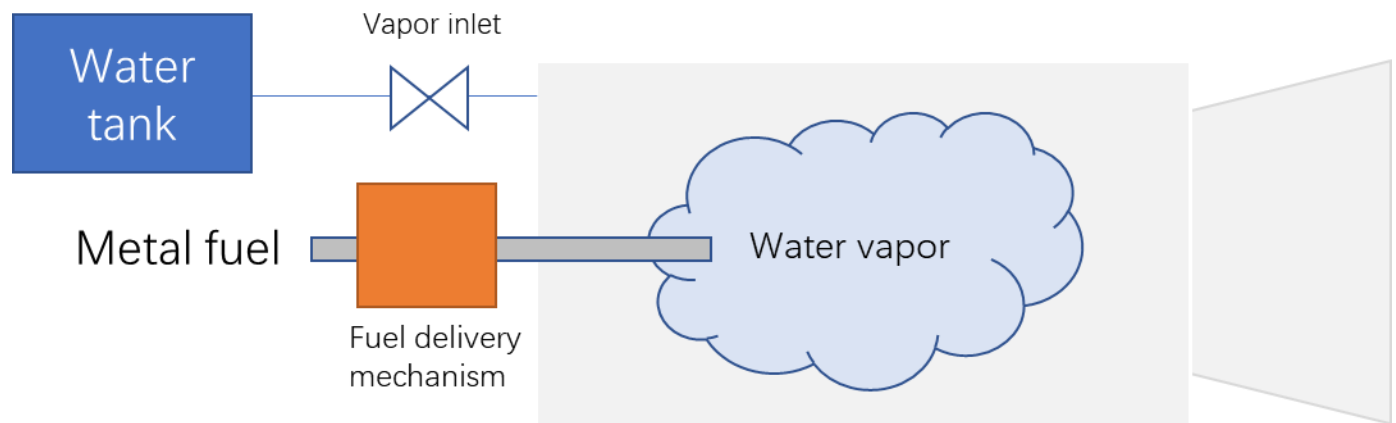


Figure 1.4 Water metal hybrid thruster illustration

1.3 1.3 Reaction

From previous research, Solid Magnesium and Liquid Water are chosen as the suitable propellant to be used for the design of Thruster. Magnesium and Water reacts with the following equation.



This reaction is exothermic and the combination of released energy and Hydrogen are expected to produce thrust.

1.4 Water as Oxidizer

Water as a propellant is being studied as an alternative propellant. Some water based propulsion systems such as the AQUARIUS, a resistojet based thruster system, developed by University of Tokyo¹³, had successful in flight demonstration. Water has a few main advantages. First, it is an abundant resource on Earth. Second, it is low cost to acquire. Third, it is easy to handle without specialized equipment, a trait desired for any propulsion system designed for CubeSats. Last but not least, water exist as liquid under standard room temperature and atmospheric pressure, meaning that it is easy to store onboard spacecraft without high pressure container.

1.5 Magnesium as Fuel

There are few metals that can react with water to release energy. From previous studies, Magnesium was found to be a suitable fuel for use. Wire shaped Magnesium was a potential candidate. Lithium and Beryllium both have higher combustion heat. They don't however satisfy the safety requirements for CubeSats. One of the alternatives to Magnesium is Aluminum. Aluminum itself has a melting point at around 1000 °C. However, when exposed to environment, Aluminum gradually forms an oxide layer. Such layer has a melting point of 2250 °C and it is required to melt before ignition is possible. Magnesium was therefore chosen for the ease of ignition.

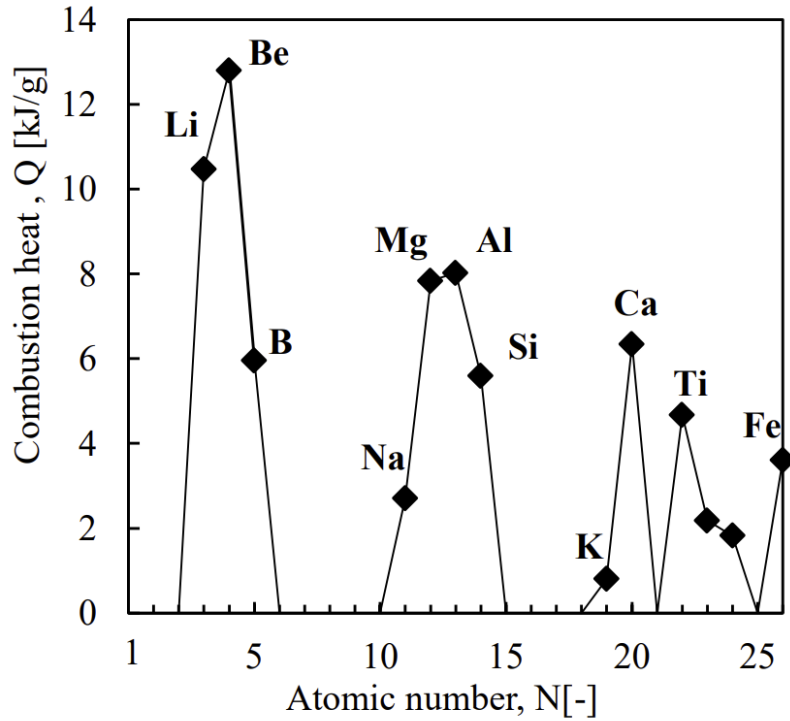


Figure 1.5 Heat Generated from Combustion¹⁴

A few shapes for fuel were considered in the previous study. Among the options are rod, plate, wire, and powder. Wire was chosen as the shape of fuel in this study. Compared to powder, wire is easier to feed due to being one continuous solid. Compared to rod and plate, due to the smaller cross-sectional area, the heat loss due to conduction is smaller so ignition and sustained combustion was easier to achieve. In previous study, wires of a few diameters were considered. 0.8 mm wire were selected as the candidate for this research. Past studies suggest that 0.8 mm wires are sufficiently thin enough to have a combustion without being too thin to create an engineering challenge for the feeding mechanism.

1.6 Research goals

This study is a continuation of prior thruster development work by Ms. Akiyama. Prior study included calculations to show that magnesium and water can produce Thrust. Magnesium wires were selected as the fuel type to study due to the advantages properties of the material and shape.

While study on ignition and combustion was already test in a closed environment, successful combustion with air and water in an open system was only first achieved after start of the study. Even so, combustion back then had been largely inconsistent, half relying on luck.

The target of the sustained combustion with the system is to have wire feed and continuously burn with water vapor as oxidizer for approximately 3-5 minutes. This number was chosen as it is the expected amount of time spacecraft would need to maneuver. It also enables enough data to understand combustion. However, in this study, any combustion that has a duration of over 10 seconds is considered a successful combustion.

Many improvements have been made to the system since to achieve the stability in the conclusion of this study. Ms. Akiyama has improved the foundation of the experimental setup, ignition system. The final product of this study is a combination of all the experience learned from various experiments to reach a more stable platform for future studies and development of the BBM thruster. This BBM thruster enables measurement of the temperature and pressure data with in the combustion chamber more directly to better quantify combustion performances. Additionally, the thruster is capable of finding the gravity and water vapor flow direction dependency during combustion.

2. Experiment Setup

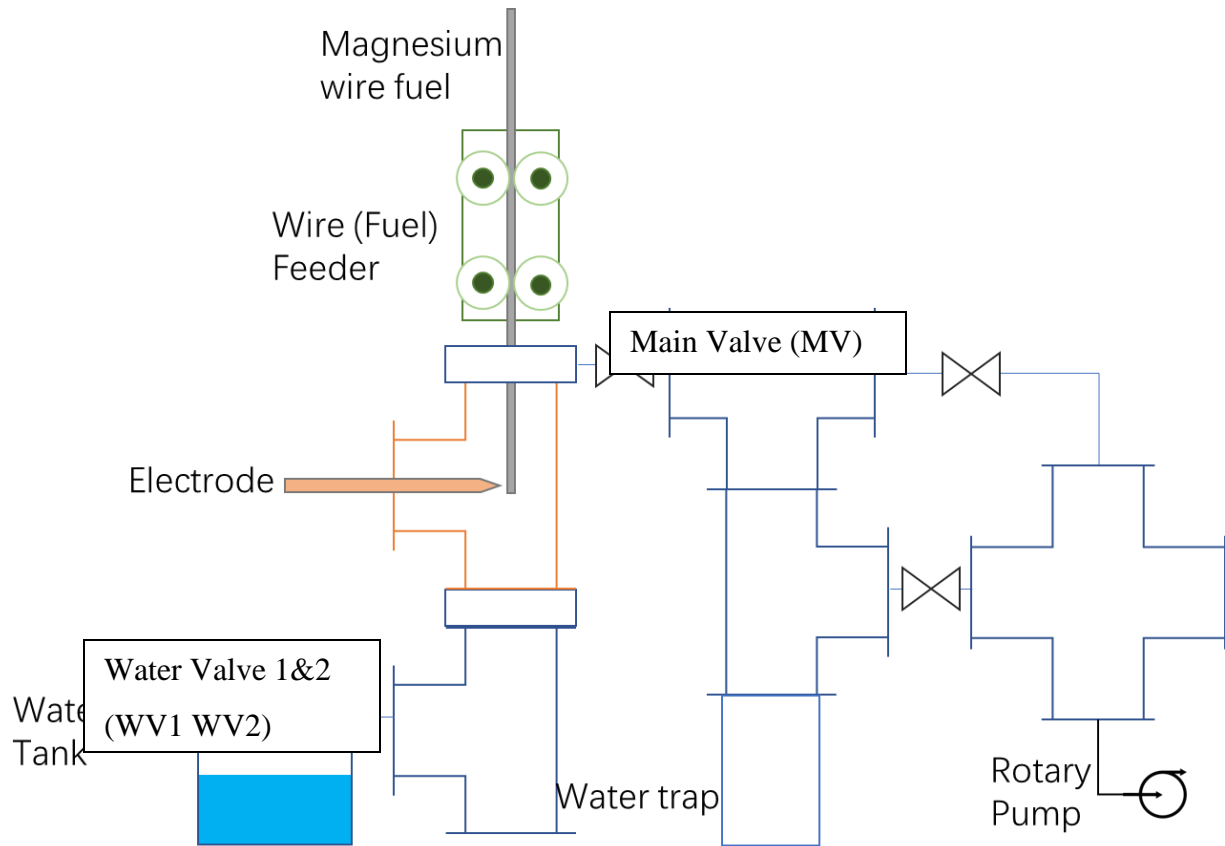


Figure 2.1 Experimental setup

Figure 2.1 shows the experimental setup that is used in this study. The water trap section is used for the measurement of oxidizer consumption rate. This study does not study the oxidizer consumption rate using this device, so it is sometimes removed. This has no effect on this study.

The main parts of the experimental setup are water supply, ignition circuit, wire feeding system, combustion chamber and vacuum system.

2.1 Vacuum Equipment

No vacuum chamber was used in this study and all the experiment setup is exposed to atmosphere. As this is a study to prepare for the eventual design of the thruster, a low-pressure vacuum is not necessary. Rotary pumps are sufficient. The experiments also use water vapor and the reaction from the combustion generates hydrogen. Either can affect the performance of the

rotary pumps. To alleviate the effect, downstream of the experiment setup, just before the inlet of the rotary pumps, a leak valve mix air with the gas downstream from combustion chamber. 2 Rotary Pumps are used to maintain a vacuum in the experimental setup to compensate for the need for extra exhaust rate. Despite such measures taken, the oil in the rotary pump can still be contaminated by water frequently. Oil needs to be replaced often as a result.

2.2 Power Supply

Several Power supplies are used for the experiment setup. The primarily function of these power supplies is to heat up the experimental setup to prevent condensations. Nichrome wires and rubber heaters are used. Heaters are taped onto the exterior of tubing so that they are heated to a temperature approximately 10 degrees above the temperature of the water vapor. Any condensation that forms lowers the pressure of the water vapor.

Power supply regulated by temperature heaters are used to control the water tank heater. These turn on and off depending on the temperature readings of the thermal couples. Having a constant temperature ensures a stable water vapor pressure. This study changes the water vapor pressure through the settings on this power supply.

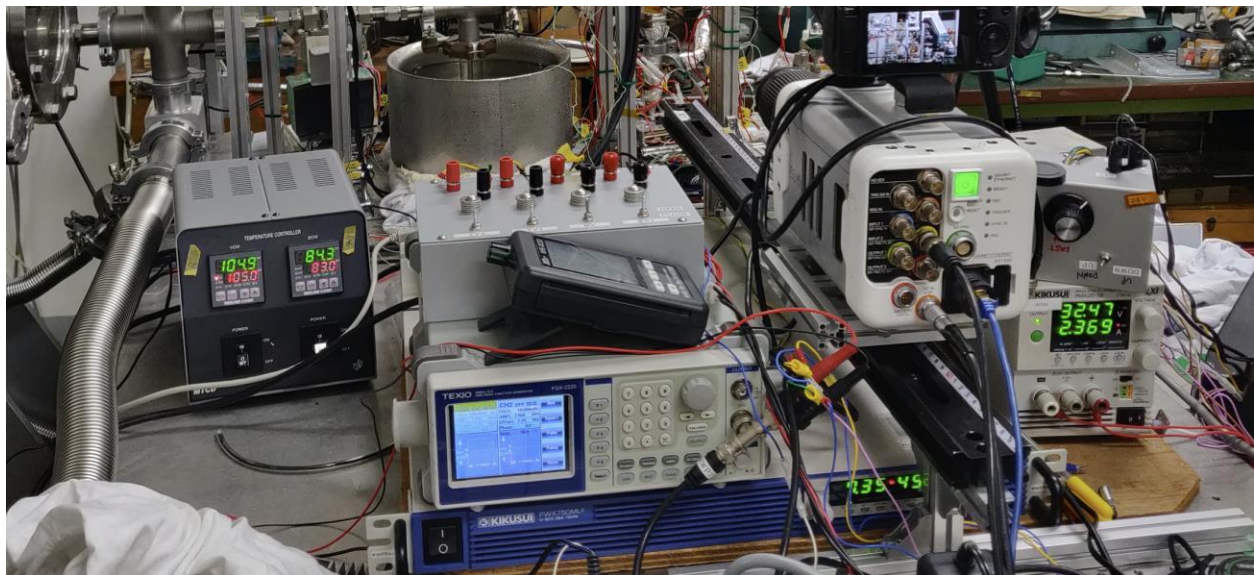


Figure 2.2 Power Supply and Signal Generator

2.3 Thermal Couples

Thermal couples are placed around the setup to monitor the temperature of the tubing, water tank and combustion chamber. The effect the temperature of the setup has on the combustion is not considered in this study as long as no condensation occur. The temperature of the water vapor is assumed to be the same as the water tank temperature.

2.4 Ignition Circuit

Ignition of wire is achieved by high voltage AC discharge arc between a tungsten electrode and the magnesium wire. The magnesium wire acts as the ground and 8 kV potential on the tungsten electrode helps forming the arc. The same circuit from the prior study was taken. The discharge voltage is controlled by the dial on the transformer. 10 on the dial corresponds to 1 kV discharge. Previously, this circuit was controlled by a signal generator, featured in figure 2.2. In this study it has been integrated into the control software. The control software automatically detects an ignition and turns off the discharge during the sustained combustion.

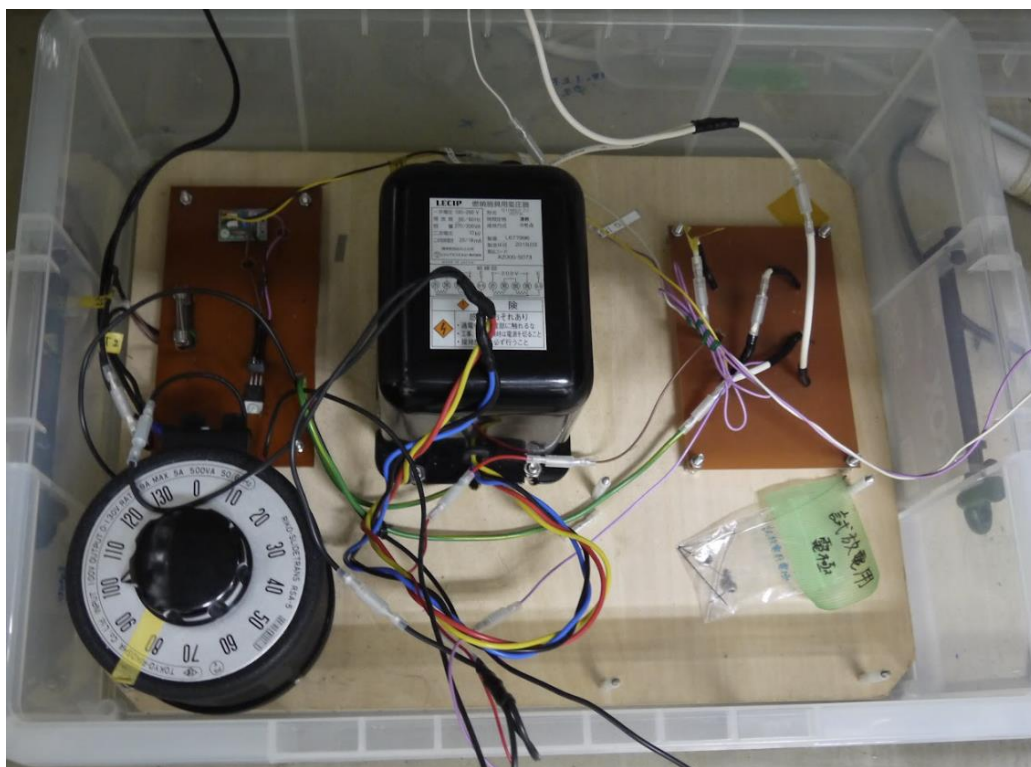


Figure 2.3 Ignition Circuit

Two types of electrodes were experimented with. Both are identical in principle. A copper rod extends from exterior to the interior of the combustion chamber. A thin tungsten wire is attached to the copper tube. First one is taken from the previous study. It has a thinner design.



Figure 2.4 Discharge Electrode

The electrodes are positioned as the figure 2.5 and 2.6 shows below. It was found during experiments that the insulation was not sufficient to prevent discharge between the copper tube and rest of the structure. The heater attached on top acted as a ground causing a short.

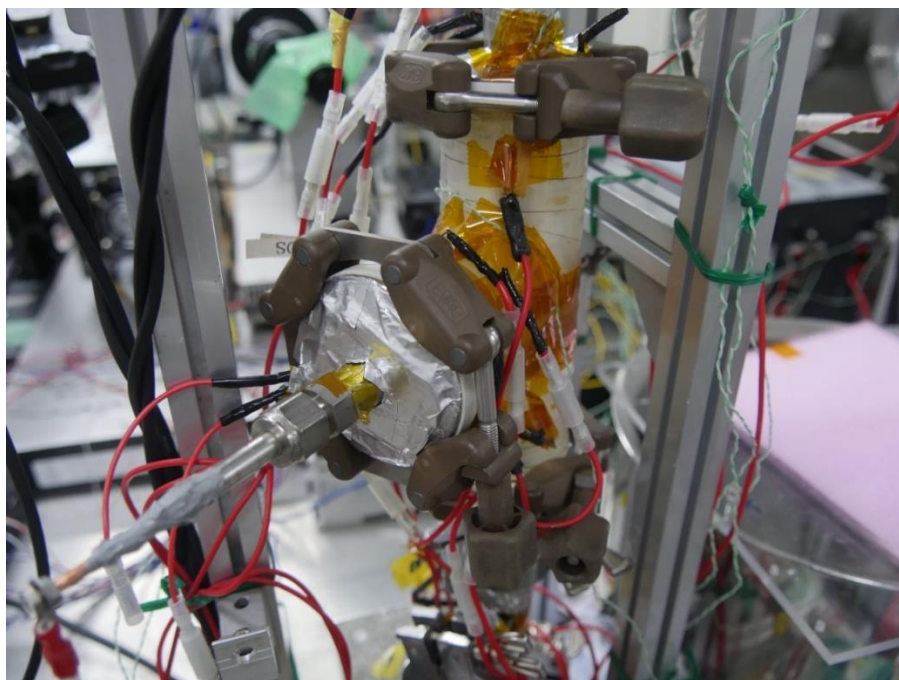


Figure 2.5 Electrode Position

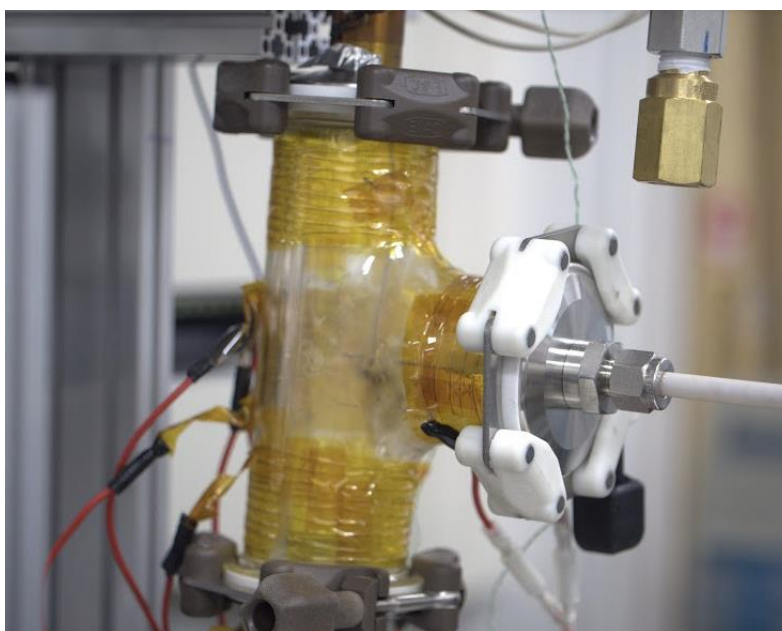


Figure 2.6 Magnesium Wire and Tungsten wire

A version designed with thicker insulation was made. The newer version is more robust, shown in the figure 2.7.

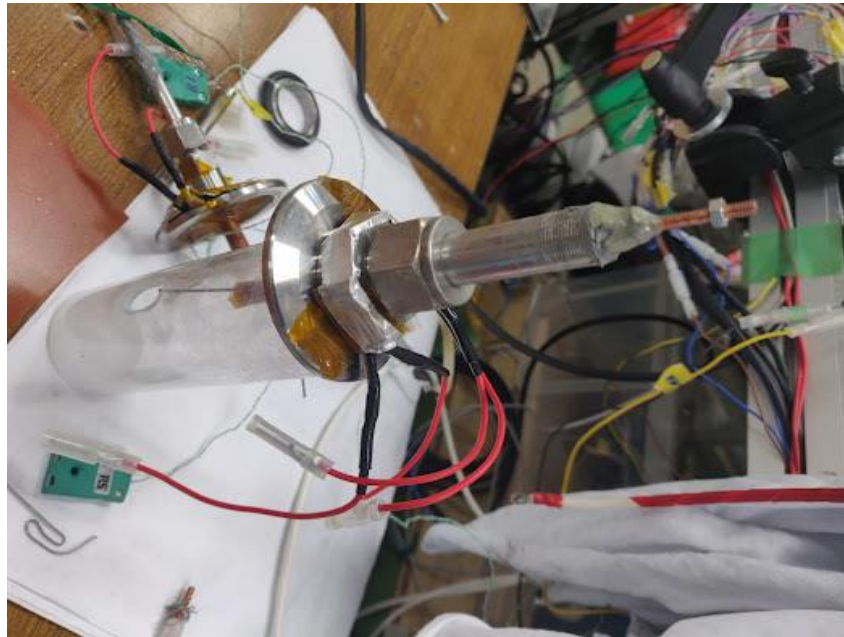


Figure 2.7 Improved Discharge Electrode

The electrode is made first by preparing a copper rod of adequate length. Kapton tapes are wrapped around the copper rod until the thickness is enough to fit within a 6mm diameter pisco tube. This pisco tube is inserted in a larger metal pipe with gaps filled with epoxy to provide further installation. Silicon adhesive is used to seal of the ends of the tube. The structure is then attached to a 1/2 inch adapter by Swagelok for easier installation and removal.

2.5 Combustion Chamber

2.5.1 Selection

In the previous study. Both NW16 pipes and NW40 pipes were used. One of the goals of the study is to observe the combustion itself. Visualization is necessary so glass nipples are used as the combustion chamber.

During experiments, the NW16 nipple used in the prior study was damaged. Figure 2.8 below shows the damaged state of the combustion chamber. Black area is from the burnt glass surface form the contact of burning magnesium wire. Hot temperature from combustion caused cracks

on the glass combustion chamber. The chamber can't be used again after damage. This damage is independent of the heaters attached to surface.



Figure 2.8 Damaged NW16 Nipple

This study only used NW40, shown in figure 2.9. There are a few considerations. First, NW40 is larger in diameter so that the wire is not as likely to touch the surface of the wall. Second, the lower flow velocity may increase the likelihood of ignition.

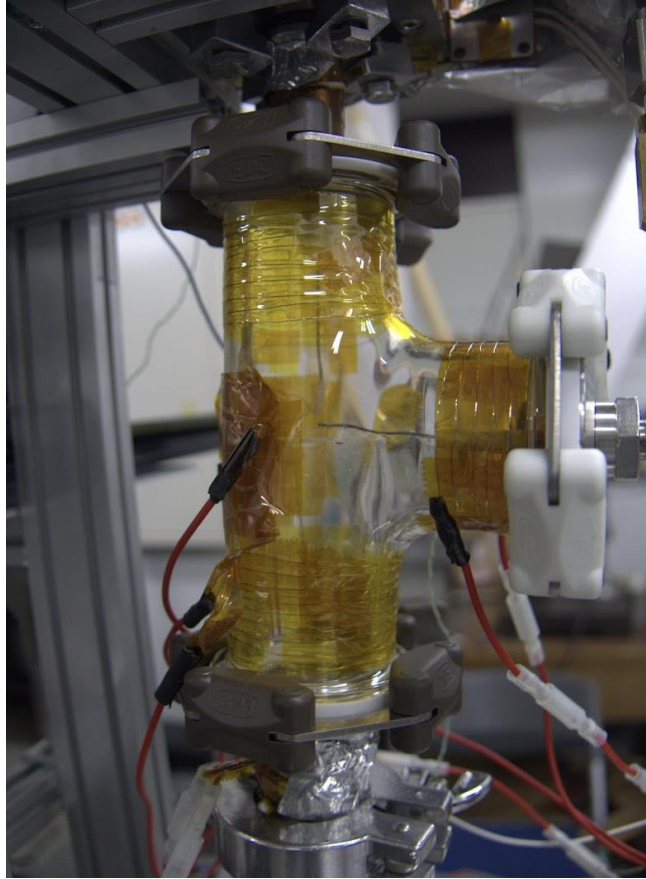


Figure 2.9 NW40 Nipple

2.5.2 Wire guide

While a wire feeder has control over the amount of the wire in the combustion chamber. It is a one dimension control and has no say on the horizontal movements of the wire tips. A guide is required to ensure that wire does not bend. In the experimental setup, the wire combustion occurs approximately 20 cm below the wire inlet. A long guide is therefore required.

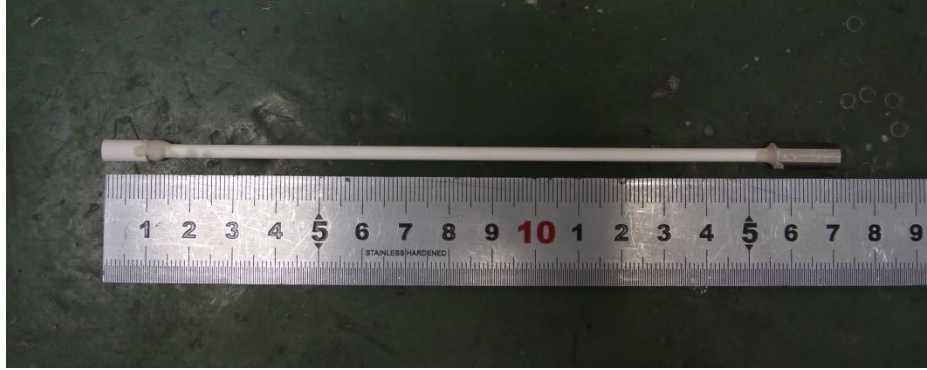


Figure 2.10 Wire Guide

The guide is made of ceramic tube and a small ceramic bracket. Alumina ceramic is used here because of the high temperature resistance and lower than metal thermal conductivity. High temperature resistance is needed to resist the temperature from combustion. Lower thermal conductivity helps with reducing heat loss through the wire guide. The ceramic tube is about 3 mm in diameter and 20 cm long. The bracket is fixed onto the tube with a ceramic screw. Figures below show the position of the wire guide. Figure 2.11 shows the end point of the wire guide.

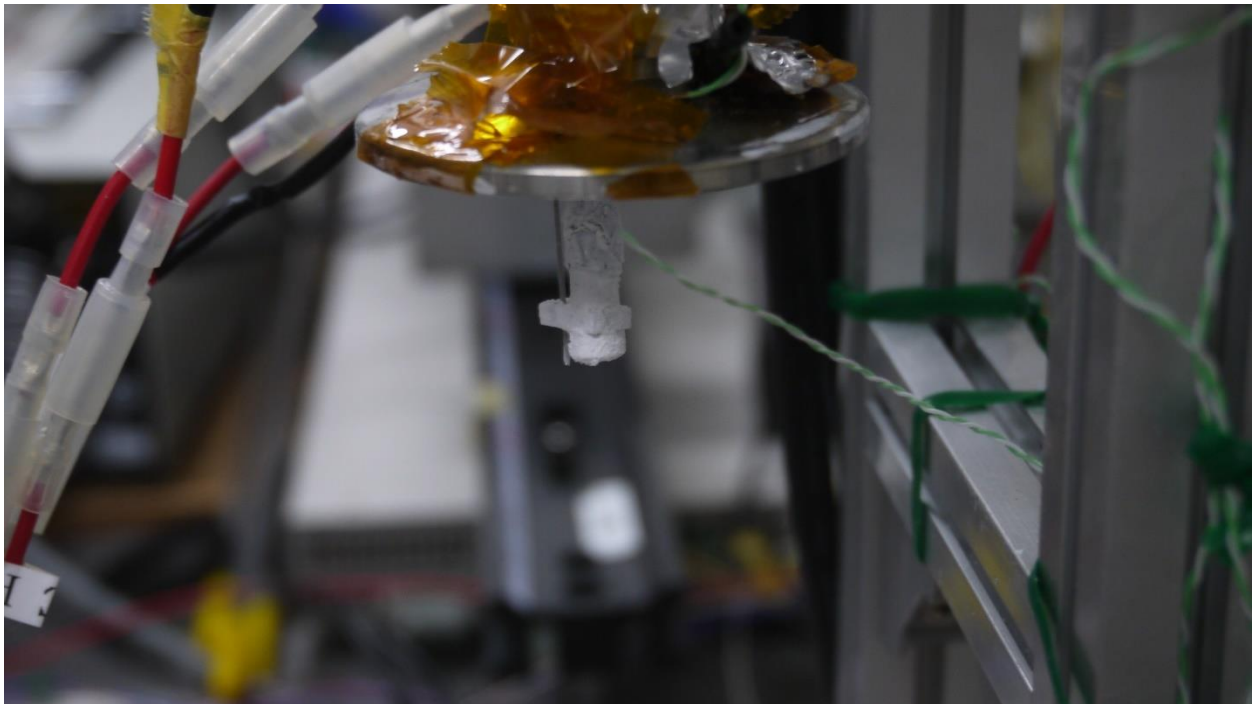


Figure 2.11 End of Wire guide

Figure 2.12 shows the path the wire guide takes and the relative position it has. The wire does not go straight down and encounters many obstacles. This is a design flaw that was not considered. Due to the brittleness of ceramic, these tubes are not only difficult to attach but can often break from smallest force. The wire guide can also force the wire to bend.

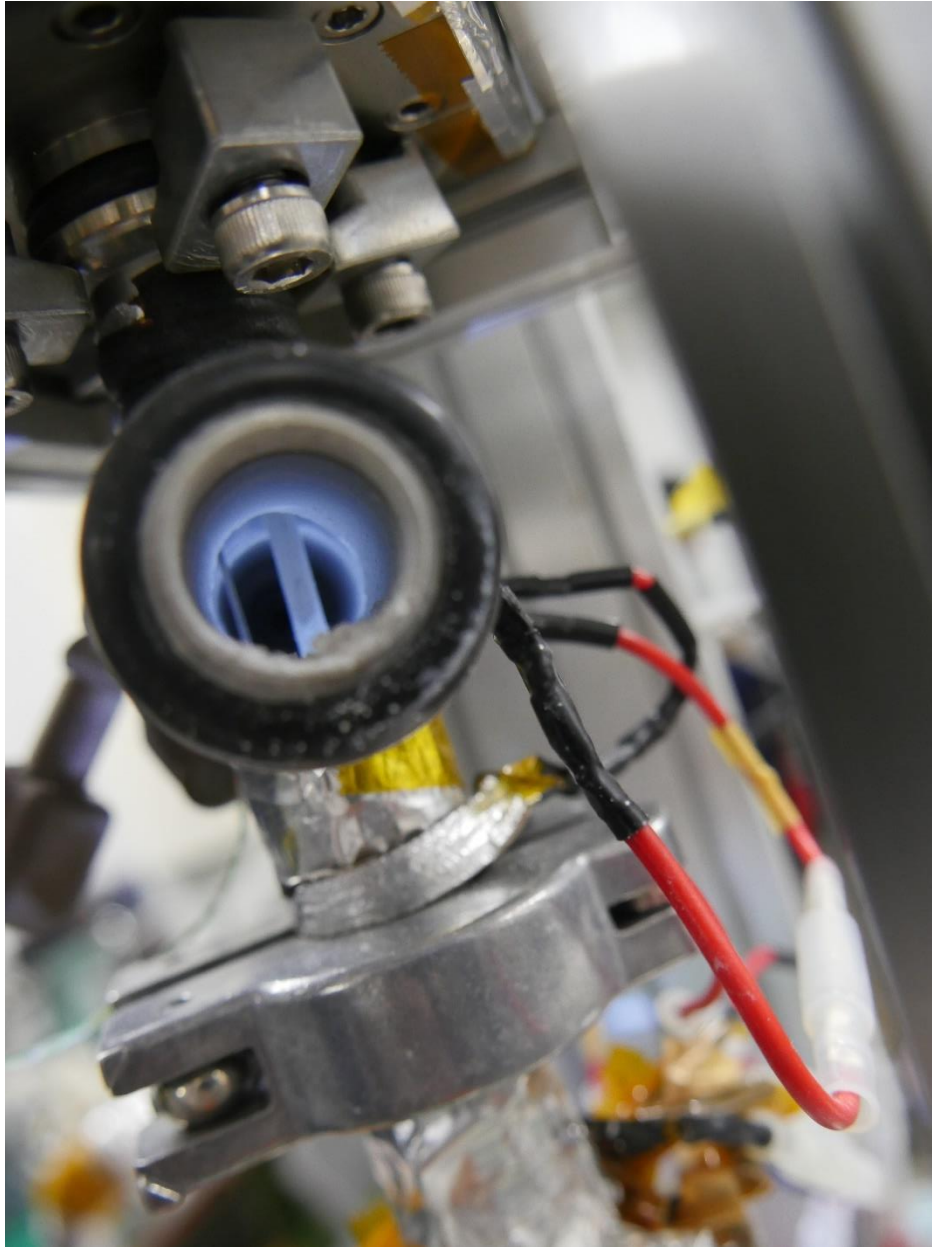


Figure 2.12 Wire guide and wire in the downstream of combustion chamber

2.5.3 Protection lining

While the NW40 Nipple is larger and therefore less likely to be damaged. The interior still needs to be protected from damage to prevent the chamber from losing clarity due to charring.

2.5.3.1 Acrylic

Acrylic shield was considered. Acrylic is cheap, clear, and easy to be modified. Modification is needed because the discharge electrode needs to be able to extend inside the chamber. A hole is drilled on the surface of the chamber. Ignition is successful with this setup.

The low melting point of Acrylic at 160 degrees Celsius made it unsuitable for long term use. Rather than charring like glass does, Acrylic melts and adhere to the surface of the glass combustion chamber. Removal is difficult and dangerous,

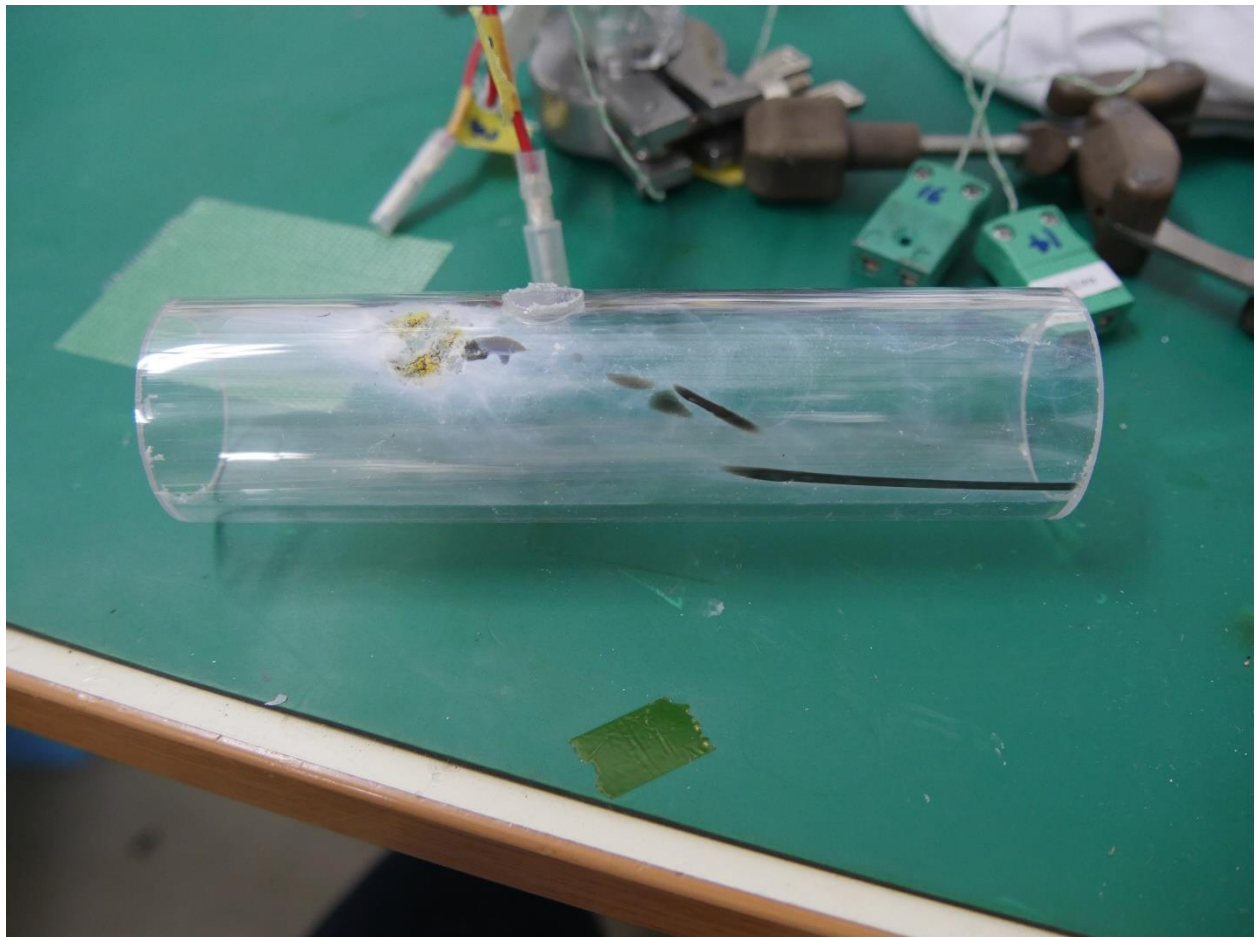


Figure 2.13 Acrylic Tube

2.5.3.2 Quartz glass

Quartz glass has the benefit of high temperature resistance without losing clarity. It is more expensive and does not allow drilling of holes. To accommodate for the electrode, two pieces of quartz glass were used instead. Electrode would fit in between the two glasses. Figure 2.14 below shows the state of the quartz glass before and after combustion. The glass after combustion has already been cleaned. Quartz glass can get charred just like the combustion chamber does. However, compare to Acrylic, it does not lose its shape which is important. These glass tubes are reused until the charring effects the ability to track combustion.



Figure 2.14 Quartz glaass tubes used for protection

2.6 Wire feeder

2.6.1 Previous solution

In previous study, because the requirement for feeding of wire is unknown. An commercial feeder used for welding was used. The mechanism is simple. The device consists of a driving roller with grooves of appropriate width for the wires used in welding. A motor connected to gears that increase torque at the cost of speed. A separate roller on a bearing that applies force on the wire which increases friction. Welding feeders comes with replaceable rollers based on the diameter of the wire used in welding. Due to the industrial purpose of such device, it was

designed to have a high torque without need for speed or precise control. By switching out the rollers, the wire feeder was compatible with 0.6 mm wires, 0.8 mm wires, 1mm wires. As this study focus on the use of 0.8 mm wires, it was considered suitable.

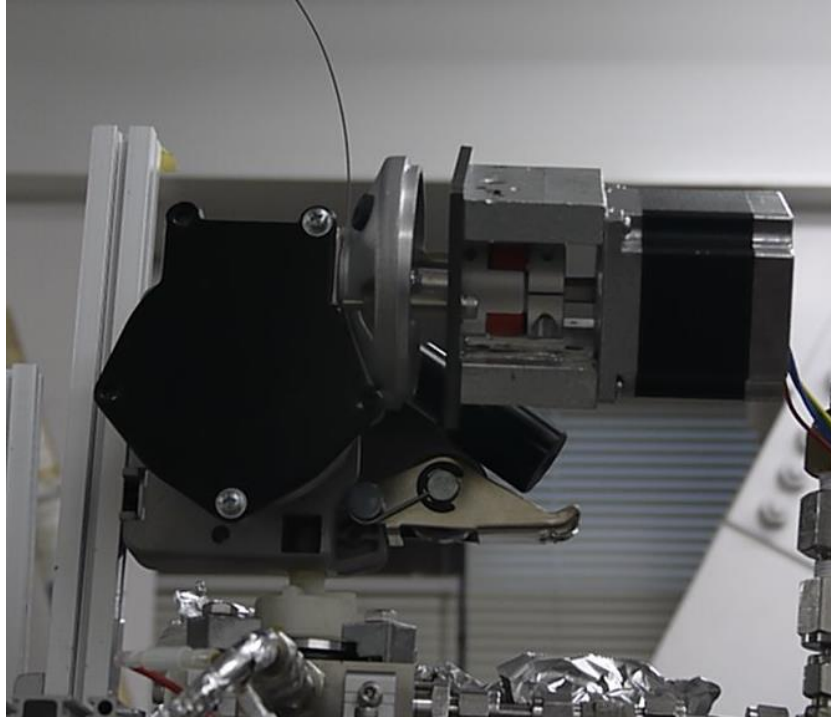


Figure 2.15 welding wire feeder (backside)



Figure 2.16 Welding wire feeder (front side)

With this wire feeder, a sealing mechanism using two o-rings helped the sealing of vacuum at the wire inlet. An off the shelf driver was used for the control of the motor on that wire feeder. A 24V power supply was used to power the driver and the motor. The driver is controlled by an Arduino. The Arduino accepts signal from a potential meter and converts the voltage into signal readable by the driver.

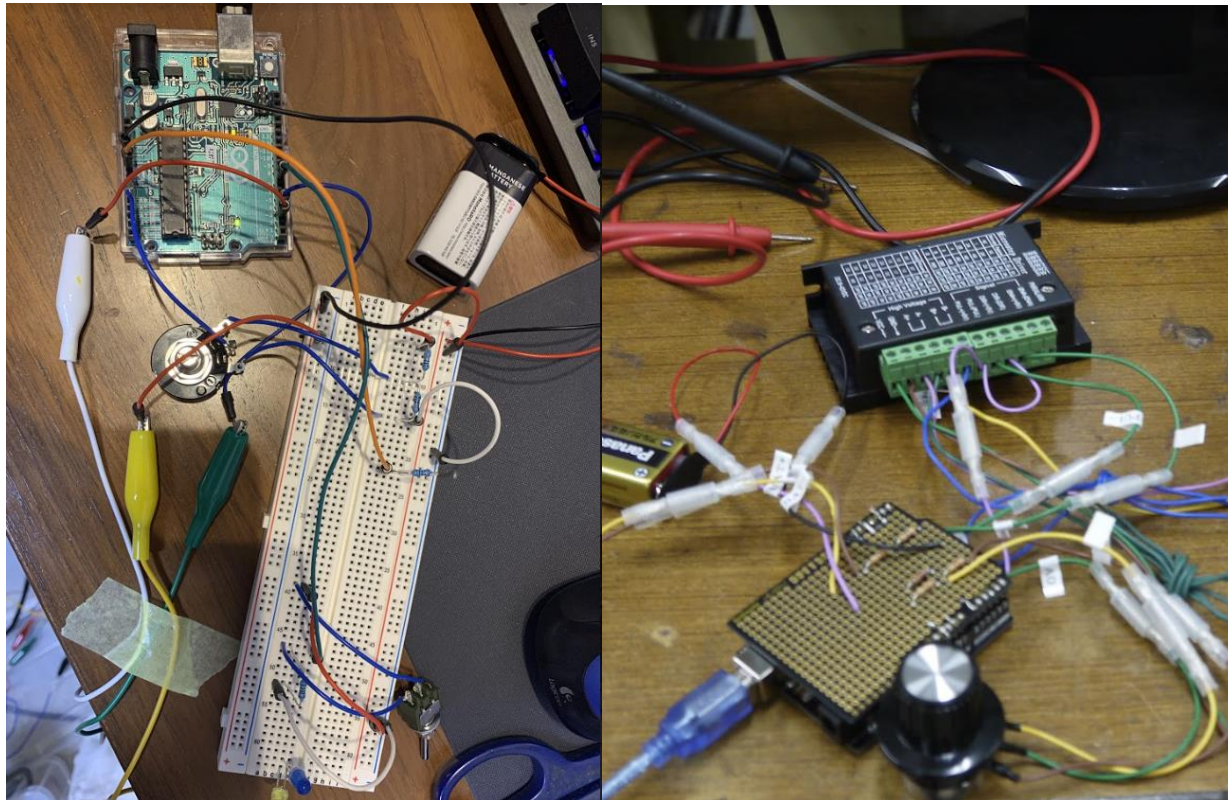


Figure 2.17 Previous manual control system

2.6.2 Problem

While the feeder was setup at low cost, combustion experiments using this system found the specifications of the feeder unsuitable for sustained combustion.

First, the max speed capable by the feeder was too low compared to the combustion velocity. The feeding rate of the wire is determined by the diameter of the roller and the RPM of the driving roller. Because of the gear reduction box, the feeder was specialized to feed wire with high torque rather than speed. During combustion, wire would combust faster than the feeding rate, resulting in extinguishment.

Second, the range of the speed wire feeder was capable of was also too narrow. The motor doesn't spin unless a voltage threshold is reached. This threshold is too high so that the feeder wasn't capable of finer adjustments to wire position.

Finally, this wire feeding system was ultimately controlled by a human operator. It requires fewer setup in terms of hardware and software but can be unreliable and most importantly inconsistent.

2.6.3 Redesign

The principle of the temporary solution had worked. However, the specs weren't up to what was needed. Of the commercially available solutions, They all tend to be bulky, not fit for use in experiment. There specs were however a good reference. Based off those larger industrial feeders. A target of 1m/s feeding rate was chosen as the target.

A new wire feeder was designed and manufactured using 3D printers Instead of designing new rollers, the same rollers are reused in this wire feeder. These rollers are 30 mm in diameter and have grooves for 0.8 mm wires.

One of the issues discovered during testing of the previous wire feeder was that excessive force causes deformation on the wire cross sectional area, potentially leading to inadequate sealing at the inlet. Having multiple rollers means that less force is required per roller to have the same performance without slipping, reducing the deformation. Because these rollers all needed to be in sync and considering the side of the wire feeders. The wire feeder opted for a two roller design. Having multiple rollers additionally helps the wire to remain somewhat straight. The two shafts for rollers are connected by a toothed belt which helps the rollers to spin at the same speed. Toothed belt ensures that slipping is near impossible compared to flat or v shaped versions. Slipping is likely not completely inferior, however. If the difference in roller speed due to slipping create a small tension on the wire, such tension can help the wire straighten.

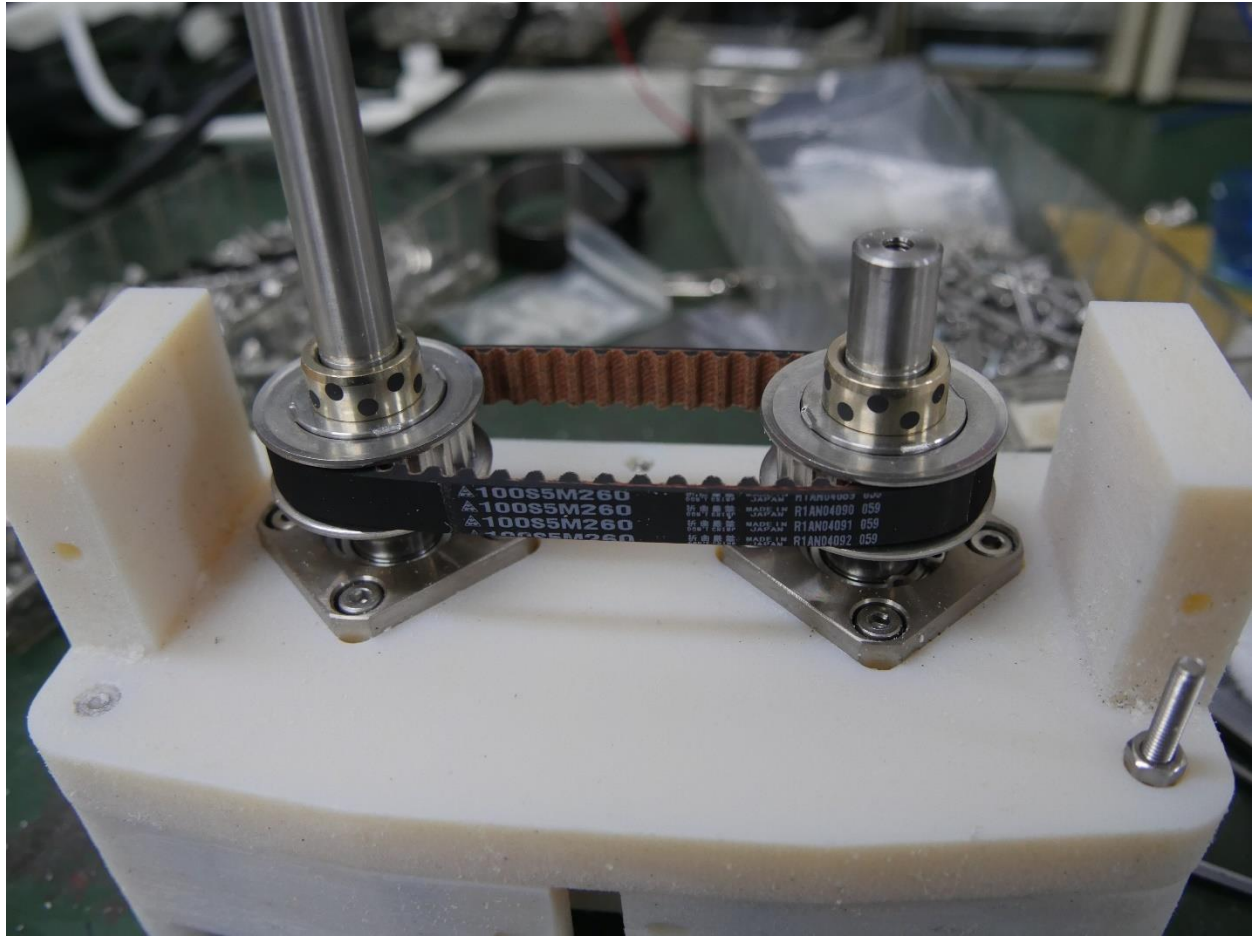


Figure 2.18 Connection belt

There was some difficulty designing the mechanism needed to apply force in between rollers and the wire. The commercial solution used a spring and clamp setup. Due to the light weight of the metallic parts used, it was effective. 3D printed parts do not have the strength of metal parts. The designed opted for a spring, bolt and nut setup, shown in the figure 2.19. 3D printed part doesn't have the durability to allow for thread, so nuts are embedded within the structure in the center. In combination with the springs, the tightening of the bolts helps clamping the free roller on top of the wire. 7.394 N/mm springs are used. Instead of metallic rollers used in the temporary solution, silicon rubber rollers are used to further help with increasing friction without increase in force.

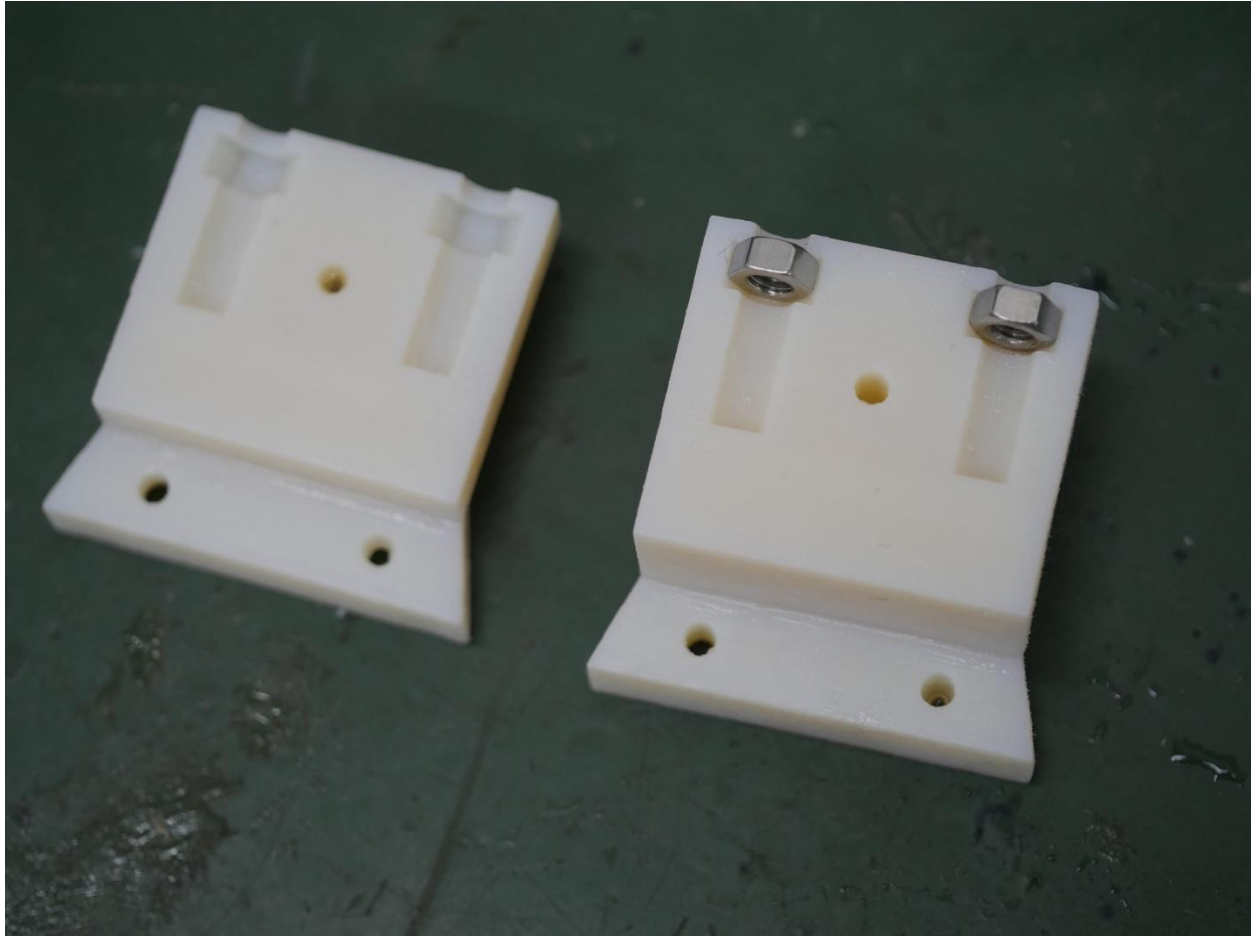


Figure 2.19 Clamping mechanism

The advantage of 3D printed part is that parts can be replaced easily. This offsets the lower durability of the plastic. During its use, some of the original parts printed in white resin are replaced with the black ABS parts due to wear. These replacements had no effect on the performance of the wire feeder. Figure 2.19 shows the state of the feeder before on the left and current on the right.

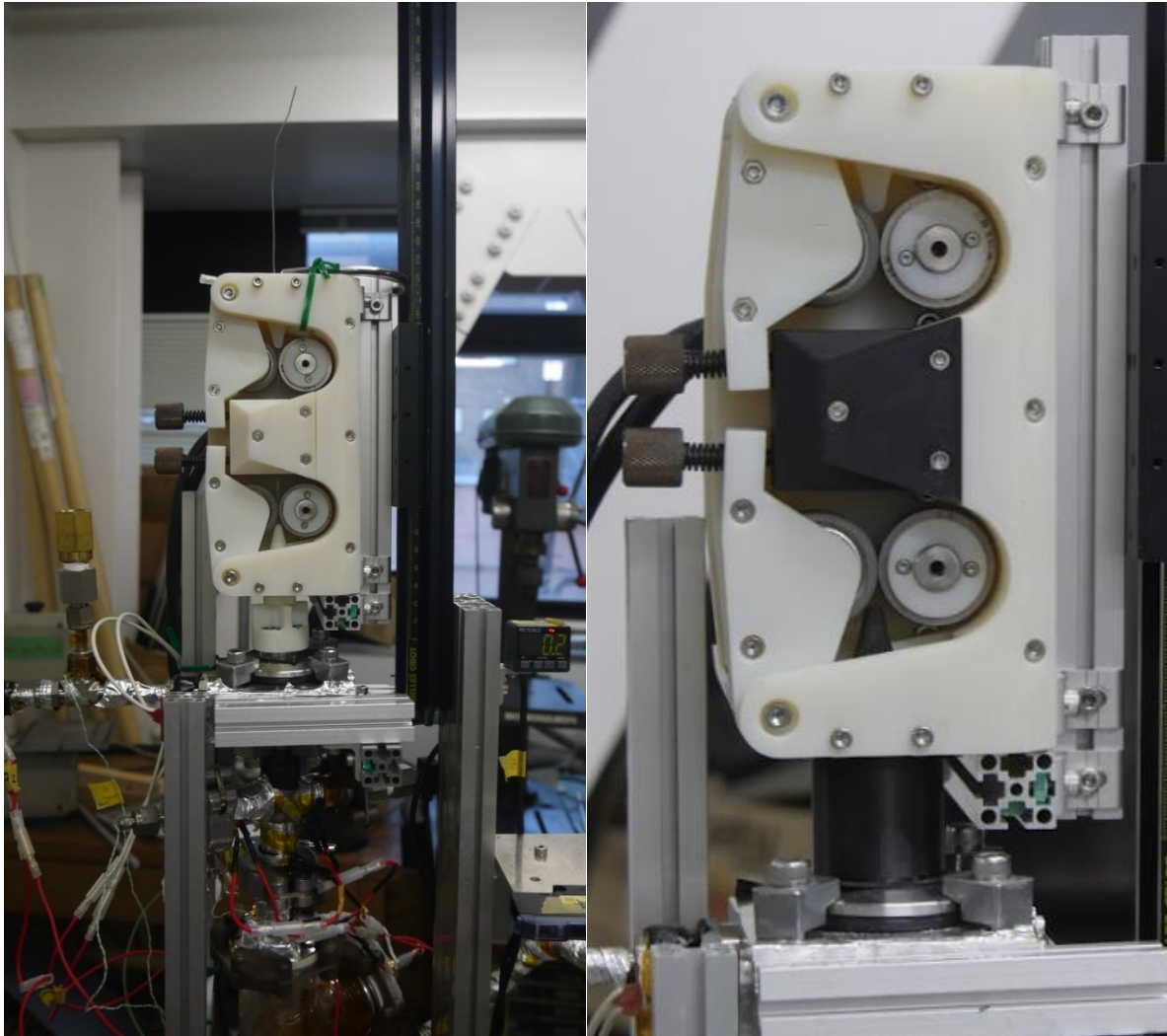


Figure 2.20 Installed Wire Feeder Original (left) Repaired (right)

The motor driver combination used is BXM230-A2 and BXSD30-A2 from oriental motors. The motor itself has a range of 2-4000 RPM and a 1:5 gearbox built on top of it reduce the actual roller speed to 0.4 – 800 RPM. These motors are selected for the inbuilt encoder allowing for precise control of speed and the wide range of speed possible. The hollow shaft as part of the gearbox is directly connected to the driving shaft of the roller. Hollow shaft was used as the design to enable easier installation and removal of the motor assembly as it doesn't require additional linkage.

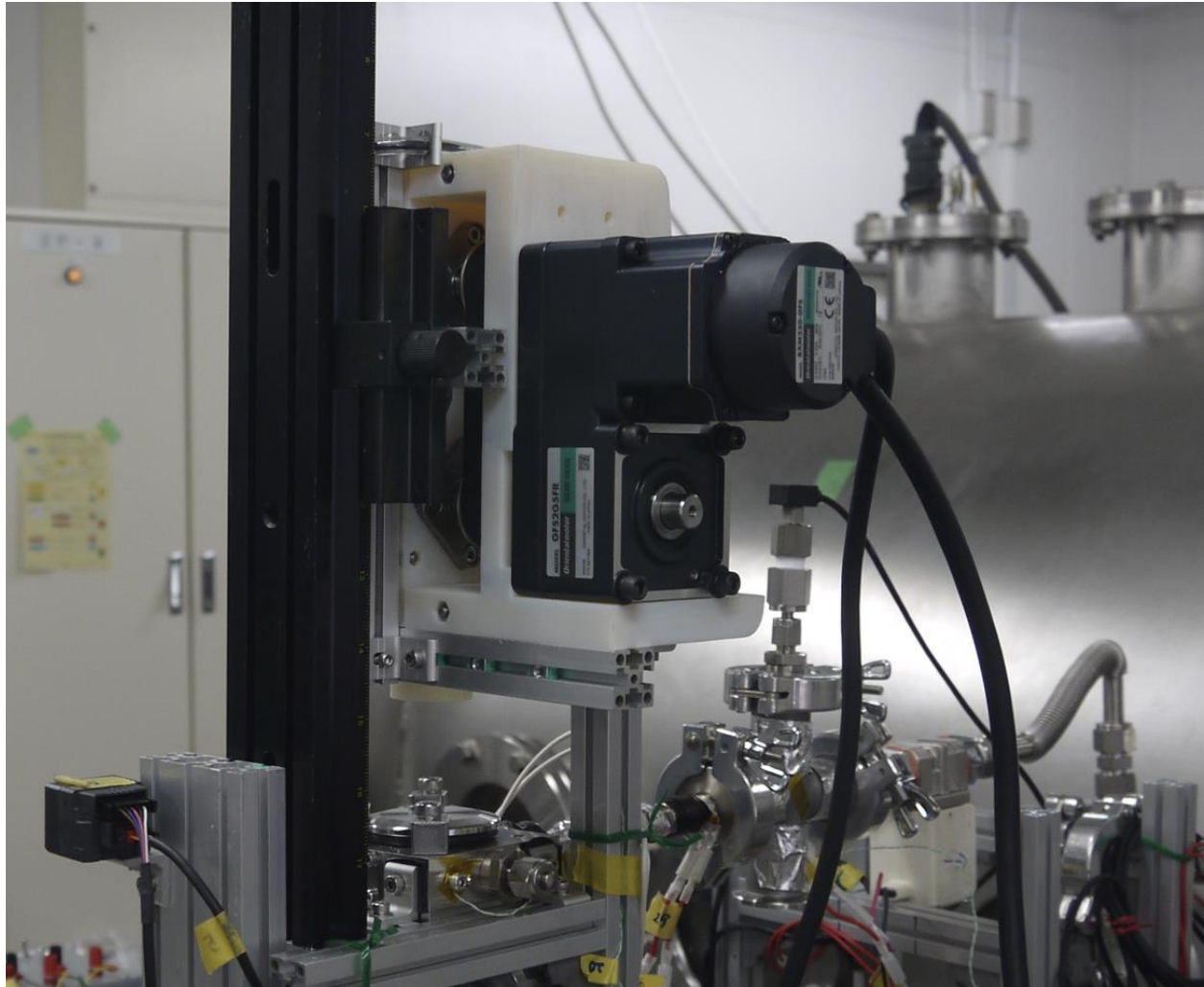


Figure 2.21 BXM230-A2 Motor

This driver has several control methods. It can accept several tiers of fixed speed using digital control or alternatively an analog control through varying input of voltage. Analog control is used as it is simple to setup. A potential meter that can output voltage from 0 to 5 V is used for initial testing. The driver has a built in settings to convert input voltage into RPM and it is set to 200 per volt after some initial testing. The feeder was able to feed wire at the designed rate.

The new feeder takes the place of the old feeder and is installed on a sliding rail to help with easier installation of the wires.

2.6.4 Flaws and Rooms for improvements

As this is the first prototype made with 3D printed parts, all the parts are designed to be thicker than what is required with minimal use of custom metal parts. As a result, the device without the motor installed weighs over 1.9 kilograms. Additionally, 3D printed parts while convenient can result in warping. Both the white resin used and the black ABS material resulted in warping. Replacing with stronger lighter parts such as ones manufactured Aluminum can reduce the structural material required.

Another unfortunate aspect is the size of the wire feeding device. It is not only heavy but also quite larger than desired. Part of the reason is the motor size. From experience using such motor driver combination, it is way over spec. In any future improved version, a smaller profile is likely beneficial. One area that needs to improve to achieve the smaller profile is the clamping mechanism. With the lighter and stronger material like metal, this part can become a lot smaller.

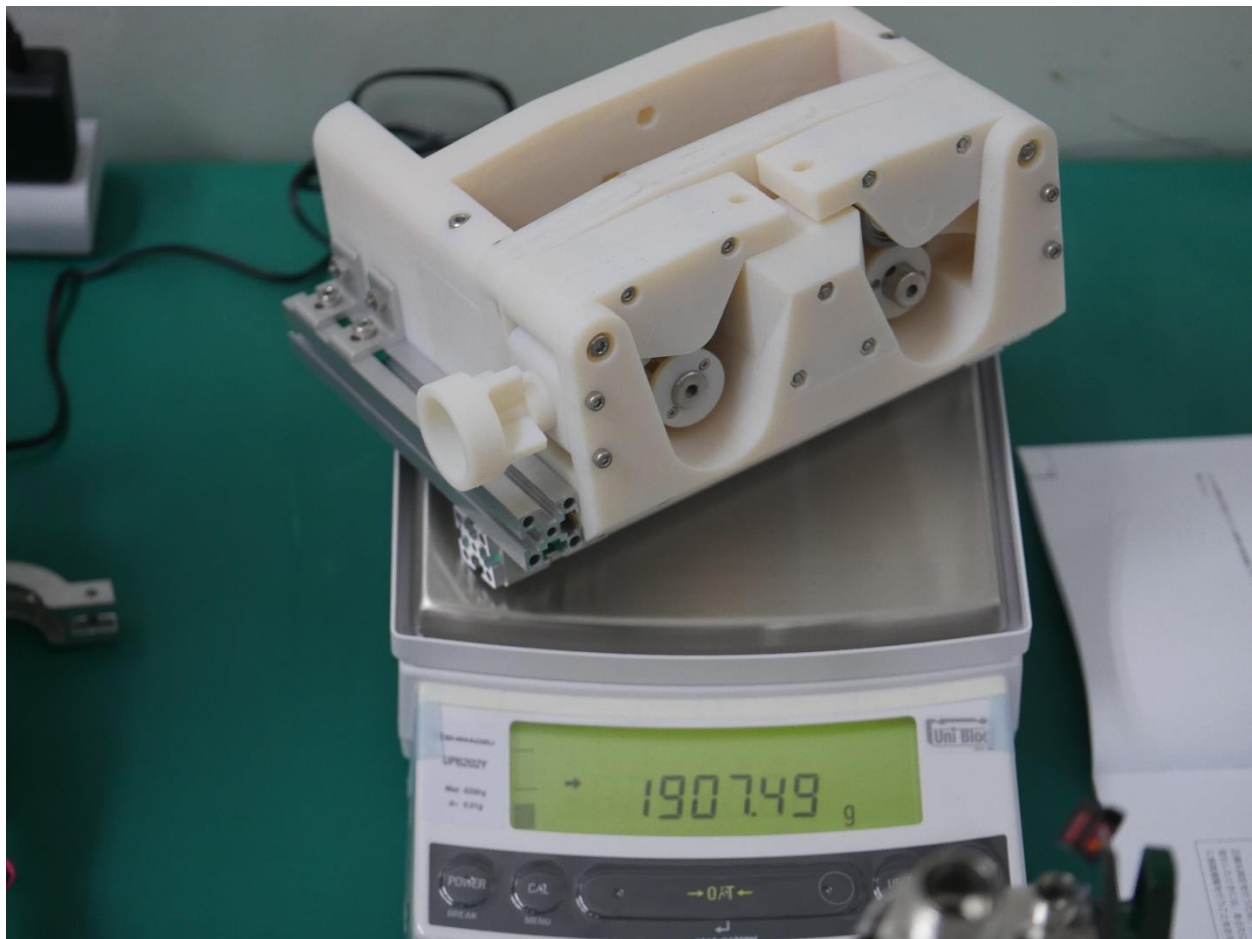


Figure 2.22 Wire feeder mass

2.7 Automated Program

While the final thruster design expect a system to use a control mechanism without feedback loop, having an automated control with feedback loops built in helps with this stage of experiments where ideal feed rate parameters are not known and dynamic adjustments are required.

In the previous system, this control is done by a human operator. The person is responsible for identifying the amount of wire left with in the combustion chamber and adjust the feeding rate accordingly. This poses a few challenges. First the response time of such control method can be slow. In general, there is a delay between the ignition and the operation of wire feeding. Second it can be difficult to match the feeding rate to combustion rate.

2.7.1 Flame Tracker

The flame tracker is coded in Python. What the flame tracker needs to do is to act as the eyes of the automated control system. It needs to be able to determine the location of the flame, the situation of the combustion just like eyes of the human operator would.

The most important from the tracker needs to obtain is the location of the flame. The problem of matching the combustion speed and feeding speed is a one dimensional problem. In this study, wire is fed downwards where as the combustion is opposite to the feeding direction.

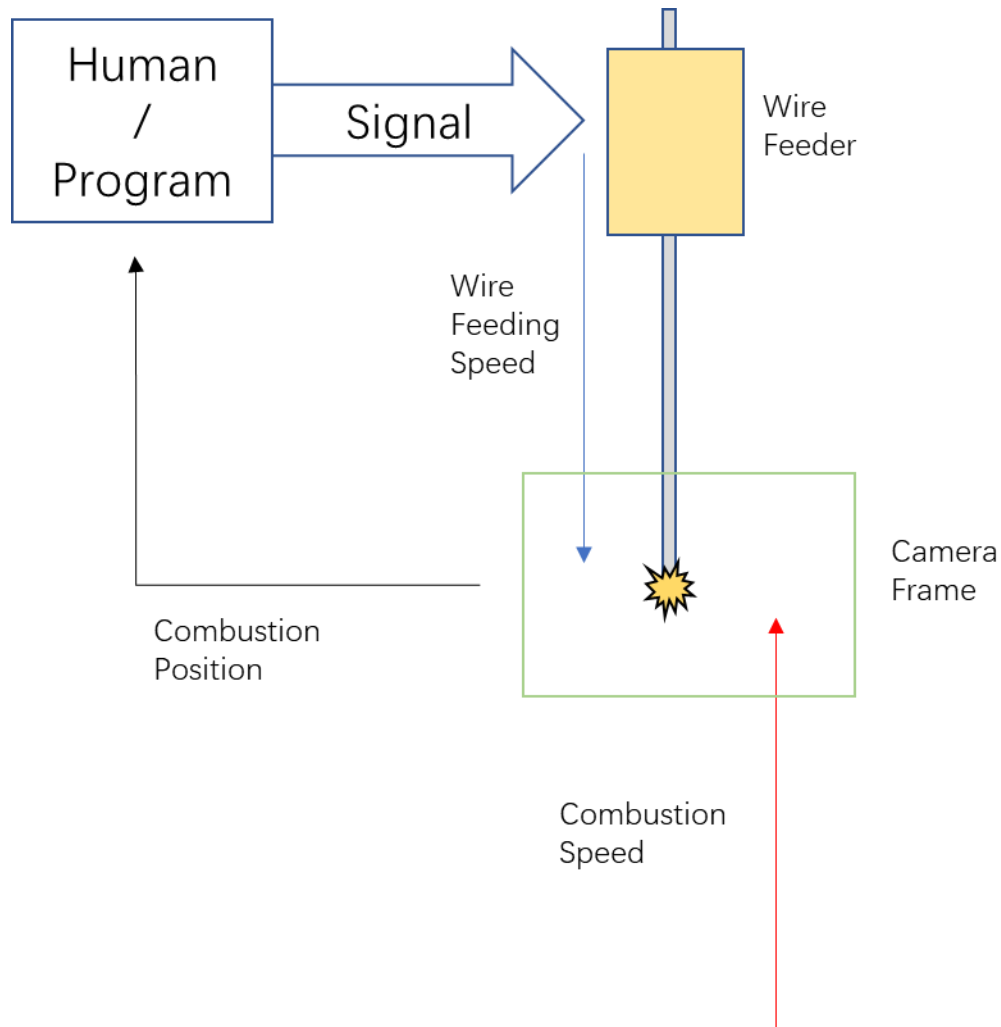


Figure 2.23 Feeding system illustration

2.7.1.1 Sensors

This study considered two potential implementations of sensor. Photovoltaic sensors and Video based method.

Photovoltaic sensor works by outputting voltage based on the luminescence, a relationship that is mostly linear. A closer light source outputs a voltage that is higher. Two photovoltaic sensors can be installed a significant distance apart. By calculating the difference in the reading of two sensors, the position of the flame can be approximated. The workings of the setup is better illustrated in the figure 2.23. For example, if the desired location of the flame is exactly between

the two sensors, a feedback loop can be implemented so that the resulting difference between two sensors is 0.

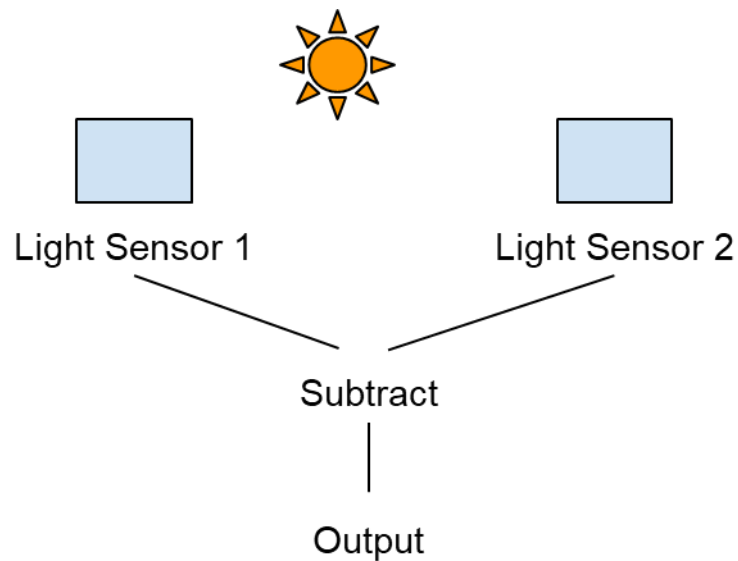


Figure 2.24 Photovoltaic based method

A video based method uses a usb web camera. This method is closer to how human would perceive the combustion. Every frame can be compiled into a 2D matrix. Through algorithms, the position of the combustion can be estimated as an (X,Y) coordinate based on the camera frame shown like the figure 2.24. A control program would then interpret the position of the flame and adjust the feeding rate.

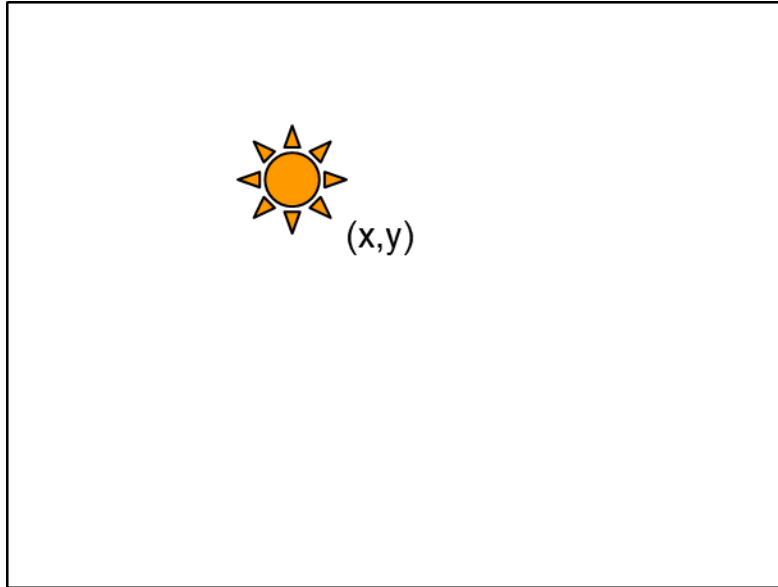


Figure 2.25 Camera based method

2.7.1.2 Benefit of each solution

Video camera based solution was chosen. The benefit of the video based solution is that it can be applied to all system where as photovoltaic sensor based system require a setup tailored to the hardware. With the changing hardware, it is impractical to be calibrating a photovoltaic system every time. The benefit of a photovoltaic sensor based system is that it does not require visualization of the combustion chamber, perhaps suited more to the finalized version of the thruster if a feedback system is necessary. It also can be a completely analog circuit where as the video based processing method requires a computer.

2.7.1.3 Camera system

A simple USB camera is used. The camera only requires a resolution of 640 x 480, a common resolution used for image processing. There are no noticeable benefits to using higher resolution images with the massive downside of slower processing time. At 640x480, the frames can be processed at 40 fps. At 1920x1080, it can only be processed at 20 fps or so. The approximation is

not improved.

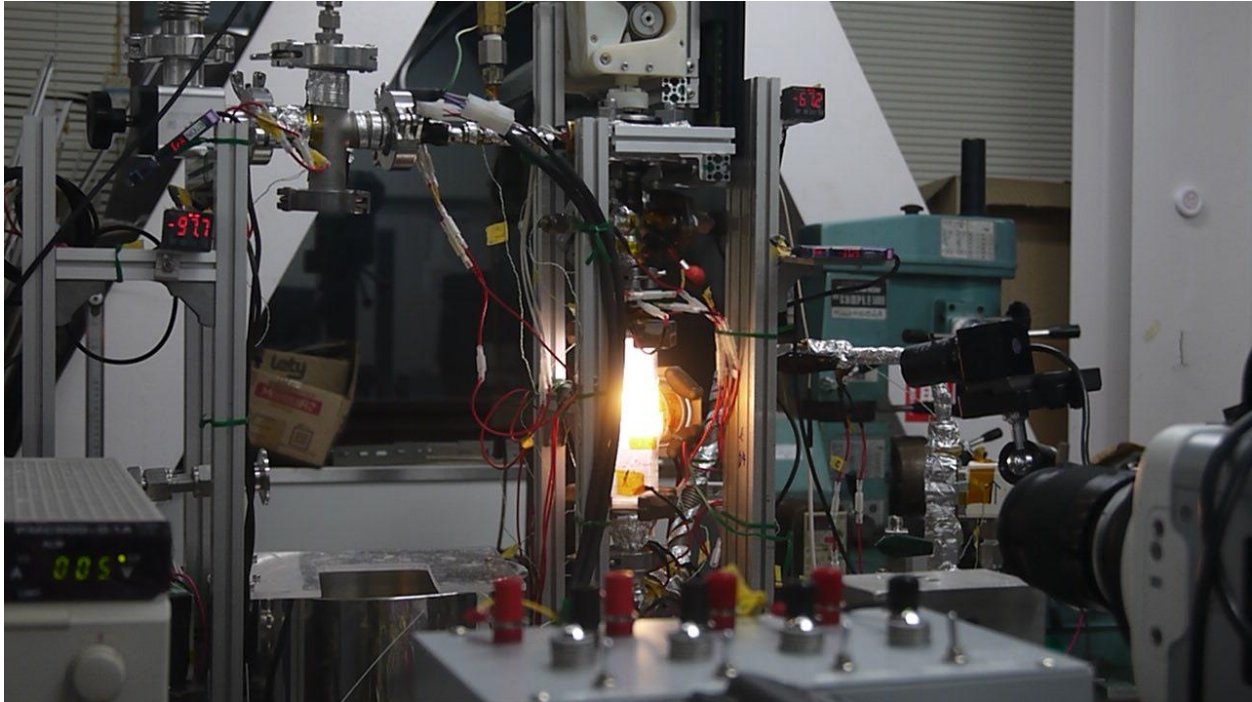


Figure 2.26 Experiment Setup

2.7.1.44.5.1.4 Combustion Search Algorithms

To identify the combustion point, a program is written in python. Python is language that is easy to learn albeit a bit slow to compile and execute. The principle of the program is quite simple. First, one frame is taken out of a live video feed. The example of which is shown below. First figure, figure 2.27 shows the original frame that is captured. Combustion chamber is positioned to fill the camera frame. The bottom figure, figure 2.28, shows the desired outcome. The green cross represents the point of combustion the program should be able to identify.

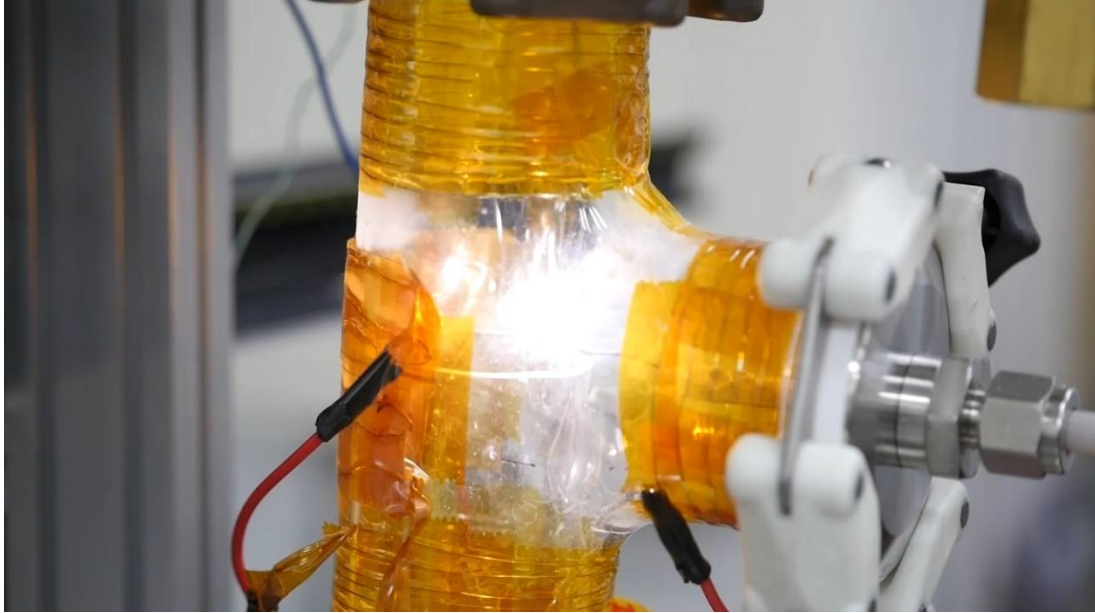


Figure 2.27 Raw image from video

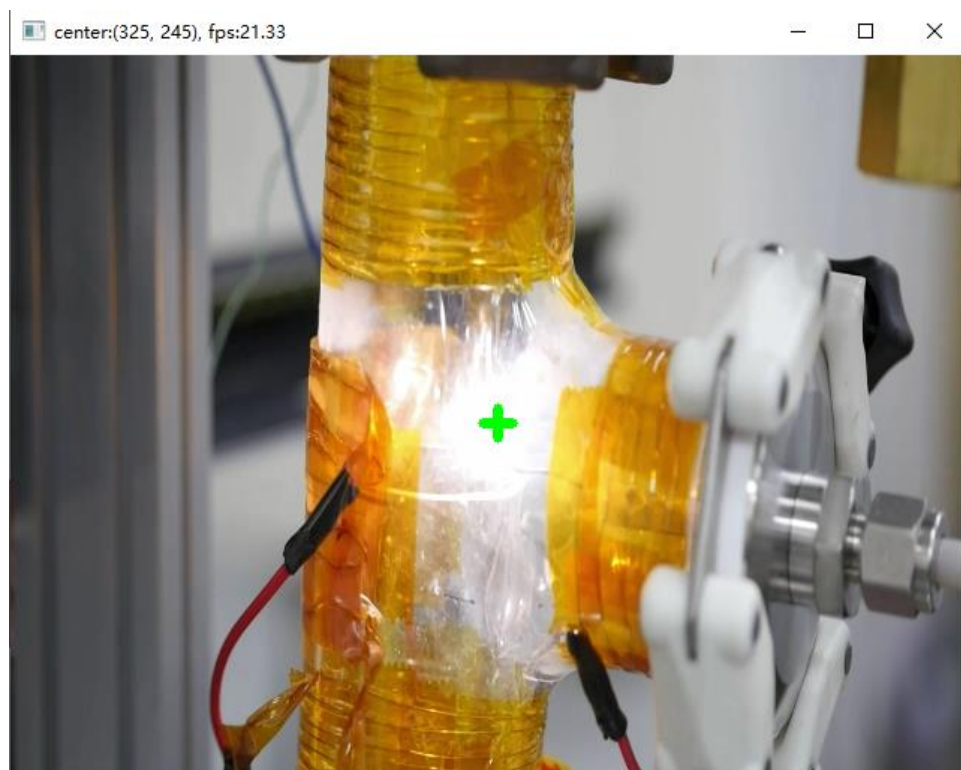


Figure 2.28 Tracked image

Each frame captured needs to be converted into matrix data that can be processed. Generally, there are 3 matrices, each one representing one of the 3 colors among red, green and blue. Only

one matrix can be used for the processing, this can be one of the 3 color matrices or a combination of three.

Greyscale, a common conversion is based on the following formula for example. For the purpose of this program, a greyscale is not necessarily ideal. The following figure 2.29 illustrates the differences in the ability to process based on the matrices used. This can be objective but matrices of the color blue showed the flame more clearly. However, Kapton tapes that cover the exterior of the combustion chamber completely absorbs all the blue lights. Matrices of red does not have such issue despite the slight blurry flame shape. Greyscale shows the middle ground where the Kapton tape still obscures the combustion but not so much that combustion is not visible. This is natural considering the formula used for greyscale.

Ultimately, matrix of red is used for the processing. The matrix has a height of 480 and a width of 640. The values have a range from 0 to 1, where 0 represents black and 1 represents white.

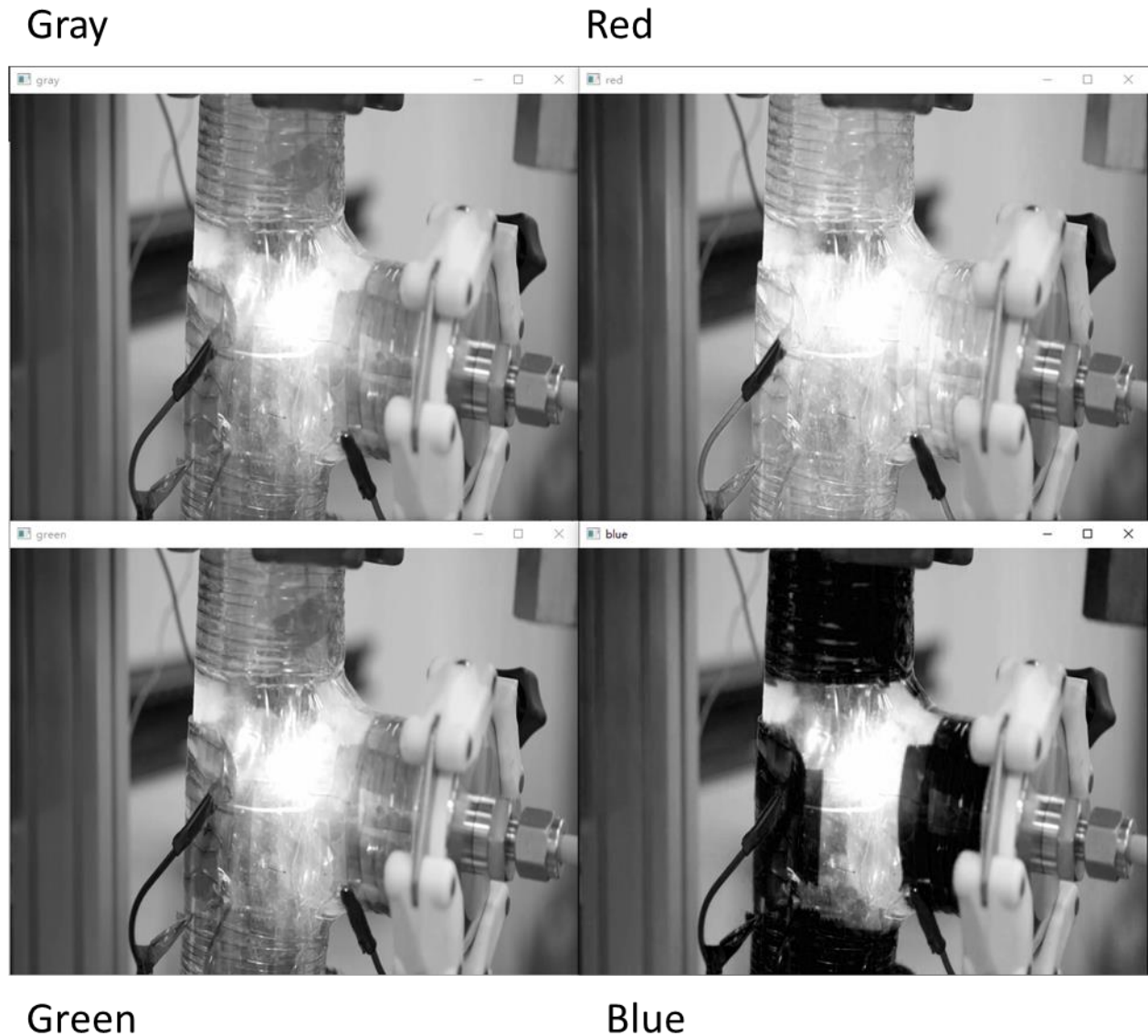


Figure 2.29 Effectiveness of color channels

The technique for finding the center of mass this program use is the center of mass formula. In order to do so, the patch of combustion needs to be identified.

After a matrix is built, the image is processed with blur so that small noises are removed, and shape is more uniform. This is a common technique used in image processing. Blur generate an image that takes the average of the pixel around using a formula. Small noise gets removed from the process of averaging. Then a threshold function is applied. This function essentially sets any unit that has a value above the threshold as 255. After trial and error, the threshold is set to 245.

The optimal value can change depending on the exposure and whether ND filter is used. The matrix after threshold process looks something like the center figure in figure 2.30.

In some cases, a hole may be present within a blob of white area. This could be the result of particle obstructing the view of combustion. This is processed using erode and dilate. This technique first expands each of the area, then shrinks the area. Any small gaps get filled.

As shown in the center figure below, reflection of the combustion also exceeds the threshold value and shows up as a white spot. However, this spot is much smaller than the point of actual combustion. A filter is made so that only one and the largest area is considered the combustion. This filter first finds all the white areas that has a size of over 200 pixels. This helps prevents false identification of any environmental light sources. Then each area is compared so that only the largest one remains. The result of the processing is shown as the figure in farthest right. The center of mass of this area is calculated as the combustion position.

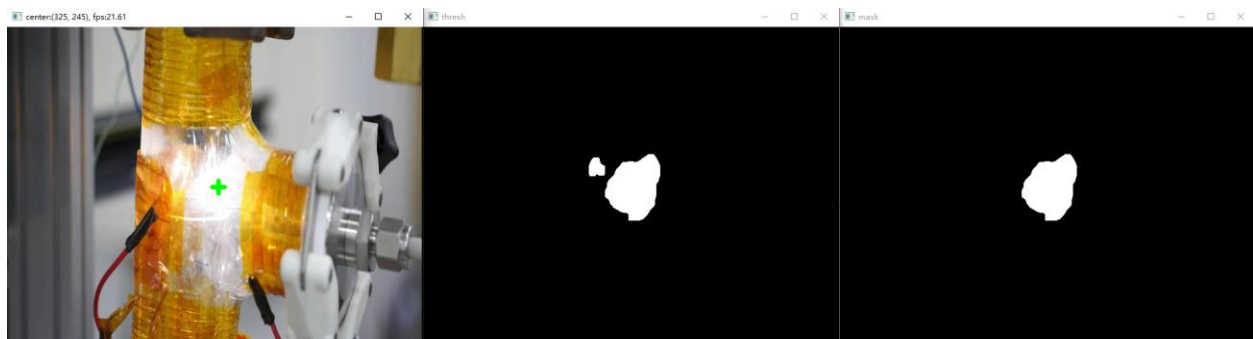


Figure 2.30 Image processing

2.7.2 Feeder control

Feeding control is coded in LabVIEW. The advantage of using LabVIEW is the ease of programming an interface. The feedback loop designed is shown below. The program takes the coordinates from the flame tracker, the desired position, and outputs voltage after conversion from the desired motor speed. Due to the rapid changing movement, only proportional and integration controls are used.

$$Motor\ RPM = (Y - Y_{target}) \times P\ parameter + \int (Y - Y_{target}) dt \times I\ parameter$$

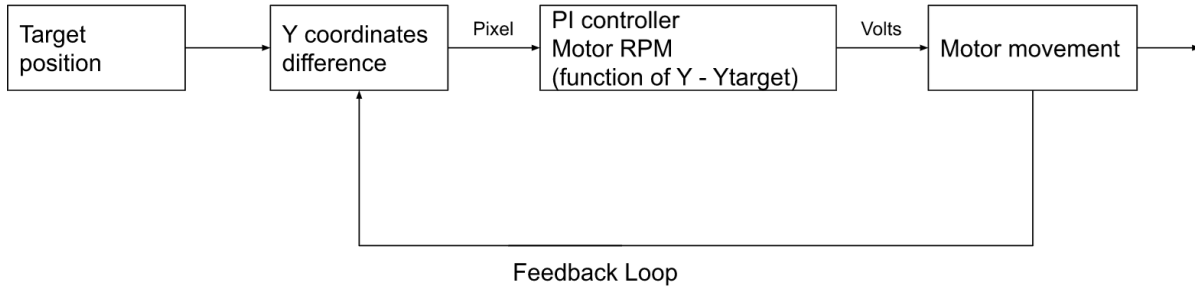


Figure 2.31 Feedback Loop

2.7.3 Communication

TCP protocol are used to communicate. LabVIEW is setup as the client and Flame Tracker is setup as the server. Both program run on the same machine so localhost is the address. In the case where there is combustion, Flame Tracker sends the coordinate of the combustion point. When there isn't a combustion, Flame Tracker sends (-1,-1) to the client. The programs are coded so they can operate independently.

2.7.4 Code structure

The code is programmed so that each function has its own while loop. In proper multithreading. This ensures that every major function is independent and one slow operation does not slow down other critical operation.

2.7.4.1 TCP + PI loop

The main loop of consists of communication with TCP. This loop runs at the frequency of Flame Tracker. It also consists of the PI controller and outputs the desired RPM of the motor. This loop does not contain any utility functions that does not require to be synced to data reading rate to prevent them from slowing down the Flame Tracking and PI controller.

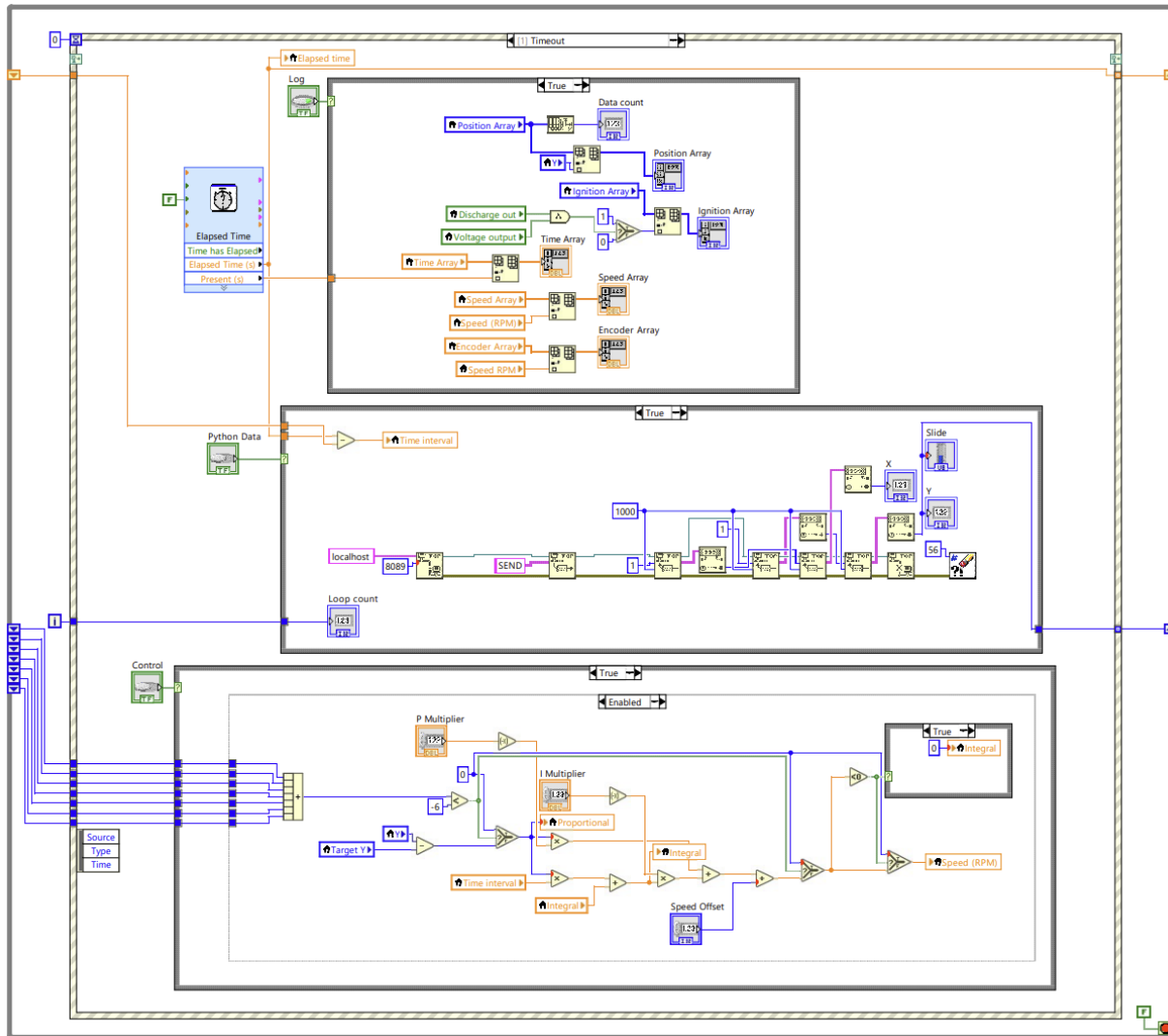


Figure 2.32 LabVIEW PI loop and TCP communication

2.7.4.2 Ignition Detection

The bright spot from ignition is used as the detection of start of combustion. This detection is on a separate loop. The program records the first appearance of brightness as the point of ignition. This point is generally the same position as the tip of the magnesium wire in the combustion chamber. Sparks generated can create instantaneous bright spots that exceed the threshold defined in the flame tracker. To prevent misjudgment, the ignition detection is coded so that only bright spots that lasts over 100 milliseconds are considered ignition. This criterion is sufficient to prevent misjudgment without adding excessive delay to the detection. The controller is only active after ignition has been detected.

2.7.4.3 Encoder output

The motor has a built-in encoder. An encoder is a sensor that helps detect the rotation of a shaft. The driver use this encoder signal to help run at a consistent speed. While the driver has the display of the speed, there is no way to output the speed directly easily. However, the driver outputs 500 pulse for every rotation of the motor shaft. By measuring the frequency of the pulse, the actual rotational speed of the motor can be obtained.

$$\text{Feeding rate} = \text{RPM} \div 60 \div 5 \times (30\text{mm} \times \pi) \quad (2)$$

Equation for the feeding rate

■ エンコーダ出力

エンコーダからは、ASG出力、BSG出力、および ZSG出力の 3 種類の信号が出力されます。

ZSG出力は OUT0 ～ OUT2 のどれかに割り付けないと確認できません。

ASG出力、BSG出力ともに、モーター軸 1 回転あたり 500 パルス出力されます。

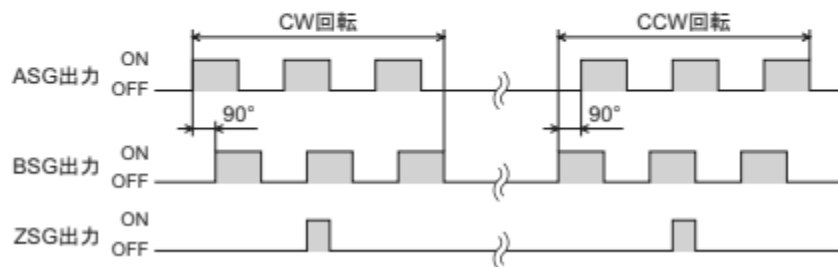


Figure 2.33 Motor driver encoder output

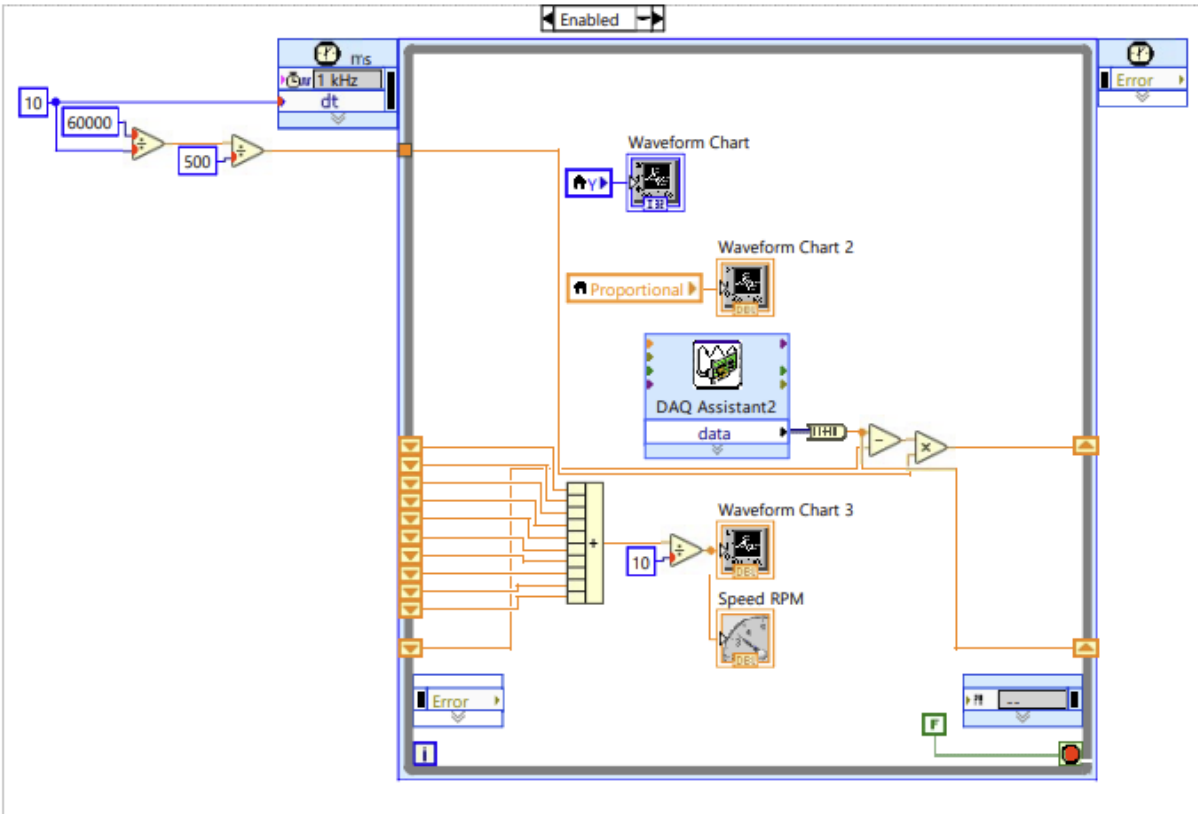


Figure 2.34 Encoder reader

2.7.4.4 Signal output

All of the output signals are handled by a single loop. This is separate from rest of the codes so that any changes to the output is reflected immediately. This also enables ability to override any of the output signals. Ignition circuit is also integrated as part of this loop.

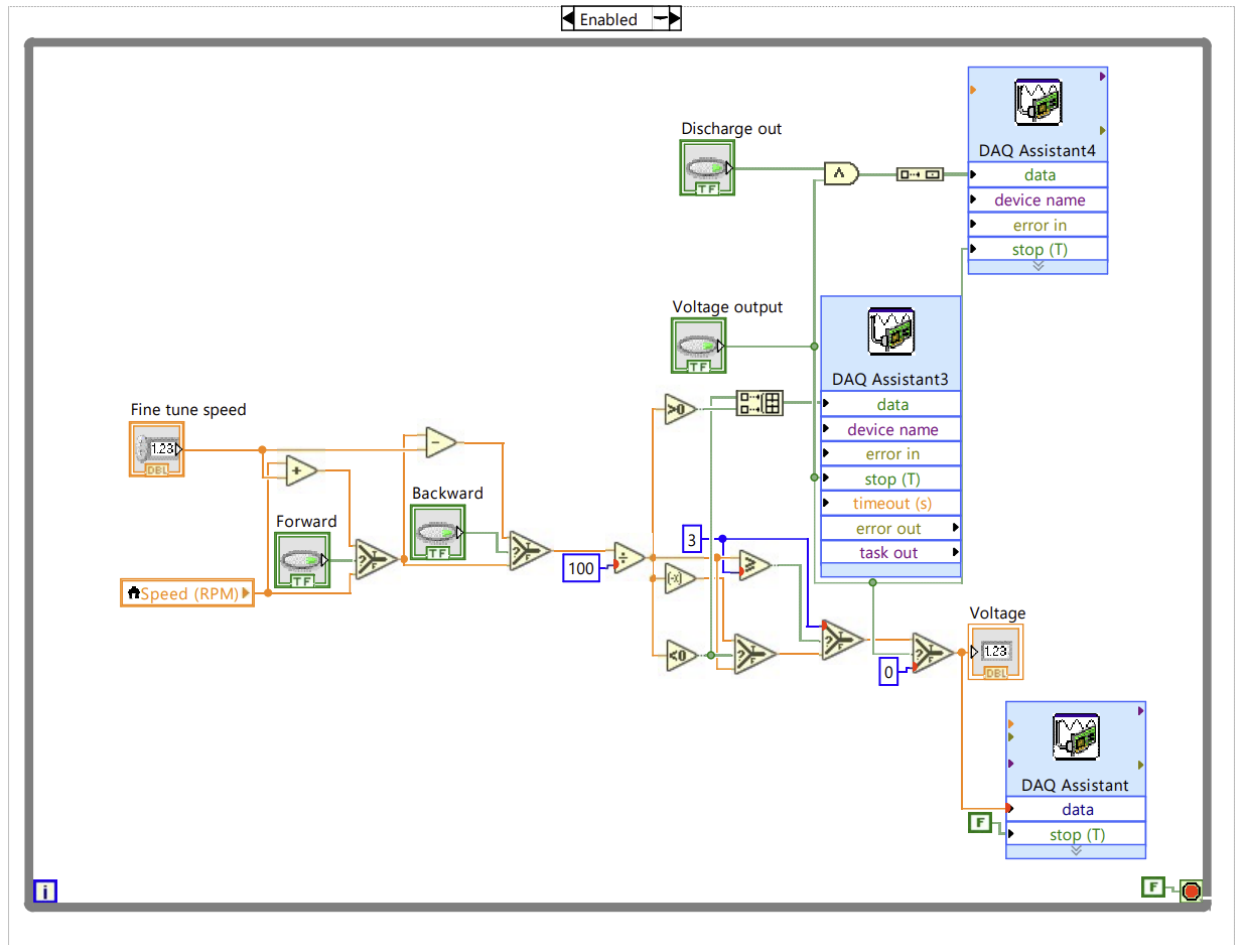


Figure 2.35 LabView output control

2.7.4.5 DAQ

USB 6001 model DAQ from National Instruments is used for the signal inputs and outputs. This is a basic model that has two analog outputs which can output voltage from -10 to 10. One of the analog inputs are used for the motor control. It has 13 digital inputs/outputs with one of them capable of working as counter. This counter is used for the encoder. Digital outputs output 3.3 V signals.

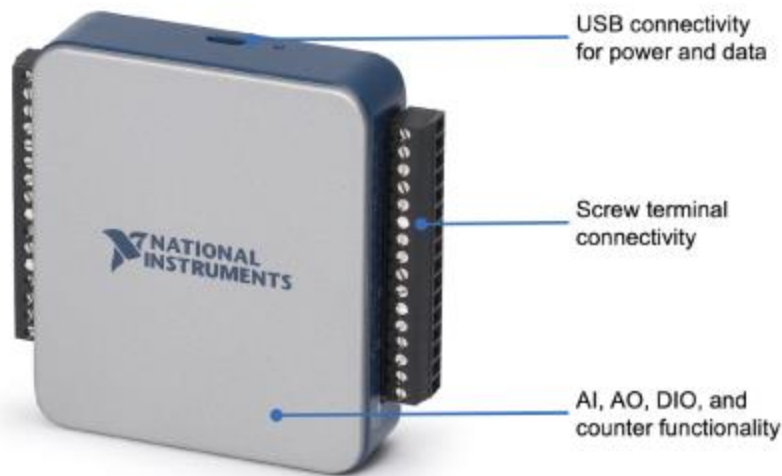


Figure 2.36 USB 6001 DAQ¹⁵

2.7.4.6 Simulation

A python based simple combustion point simulation was used to test out the control program. The simulation simulates the combustion point by rendering a white dot that rises at a constant rate to simulate combustion. Output from the LabVIEW control controls the falling rate of the white dot. This simulation showed the control works and help determine the PI parameters that can be used.

2.7.4.7 Optimizations

Unlike the simulation, the real combustion does not behave consistently. The brightness of combustion can change over one combustion. Because the control program is setup to stop automatically on extinguishment, optimizations were required to prevent feeder from sudden change in feeding rate due to changing luminance. This codes ensures the integral part of the decays during the 6 frames after disappearance of flame. This translates to approximately 200 milliseconds.

The feeder is also set only feed wire in one direction. Because the control system's main purpose is to counter the movement of combustion point from the process of combustion, it is unnecessary to pull out wires from the combustion chamber during a combustion. In the

programming, any negative RPM values PI controller calculates is reset to 0. This is unlike a conventional PI controller. This is an effective way to prevent wires from leaving the wire guide.

Because of the residue generated during the combustion. The target combustion point is set at a small distance above the discharge electrode. Figure 4.37 illustrates the difference. Ignition point refer to the tip of the wire that is ignited first, target point refer to the location This helps prevent residue build up at a location too close to the electrode. On the LabVIEW interface, the target is set to be 70 pixels above the ignition point, it translates to about 2 cm in real world. This is a value found after multiple trail and errors. It is closer to the wire guide, so the wire is less likely to drift but far enough away so that wire does not burn too close to the guide.

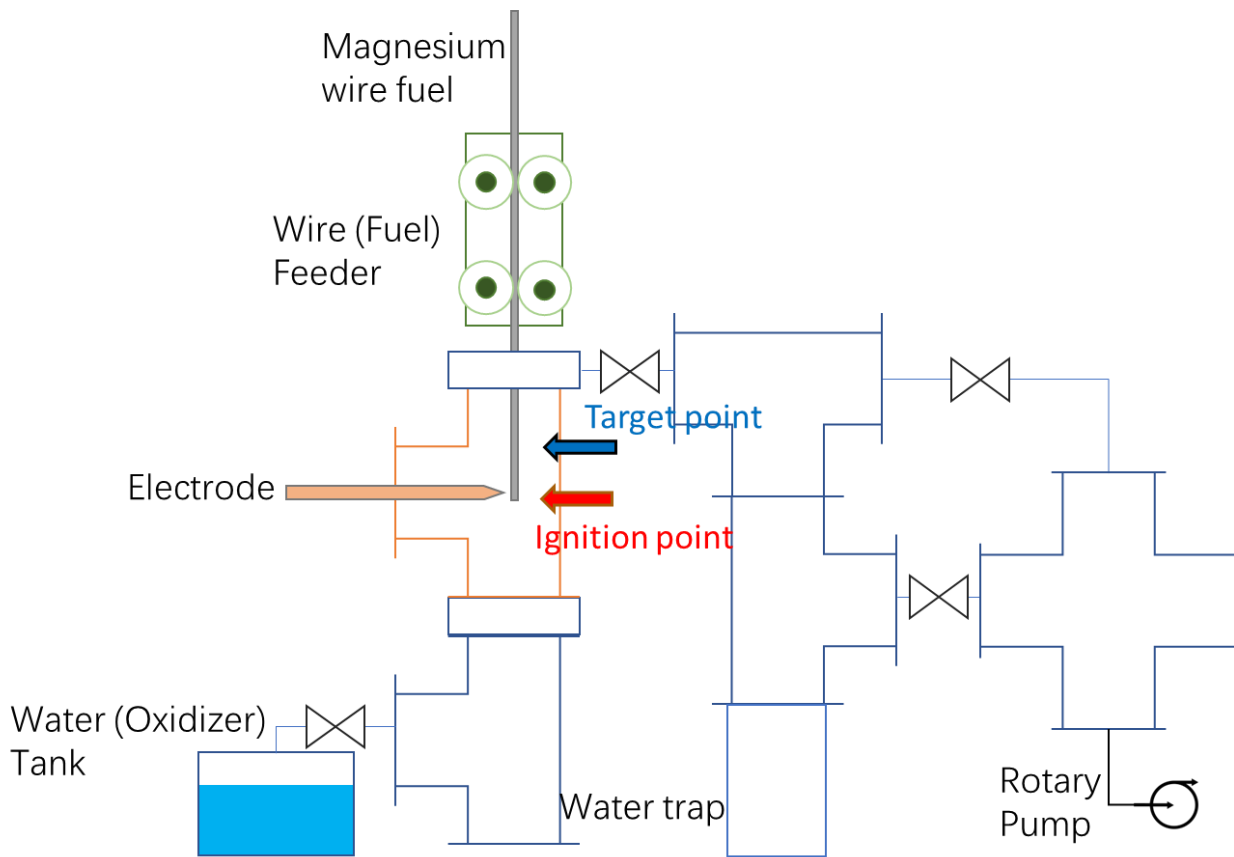


Figure 2.37 Target and Ignition point

2.7.4.8 Potential Improvements

Currently the web camera only reads Red, Green, and Blue. It is possible that there are wavelengths that can produce an image that is better than what the current camera is capable of. Perhaps the use of filters can help enhance the accuracy of the combustion point prediction.

Under different combustion conditions, the brightness of the combustion varies. A potential mechanism to automatically apply an ND filter could be useful to help prevent overexposure.

2.8 Water supply

Water tank is one reused from previous study. This water tank has a built in heater which helps maintaining the temperature of the water at a consistent temperature. The tank has a leak valve, a pressure sensor. The heated water vapor leaves the tank through a 1/2 inch tube.

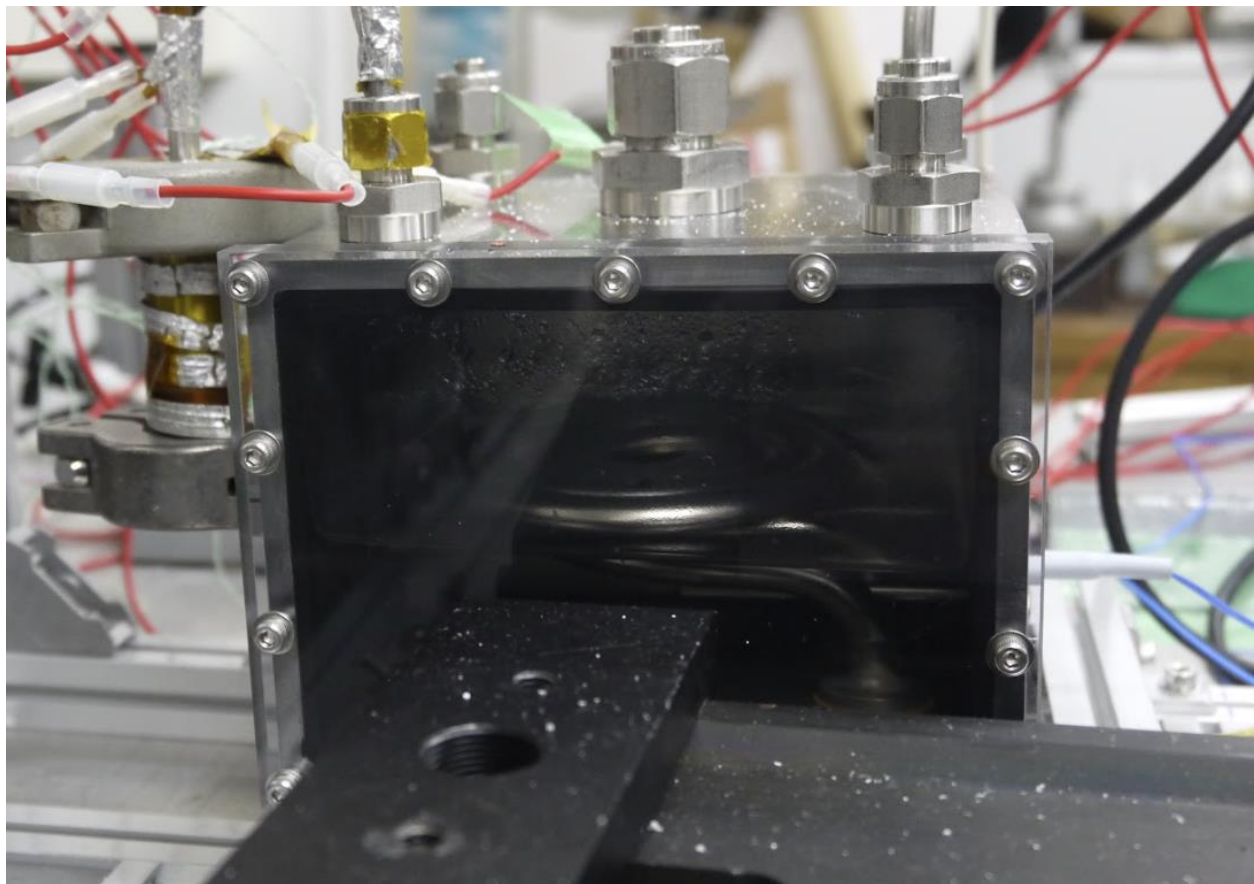


Figure 2.38 Water Tank

The gas flow path is shown below. Without any combustion, the water flows from the bottom of the combustion chamber as shown in figure 2.39. The water then leaves through the top flow path.

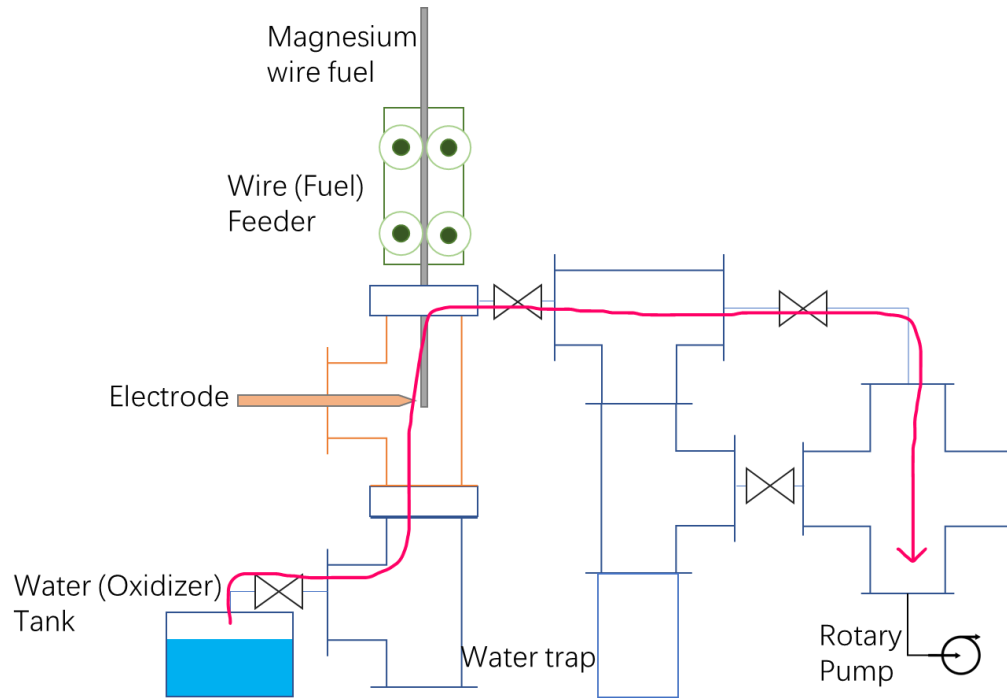


Figure 2.39 Water vapor flow path

2.9 Orifice

To limit the flow rate and flow velocity in the combustion chamber, an orifice is used downstream of the combustion chamber. The orifice is located at the location marked below.

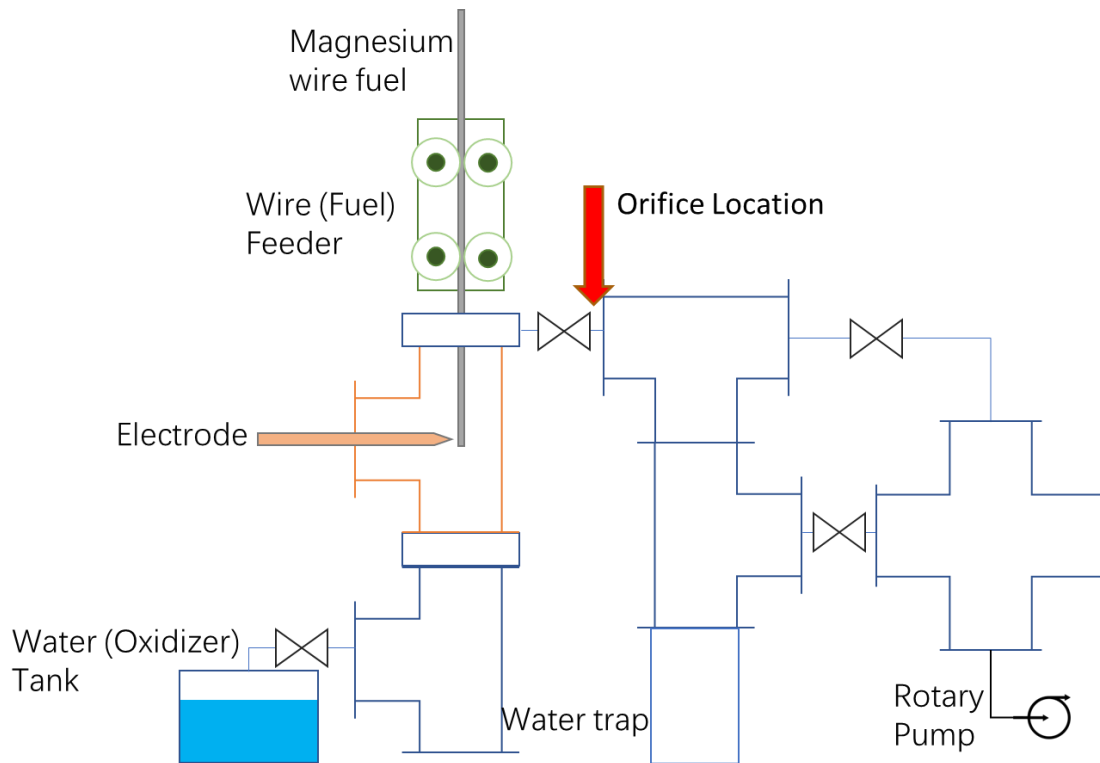


Figure 2.40 Orifice location

In prior studies, orifice of diameter from 0.5 mm to 2 mm were used to test out combustion condition. In this study, only 1 mm orifice is used as varying flowrate based on the orifice is not necessary.

Orifice is drilled onto a thin aluminum plate first. It is then attached an insert with Kapton tape. Any adhesive works and the use of Kapton tape does not have an impact. Figure 2.42 shows the insert with orifice plate attached.



Figure 2.41 1 mm orifice plate

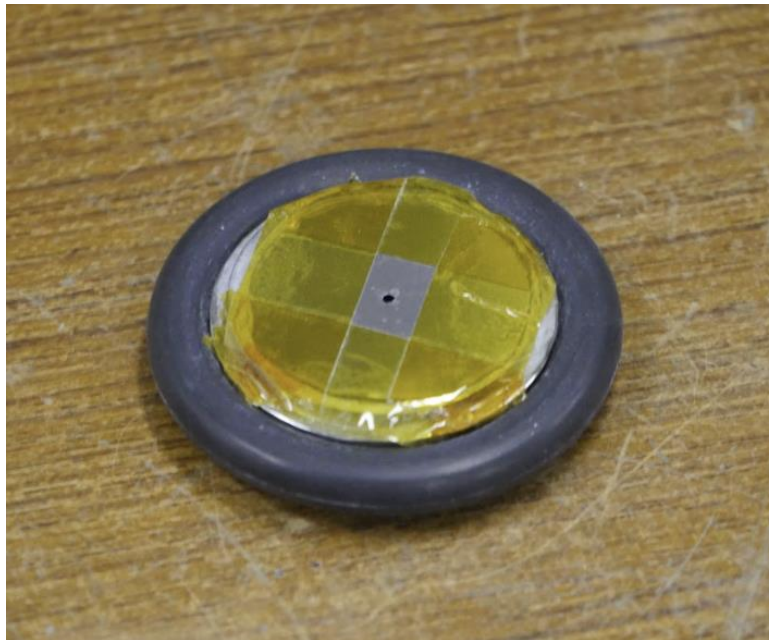


Figure 2.42 Orifice clean

The two figures below show the orifice after each combustion. Residues can get trapped on the surface of the insert. However, these residue do not obstruct the flow path. This part is cleaned after each experiment.



Figure 2.43 Orifice upstream side



Figure 2.44 Orifice downstream side

2.10 Efficiency Measurement

2.10.1 Overview

A system to measure the combustion efficiency of fuel was developed. It is a chemical based measuring system. Part of the samples that need to be measured reacts with the solution. The gas generation from the reaction are used to the validation process suggests the system has the following relationship.

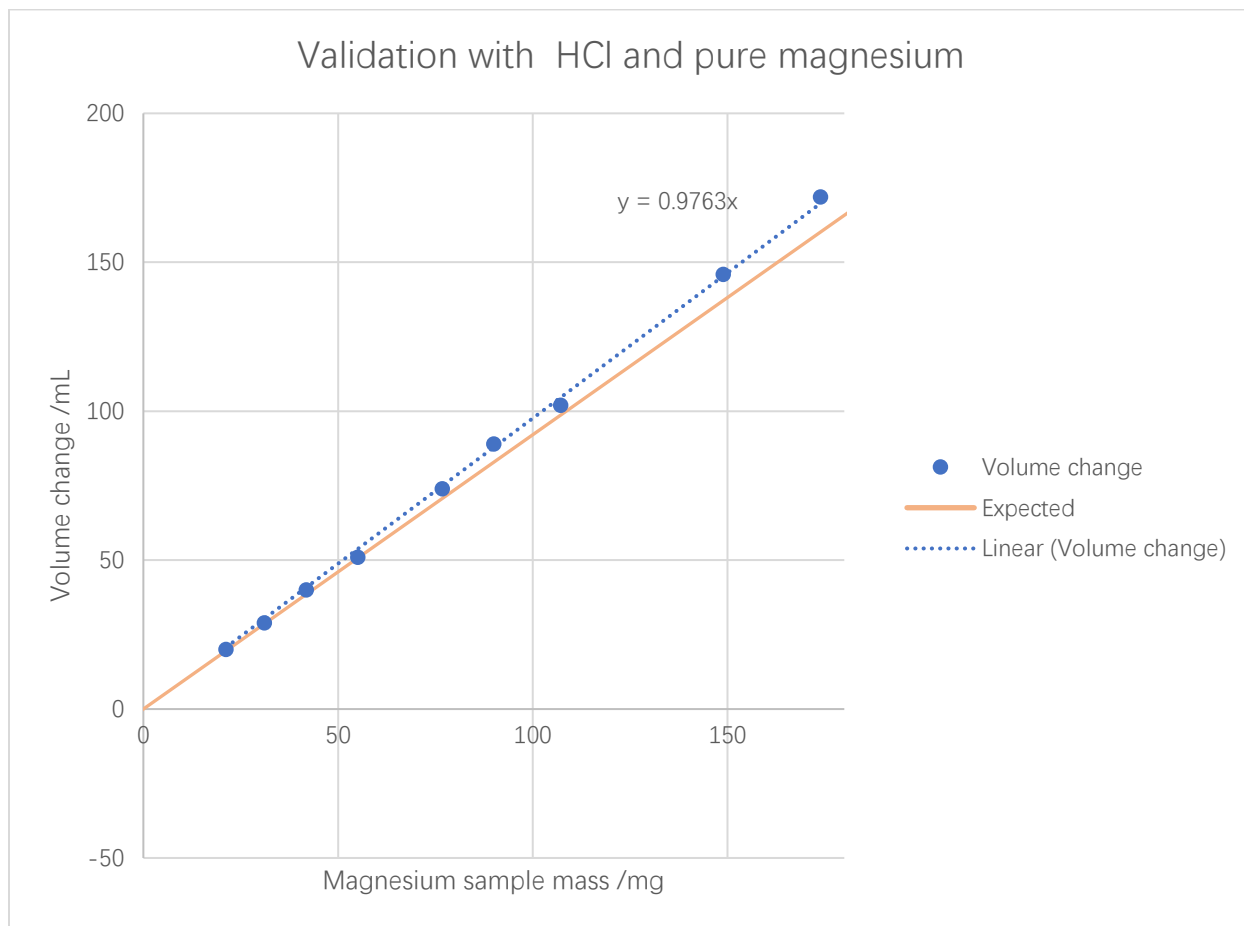
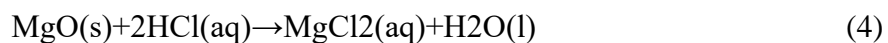
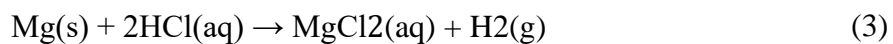


Figure 2.45 Mg measurement system, Pure Mg Calibration

The system is a combination of hydrogen generator and eudiometer. Magnesium, when reacted with HCl, generate Hydrogen gas and MgCl_2 . MgO , the bi-product from the combustion, reacts with HCl and does not form any gas. The following formulas show the relationships that were used.



By measuring the gas generated, knowing the molar mass of magnesium, hydrogen, the amount of pure magnesium reacted can be calculated.

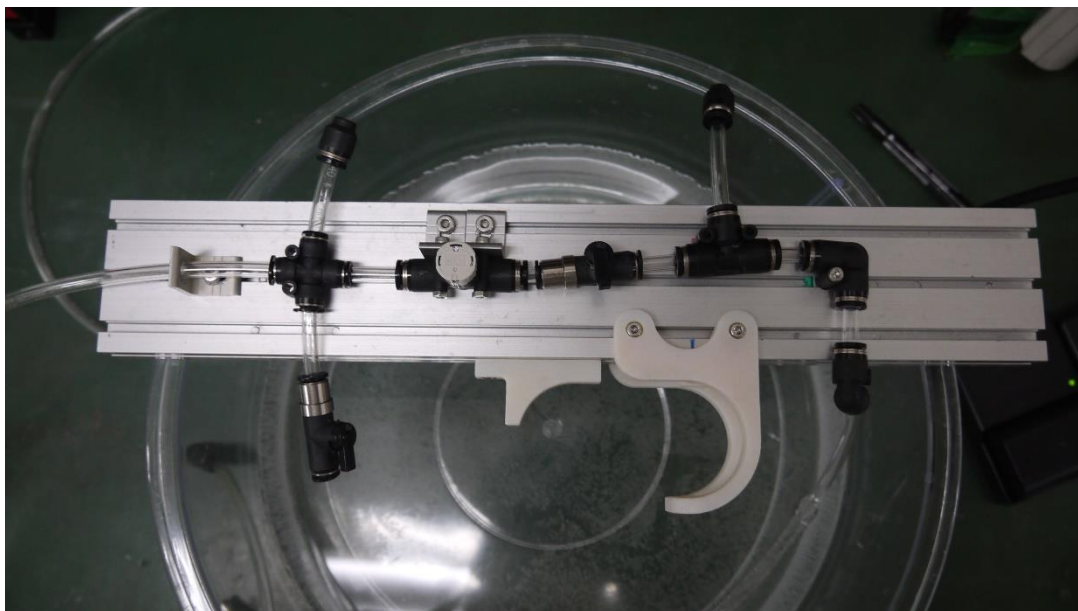


Figure 2.46 Fuel efficiency measurement system

2.10.2 Device setup

The setup consists of a container for reaction, 2 mol/L HCl solution and a cylinder for the collection of hydrogen. 2 pressure sensors are only used during validation.

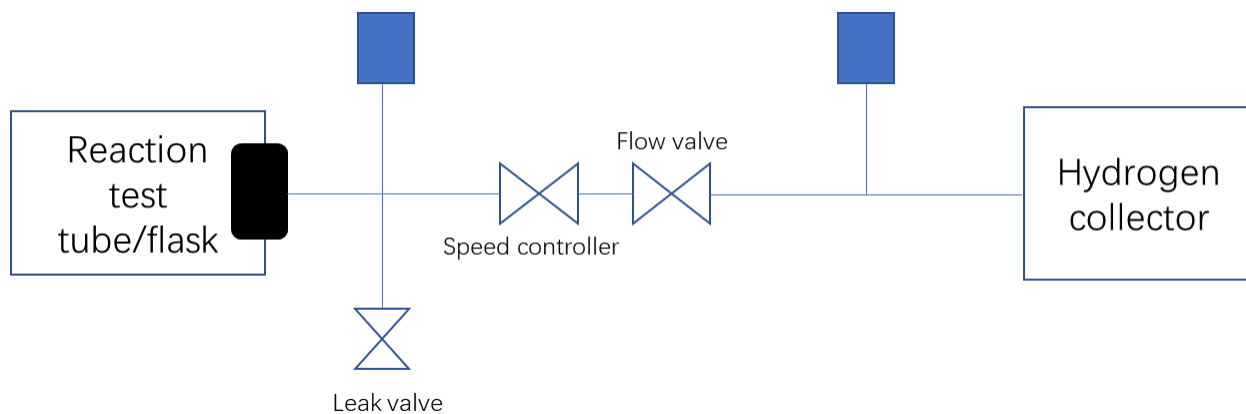


Figure 2.47 Fuel efficiency system

2.10.3 Assumption

The successful measurement assumes the following conditions.

- Constant Pressure and temperature.

Some amount of gas exist in the system before any actual measurements. This gas can subject to expansion and contraction from changes in the gas temperature. Such change will result in in accurate measurements. The temperature change can come from simple interaction such as touching the reaction flask

- No other gas generated.

It is essential that hydrogen generated from reaction with pure magnesium is the only gas generated during the measurement. In practice small amounts of HCl acid and water vapor may contribute to the change in volume.

- Sample consists of only magnesium and magnesium oxide.

This is necessary and expected as only magnesium and water vapor should react. Any other reaction would indicate impurity in the fuel or oxidizer.

2.10.4 Cylinder

The measurement system is tested with two cylinders. A 10 mL one and a 200 mL one.

Which cylinder is appropriate is dependent on the amount of pure magnesium expected.

200 mL cylinder has a measurement error of 2 mL and the 10 mL cylinder has a measurement error of 0.2 mL.

2.10.5 Expected Value

Hydrogen per mass of pure magnesium sample can be calculated. 1 mol of Magnesium can generate 1 mol of Hydrogen gas based on the reaction. Knowing that molar mass of Magnesium is 24.305 grams and that 1 mol of any gas at standard temperature and pressure is 22.4L

mL of hydrogen produced per mg of aluminum: $22.4/24.305 = 0.921$ mL/mg

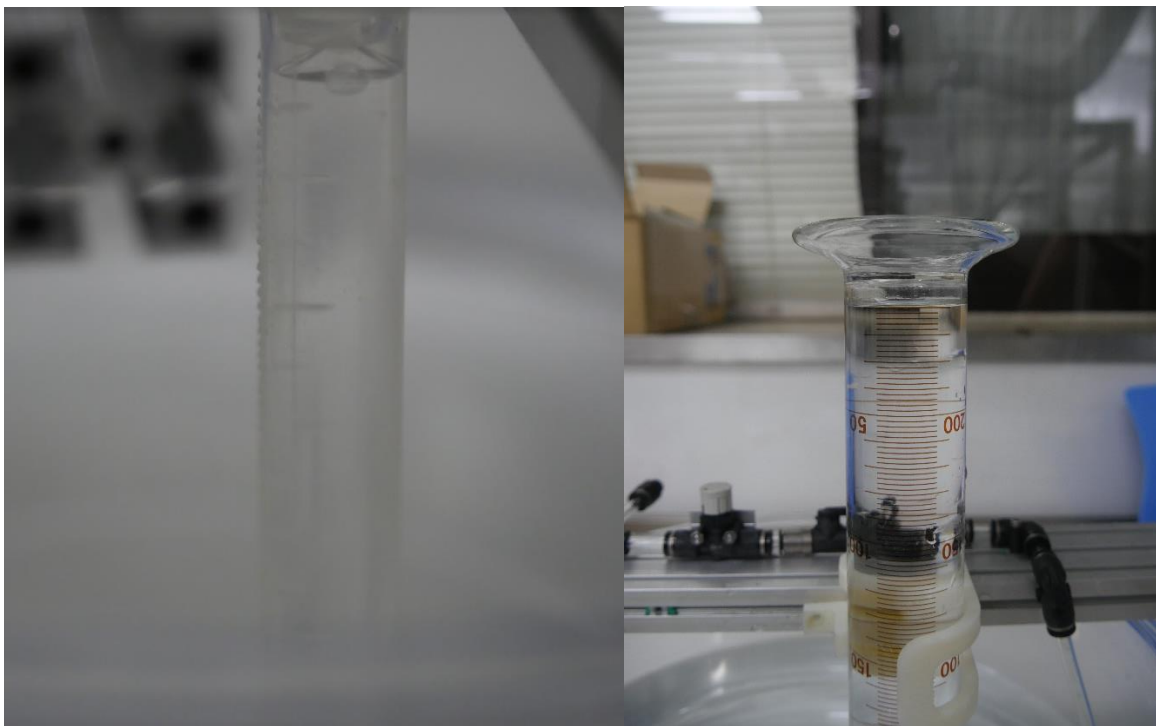


Figure 2.48 Cylinder 10mL (left) 200 ml (right)

2.10.6 Error assessment

In larger sample and Mg contents, deviation from calculated is more significant than the measurement error.

In smaller sample and Mg contents, the deviation from the calculated is less significant than the measurement error.

2.10.7 Deviation cause

The hydrogen generation deviates from the calculated value by 6%

Water vapor from the heat generated during reaction can contribute to the extra volume.

Hydrochloric acid exists as a gas that can be released from the solution. The exhaust gas of the system was found to be acidic. Hydrochloric acid release can be contributing to the volume change.



Figure 2.49 pH test paper showing acidic exhaust

2.10.8 Cooling bath

Cooling bath were used during testing of this system to eliminate effect from temperature.

Minimal improvements were found. Cooling bath is therefore determined to be unnecessary.

Figure 2.50 shows the setup that was used. Reaction chamber is submerged in water at 5 degrees Celsius with an environmental temperature of 20 degrees Celsius. A thermal camera was used to find the temperature of the test setup. The result of which is shown in figure 2.51

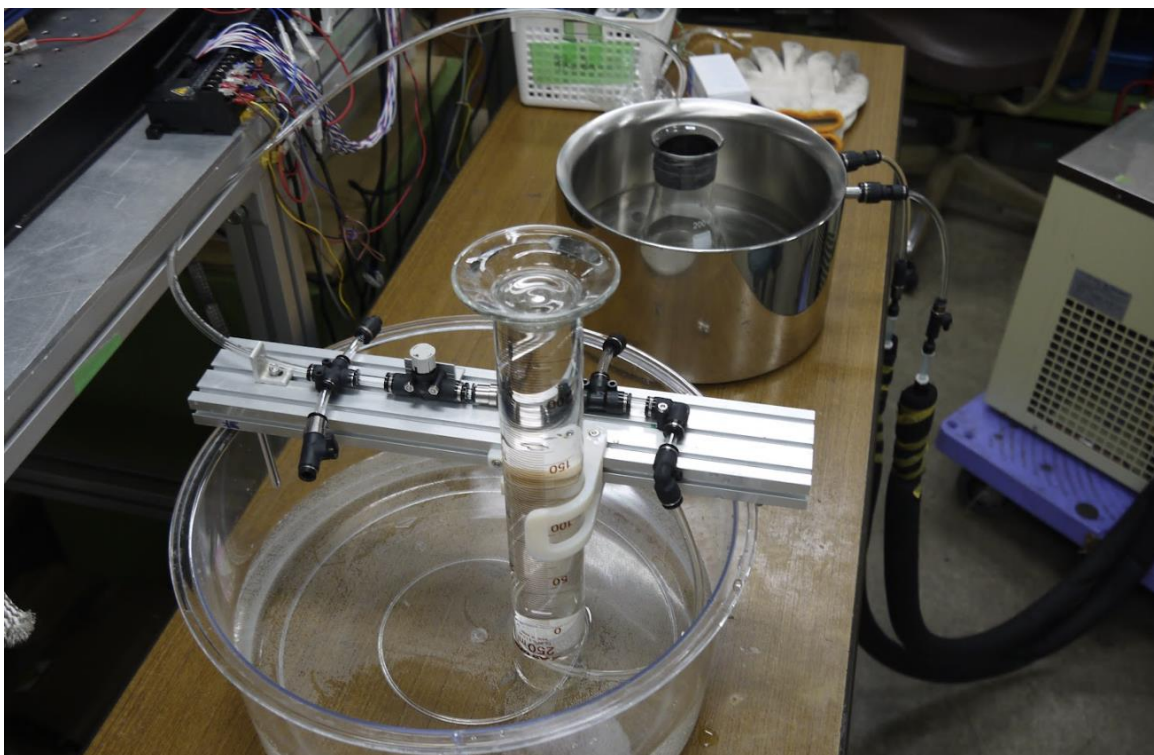


Figure 2.50 Mg measurement with cooling bath

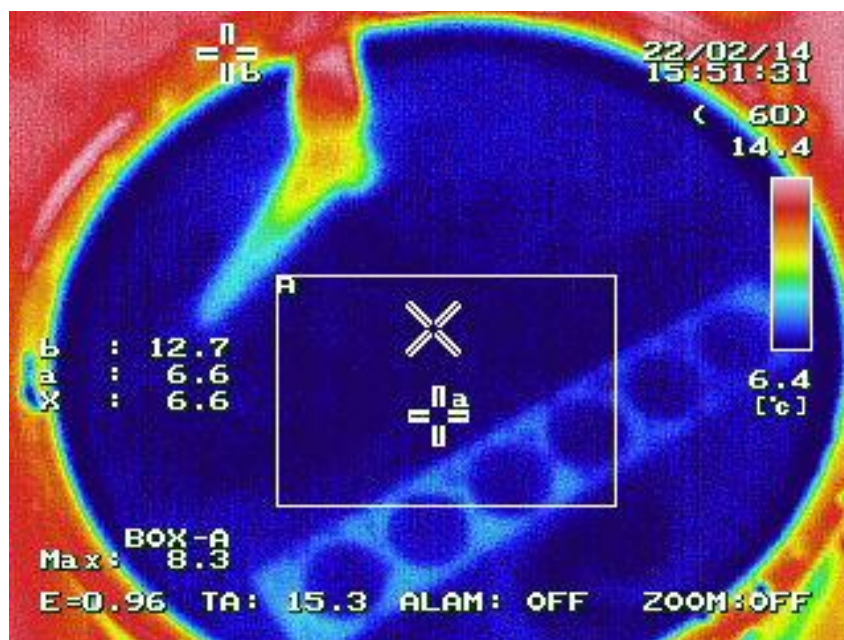


Figure 2.51 Thermal imaging of cooling bath

2.10.9 Compatibility

This system was originally designed and built for both magnesium wire-based combustion and aluminum powder based combustion results. Validation for aluminum powder was also conducted and the result values had minimal deviation from the calculated expected values.

2.11 Safety

Hydrogen is flammable and potentially explosive. Measures are taken for safety.

A draft chamber was used in all efficiency measurement to remove hydrogen from the laboratory.

Combustion gas downstream of the combustion chamber is mixed with air to reduce the concentration of hydrogen.

2.12 BBM Thruster Design

The proof of concept was a platform to achieve a combustion. However, it was insufficient to quantify data. Temperature within the combustion chamber couldn't be measured due to constraints presented by the glass chamber. The fragile chamber also wasn't suited to test out different water vapor flow direction configurations and combustion orientation.

A new BBM thruster is designed based on experiences from the proof of concepts.

This thruster is designed to produce thrust. The experiment setup used so far has been a proof of concept, a test bunch that observes the various phenomena in magnesium wire combustion with water. The setup is not capable of producing thrust in the traditional sense. Additionally, there are data that couldn't be collected. This BBM thruster hopes to help collect these missing data.

2.12.1 Concept

Mechanism designed for current experiment setup is reused in this design. The Thruster consists of a combustion chamber, water supply system, magnesium wire supply system, ignition circuit just like the current test bunch setup. A nozzle is designed. To accommodate for the nozzle, the thruster is designed to directly attached to a vacuum chamber through a flange. The thruster itself is designed to be in atmosphere to accommodate for the water supply system and wire feeding system.

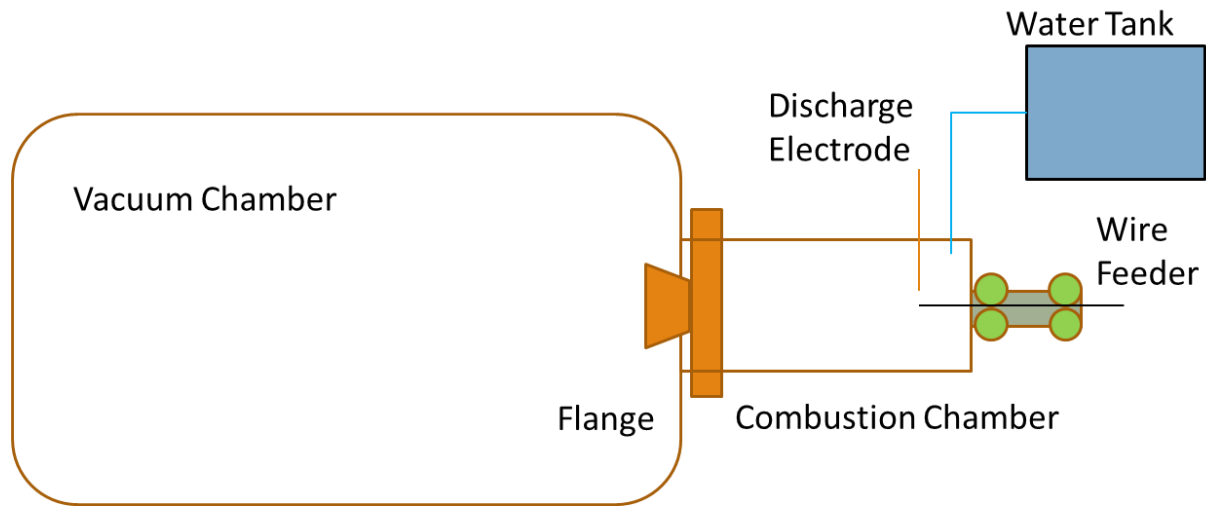


Figure 2.52 BBM Model concept

The final thruster design with the wire feeder attached resemble the model in the figure 2.53 shown below.

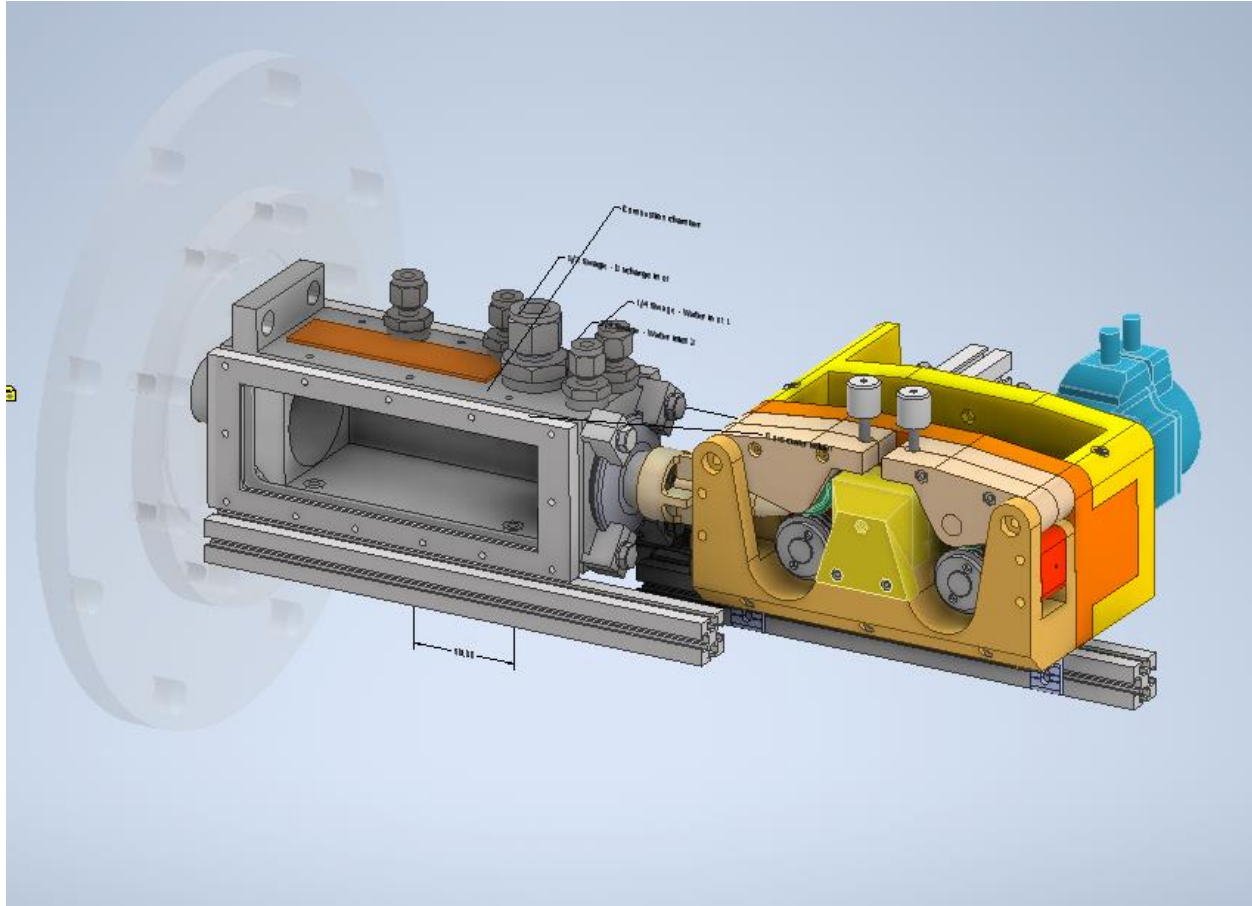


Figure 2.53 Thruster illustration

2.12.2 Combustion chamber

The combustion chamber is designed based on the specification of the current combustion chamber. The combustion chamber needs to satisfy a few requirements. First, visualization of the combustion is necessary, both for data collection and control system. Second, ports are required on the combustion chamber to allow for sensors that was previously impossible to implement.

While a cylindrical chamber is desirable, it can't be manufactured with glass while satisfying all of the requirements. A rectangular combustion chamber enables the installation of windows and ports.

The diameter of the NW40 nipples that is used is 39 mm, the cross section of the new chamber is 40 mm by 50 mm. The effective cross-sectional area can be further reduced by inserting extra

glass panels. To ensure enough length is available for the wire combustion, the length of the combustion chamber is designed to be 150 mm.

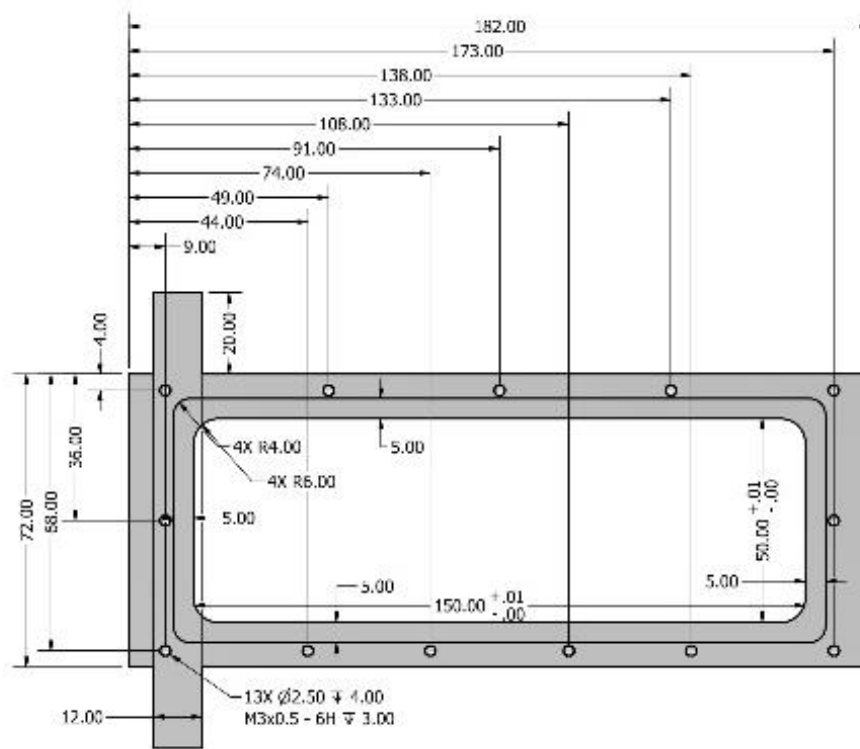


Figure 2.54 Combustion chamber dimensions

2.12.3 Sensor ports

This new thruster is designed to measure temperature in finer details. A temperature gradient likely exist in the combustion chamber. The symmetric distribution of thermal couples enables a better understanding of the temperature distribution during a combustion. Additionally, these ports are located off the center to prevent interference with the combustion itself.

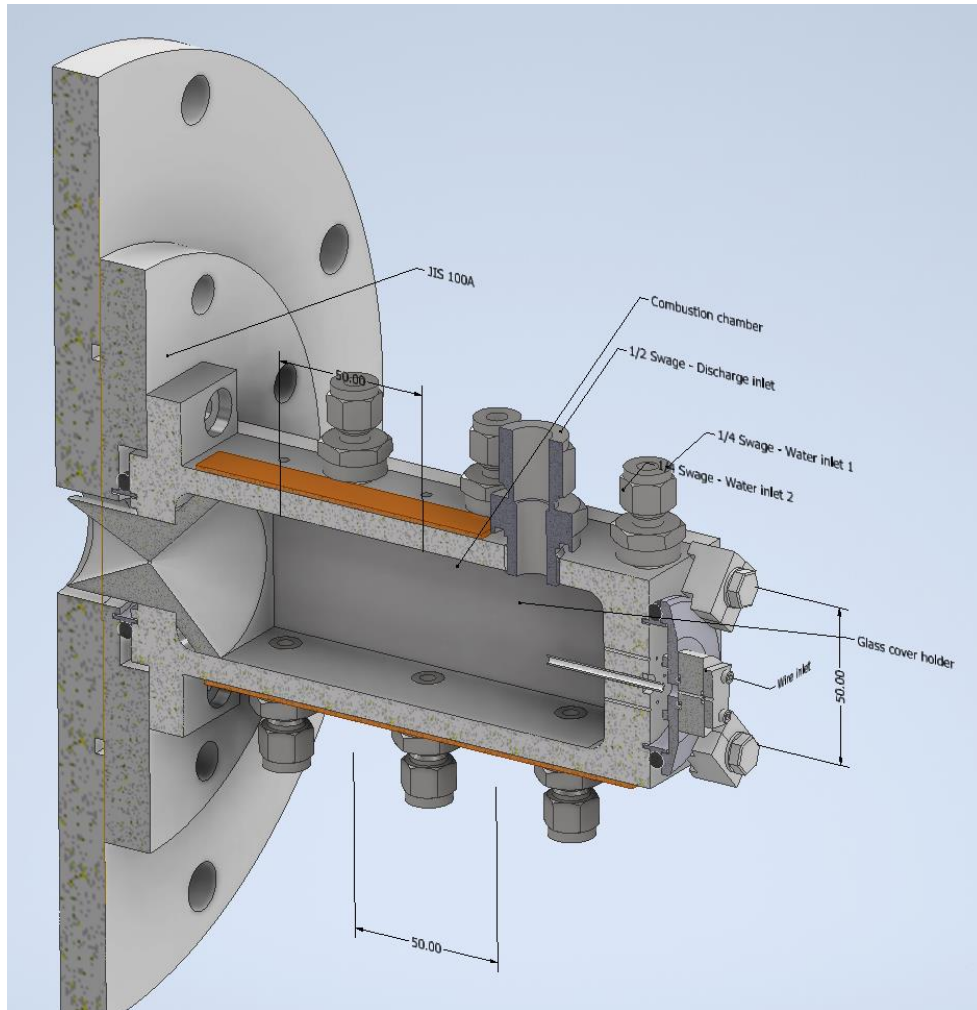


Figure 2.55 Cross Section

2.12.4 Discharge electrode

Discharge electrode is placed closer to the wire guide. In a horizontal configuration, the electrode is positioned on top of the wire. This helps with the issue of residue as the gravity will keep the residue away from any obstacle. This port uses the same Swagelok 1/2 adapter current experiment setup uses.

2.12.5 Wire inlet and guide

The wire inlet uses the same design as current experiment setup. The wire guide is changed to a shorter tube instead of a ring. This resolves the issue of loose wire guide. Shorter wire guide also reduces the chance of breaking.

2.12.6 Nozzle design

Figure 2.56 shows the nozzle cross section. The nozzle size is currently limited by the combustion chamber size. This is a temporary nozzle to help calibrate the new thruster design into working order. The inlet converges gas from the rectangular cross section of the combustion chamber. Some stagnation may occur. The nozzle is designed with a 25 degree angle. This angle is chosen to help extend the nozzle as far as possible into the vacuum chamber. The throat of this nozzle has a diameter of 1 mm. Mass flow rate of this nozzle should be the same as current setup.

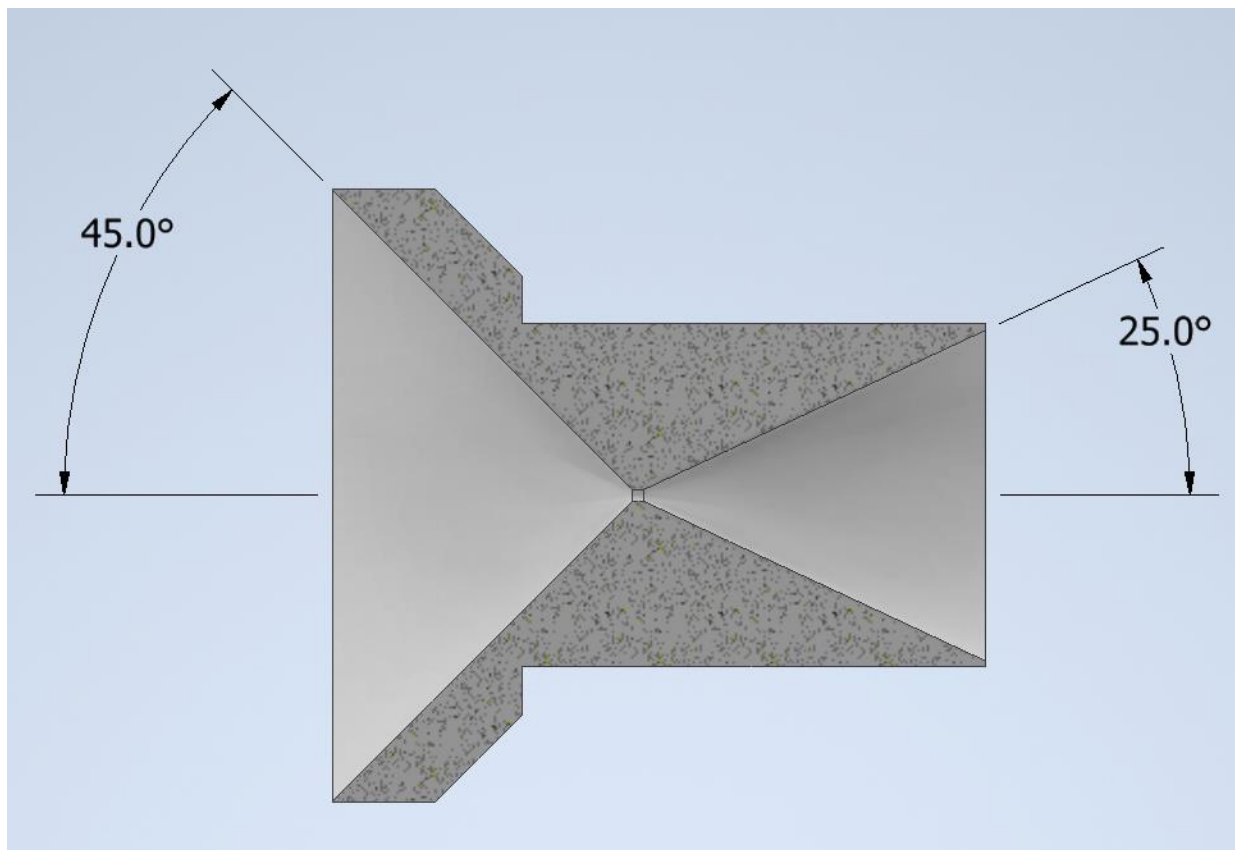


Figure 2.56 Nozzle cross section

2.12.7 Valve

Unlike the current experiment setup, the BBM thruster does not have any valve downstream. In prior study, the research concluded that ignition while oxidizer is flowing is difficult. This study however found that such ignition is possible at low pressure conditions.

2.12.8 Residue

This study ignores the effect of residue within the system. In this BBM thruster, residues are expected to remain in the combustion chamber during each combustion.

2.12.9 Water flow direction

Water in this thruster is designed to flow in the same direction as wire feeding direction. Ports on the side walls of the combustion also optionally can act as a water vapor inlet. This should be able to verify the effect of flow direction on the combustion.

2.12.10 Compatibility

This thruster is fully designed to be compatible with current experiment setup. This helps with easily verifying the performance with existing data.

2.13 Initial BBM Thruster testing

2.13.1 Parts

All parts are manufactured with stainless steel and with a tolerance of 0.1 mm at touching surfaces. Nozzle is attached with bolts as shown in figure 2.57. Gap between the nozzle and combustion chamber shown in figure 2.58 is not sealed. Measures should be taken in future studies if there is a significant leak at the location.

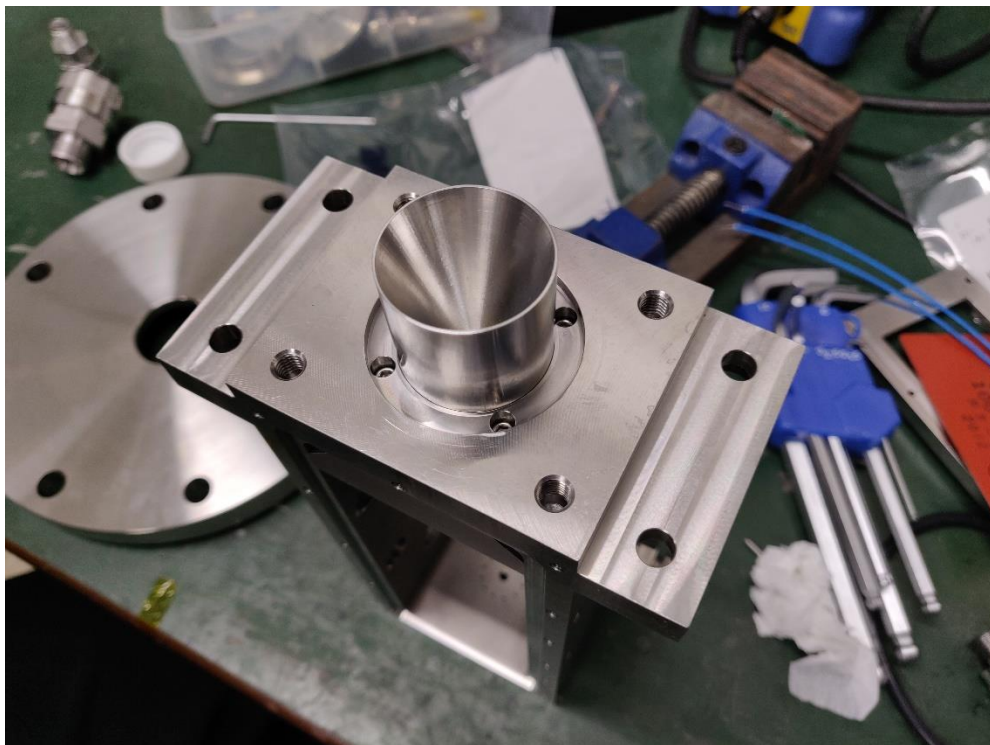


Figure 2.57 Attached Nozzle

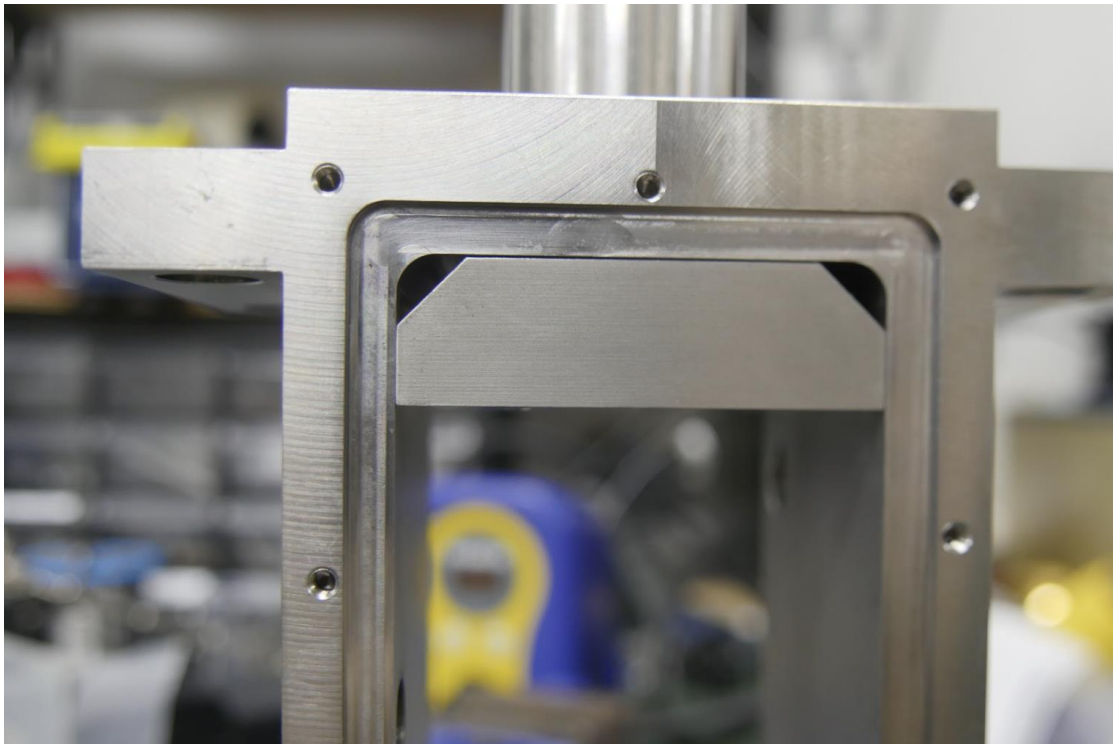


Figure 2.58 Nozzle

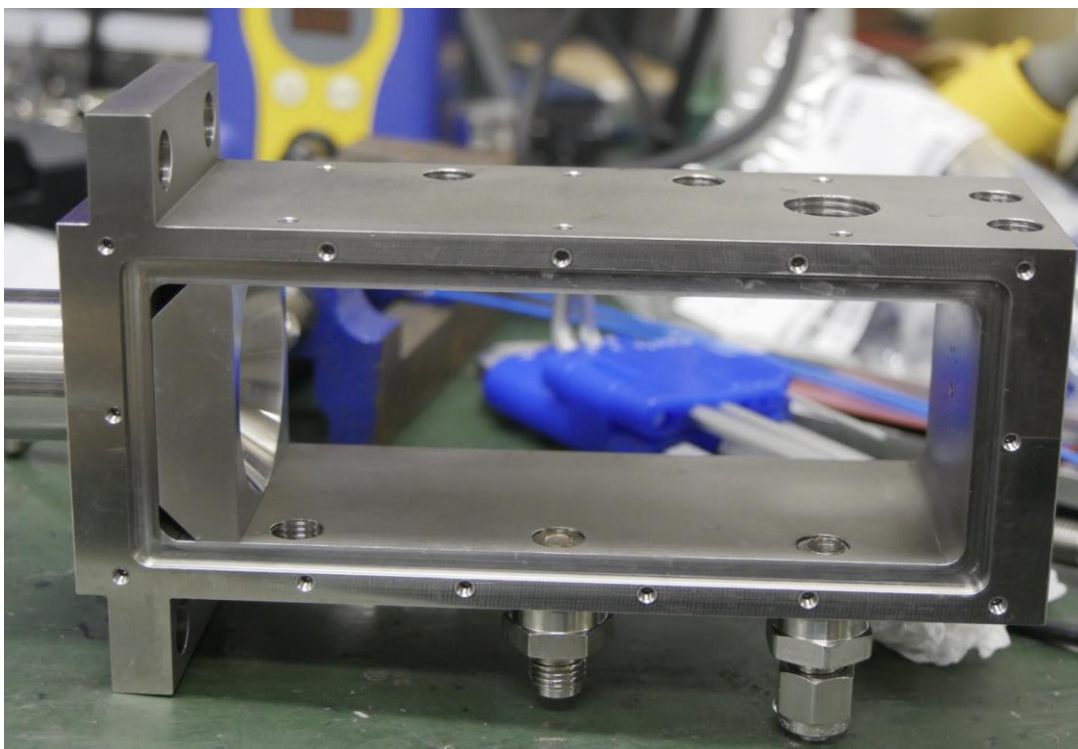


Figure 2.59 Combustion chamber



Figure 2.60 Quartz glass

2.13.2 Setup

For this study, the chamber is assembled to NW40 pipes for testing. The chamber is connected as the figure below. A viewport is installed downstream of the nozzle to observe any generation of residue past the nozzle shown in figure 2.62. Wire feeder is upstream of the oxidizer inlet, on the right side of the combustion chamber in figure 2.61.

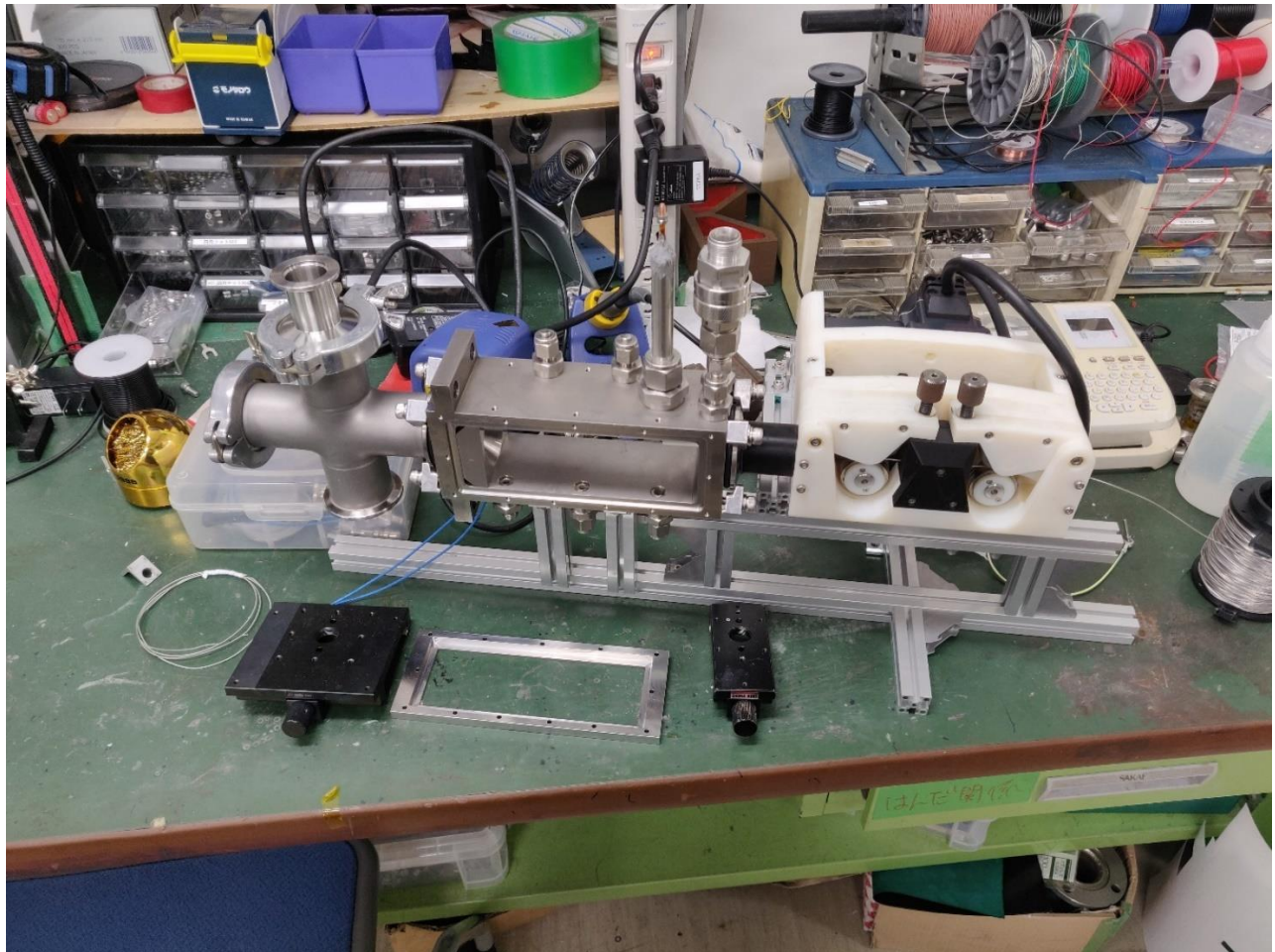


Figure 2.61 System overview

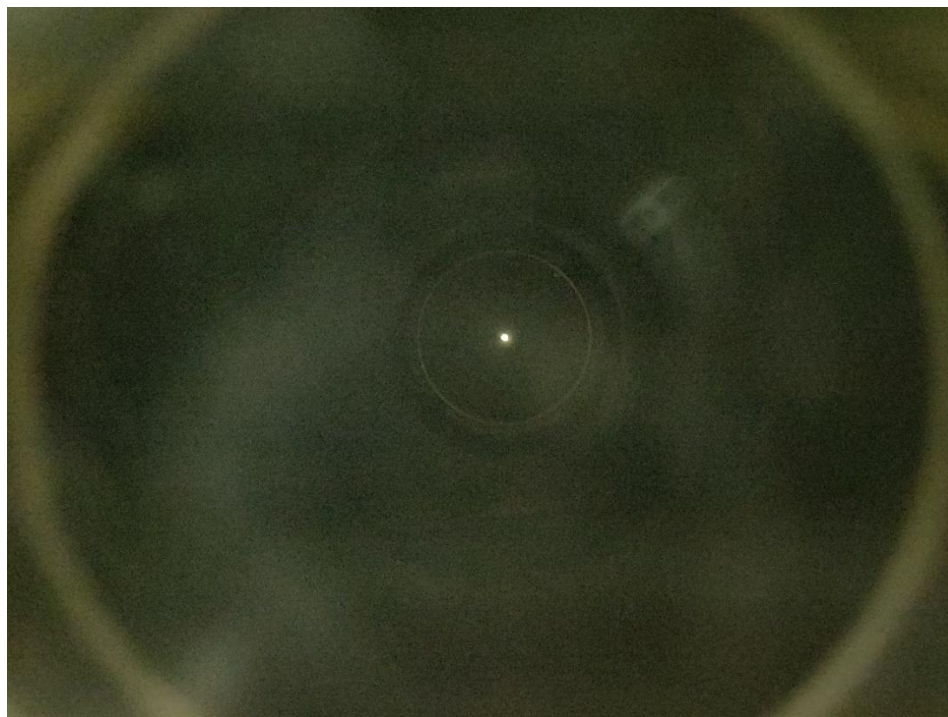


Figure 2.62 Nozzle from viewport

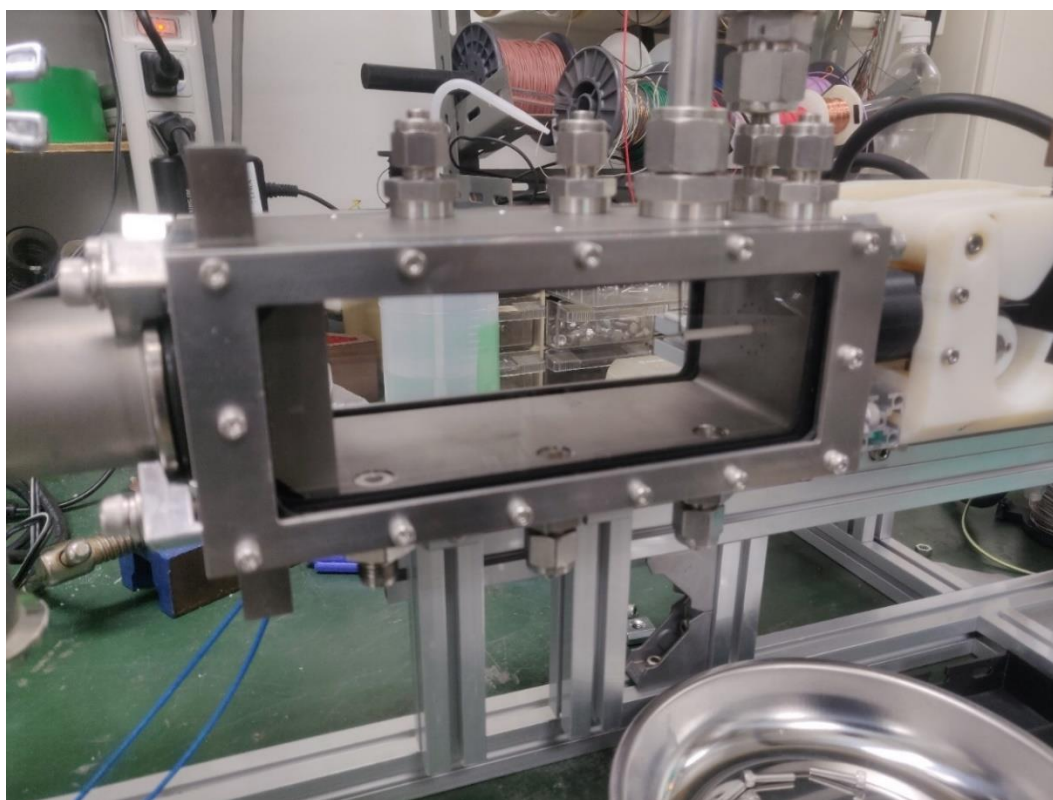


Figure 2.63 Installed combustion chamber

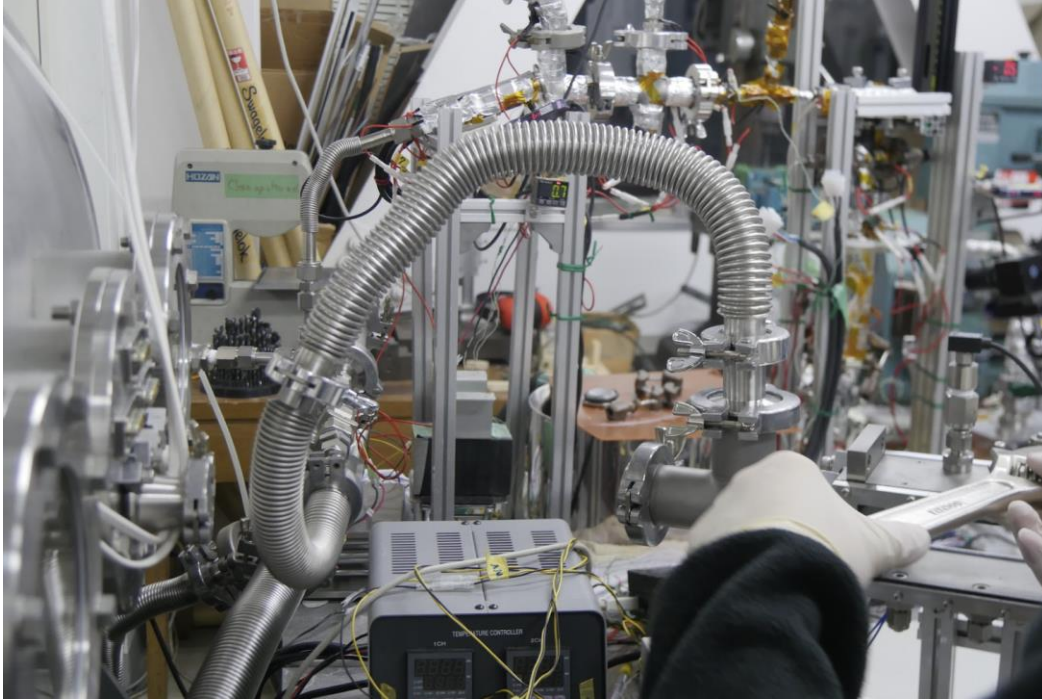


Figure 2.64 Vacuum system connections

Downstream of the chamber, the same vacuum system is connected. The system is shared with the other experiment system, but this doesn't affect the performance in any meaningful way.

Guide is replaced with a ceramic tube version that does not affect the discharge, shown extending from the left in figure 2.65.

To prevent discharge between the combustion chamber wall and the electrode. A ceramic tube cover was used in some of the experiments, visible in the figure 2.66. A longer tungsten wire was also used to adjust the position of the ignition during the initial testing, shown in the same figure.

Wire feeding system is applied to the BBM thruster as well. To accommodate the horizontal configuration, the camera used for tracking is rotated 90 degrees so that relative to the camera, the wire is fed downwards. The sequence of the combustion in the result section is rotated to have the same orientation as real-world thruster configuration.

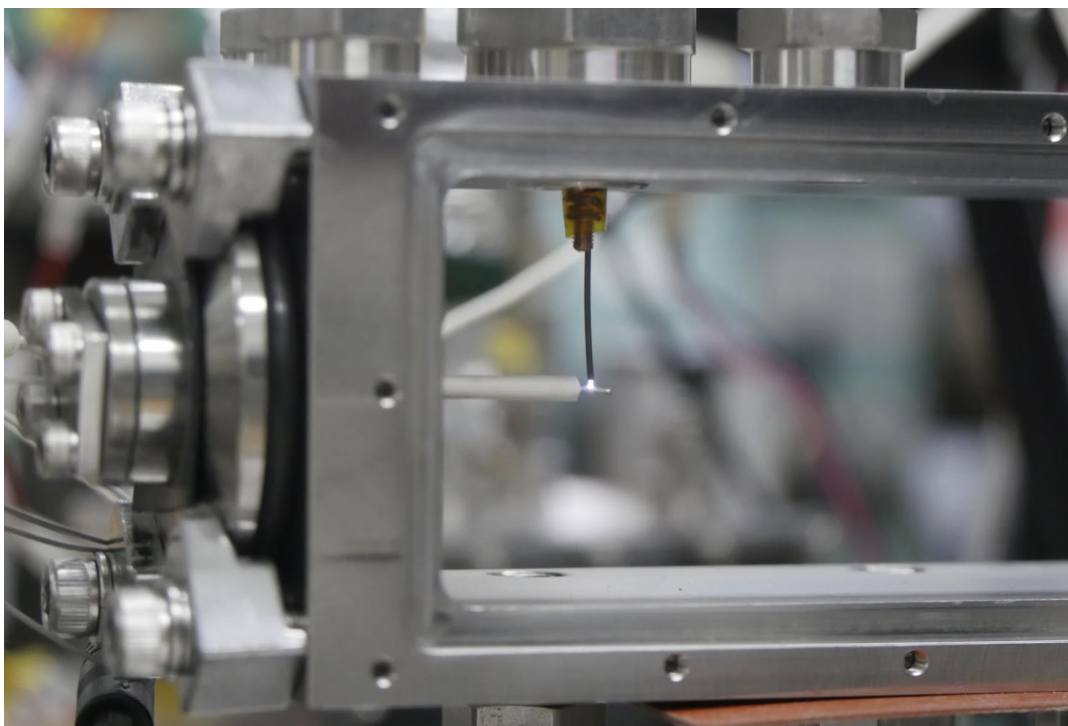


Figure 2.65 discharge confirmation

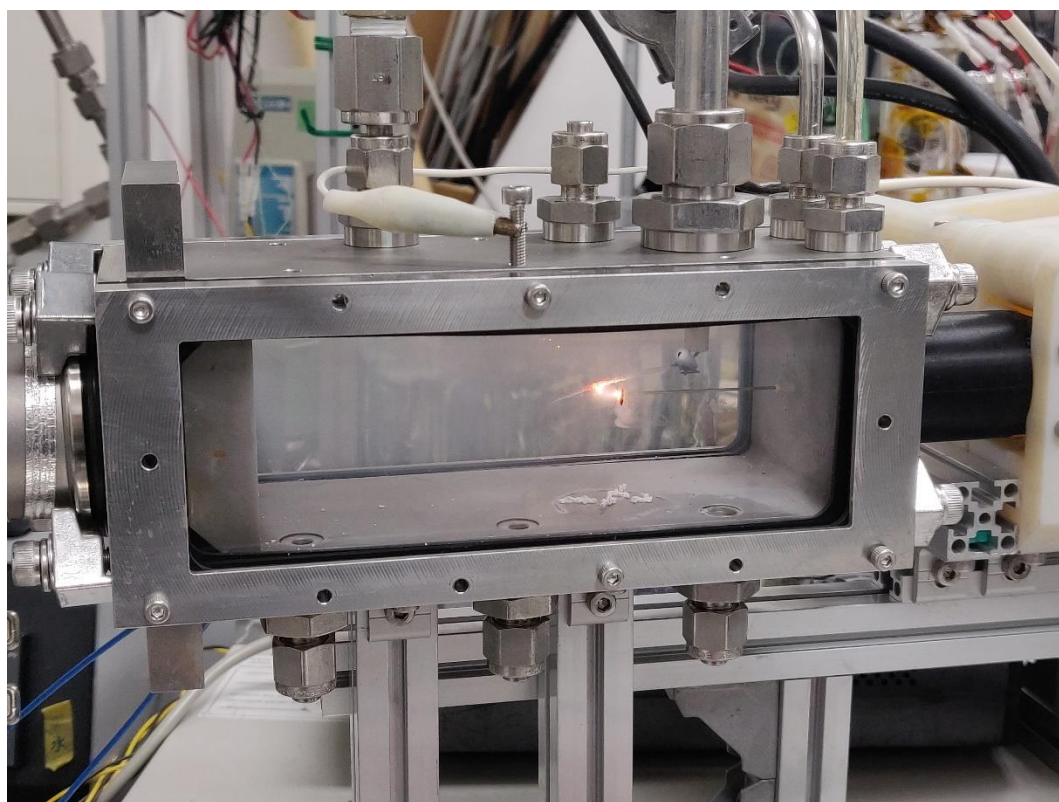


Figure 2.66 Alternate electrode configuration

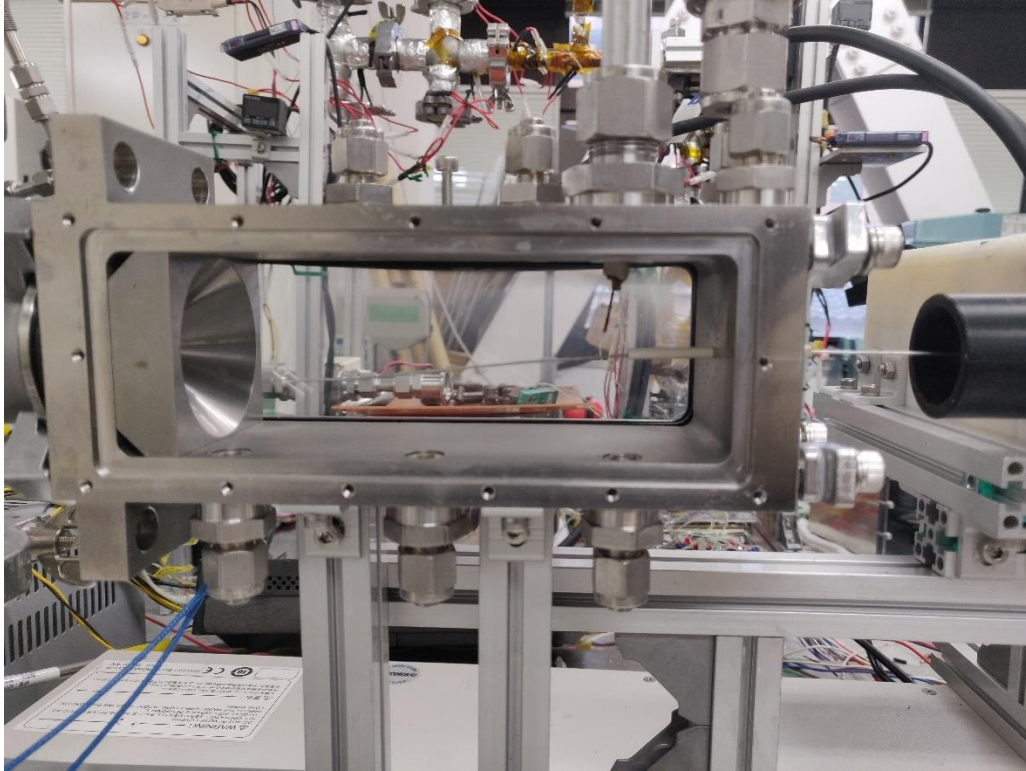


Figure 2.67 Wire guide effectiveness

2.13.3 Ignition confirmation

Three cases of ignition were attempted, all in horizontal chamber configuration. First configuration is in air without vacuum system. This condition doesn't have heat loss due to the absence of air flow. This resembles the closed system. Second configuration has ignition in air without vacuum system at first but opens valve to vacuum system on the confirmation of ignition. This is same configuration in the prior study. Because air is used in this set of experiments, the inlet mass flowrate is controlled by a speed controller rather than water vapor temperature and pressure. Third configuration is the fully open system. The discharge occurs in flowing air. This is closer to the actual thruster operation.

3. Experiment Procedure

3.1 Wire setup

- Loosen clamping bolts on the wire feeder
- Roll up required amount of wire, usually a few meters.
- Feed wire through the wire feeder and the wire inlet
- Feed wire until it goes through the wire guide
- Tighten wire inlet bolts
- Do a leak check, adjust the bolts until leak is minimal
- Lower wire feeder
- Position wire within the grooves of the rollers
- Clamp bolts on wirefeeder
- Launch LabVIEW program and test that the feeder feeds

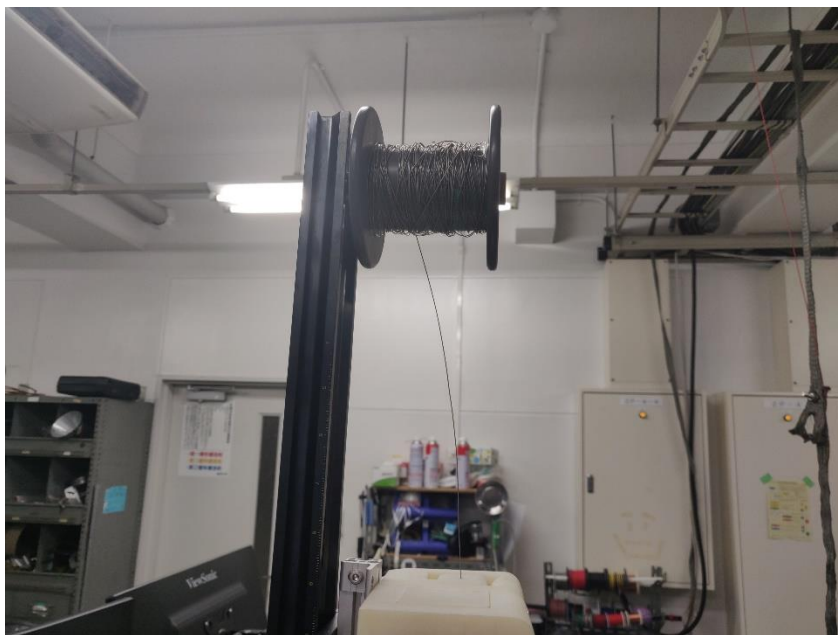


Figure 3.1 Rolled up wires

3.2 Leak checks

- After all the parts to the experiment setups is assembled. A leak test is performed.
- Turn on recording for leak checks
- Close all valves including leak valves, MV and WV2
- Turn on all Rotary Pumps
- Open MV
- Wait until pressure in combustion chamber is stabilized.
- Pressure sensor should be below -95 kPa
- Close MV
- Turn off Rotary Pumps
- Monitor Leak rate

3.3 Heater Check

- Turn off all the valves
- Check that all thermal couples return value.
- Check that all heaters are plugged in
- Set desired water temperature
- Set desired
- Turn on Tube heaters
- Check that Temperature increases
- Turn off Tube heaters
- Turn on water heaters and combustion chamber heater

-
- Check that Temperature increases
 - Turn off water heaters and combustion chamber heater

3.4 Discharge check

- Check that all valves are closed
- Lower the tip of wire until it is positioned less than 1 cm away from discharge electrode
- Turn on the rotary pumps
- Open MV valve so that combustion
- Check that transformer has dial set to 80, corresponds to 8kV on discharge
- Turn on discharge in labview for 1 second
- If discharge doesn't occur, bring wire closer until it does

3.5 Combustion procedure (Air)

- Check that all valves are closed
- Start recording of pressure temperature data
- Initiate FlameTracker and LabVIEW program
- Turn on heaters until target temperatures are reached
- Begin recording of software, LabVIEW
- Turn on Vacuum Pumps
- Open all Leak Valves
- Open MV, WV1, WV2
- Wait for pressure to stabilize
- Turn on ignition search mode in LabVIEW

-
- Turn on discharge
 - Combustion should start automatically
 - Wait for combustion to stop
 - Experiment end.

3.6 Combustion procedure (Water)

- Check that all valves are closed
- Start recording of pressure temperature data
- Initiate FlameTracker and LabVIEW program
- Turn on heaters until target temperatures are reached
- Begin recording of software, LabVIEW
- Turn on Vacuum Pumps
- Open MV1
- Open leak valve downstream of combustion chamber
- Open MV, WV2
- Wait for pressure to stabilize
- Turn on ignition search mode in LabVIEW
- Turn on discharge
- Combustion should start automatically
- Wait for combustion to stop
- Close MV, WV2
- Experiment end.

4. Results

4.1 Sustained Combustion

This records the longest combustion that was achieved using the control program and experiment setup. The length was 280 seconds. The experiment used 0.5 mm orifice and water temperature of 83 degrees Celsius.

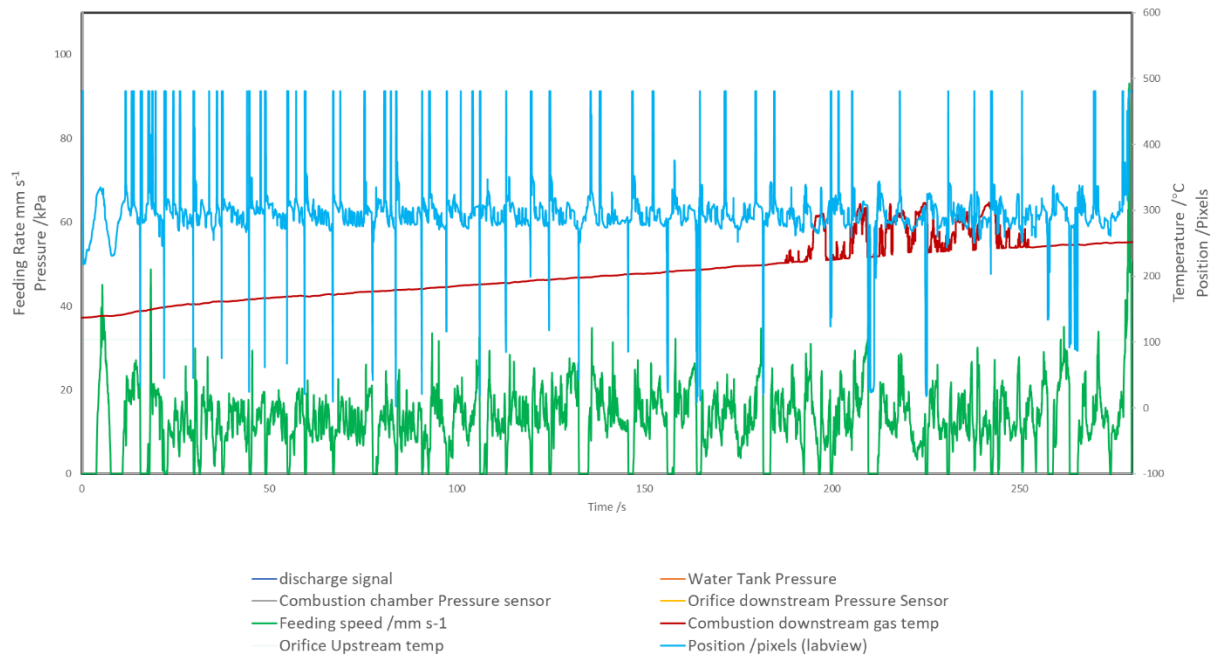


Figure 4.1 Result Sustained Combustion 280 seconds

4.2 Varying Pressure

All combustions are done with 0.8 mm wires using the automated control methods. Temperature of the water tank is set based on desired water vapor pressure.

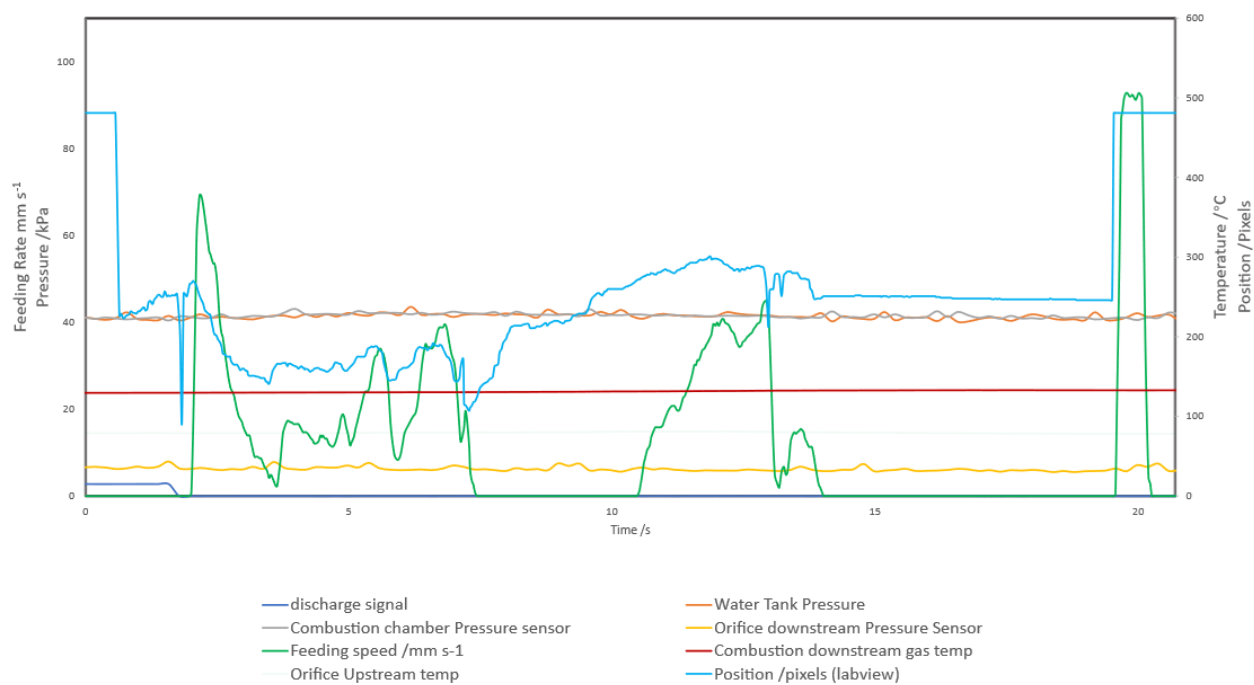


Figure 4.2 Result 45kPa 1

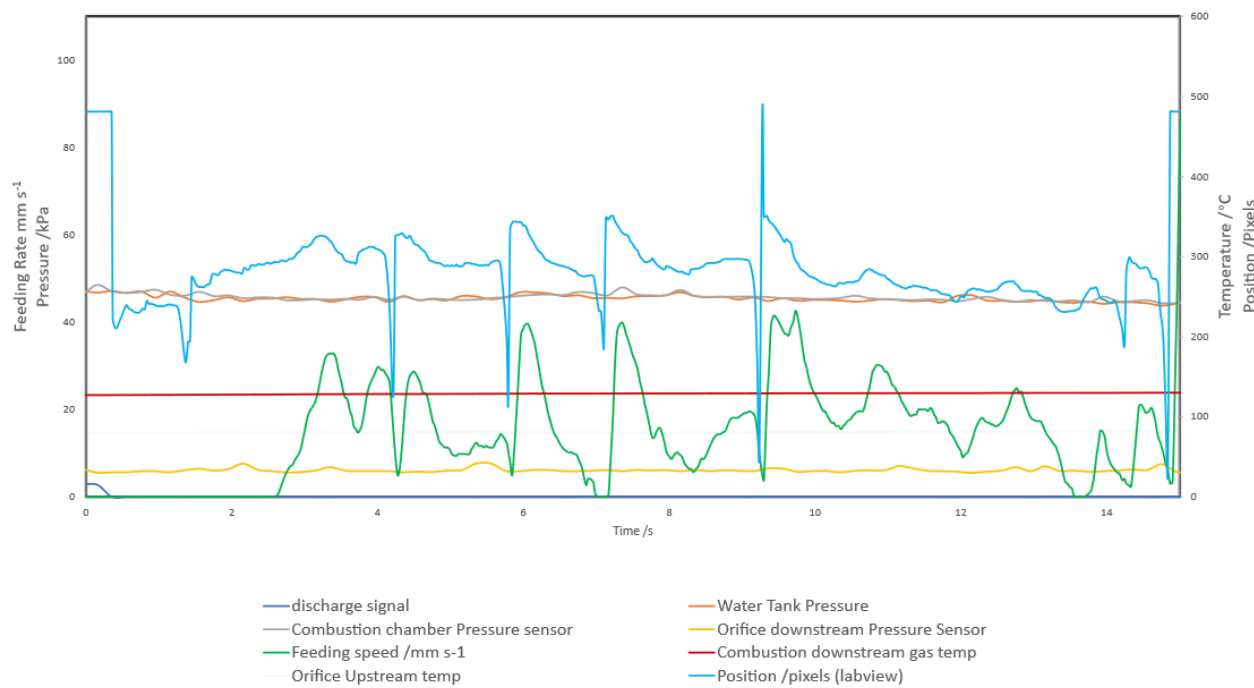


Figure 4.3 Result 45kPa 2

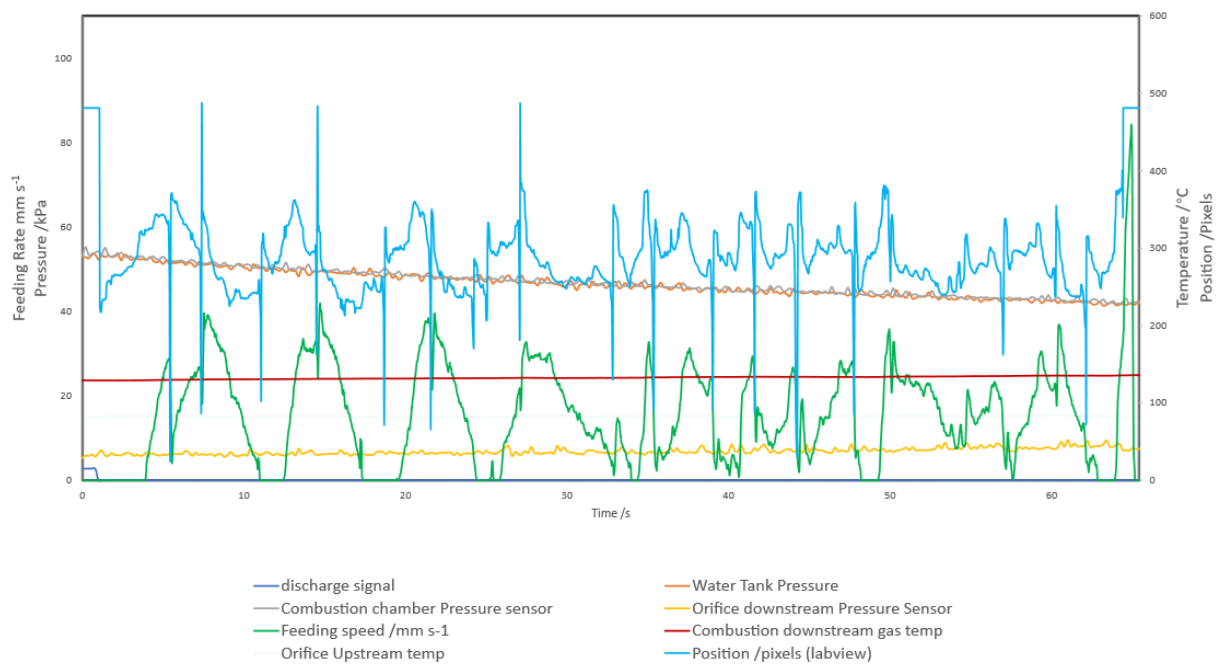


Figure 4.4 Result 45kPa 3

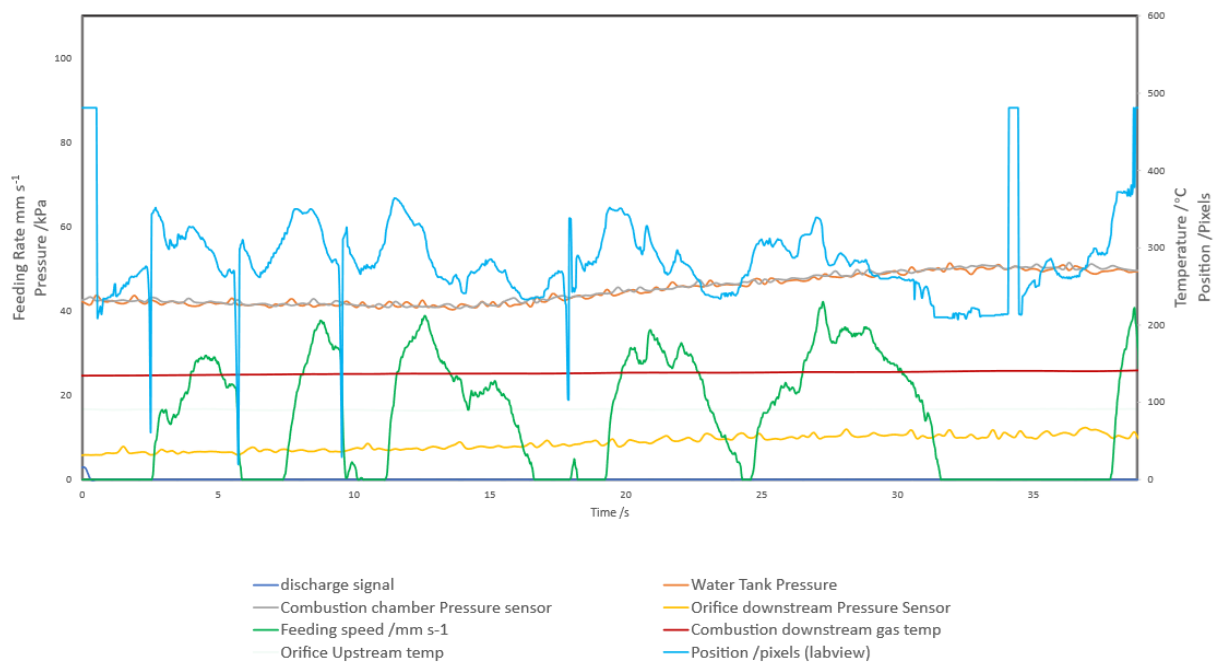


Figure 4.5 Result 45kPa 4

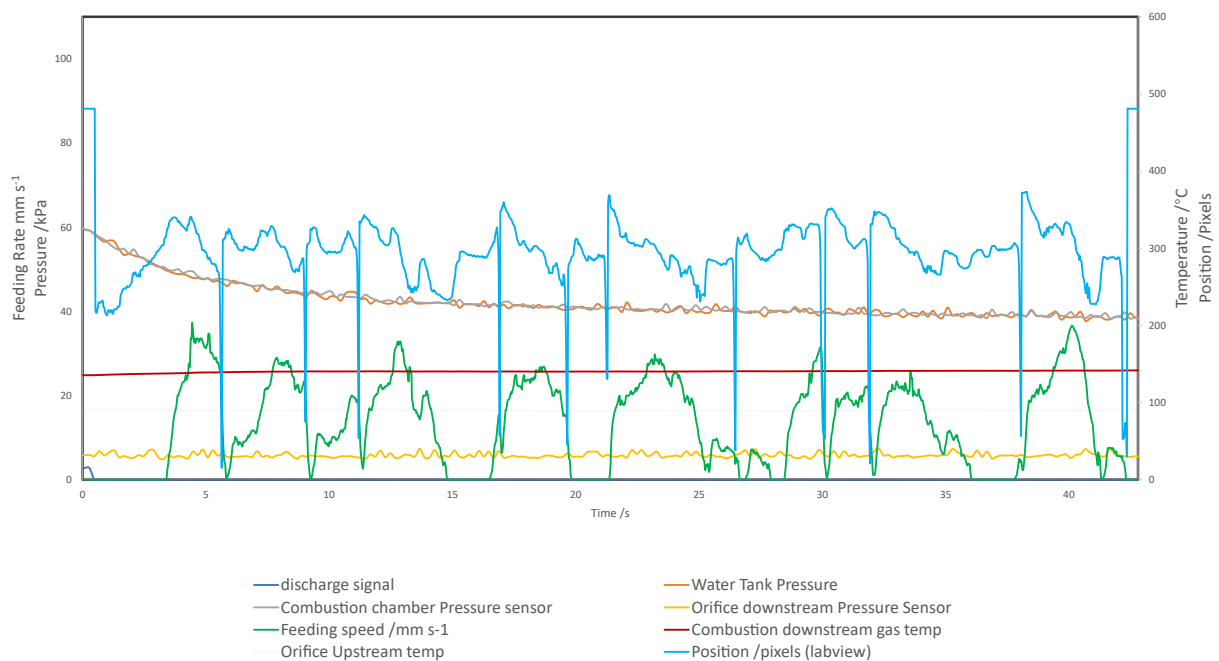


Figure 4.6 Result 35kPa 1

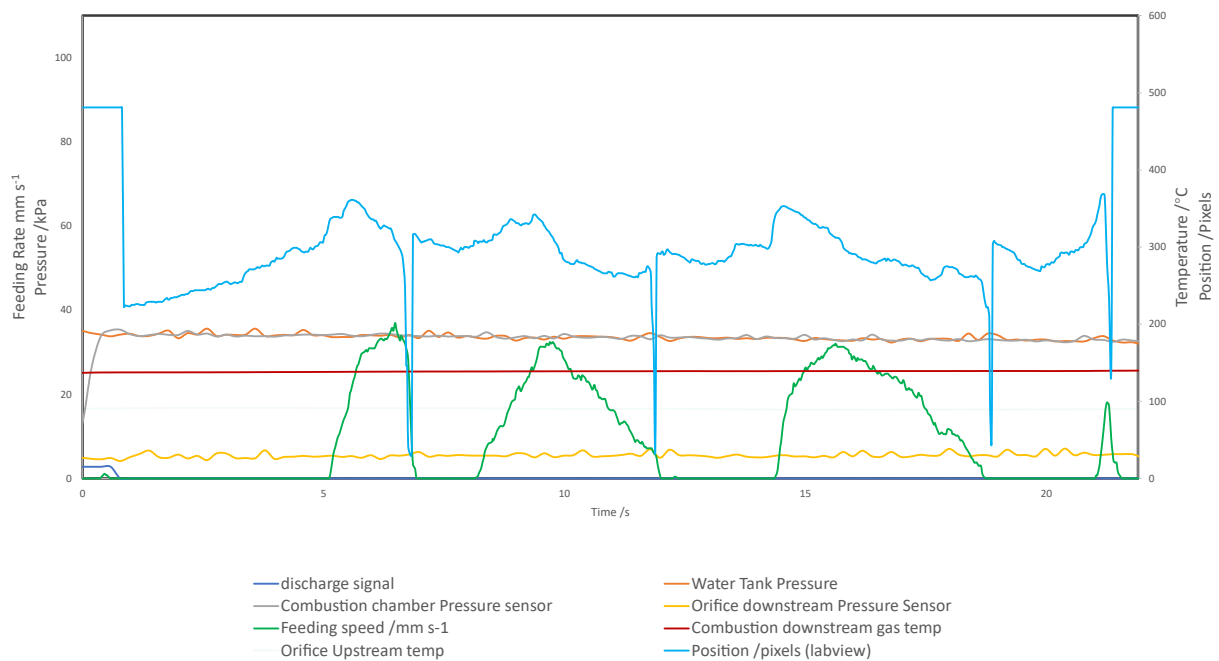


Figure 4.7 Result 35kPa 2

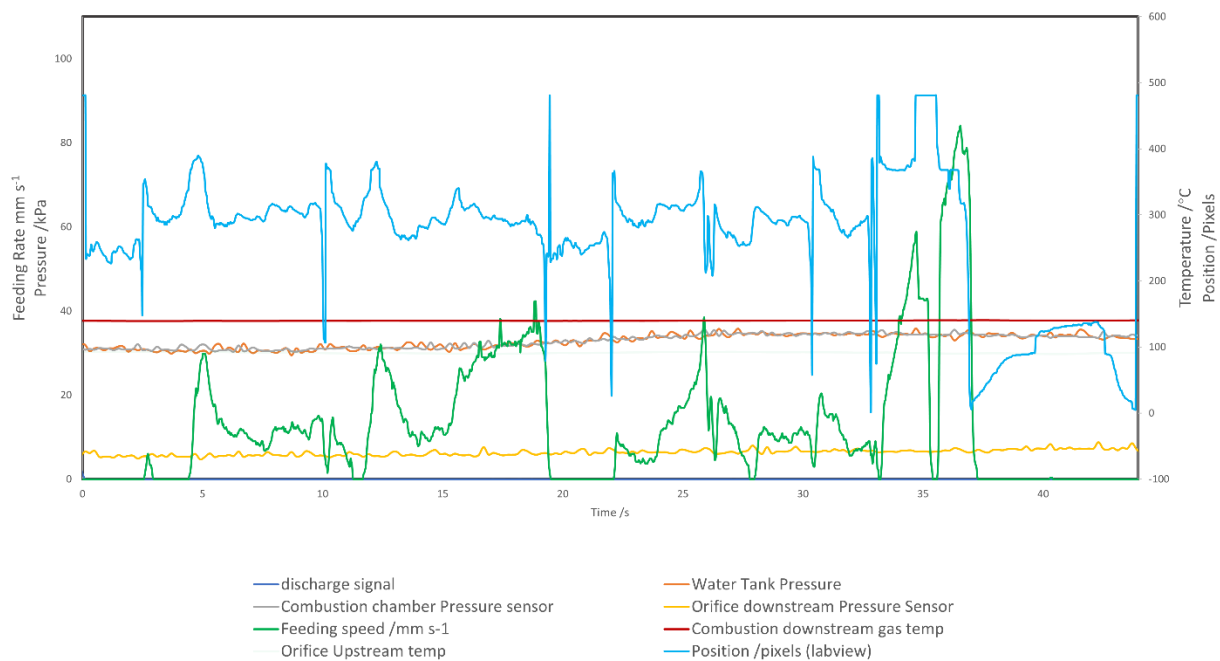


Figure 4.8 Result 35kPa 3

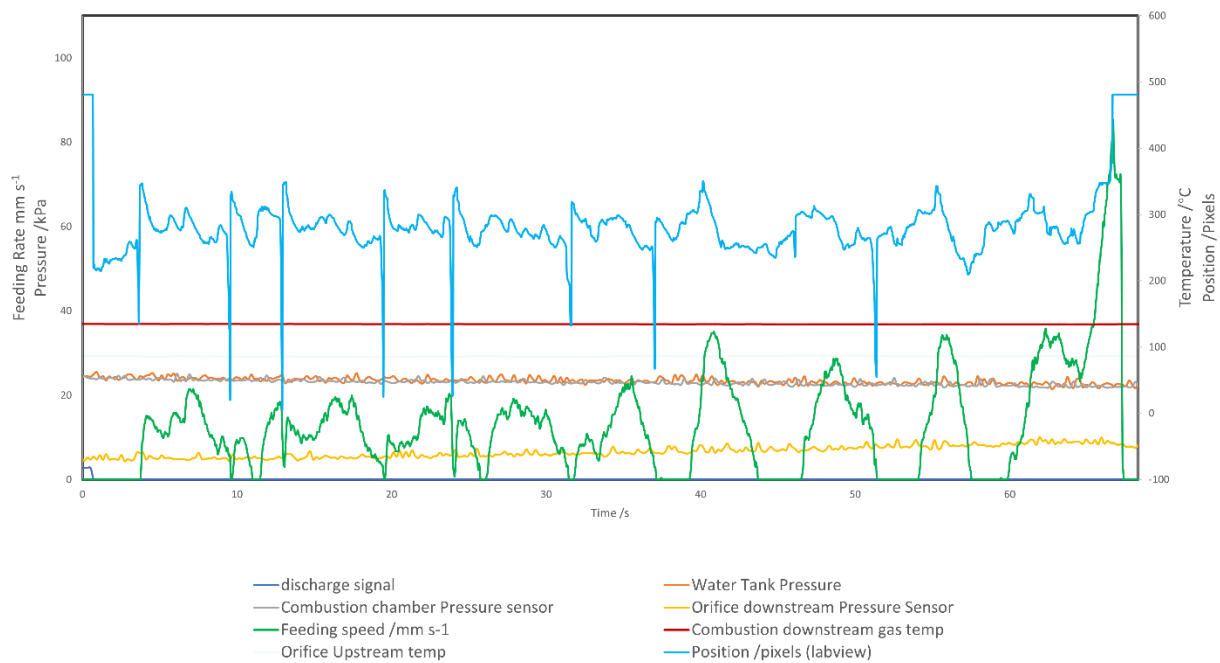


Figure 4.9 Result 25kPa 1

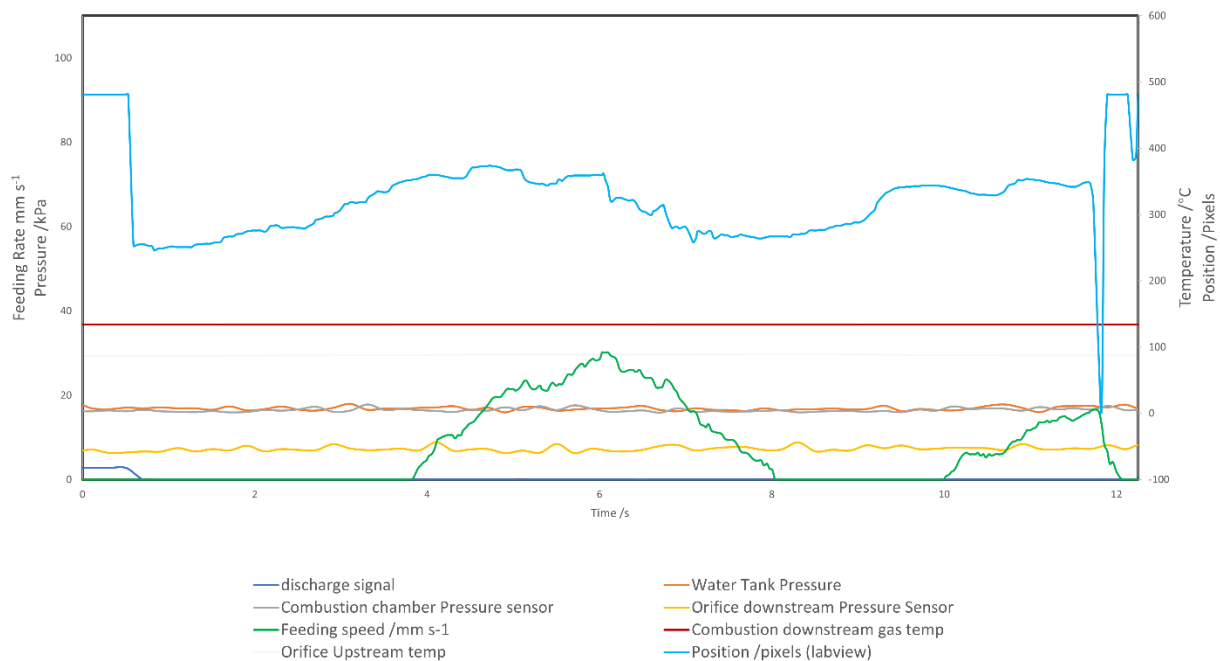


Figure 4.10 Result 20kPa 1

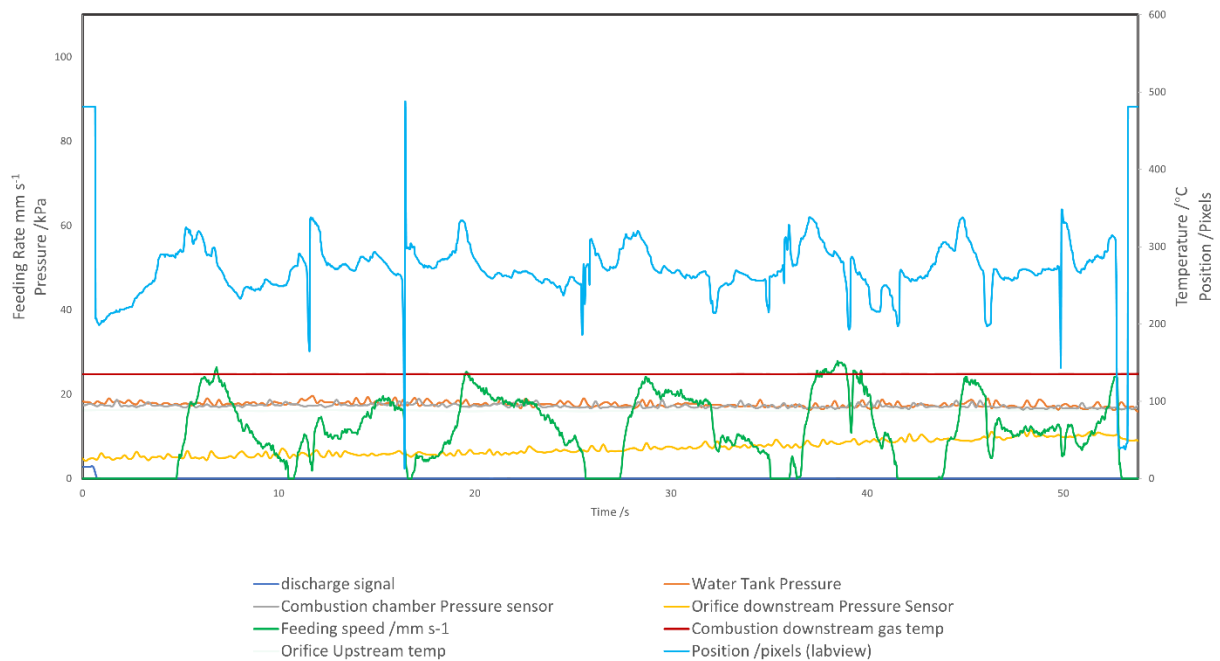


Figure 4.11 Result 20kPa 2

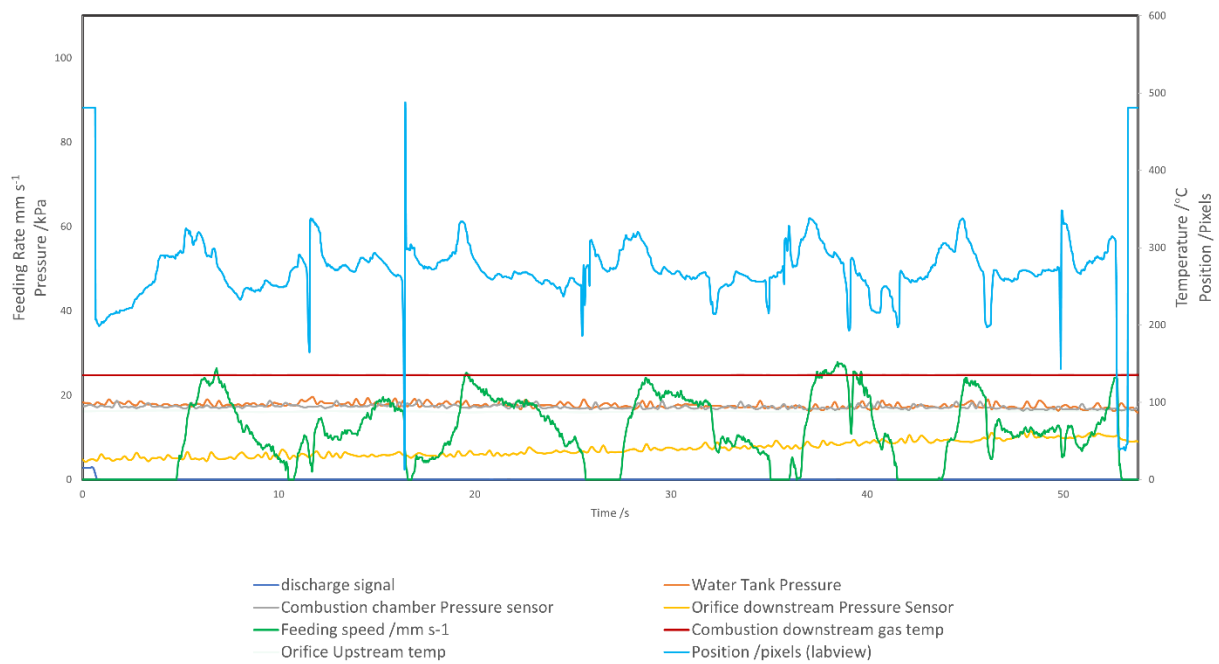


Figure 4.12 Result 20kPa 3

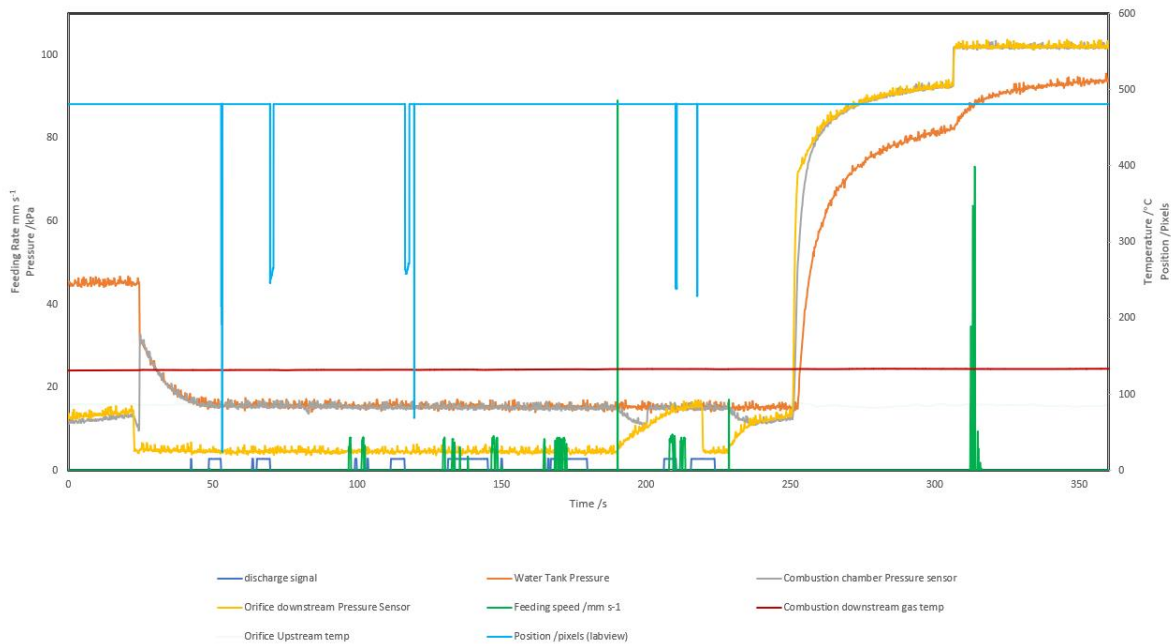
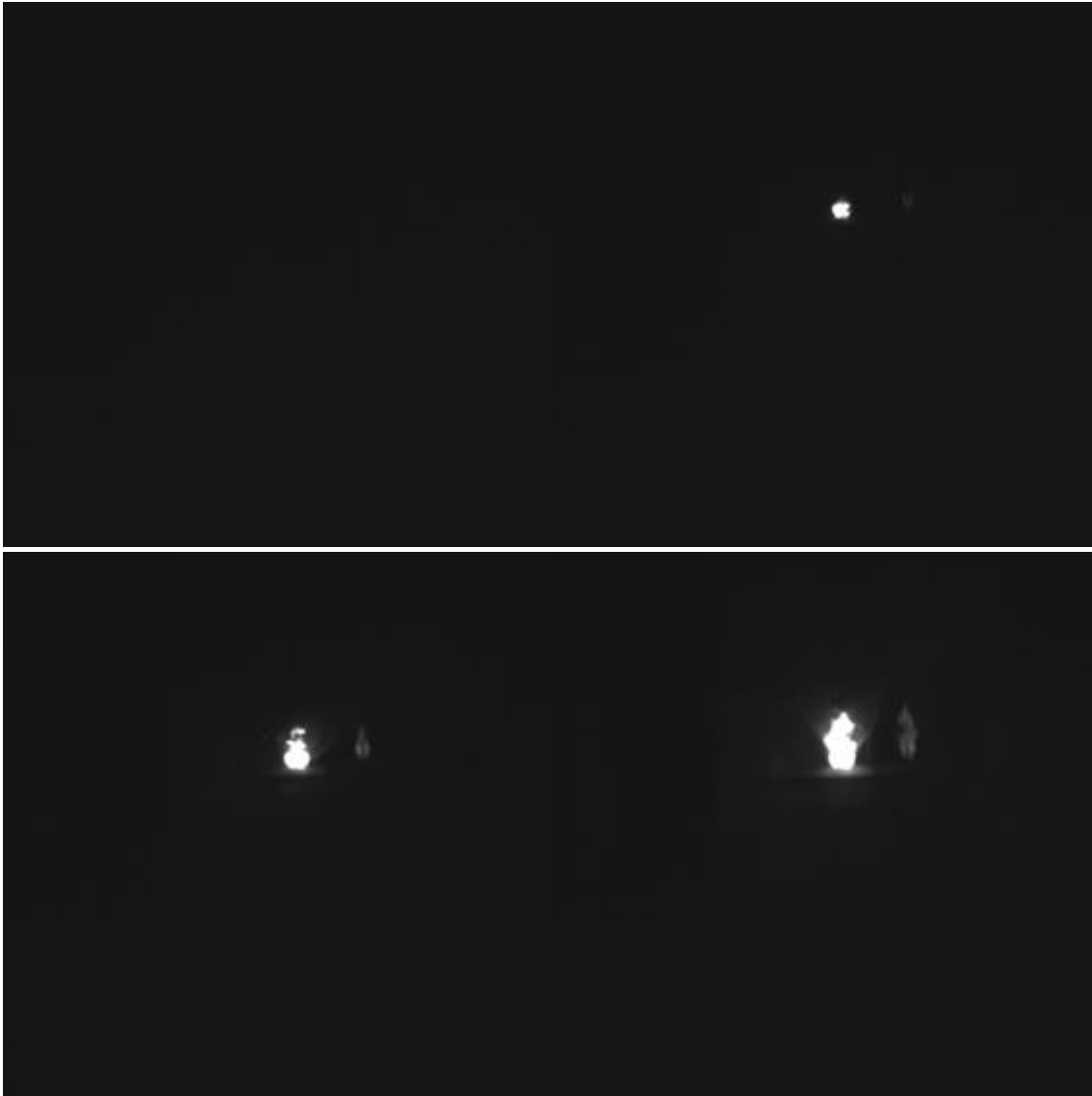
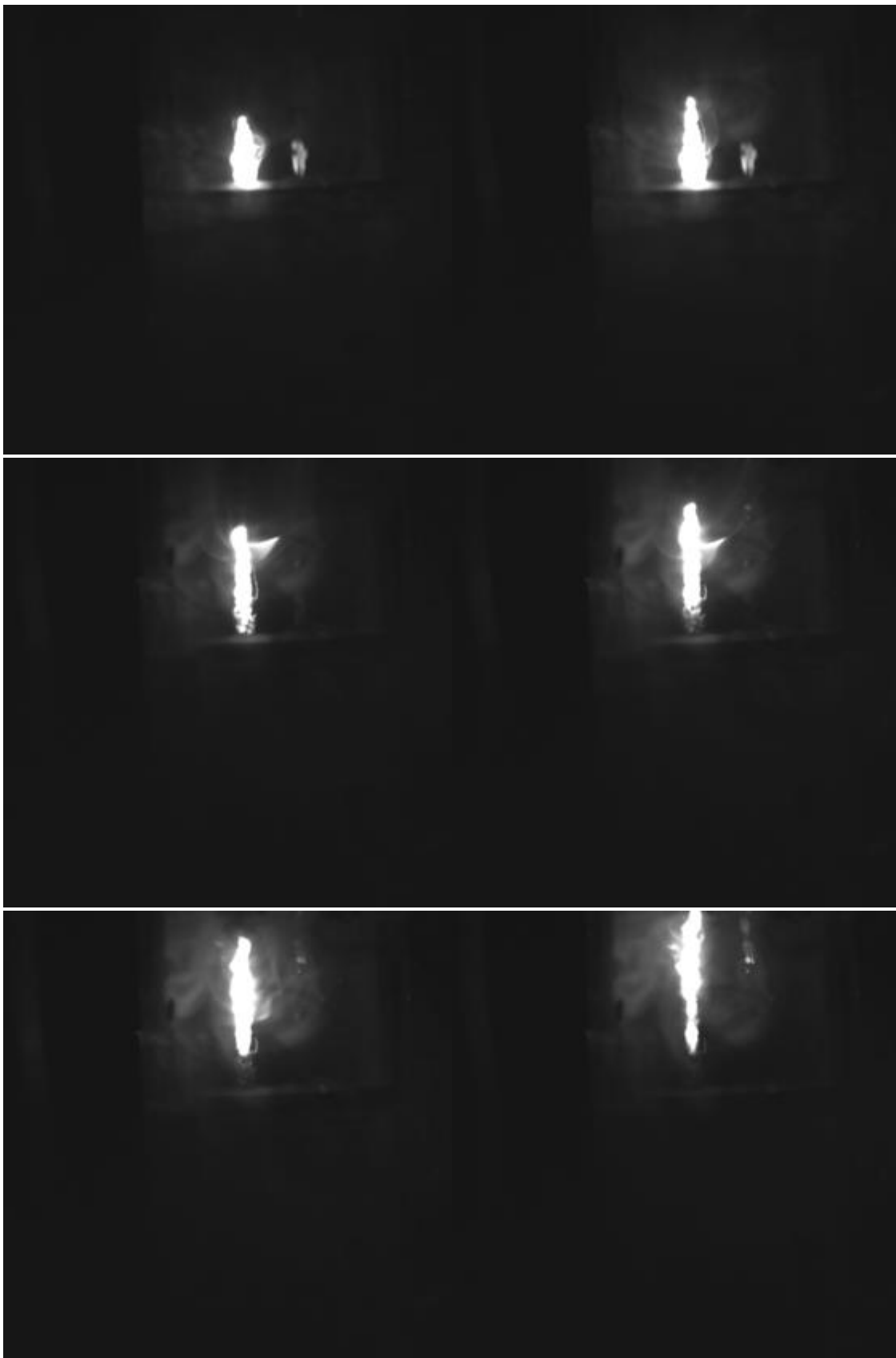


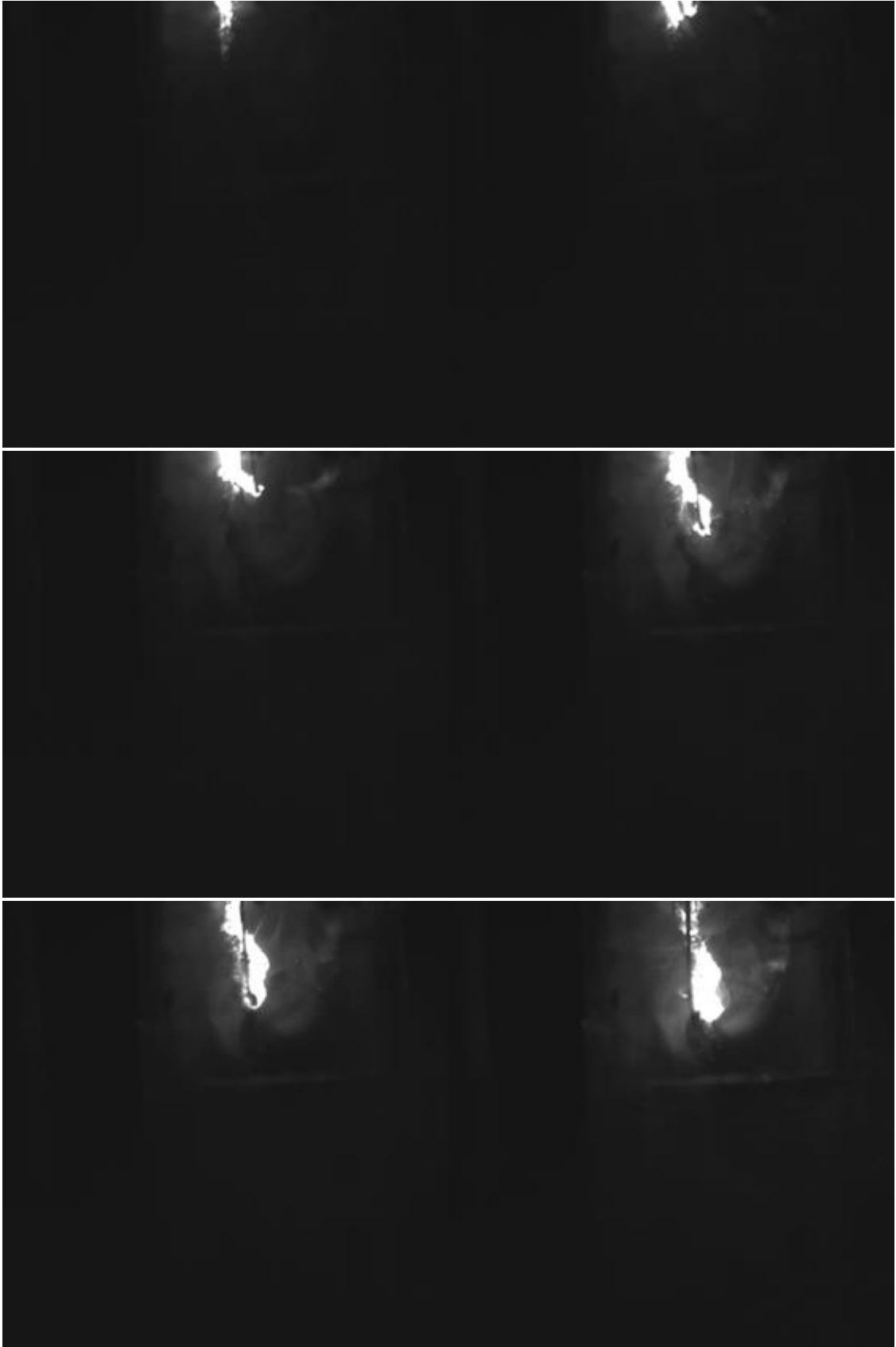
Figure 4.13 Result 15 kPa (failed)

4.3 Wire combustion under high speed camera







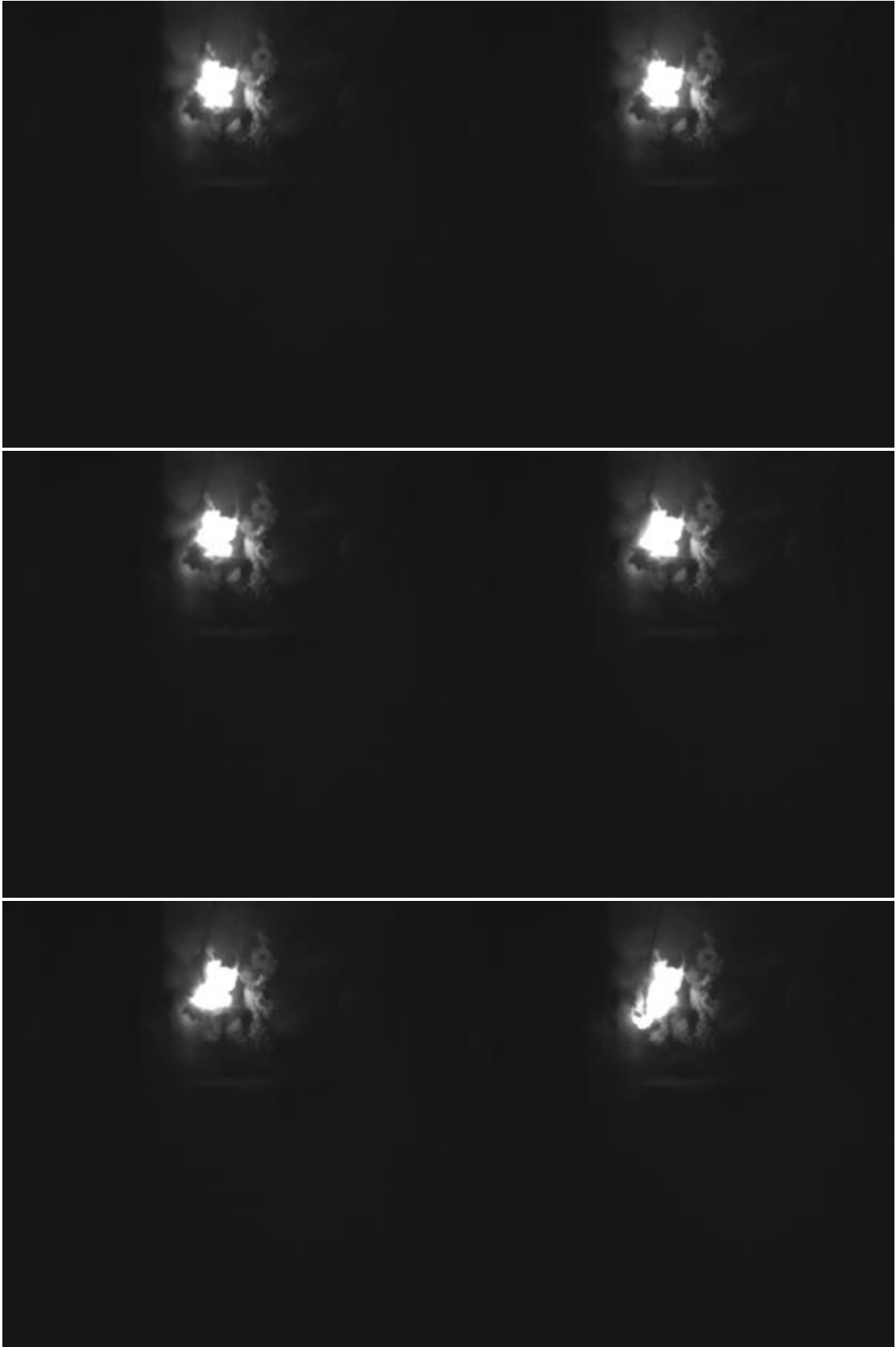


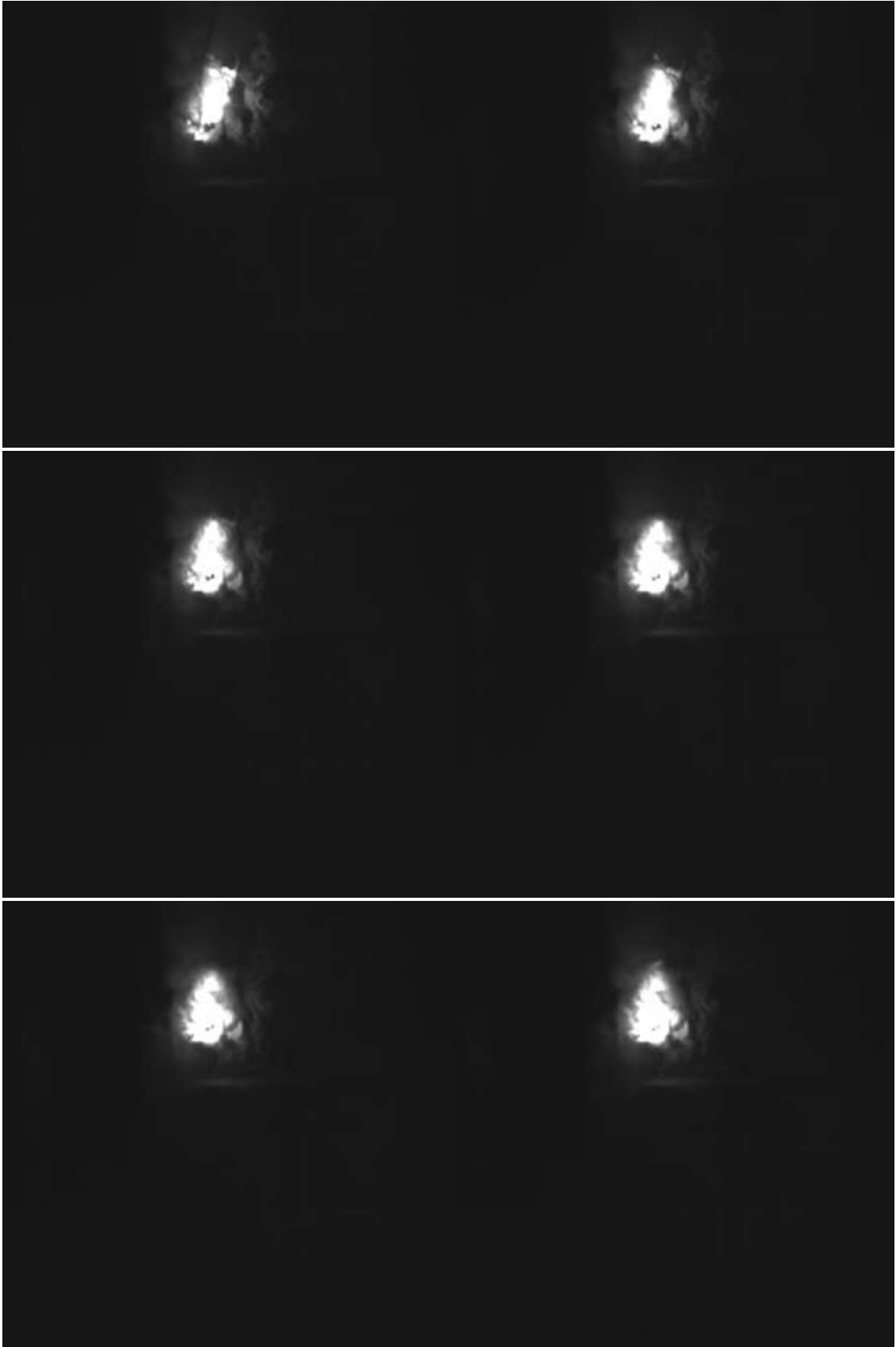


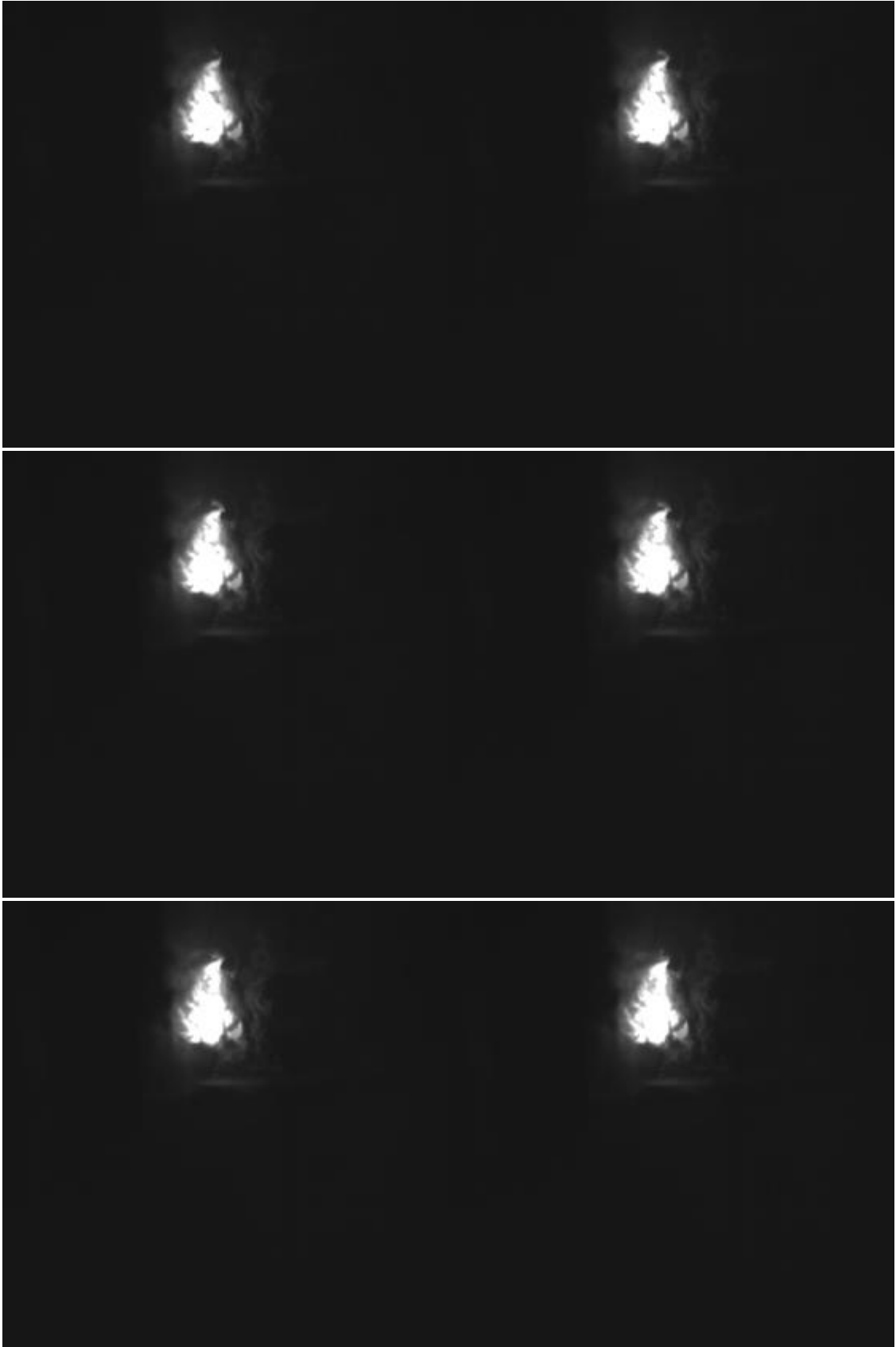


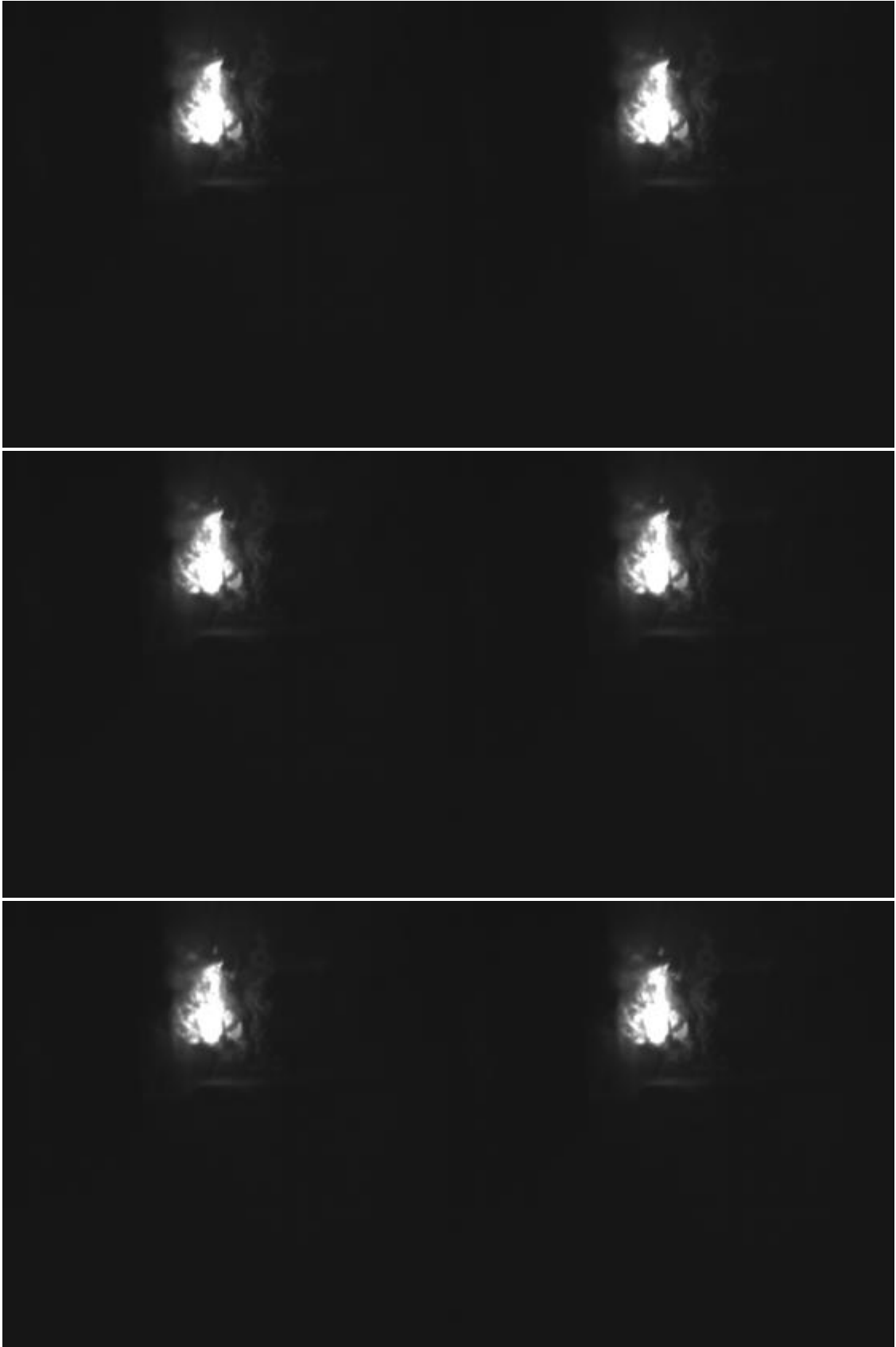


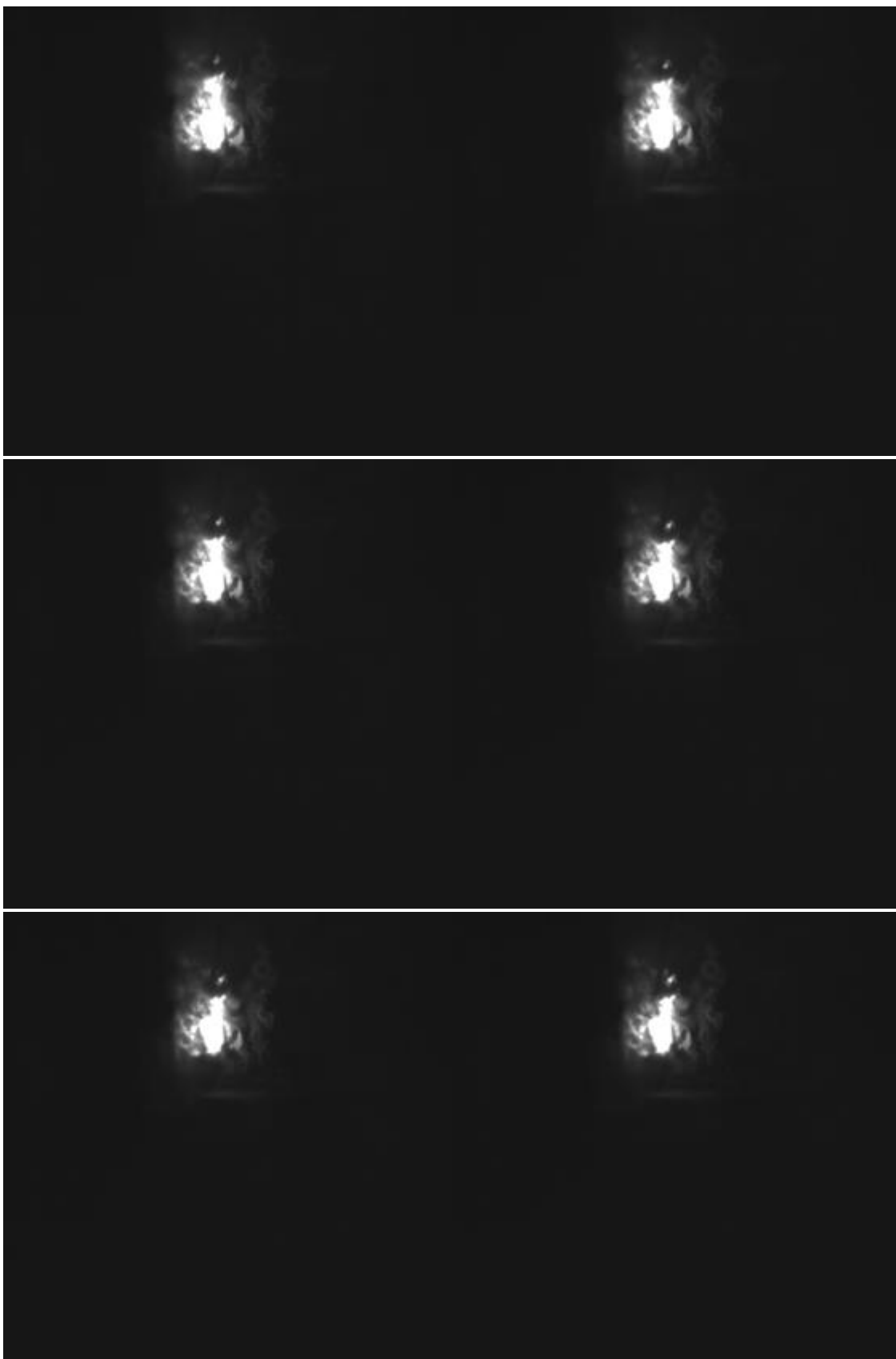


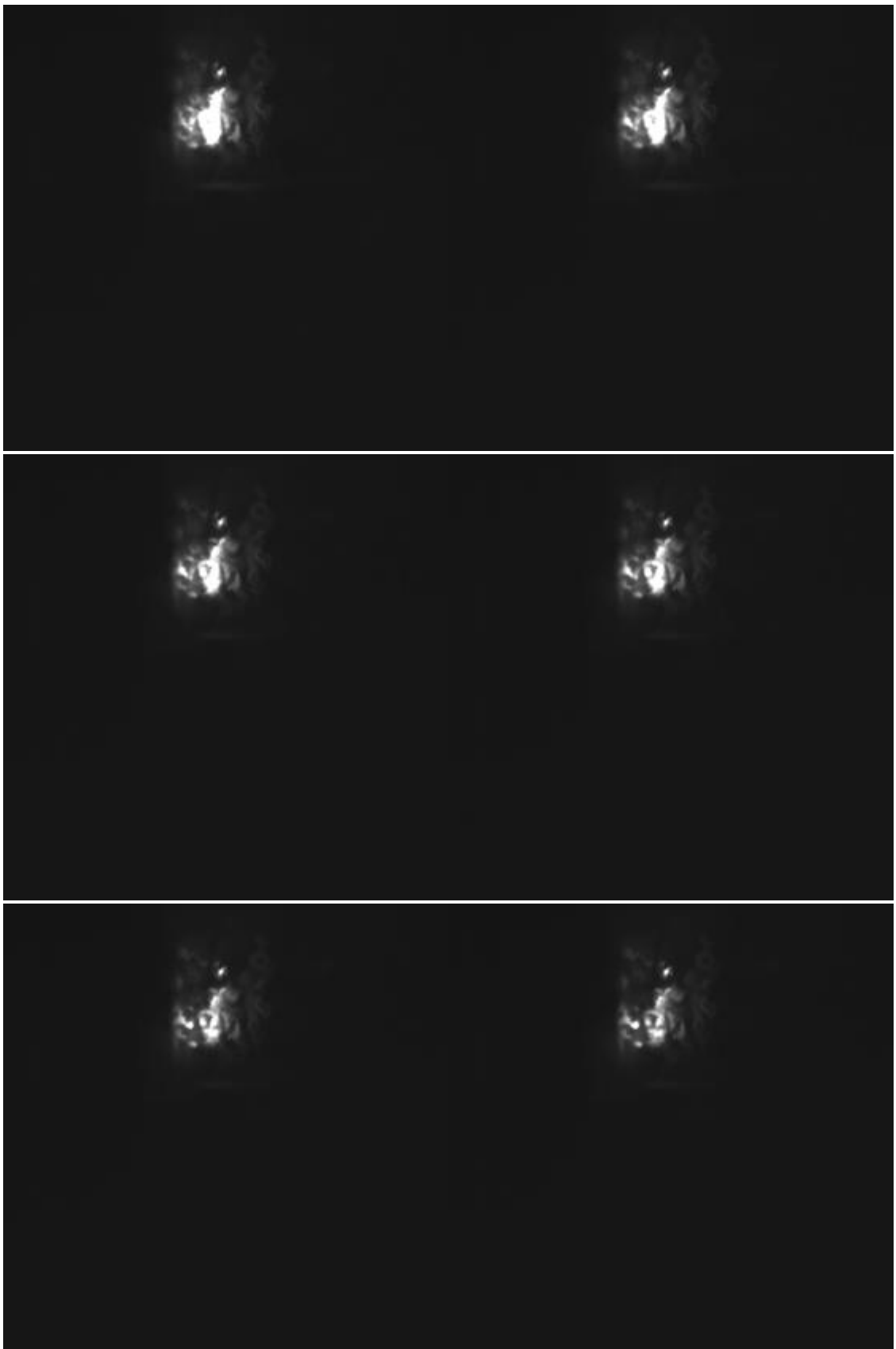


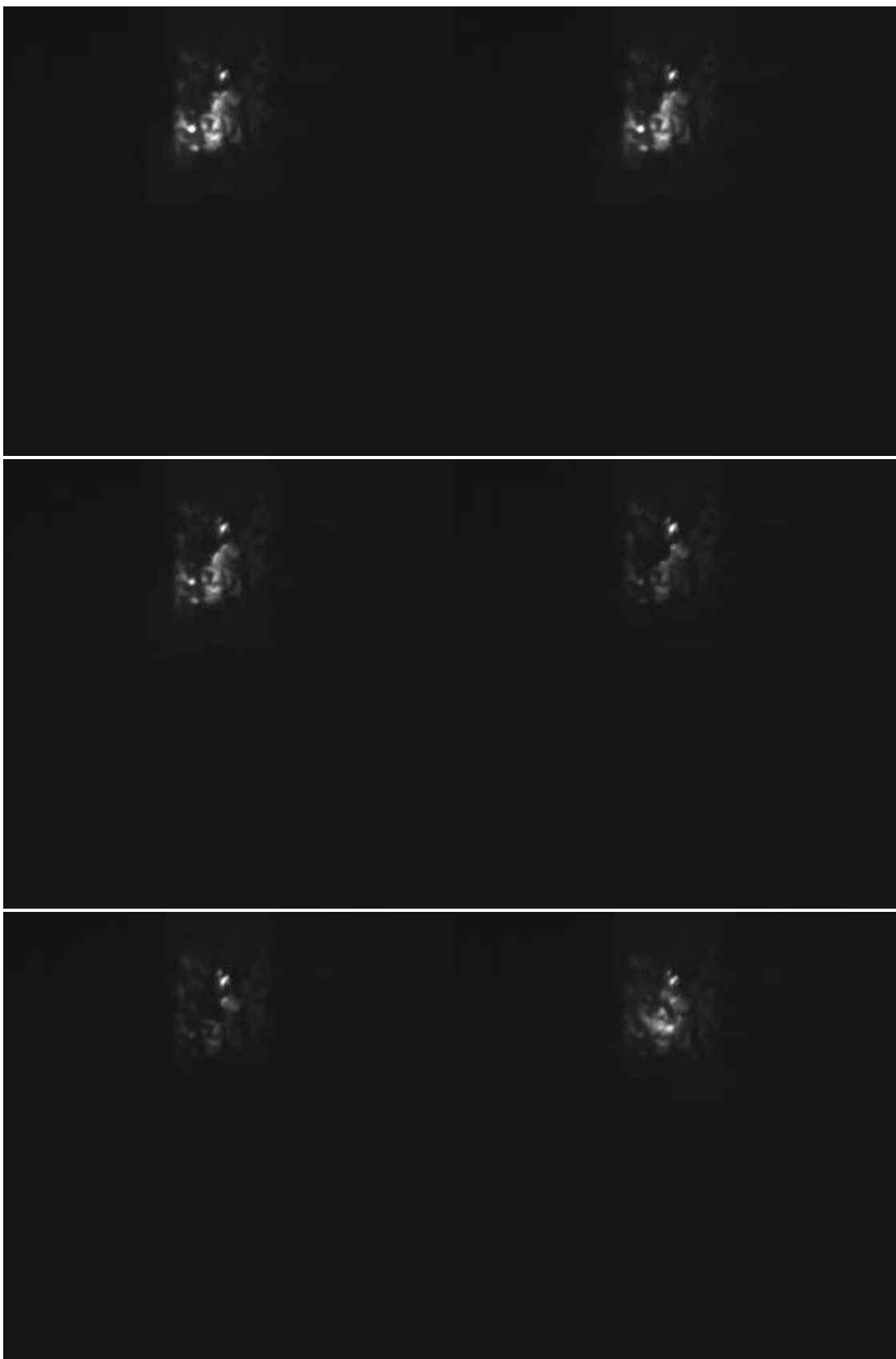












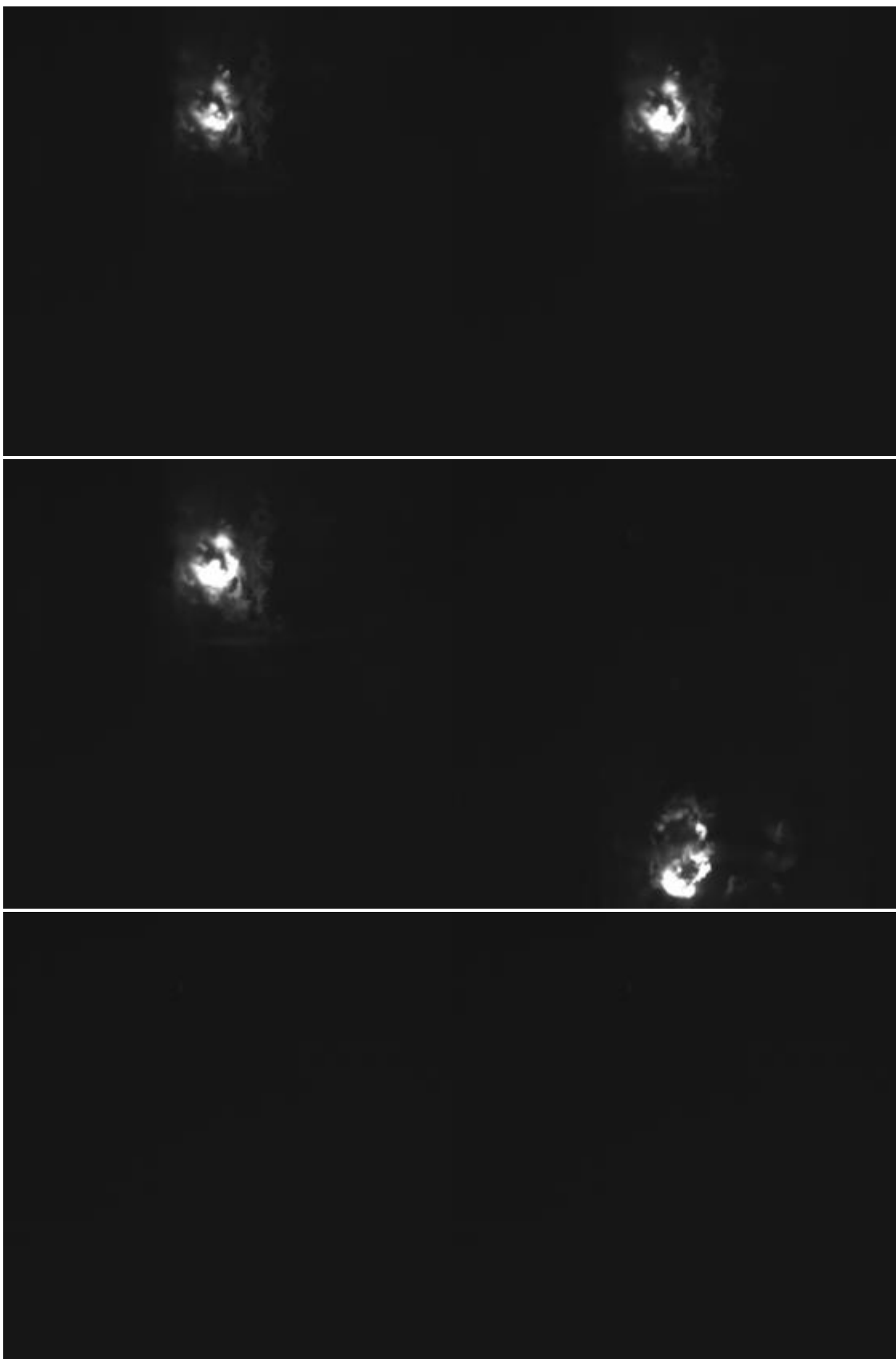
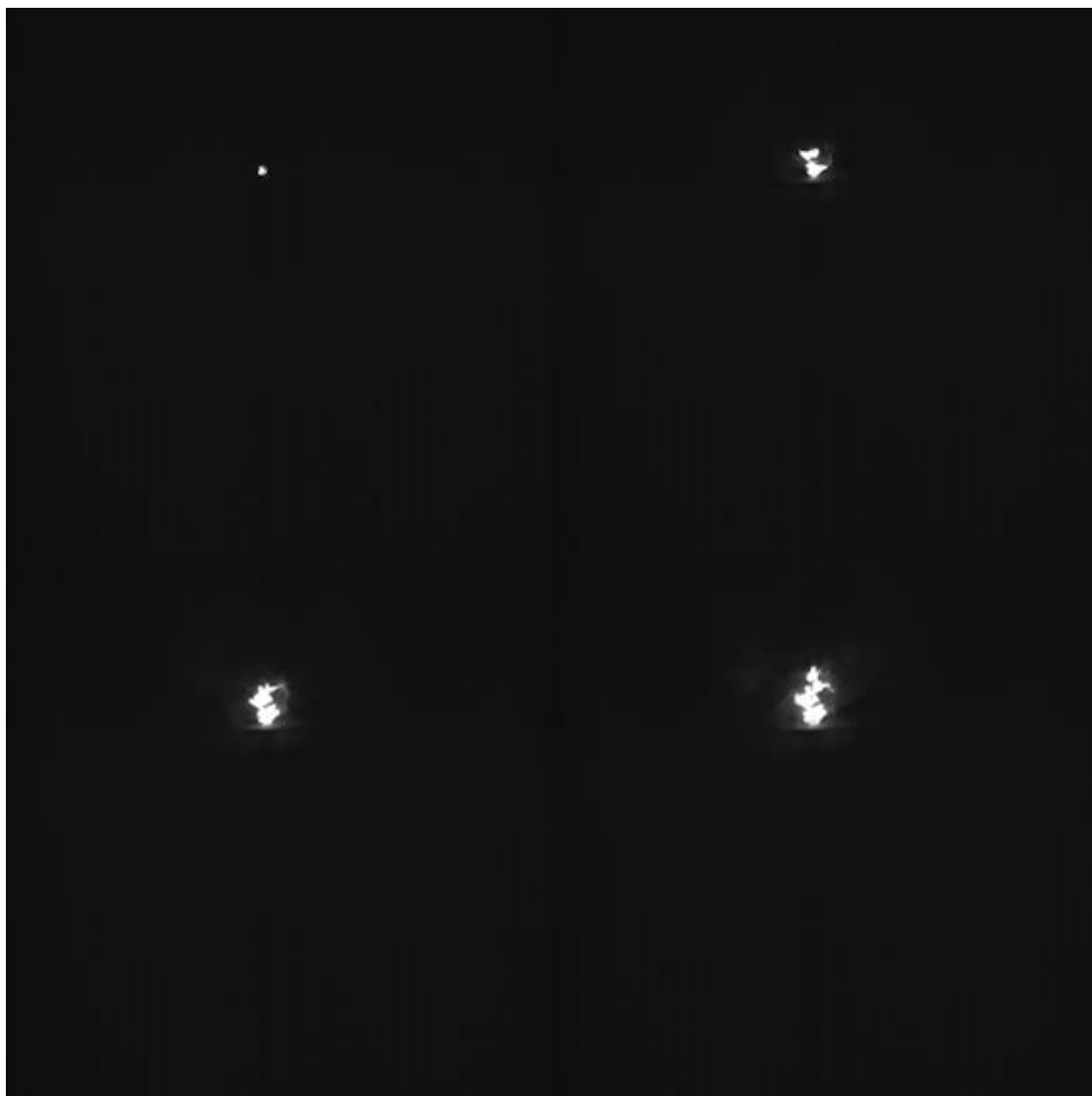
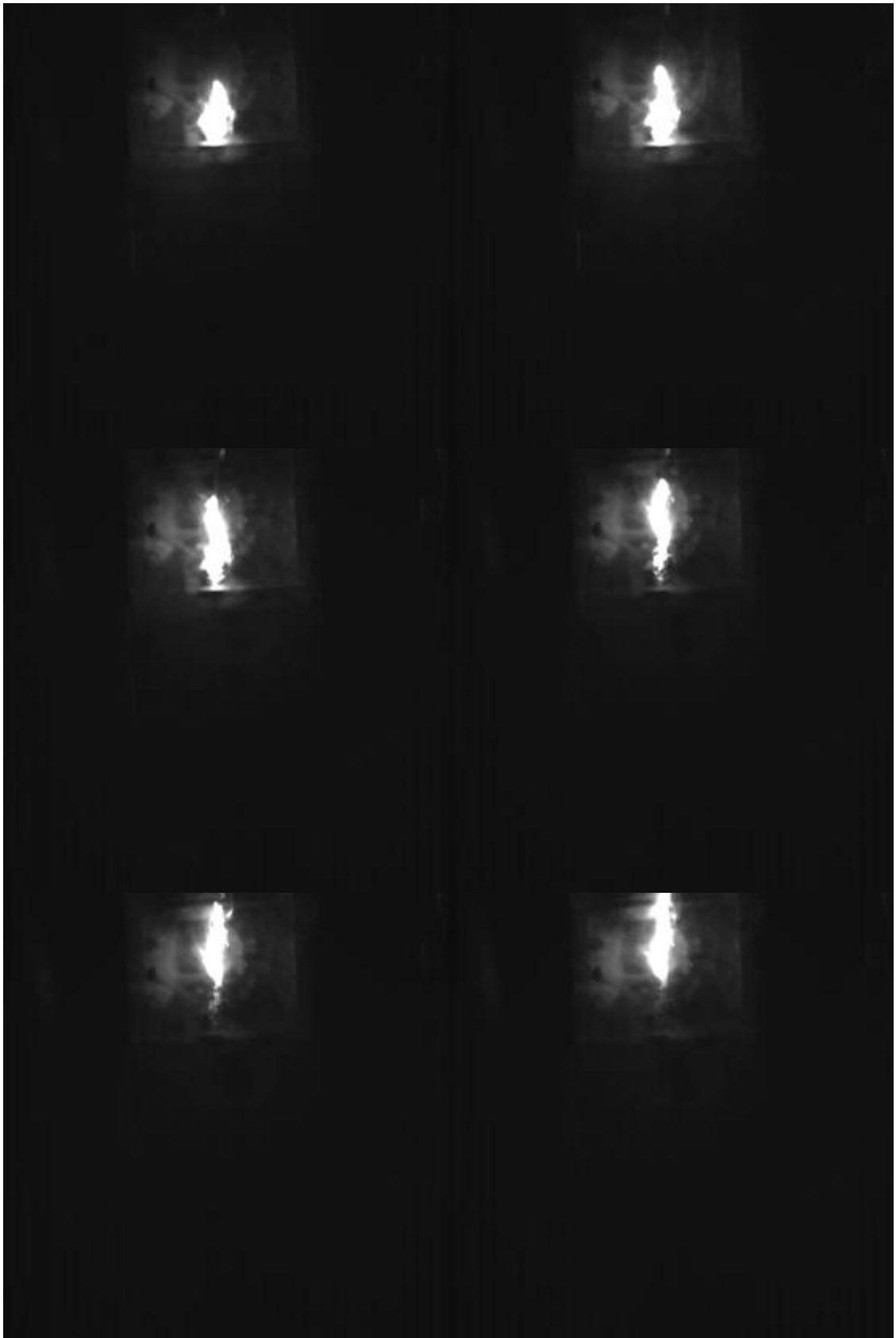
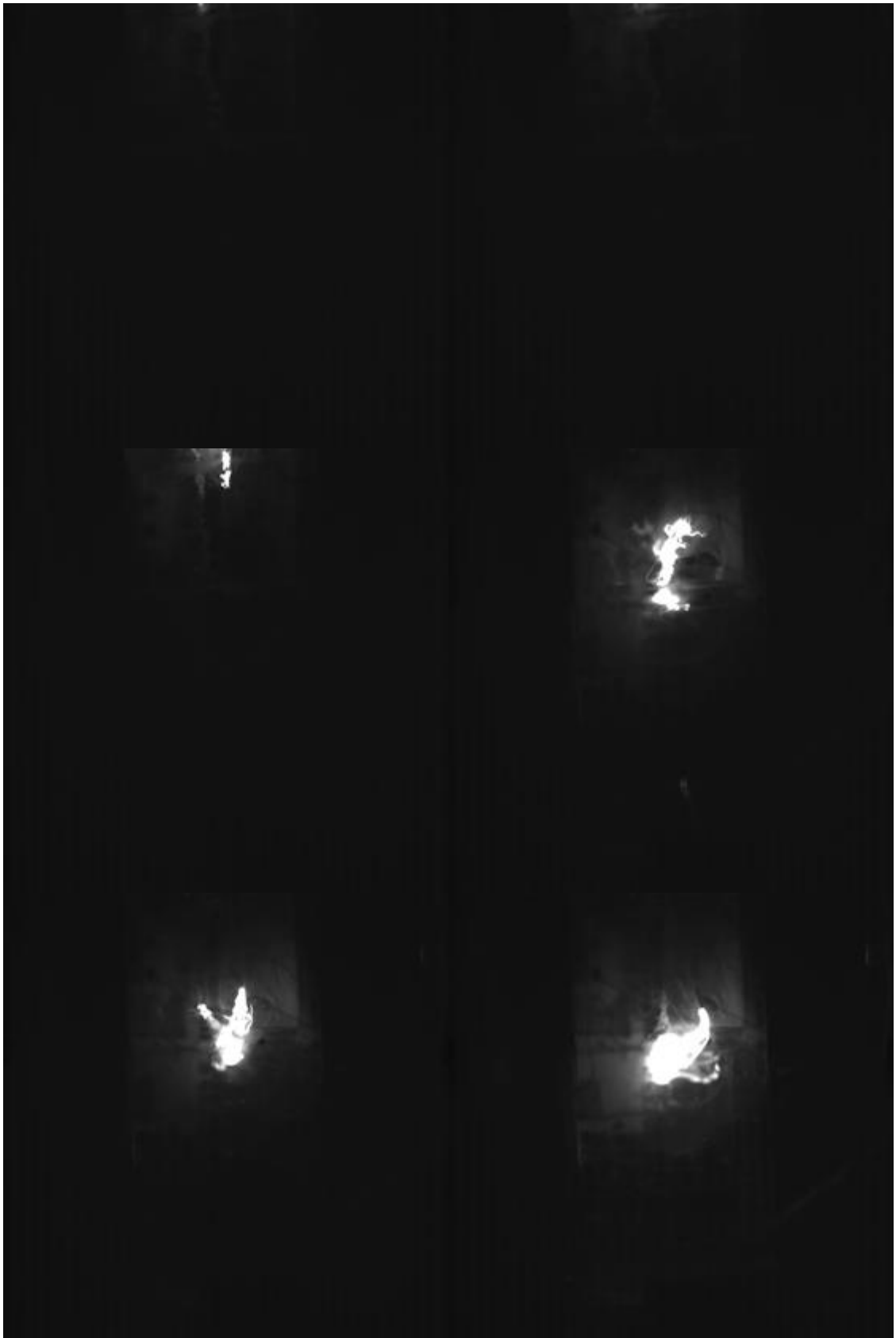


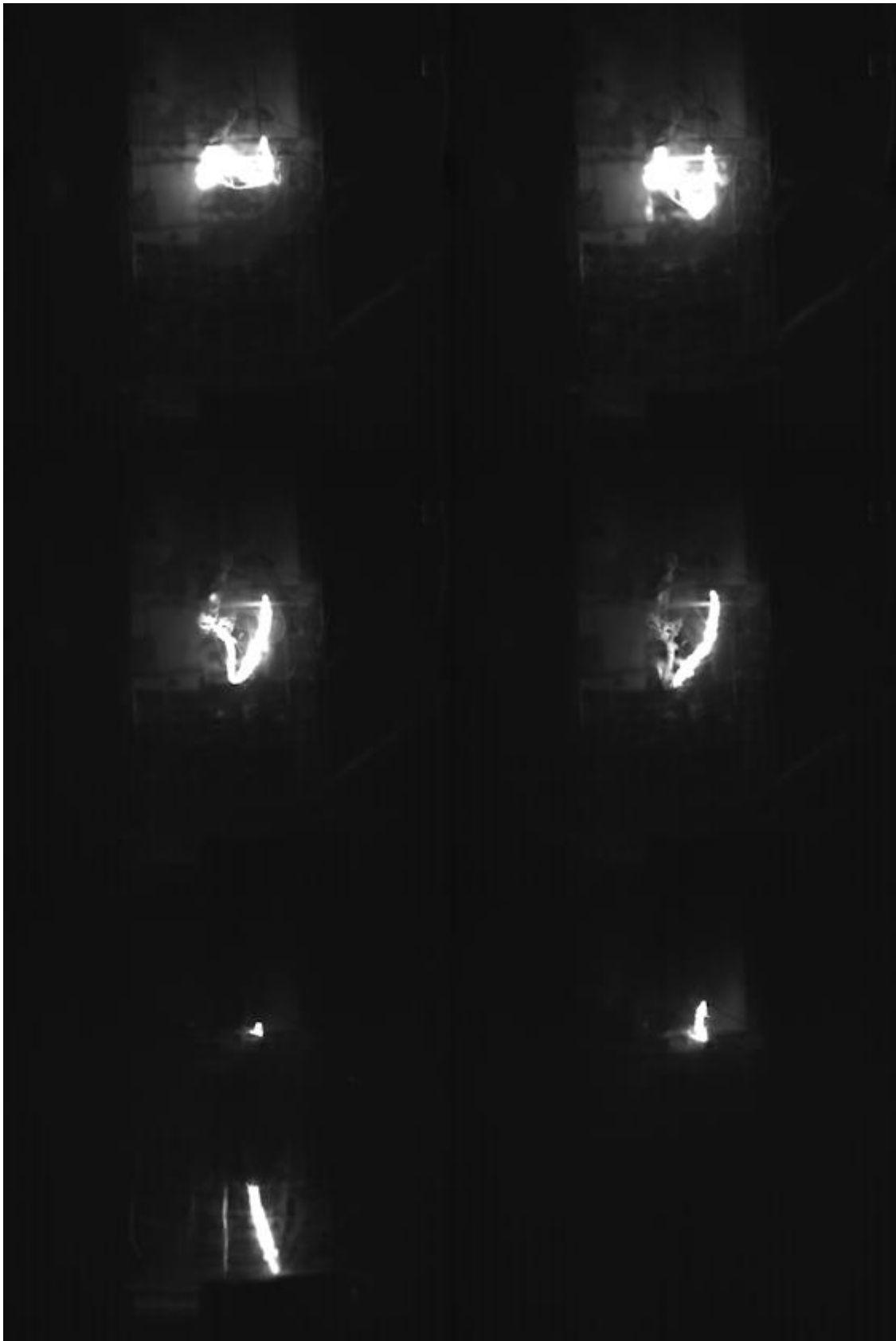
Figure 4.14 High speed camera footage from previous setup

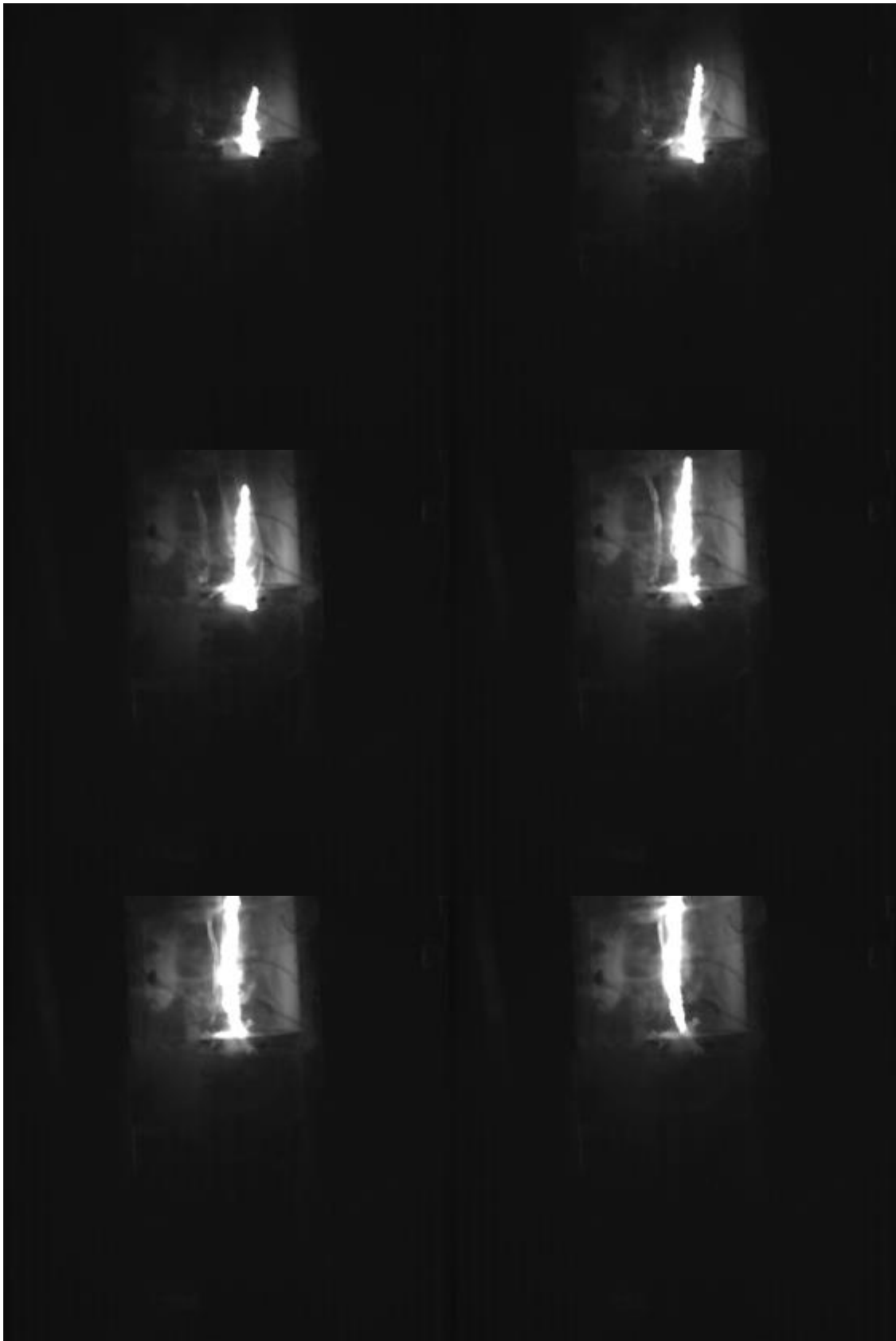




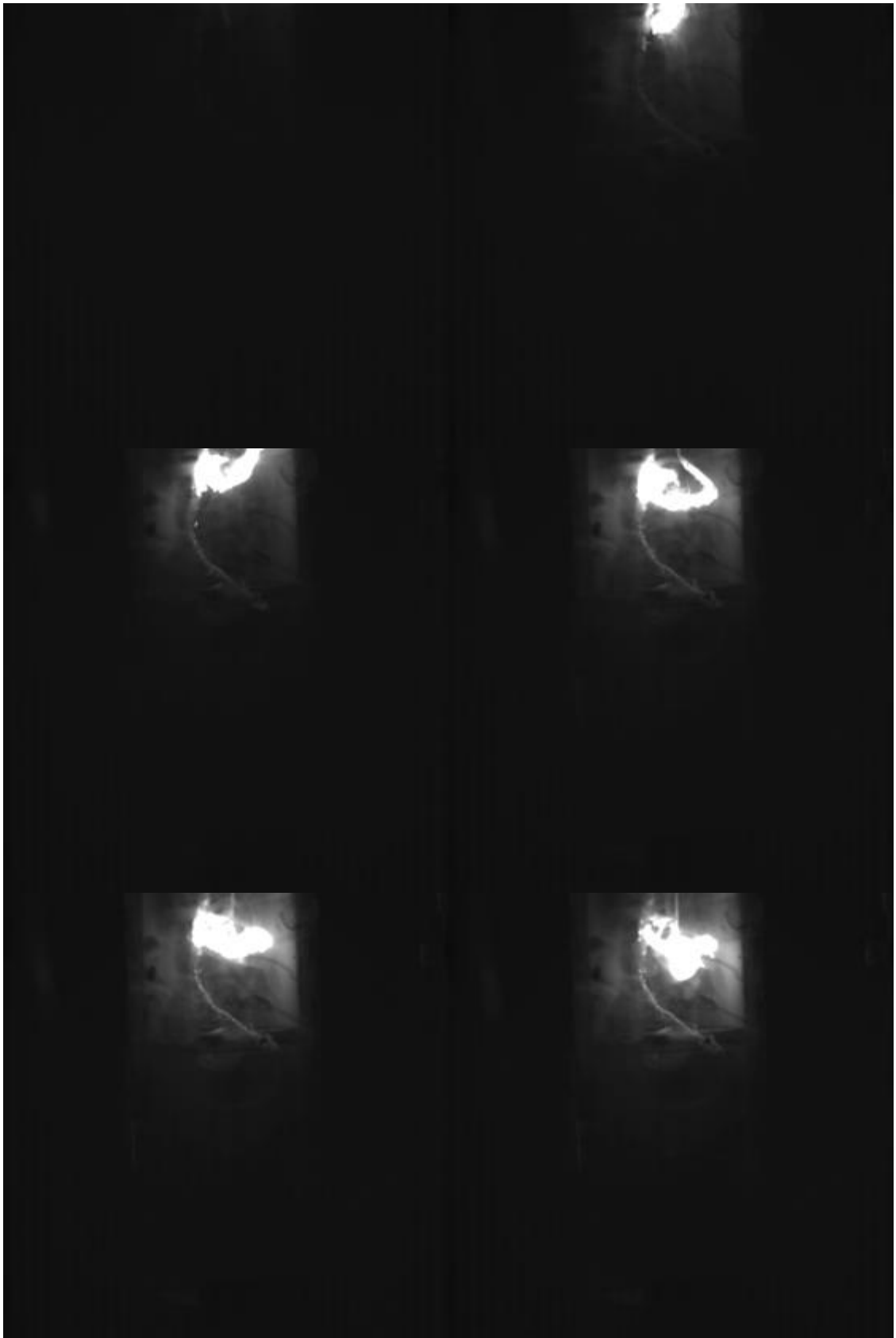


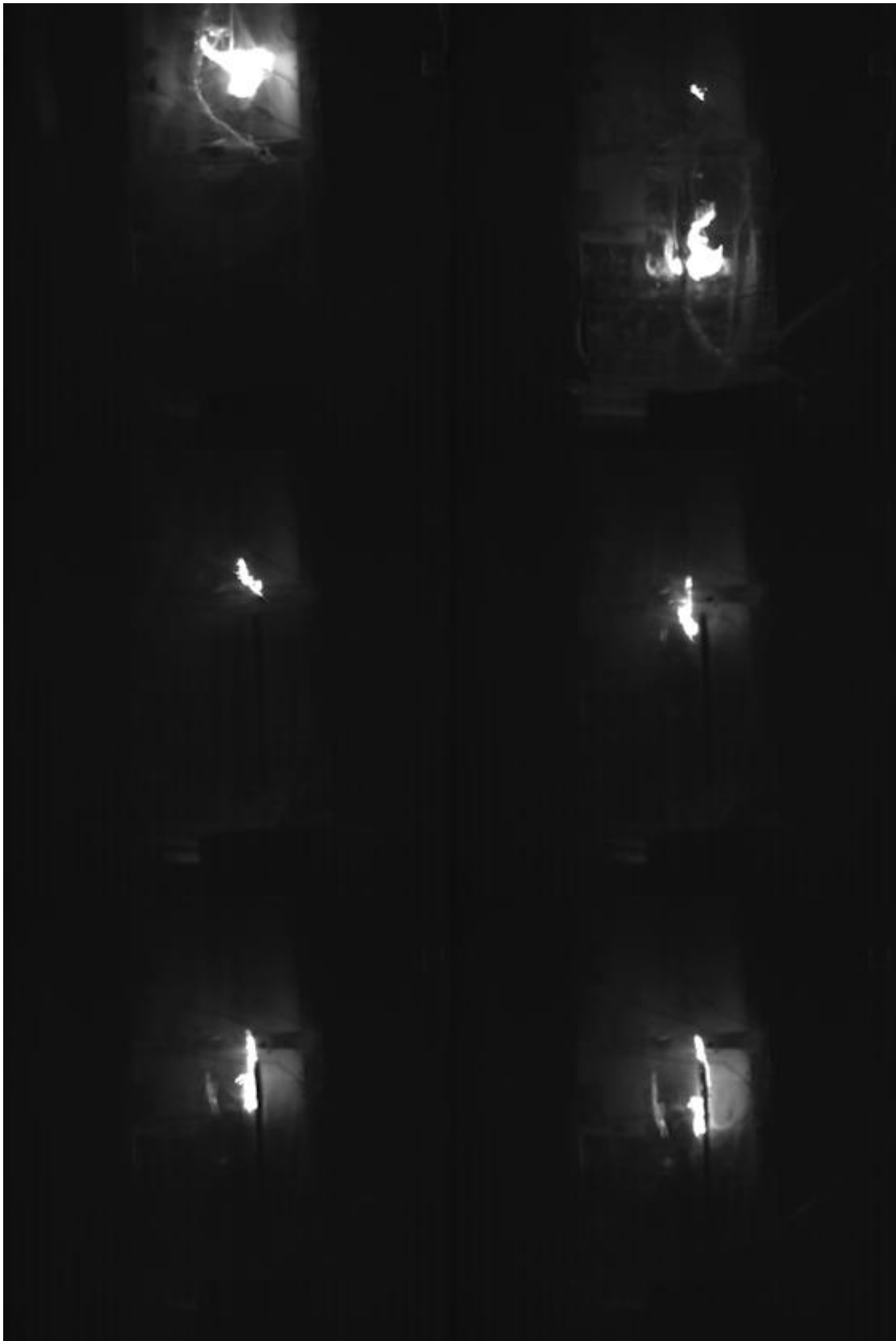


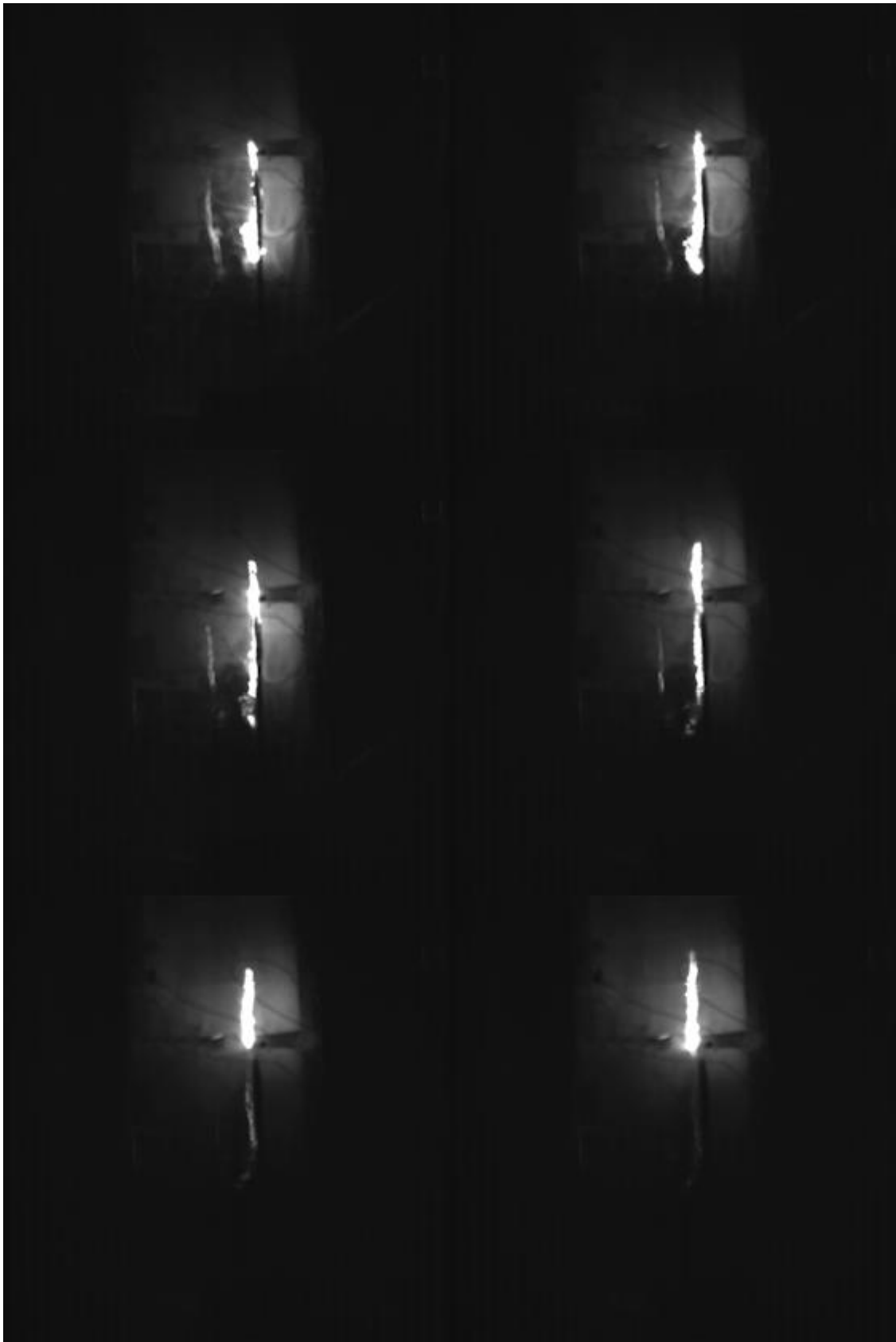


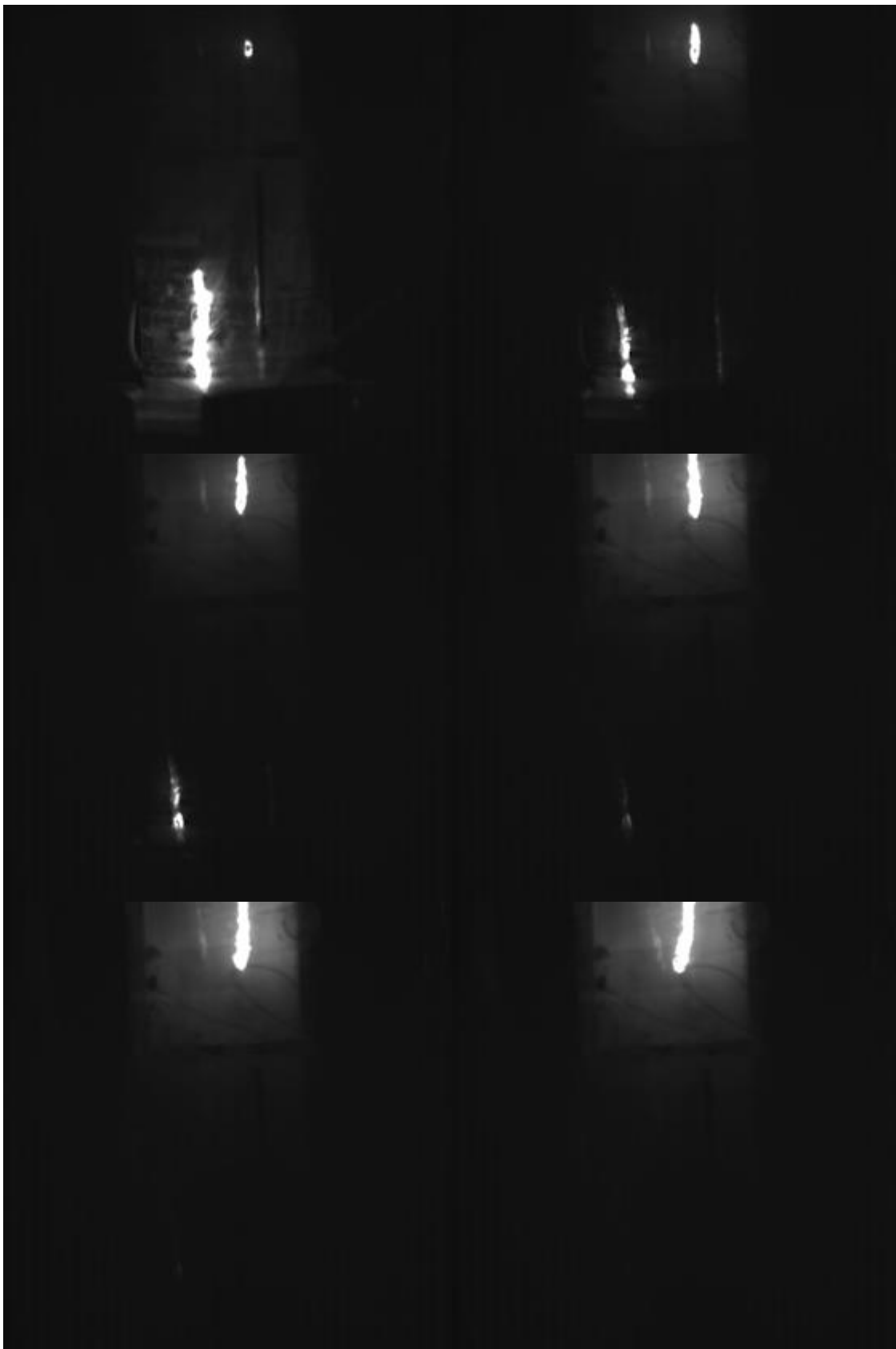


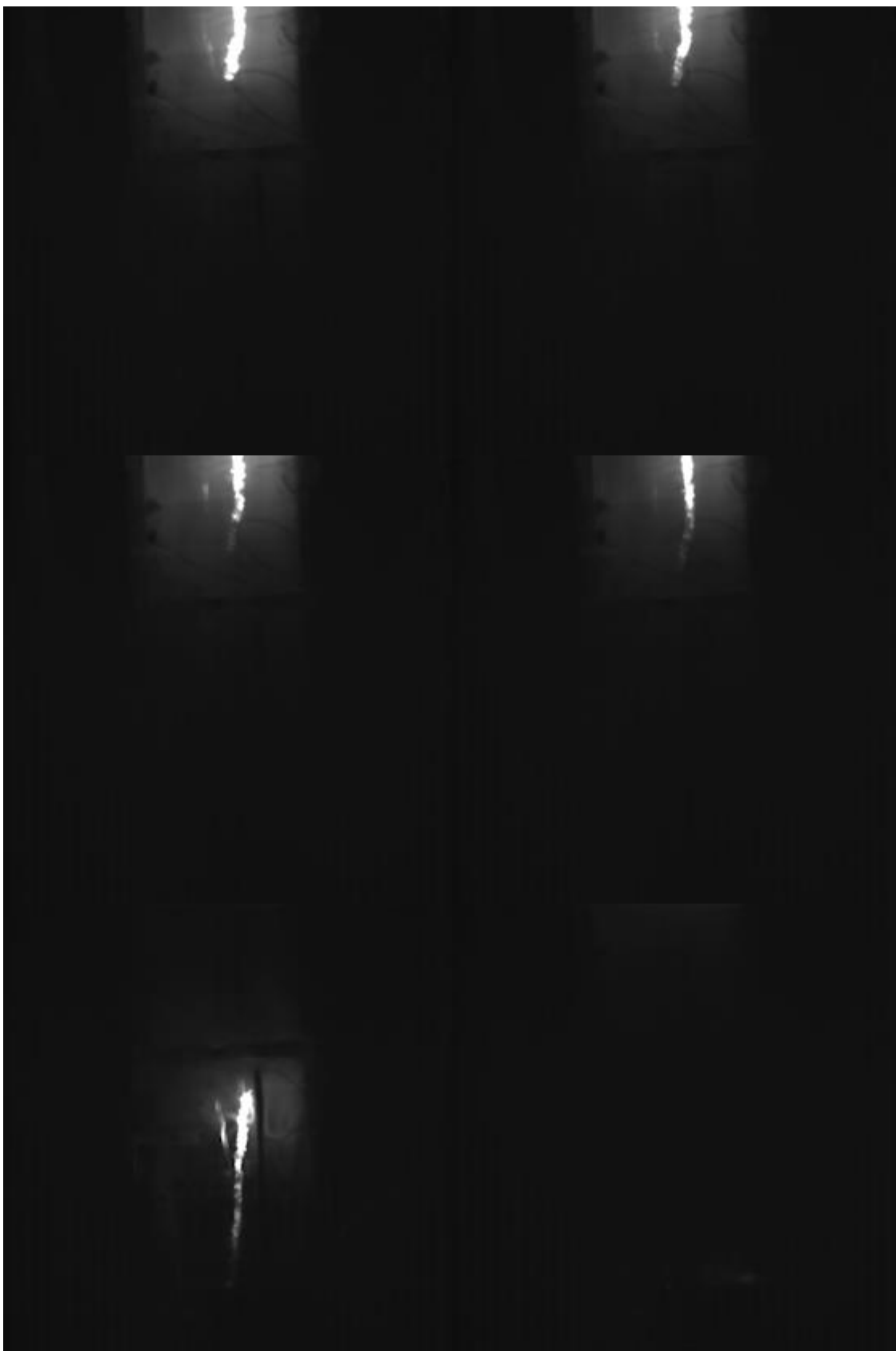


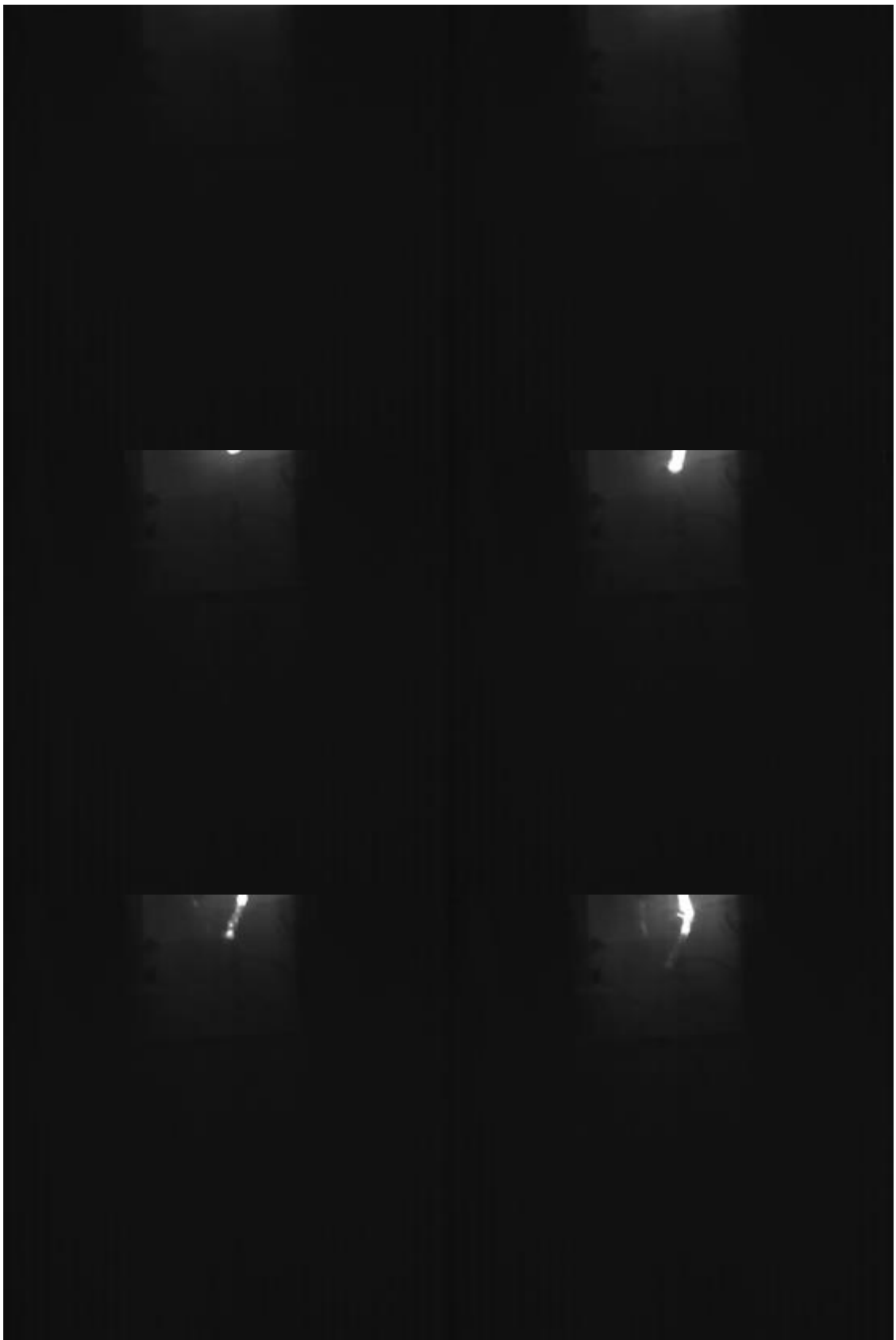


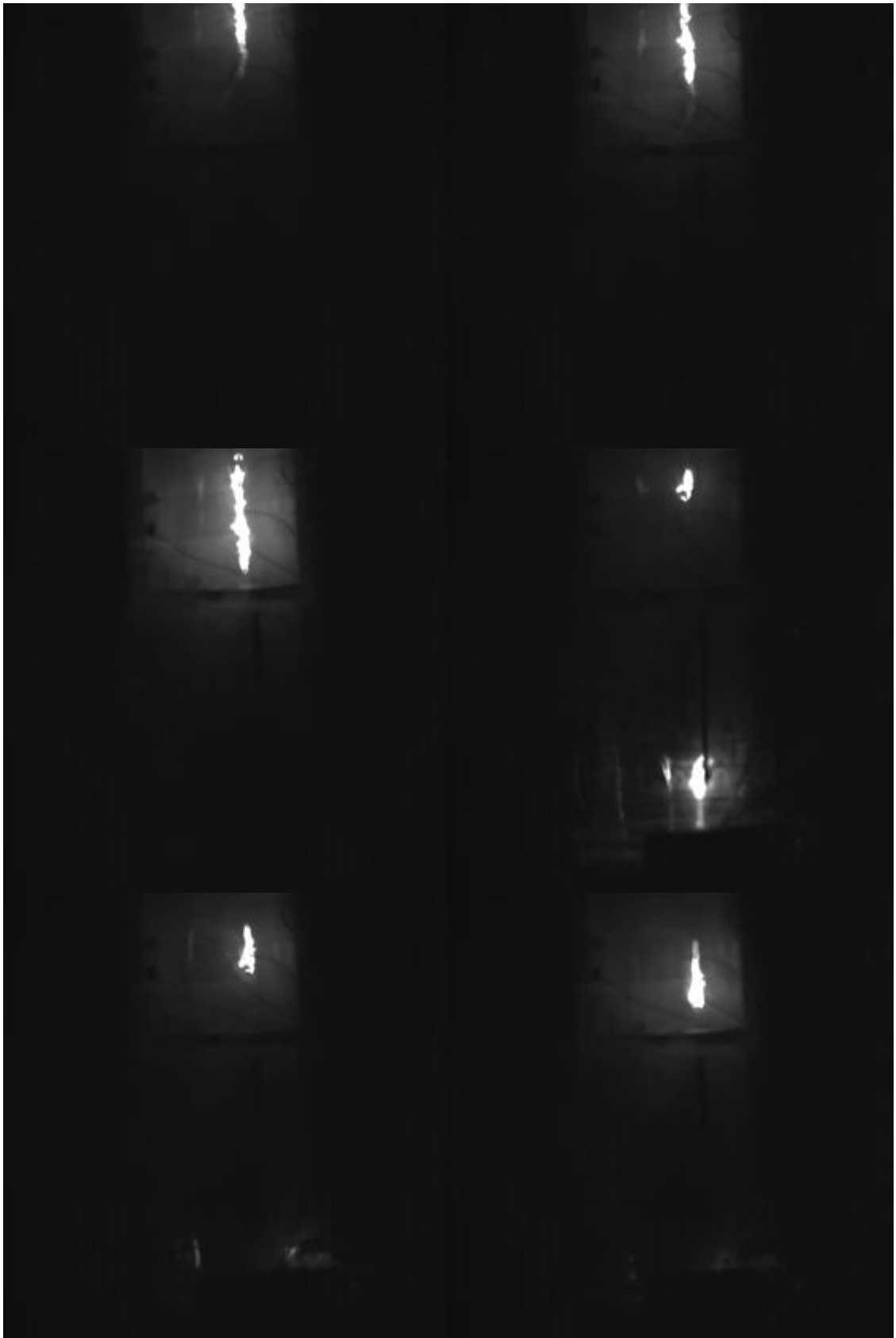


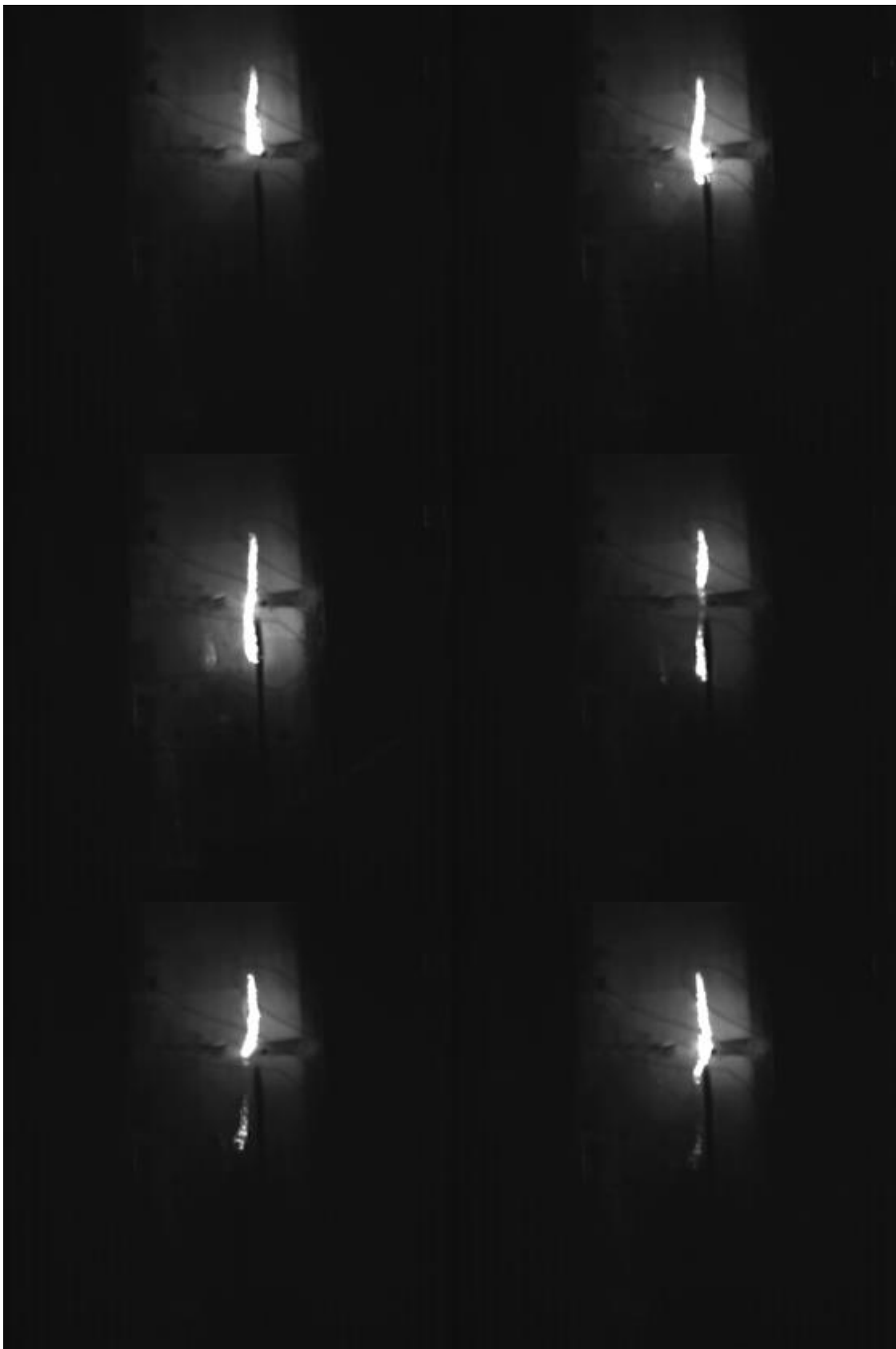


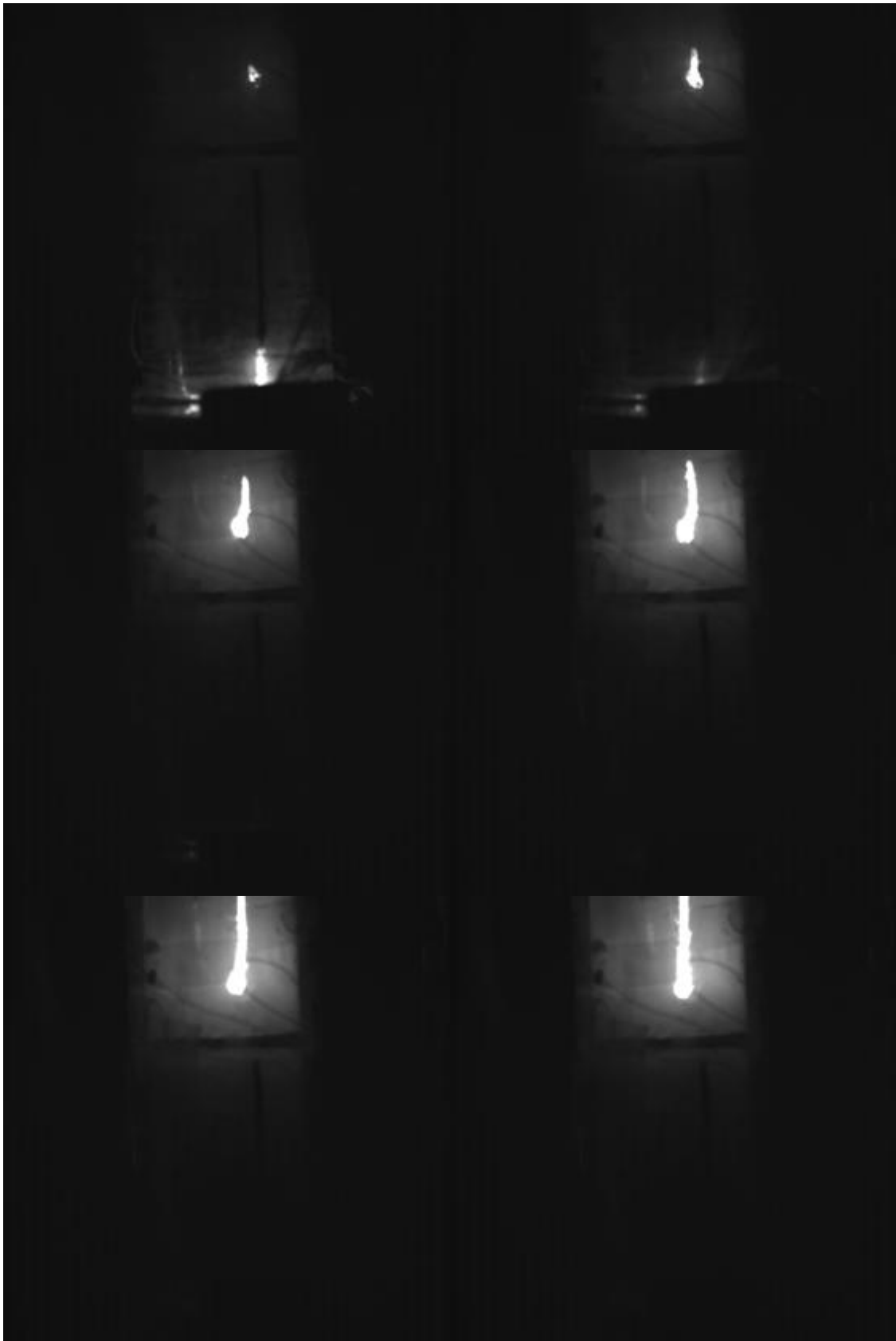




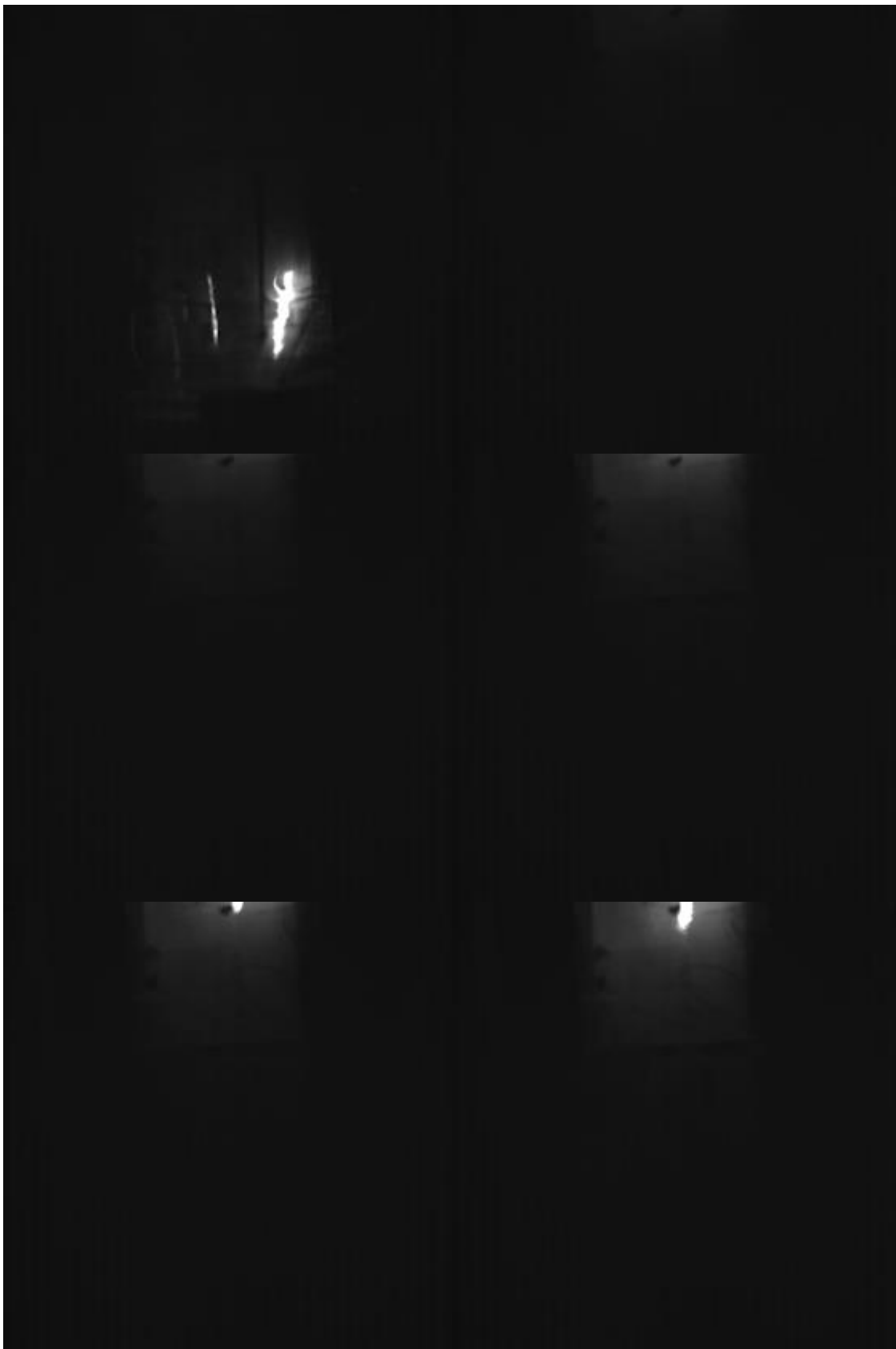


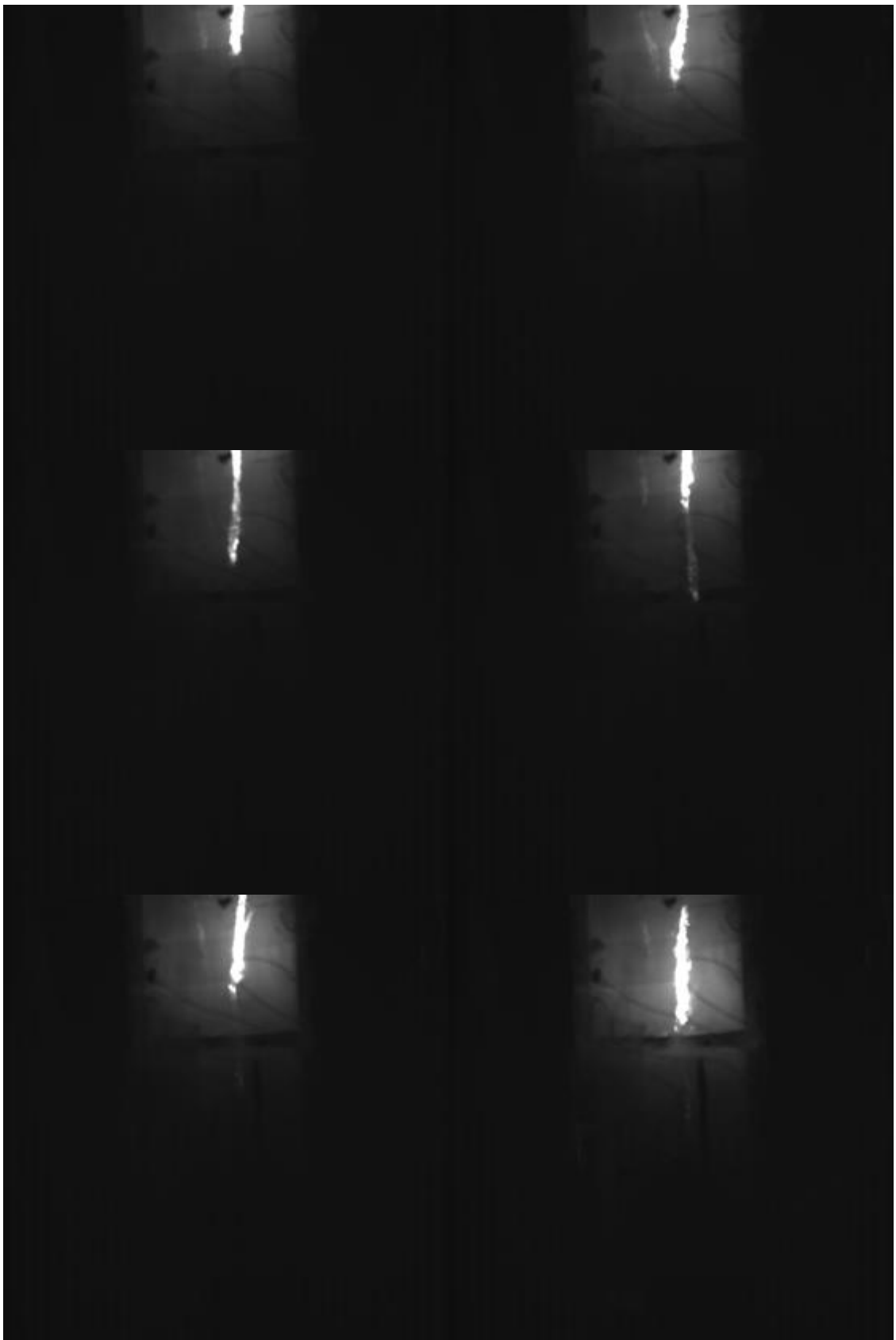












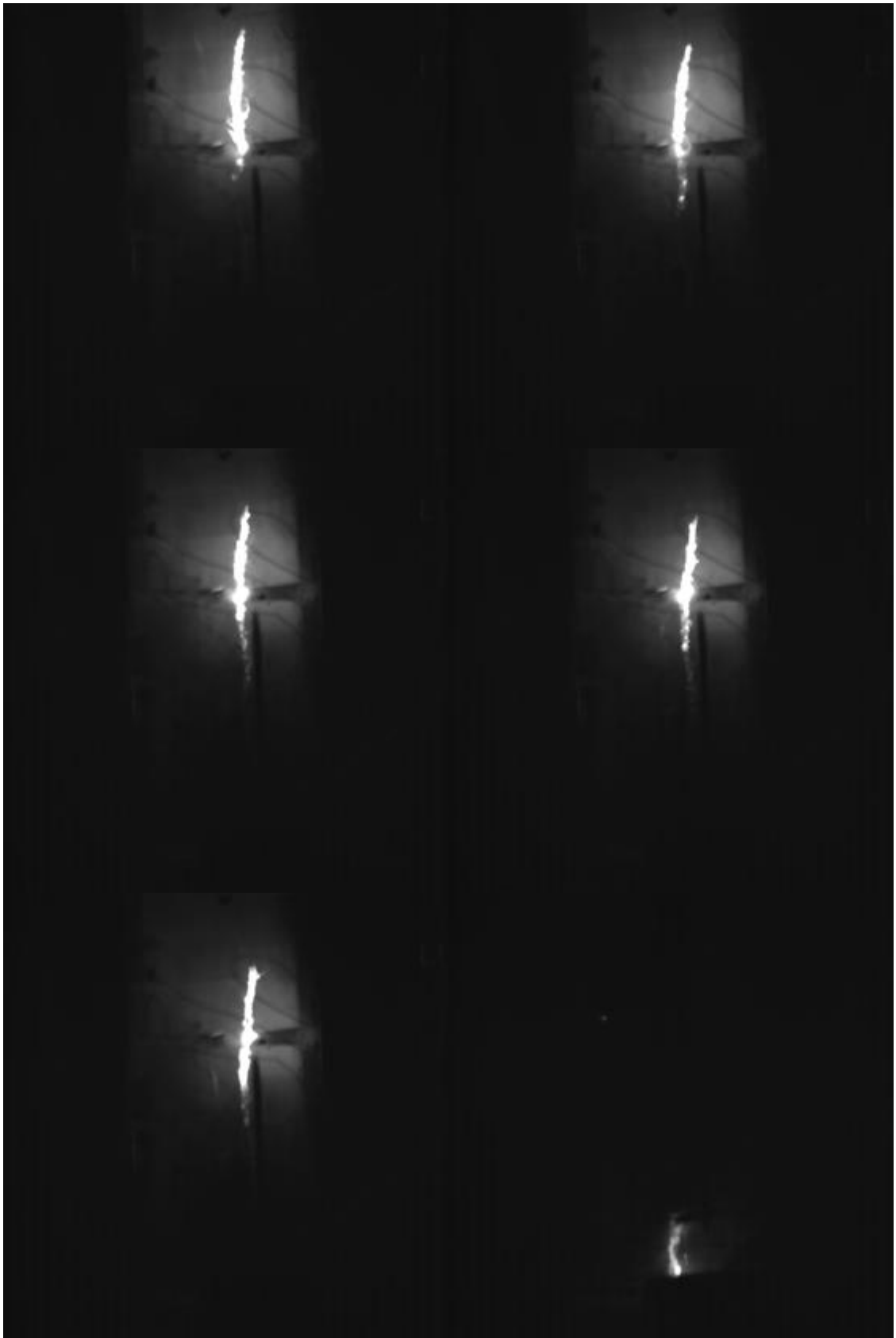


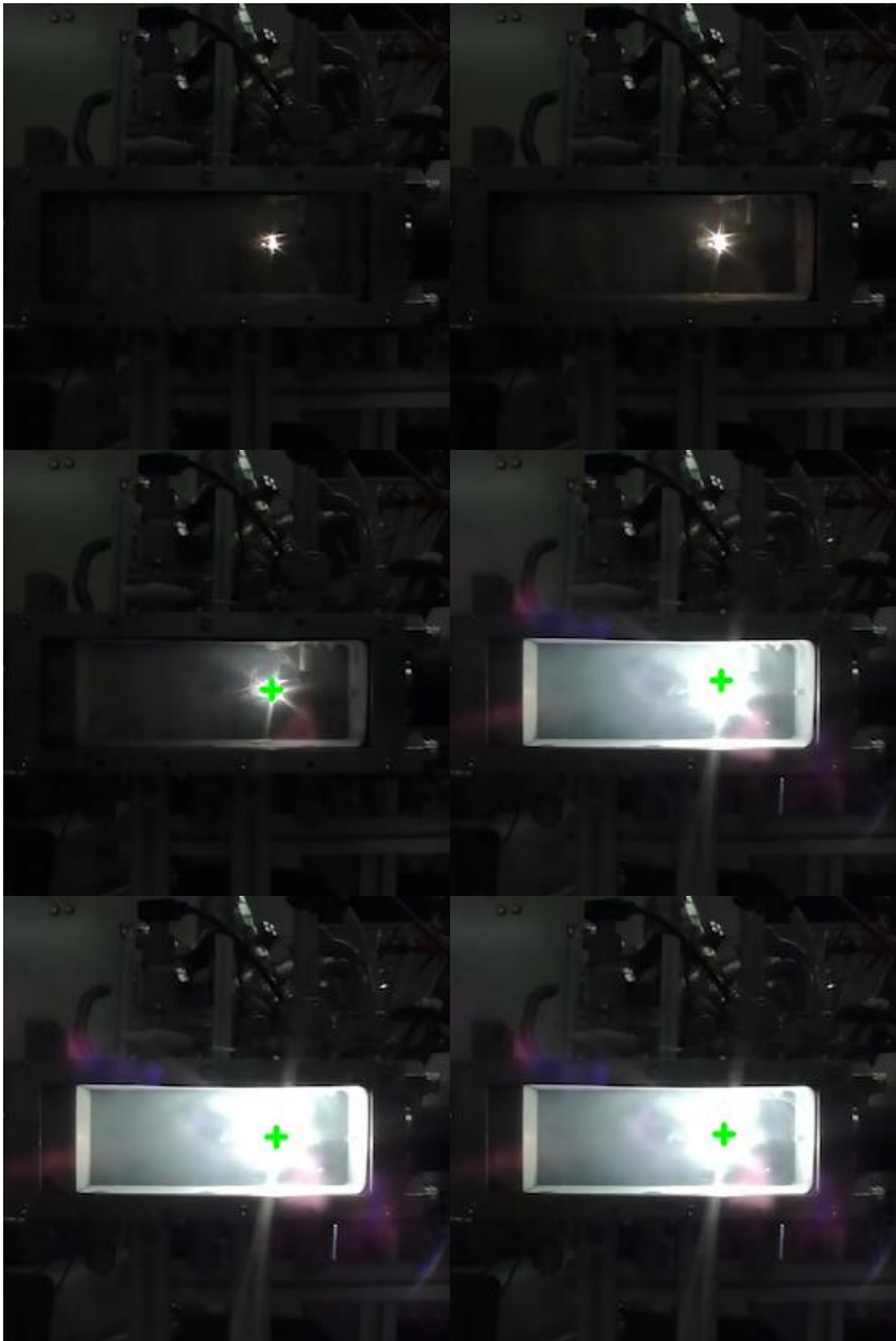


Figure 4.15 Highspeed camera footage 2

4.4 BBM thruster results

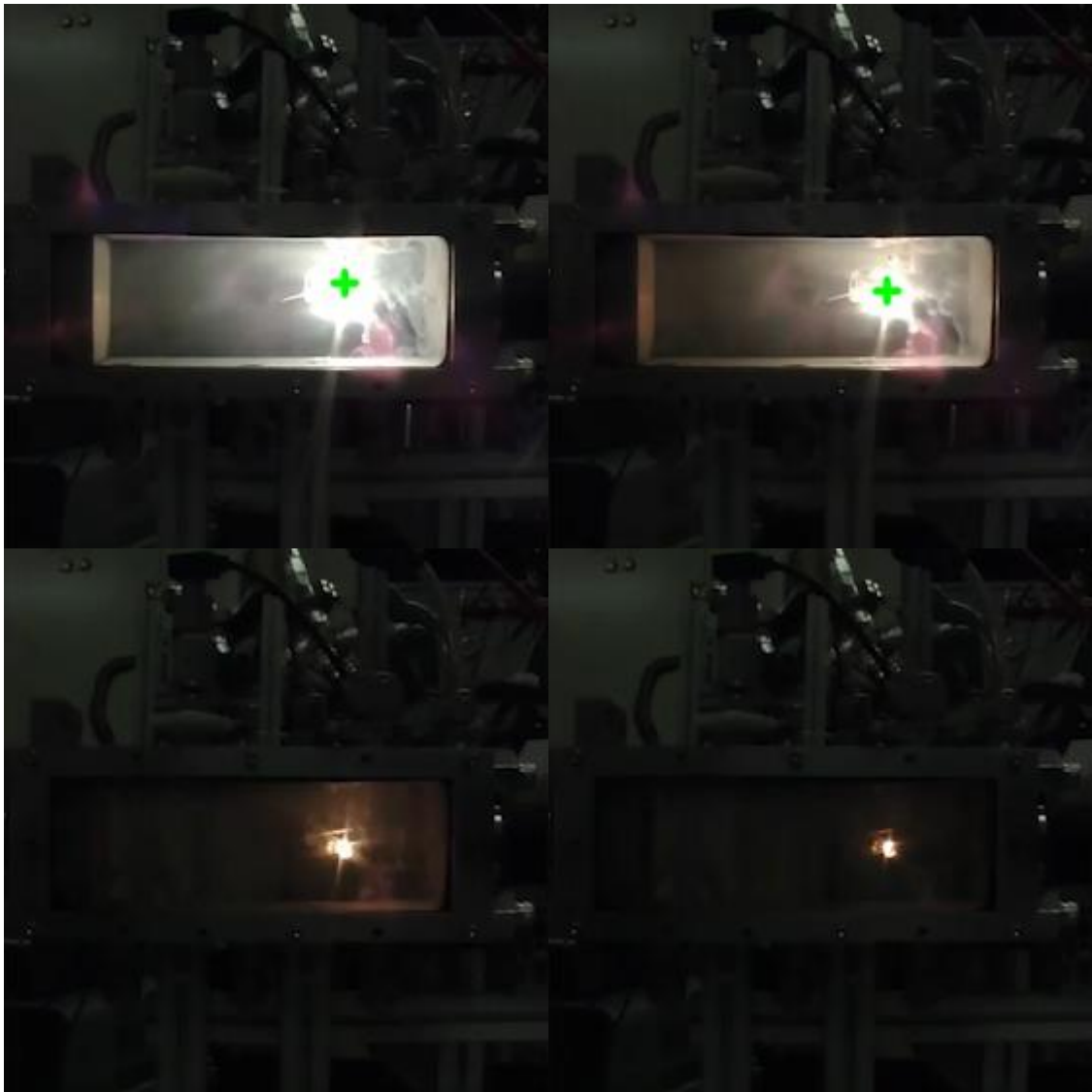
4.4.1 Closed system

Ignition was successful but sustained combustion was not. Combustion stopped by itself, lasting approximately 4 seconds.









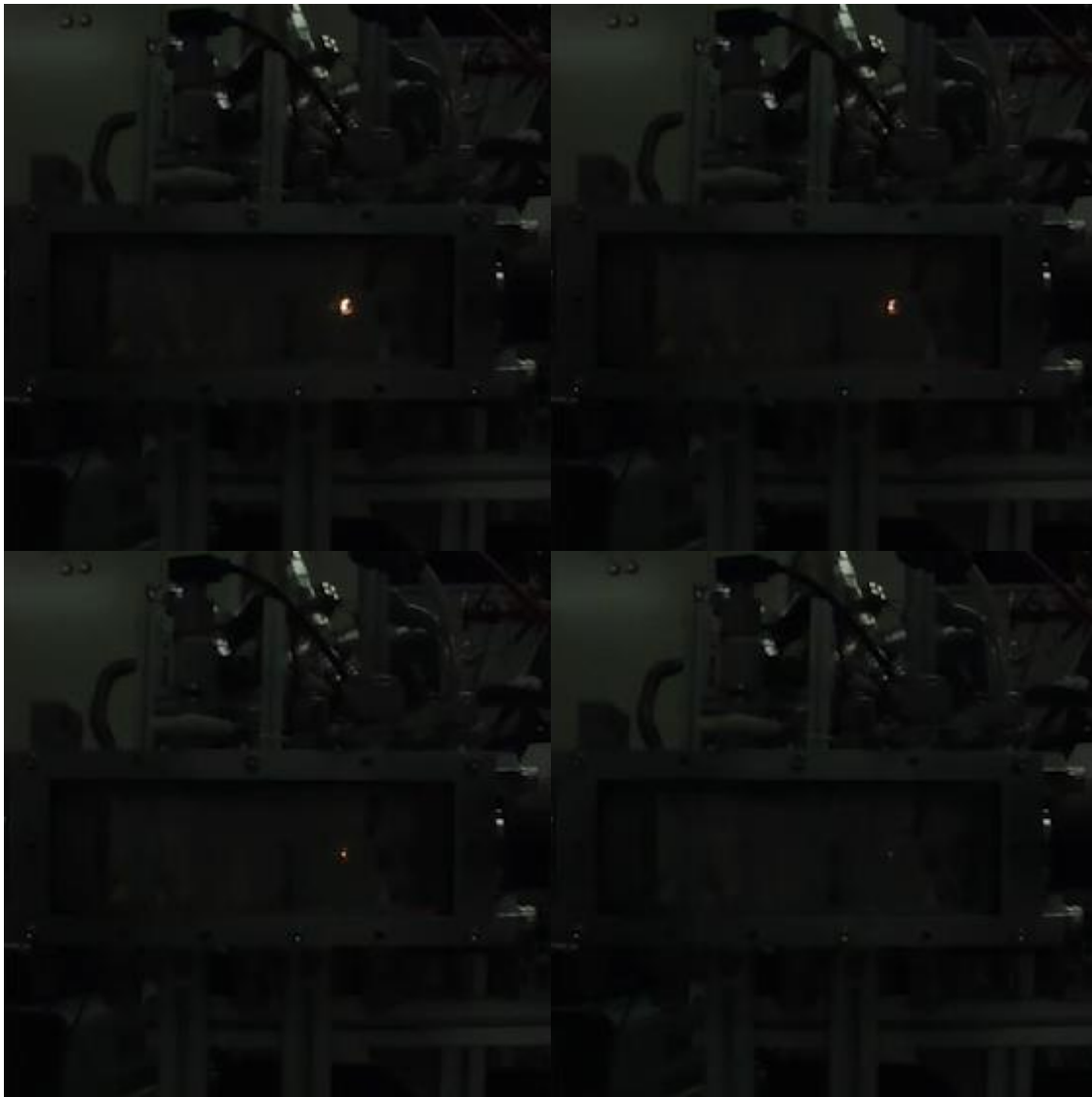


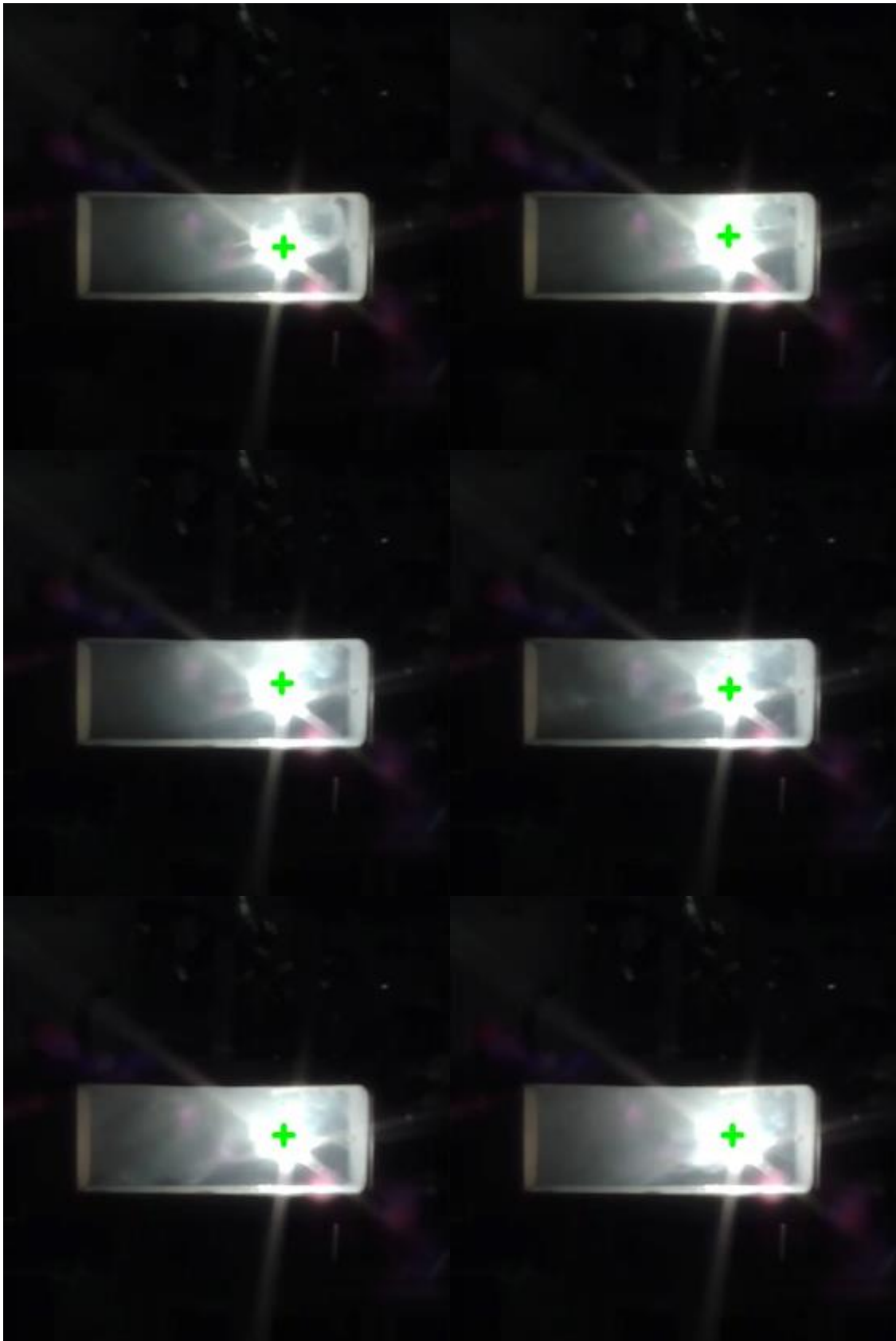
Figure 4.16 BBM closed system combustion

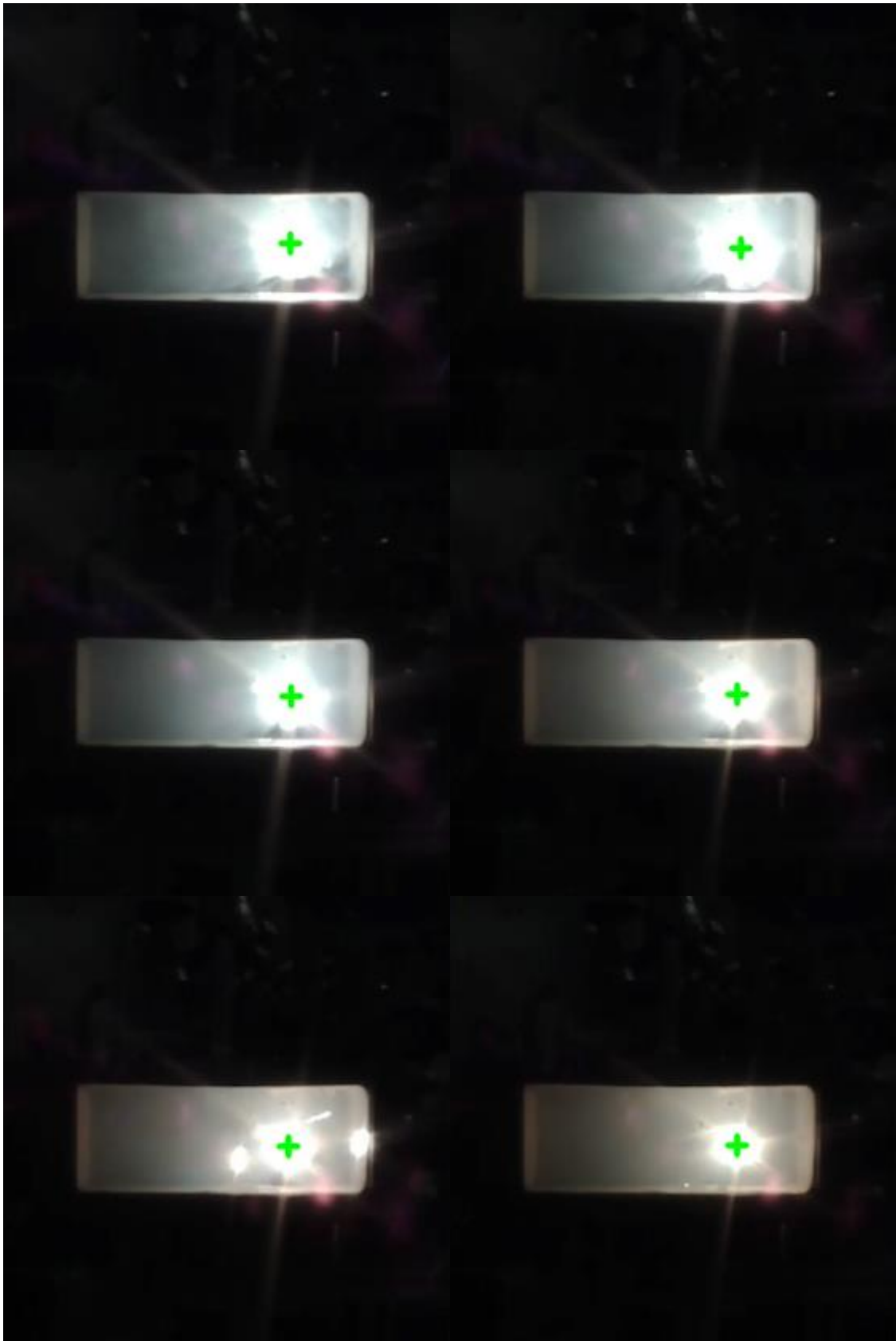
4.4.2 Closed then open system

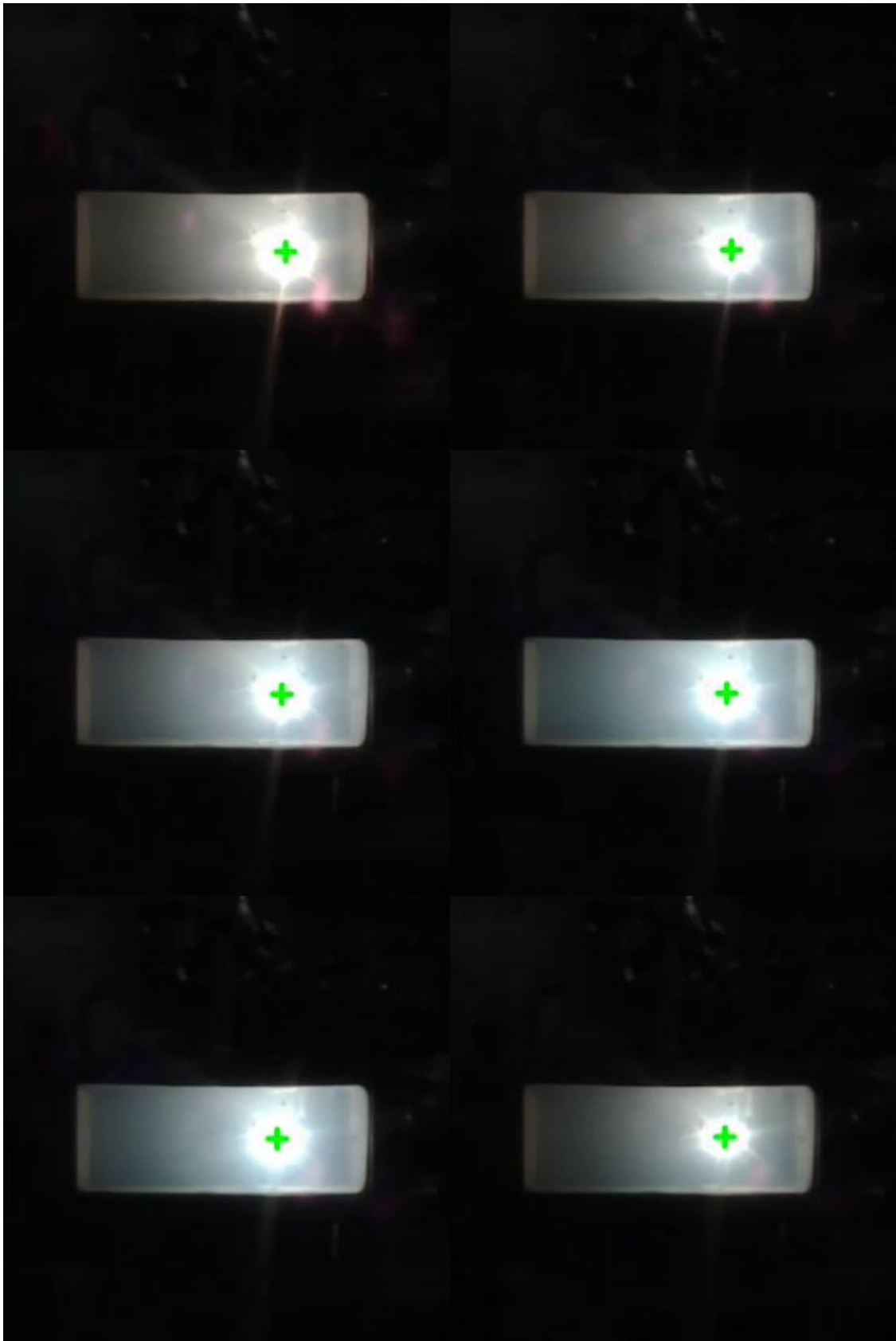
Ignition successful and no significant improvement over closed system, over approximately 10 seconds. Stopped by itself lasting approximately 10 seconds.

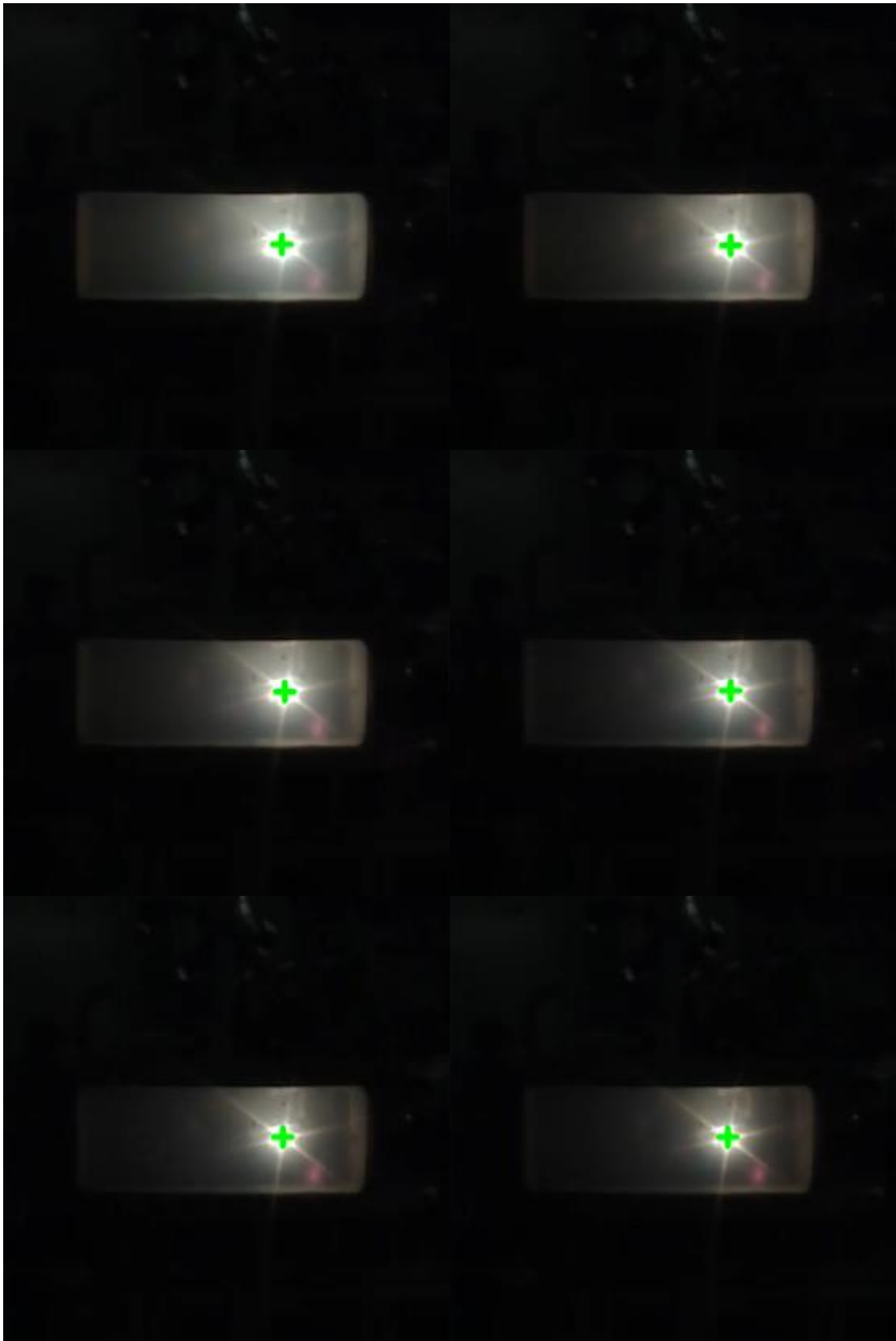


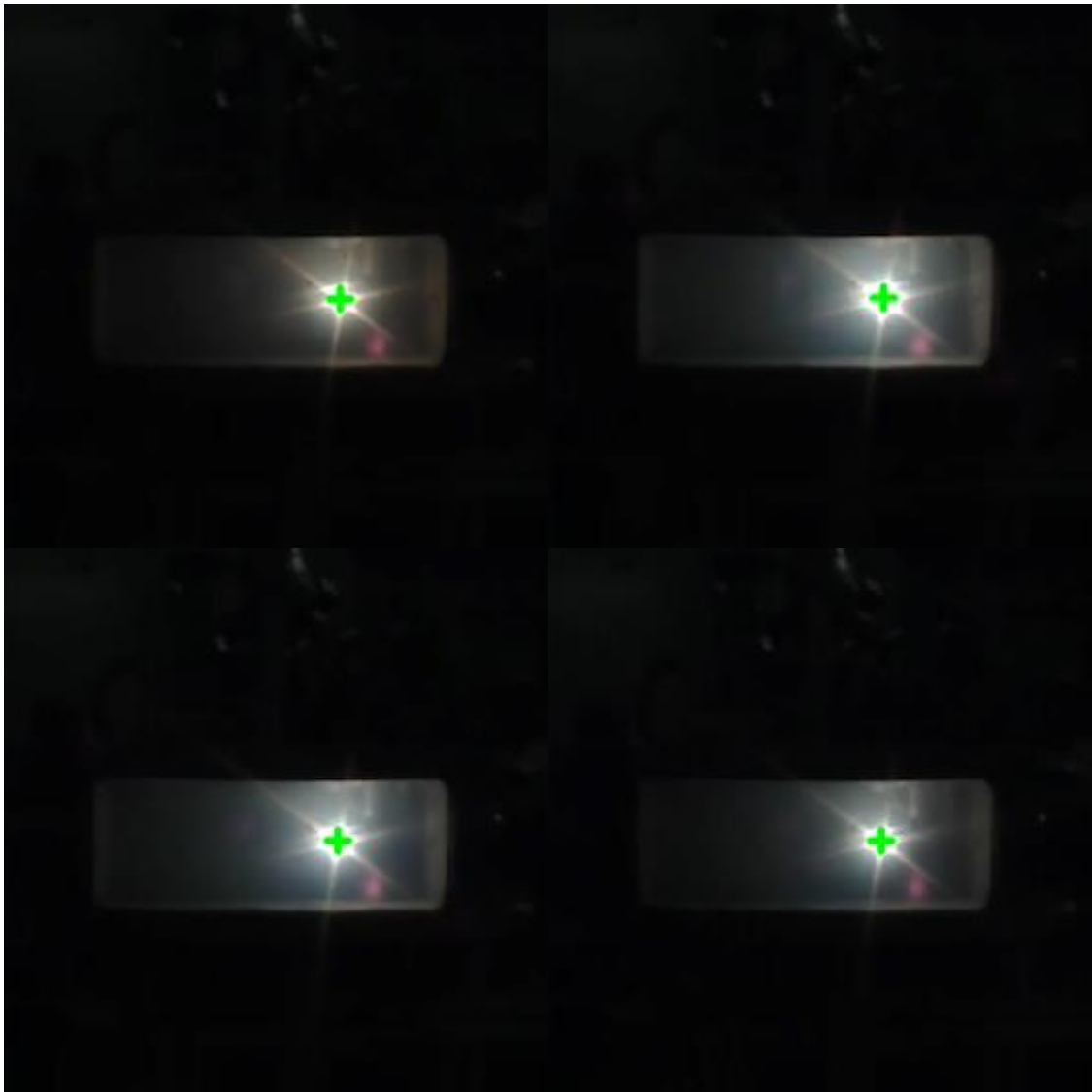












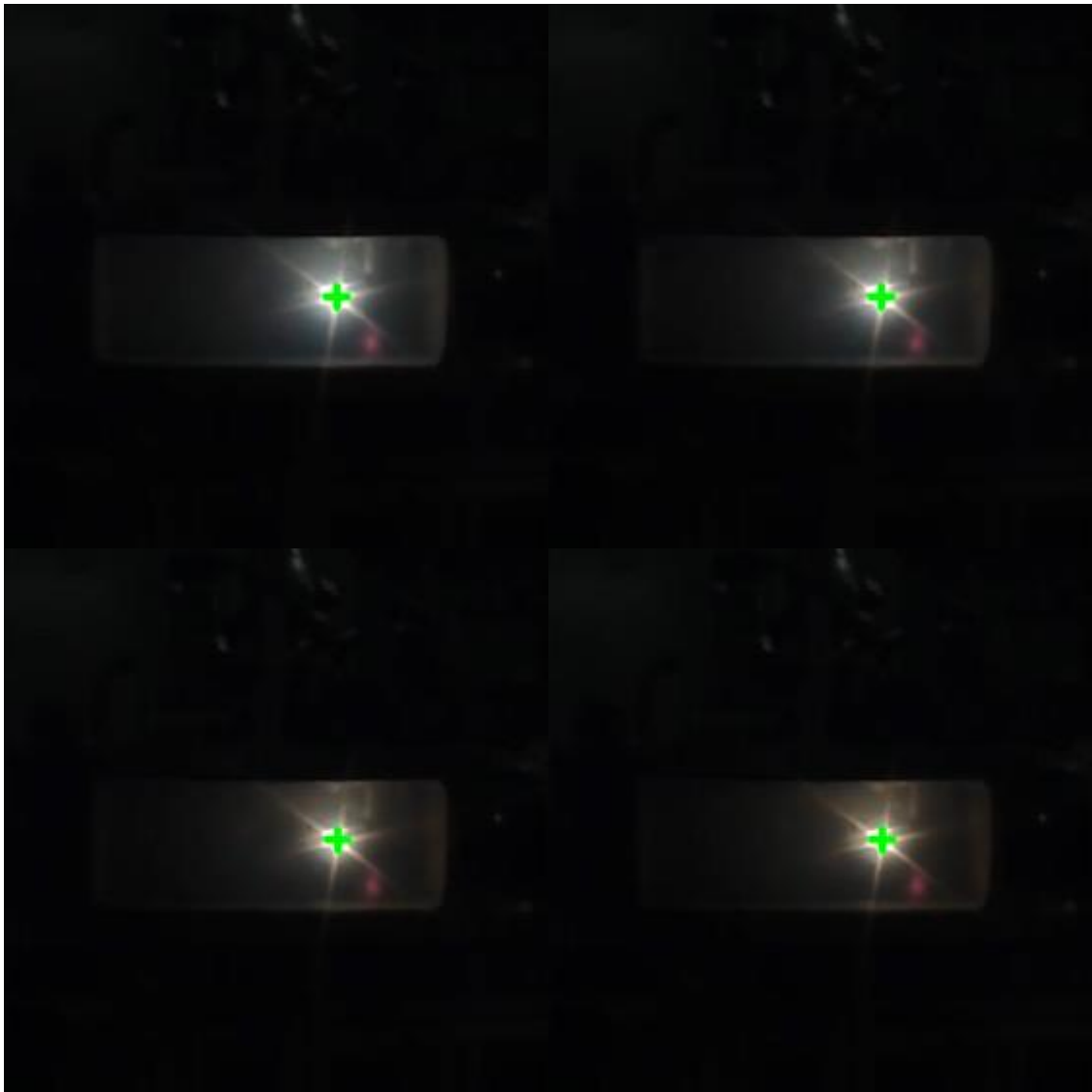




Figure 4.17 BBM Closed to open system combustion

4.4.3 Open system 35kPa

The wires failed to ignite over discharge duration of a few minutes.

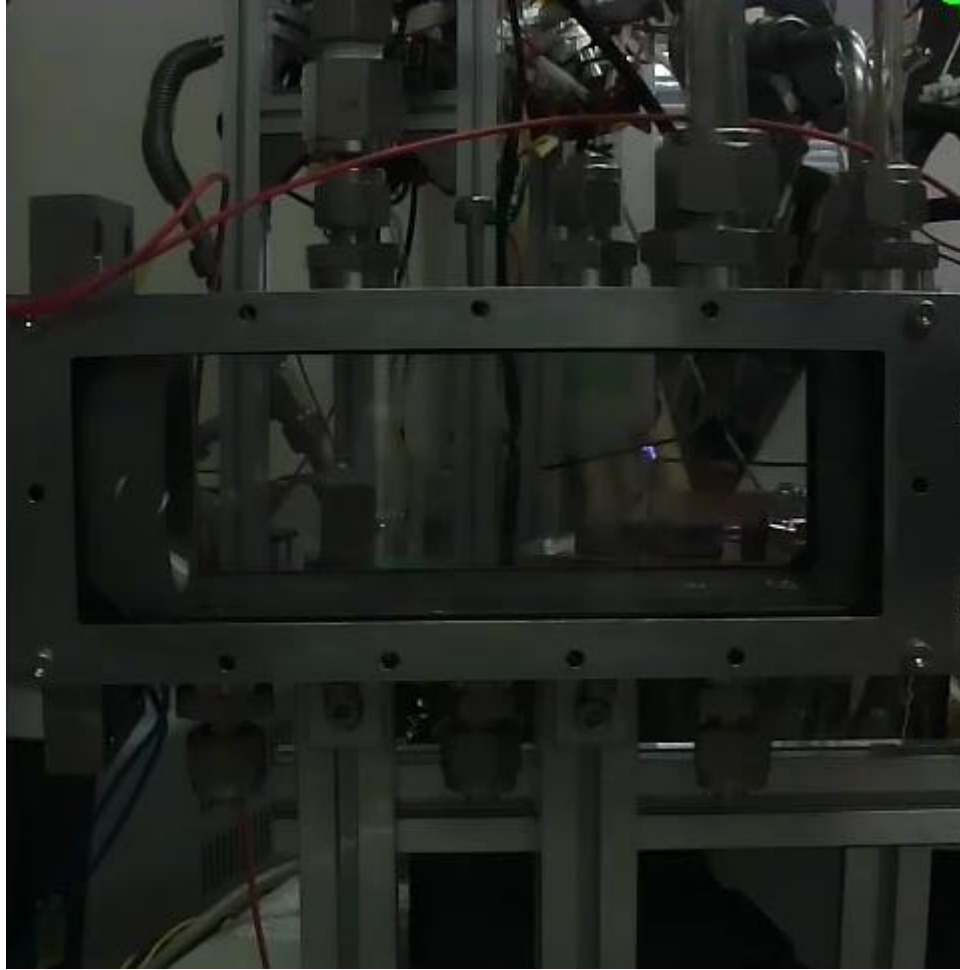


Figure 4.18 Open system failed ignition

4.4.4 Residue

Residue was formed where it barely hangs off the unburnt wire. Approximately 1 cm of wire was burnt in configuration 2 and 4 mm burnt in configuration 1. The wire formed a similar shape due to melting and force of gravity.

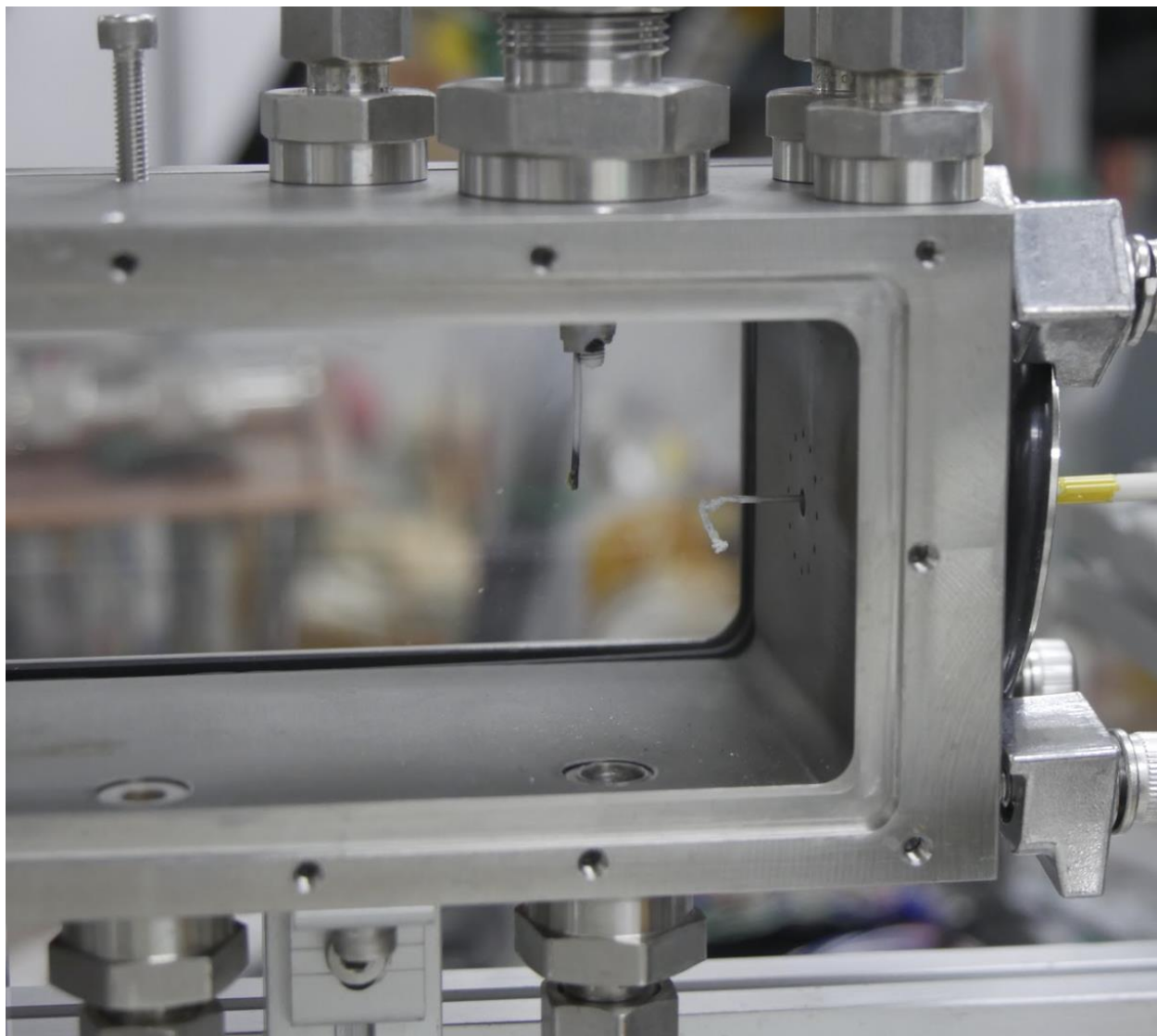


Figure 4.19 Residue shape example for both case 1 and 2

5. Analysis

5.1 Sustained Combustion results

Before the introduction of the automated control system, the longest record of sustained combustion achieved was approximately 2 minutes. The first introduction the control system resulted in a record of 1 minute.

With gradual implementation of optimizations. The longest successful combustion of 4 minutes was achieved. The feeding rate history of the combustion is in the figure.

5.1.1 Convergence

The convergence is quite slower than what was expected. In adequate PI parameters could be one of the reasons. PI parameters that are too large can lead to diverging oscillations or failure to converge at all. However, changing the PI parameters didn't improve the stability.

5.1.2 Oscillation Hypothesis

There could be factors outside of the control system that is contributing to the slight oscillation. This study hypothesized a few.

First, the combustion condition is not a constant. While the water vapor temperature and pressure is setup to be consistent, this is only true when there isn't a combustion. The flow rate can change during the combustion.

Second, the flow path of this experiment setup may have contributed to oscillation. In the experiment setup, the wire combustion direction is the same as the water flow direction. The feeding direction is opposite to the water flow direction. Because the fuel before combustion is downstream of the post combustion gas, the amount of oxidizer that is available to sustain combustion is dependent on how much is consumed already. The amount of oxidizer consumed is dependent on the combustion rate. The phenomenon can be explained by the figures below. Initially, just after ignition, combustion chamber only contains water vapor. During this moment, the wire combustion rate is the highest. However, due to the higher combustion rate, the amount of oxidizer available for the next segment of fuel is therefore lower, resulting in a slower

combustion. In the second figure, it shows the case where there is already a slower combustion. Because of the slower combustion, more oxidizer is available for the next segment.

This hypothesis could not be tested with the experiment setup available because the test bunch was not designed to allow the change of combustion chamber direction, water flow direction.

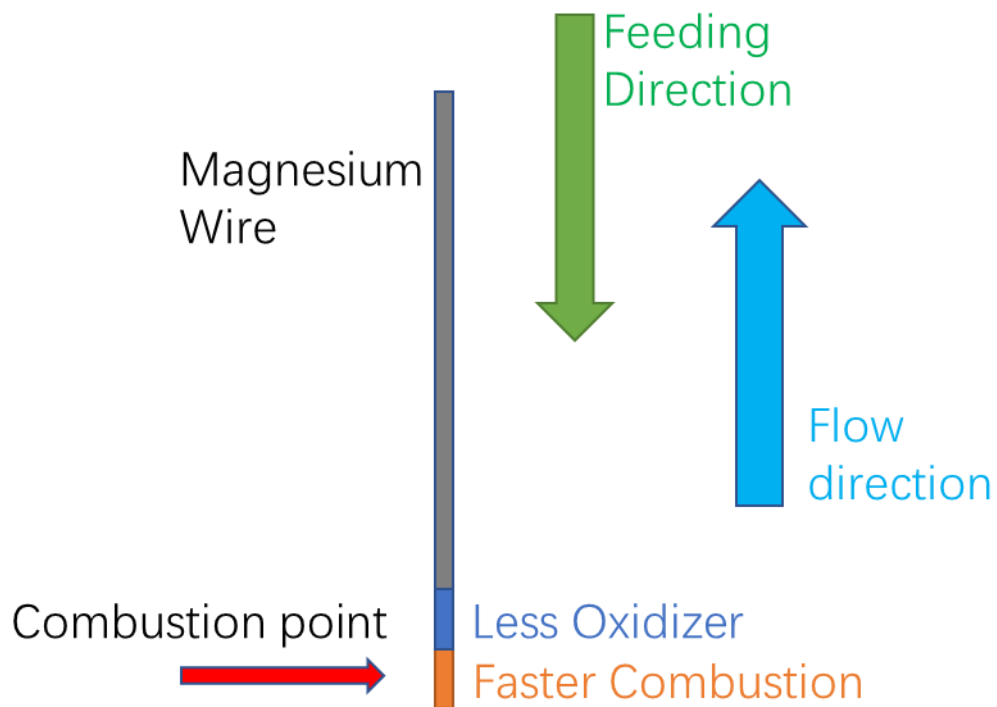


Figure 5.1 Oxidizer relation state 1

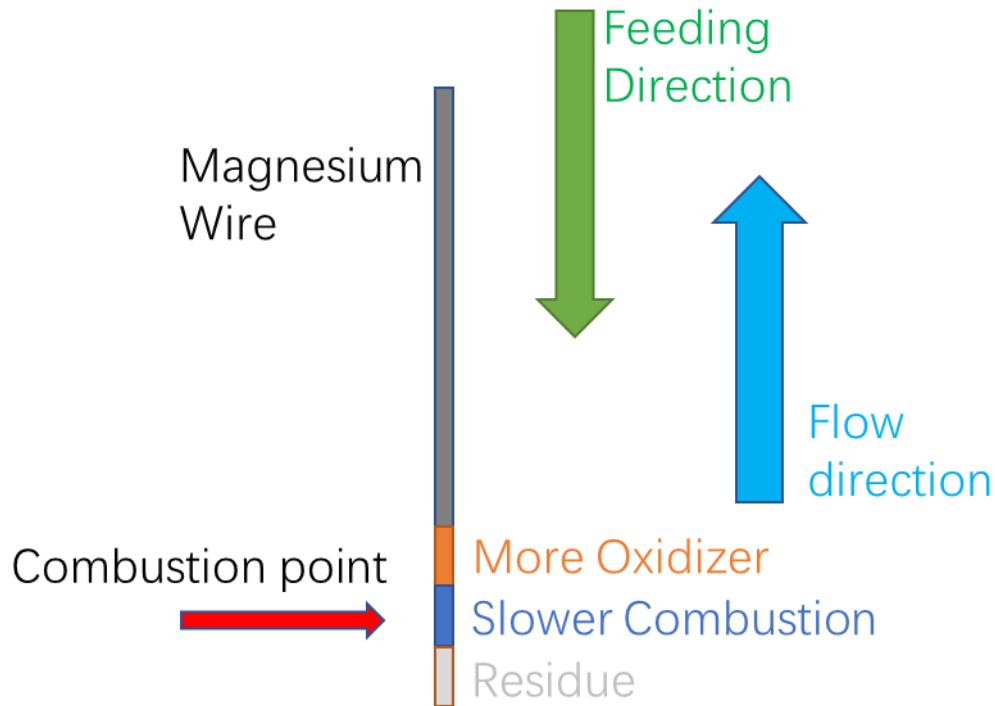


Figure 5.2 Oxidizer relation state 2

5.2 Combustion behavior

5.2.1 Ignition

Ignition detection was successful. Control program successfully stops discharge after ignition.

Figure 5.1 shows the state of the combustion chamber before discharge signal. In this state the control program searches for an ignition.

Figure 5.2 shows the discharge. Discharge shows up as a bright dot but it is small enough to not be recognized as ignition

Figure 5.3 shows the discharge just before ignition. There is usually a green flash just before the combustion.

Figure 5.4 shows the green flash from a prior study. This flash is quite apparent during experiment to naked eye.

The green flash was thought to be the Magnesium Oxide reacting at first. Magnesium however burns a color of bright white. Tungsten burns the color of green however. This unknown aspect does not interfere with sustained combustion as the discharge stops after ignition.



Figure 5.3 Combustion chamber before discharge

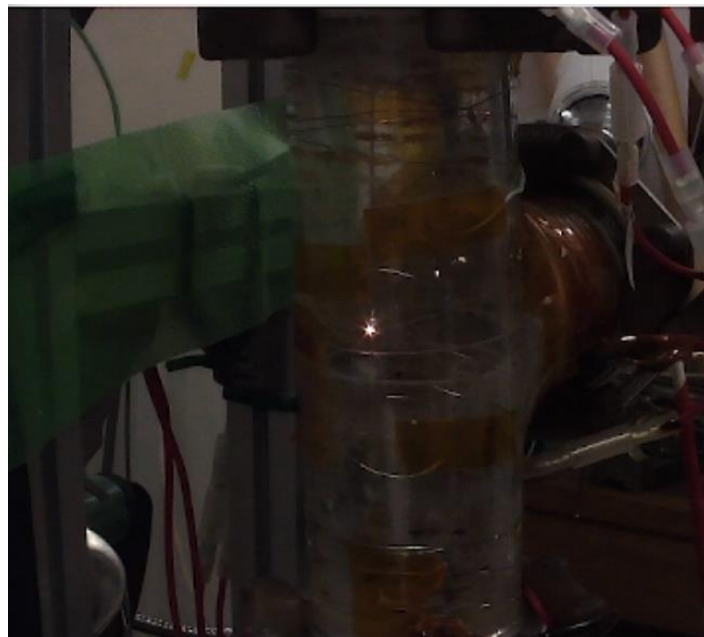


Figure 5.4 Discharge

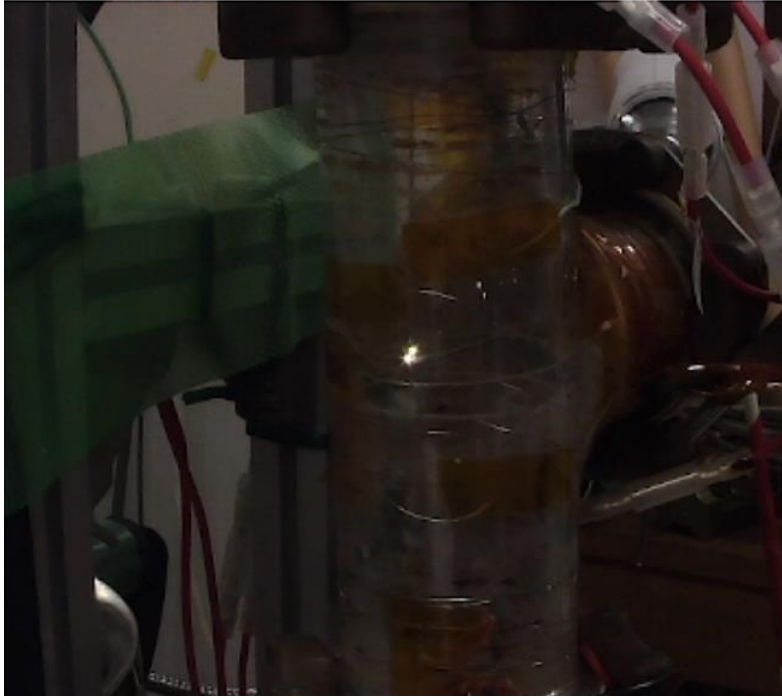


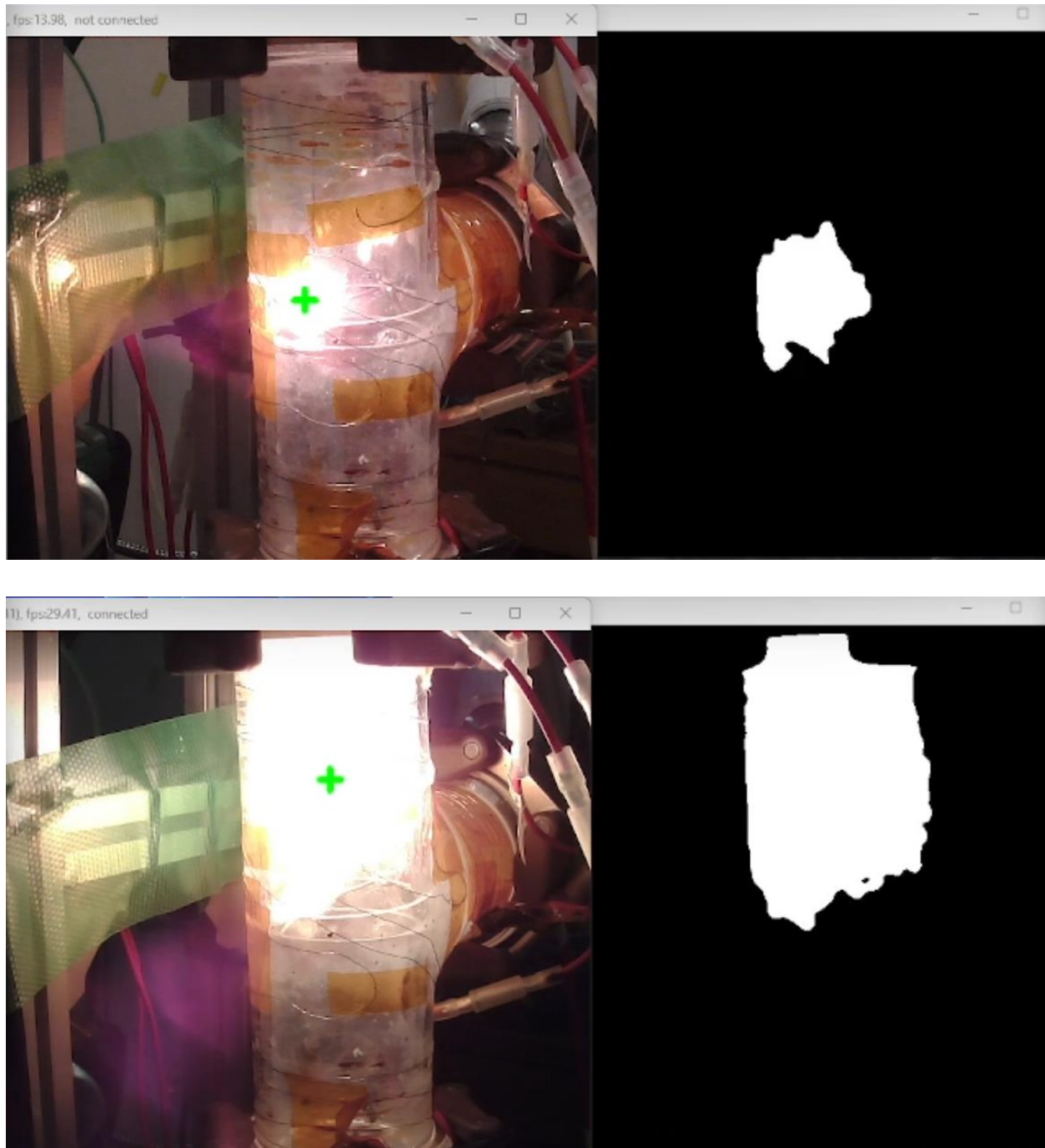
Figure 5.5 Just before ignition



Figure 5.6 Different experiment with green light

5.2.2 Flame tracking

Figure 5 shows the state just after ignition. It can be seen that the ignition was successfully detected and tracked. Figure 5 shows the frame just after ignition. Figure 6 shows the frame during sustained combustion.



Before the setup of the current experiment setup and control systems, the assumption for the behavior of wire combustion is that the combustion occurs on the very tip of the wire as a single point, similar to the combustion just after ignition. Video taken during the combustion showed that this is not always the case. The bright spots can and will fill up the combustion chamber. ND filter was adjusted so to avoid such saturation but it did not improve. Figure 7.7 shows an

example of the state of combustion during one of the experiments where ND filter was set to block more lights.

The control program assumes that the combustion point is a glowing sphere. In the figure, the combustion point occurs along the entire wire. The Flame Tracker is able to successfully track the center of the glowing area but the center of glowing area is not necessary the point of combustion.

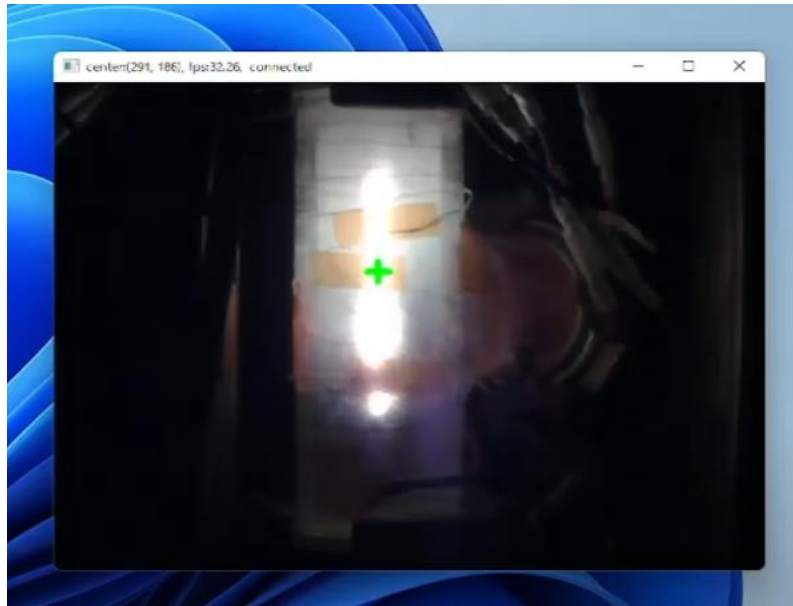


Figure 5.7 Wire combustion

It is assumed that the combustion is not uniform after this observation. What likely is happening is illustrated in the figure 7.8. The figure on the left shows what was expected in the previous study. The figure on the right shows the possible distribution of the combustion. At the tip of the magnesium wire, the combustion is nearly all complete so all that is left is residue. At locations slightly higher, combustion on the exterior just started.

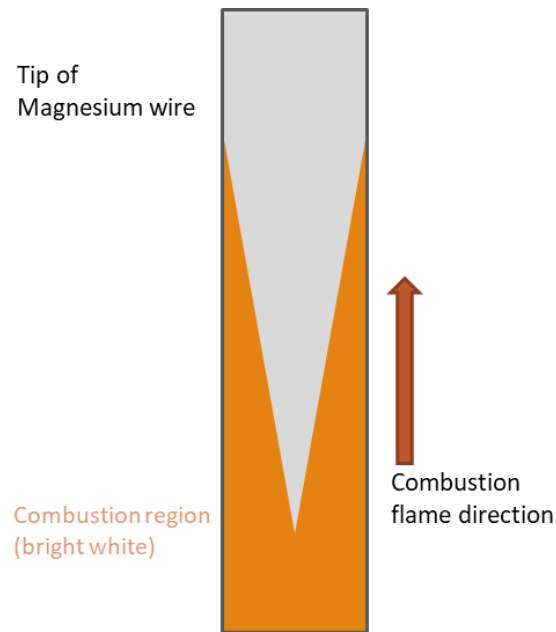


Figure 5.8 Combustion profile speculation illustration

One of the factors that could be contributing to this behavior is that the combustion gas is going up due to the gravity. This might be accelerating the combustion in a way that is specific to this orientation.

5.3 Combustion rate and Pressure

Combustion rate for each pressure is obtained from the encoder reading data during combustion. Feeding rate during each combustion is averaged to obtain the data. Because of some temperature and pressure fluctuations, pressure is also averaged. The data is shown in table and figure below. The color indicates the temperature the tank was set to, it does not represent the actual water vapor temperatures.

Data set	Combustion no.	Pressure /kPa	Feeding rate /mgs-1	Stddev /mgs-1
	1	41.52	38.47	52.65
45kPa	2	45.62	44.45	38.80
	3	47.06	54.13	38.14
	4	45.37	52.22	39.85
	1	42.64	47.21	36.46
35 kPa	2	33.42	33.96	41.59
	3	32.91	43.50	55.21
	4	51.75	32.69	30.74
25 kPa	1	23.03	37.34	29.88
	1	16.51	28.21	33.06
20kPa	2	17.07	39.76	27.79
	3	21.50	15.15	17.85

Table 7.1 Feed rate over various vapor pressure

Error bar in on the graph shows the standard deviation of the feeding rate. From the graph, it can be inferred that the combustion rate increases when the water vapor pressure increases.

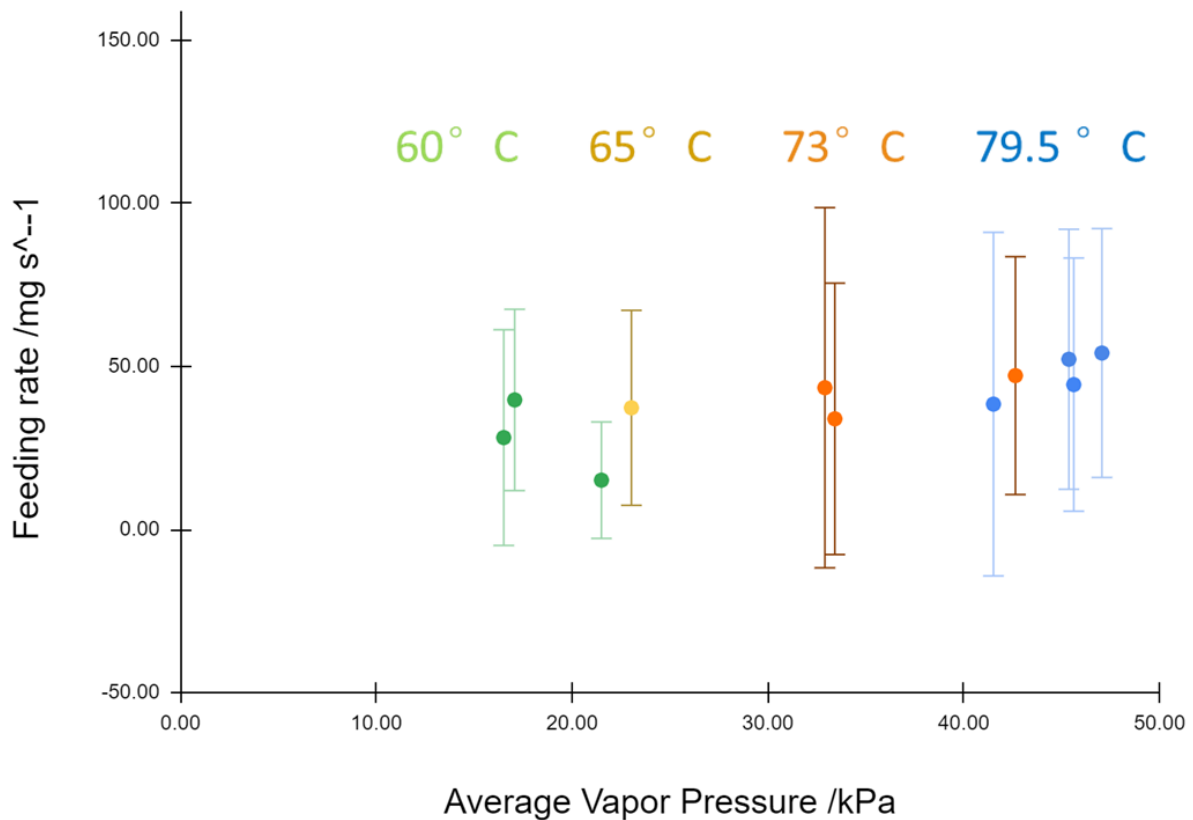


Figure 5.9 Feed rate over various vapor pressure

5.3.1 Observations

Combustion was not successful at pressure near 15 kPa. At 15 kPa, magnesium wire ignites but extinguishes within a second. 15 kPa is the lower pressure limit with the current experiment setup. Figure shows the all the combustion attempts with 15 kPa settings. Data from the flame tracker shows the observation as well.

The following graphs can be obtained from calculations of mass flowrate of water vapor when there is a choked flow at orifice. The relationship between mass flowrate and pressure is approximately linear. The combustion speed to mass flowrate relation should follow same trend as figure.

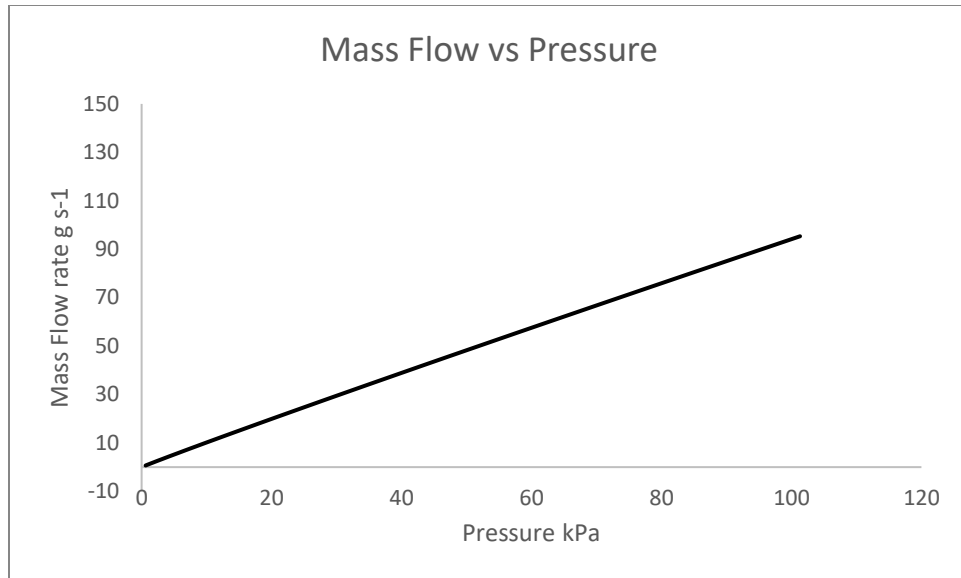


Figure 5.10 Mass Flow Pressure relationship

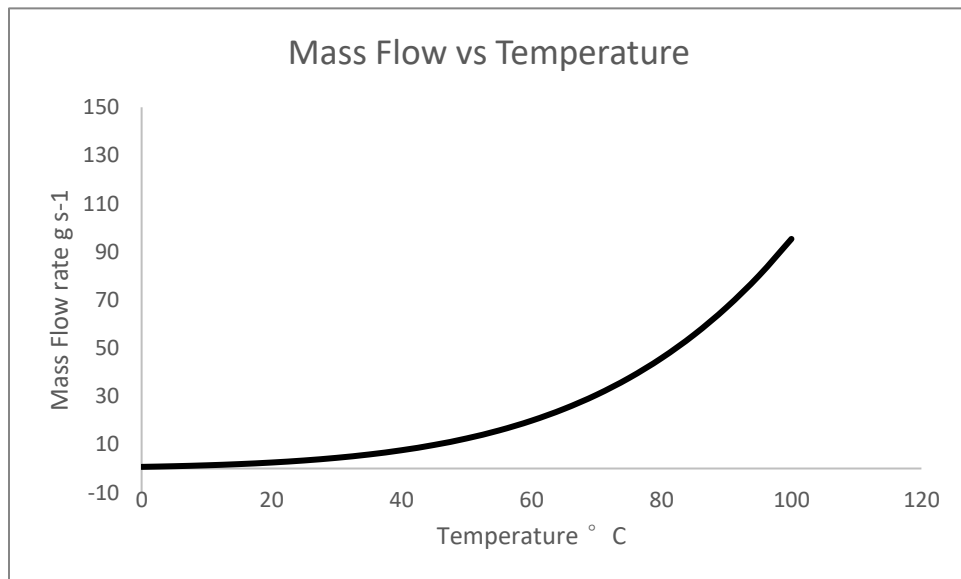


Figure 5.11 Mass Flow Temperature relationship

5.4 Combustion Efficiency / Residue

Efficiency is measured with the fuel efficiency measurement system. The efficiency was found to be close to 99%. Residue sample in all experiment cases resulted in minimal or no gas generation. Pictures of the residue are taken and shown below for some of the experiments. They show no difference in appearance from a subjective viewpoint. First figure shows the residue that is not completely detached from the unburnt wire.

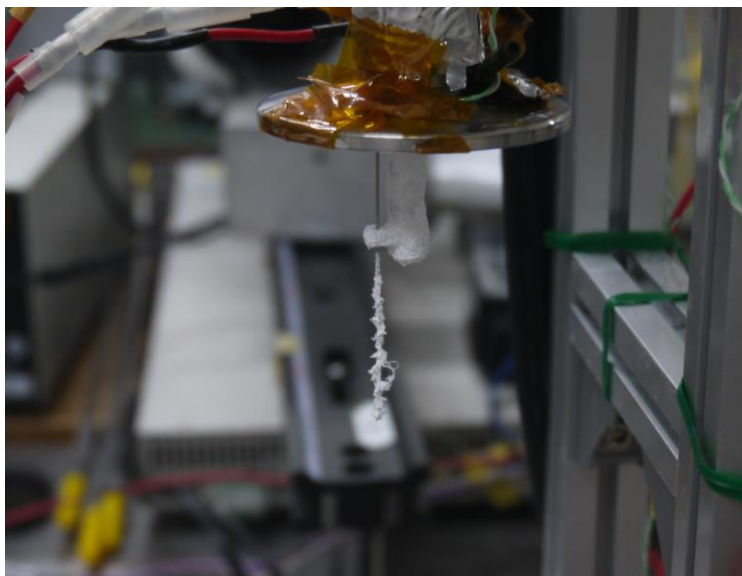


Figure 5.12 Residue hanging



Figure 5.13 Residue 35 kPa

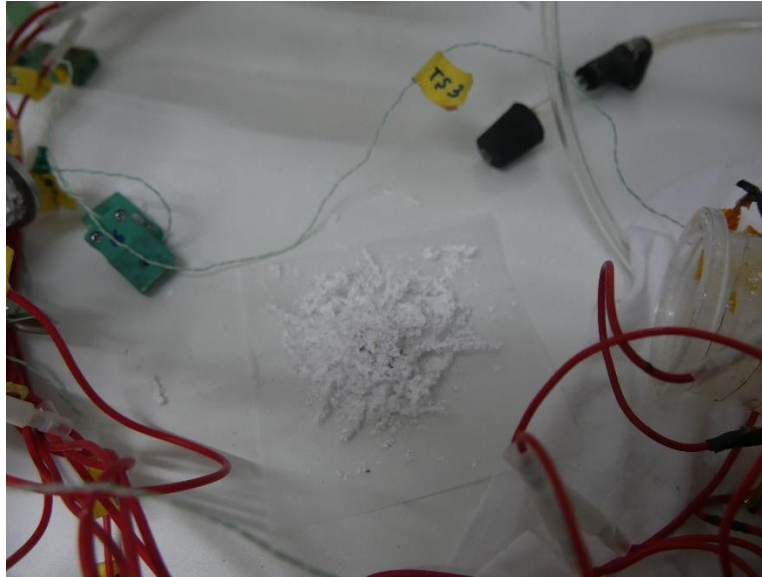


Figure 5.14 Residue 45 kPa

5.5 Extinguish case

This study does not include combustion data from experiments that were conducted by peers with the same control system and setup but different experiment conditions such as different orifice size, wire size and pressure. These data do not necessary contribute to the development of the thruster. However, the behavior of the wire during the experiments are used to draw some of the conclusions in this section.

5.5.1 Insufficient wire

There are some cases where combustion extinguished from wire running out. These cases are rare and are contributed to preparation. Only the necessary amount of magnesium wires is cut and prepared for combustion to avoid contamination. During longer combustion, the wire feeder can feed several meters of magnesium wire over 5 minutes. The simple solution is to prepare more wires. This is not a critical case of extinguish.

5.5.2 Wire touching chamber wall

When point of combustion touches the wall, the energy required to sustain combustion is lost. Wire does not go straight after exiting wire guide. The wire guide itself can also loosen as part of the design flaw. If the wire keeps feeding, the wire is likely to touch the quartz glass tubes before reaching the bottom of the combustion chamber. The direction that wire bends is also in essence, random. When enough wire is fed, in the case of the longer combustions, the wire will touch the

surface of the interior. The solution are to straighten wire, having a large combustion chamber, and limit the amount of wire after the guide. This extinguish case became less common as the combustion target point was set closer to the wire guide.

5.5.3 Wire leaving guide

There are cases of extinguishment where wire leaves the guide during combustion. This is usually a result of feeder not feeding enough wires to match the combustion rate. Before the optimization of wire feeding direction, wire can leave the wire guide if the wire is pulled back too far during combustion. The solution for this to use one continuous guide from the inlet.

5.5.4 Hanging on electrode

Discharge electrode extends through the center of the combustion chamber. By chance, the wire residue can hang onto the electrode. This results in a gradual pile up of the residue. This is the most common case of extinguishment. The solution is to either guide the wire so that the residue does not fall over the discharge probe, or to move the discharge probe out of the path of residue. This phenomenon can be visualized in the high speed camera footage in figure 4.14 and figure 4.15.

5.5.5 hardware failure

This failure condition happened when the discharge from the ignition circuit damaged one of the usb ports that connected the usb camera. Software failure occurs due to such hardware failure. However, this is least likely to occur and has been partially solved through software implementations.

5.6 BBM test analysis

At the time of the study, only the ignition was confirmed. Ground works for study on the orientation dependency only started. Based on the figure showing residue. Gravity may influence the ability to have a sustained combustion.

6. Conclusion

In this study, the experiment setup based on prior studies has been improved.

The automated control system, wire feeder, and efficiency measurement has all worked better than expected. In particular, the automated control system was able to integrate with rest of the experiment setup to produce a record combustion time of 280 seconds.

Being automated, the system was able match the feeding rate to the combustion rate without any interference. This system has drastically reduced the complexity of executing experiments since the implementation, enabling more observation of what is happening and less reliance on reply.

Experiments to better understand the relationship between pressure and combustion were also successful. One large improvement is that the ignition is now possible without the need to stop water vapor flow downstream. This is an important step to making a working thruster as controlling of the flow path downstream of the combustion chamber is not possible.

The fuel efficiency measurement system was also able to help better understand the combustion. It is discovered that combustion in all of the conditions experimented with result in a near 100% combustion efficiency of the magnesium wire fuel. It is slightly unfortunate that the time spent on reducing the error of the system in larger samples was unnecessary to draw the same conclusion. The result however is good news for the thruster as only the water efficiency needs to be optimized. Additionally, not included in this study, the same system developed is being used on measuring the fuel efficiency of aluminum powder based thruster.

Finally, based on the data collected and observation of the combustion, a BBM thruster is designed. This thruster enables collection of data such as combustion gas temperature that is necessary to better understand the interaction between water vapor and magnesium wire. Most importantly, this BBM model is able to finally produce thrust. The ability to produce thrust, to my opinion, is finally the turning point where an experiment setup can technically be called a thruster. The thruster is assembled and tested for ignition. Combustion is partially successful by the time of this study.

Appendix A

Thruster design

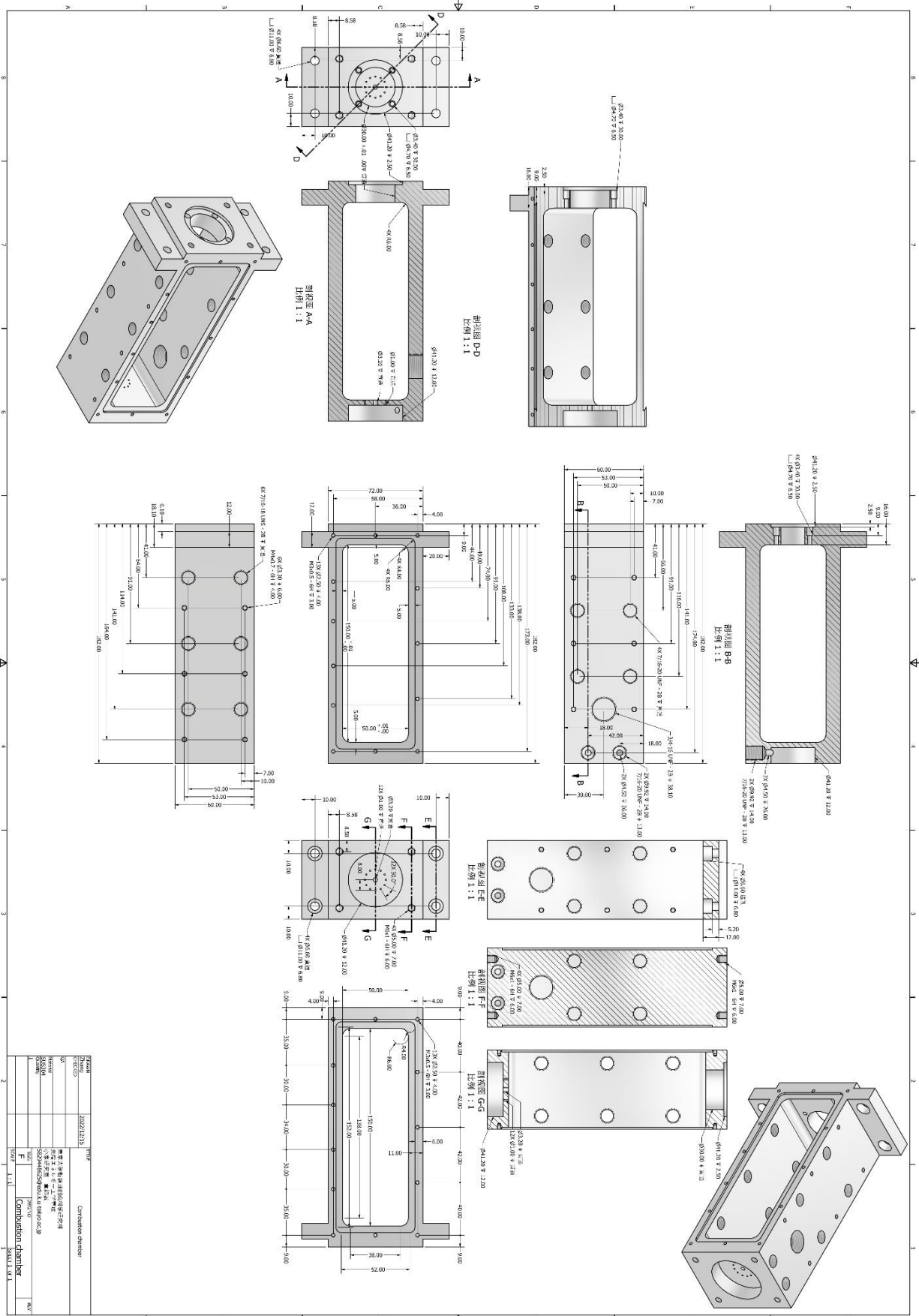
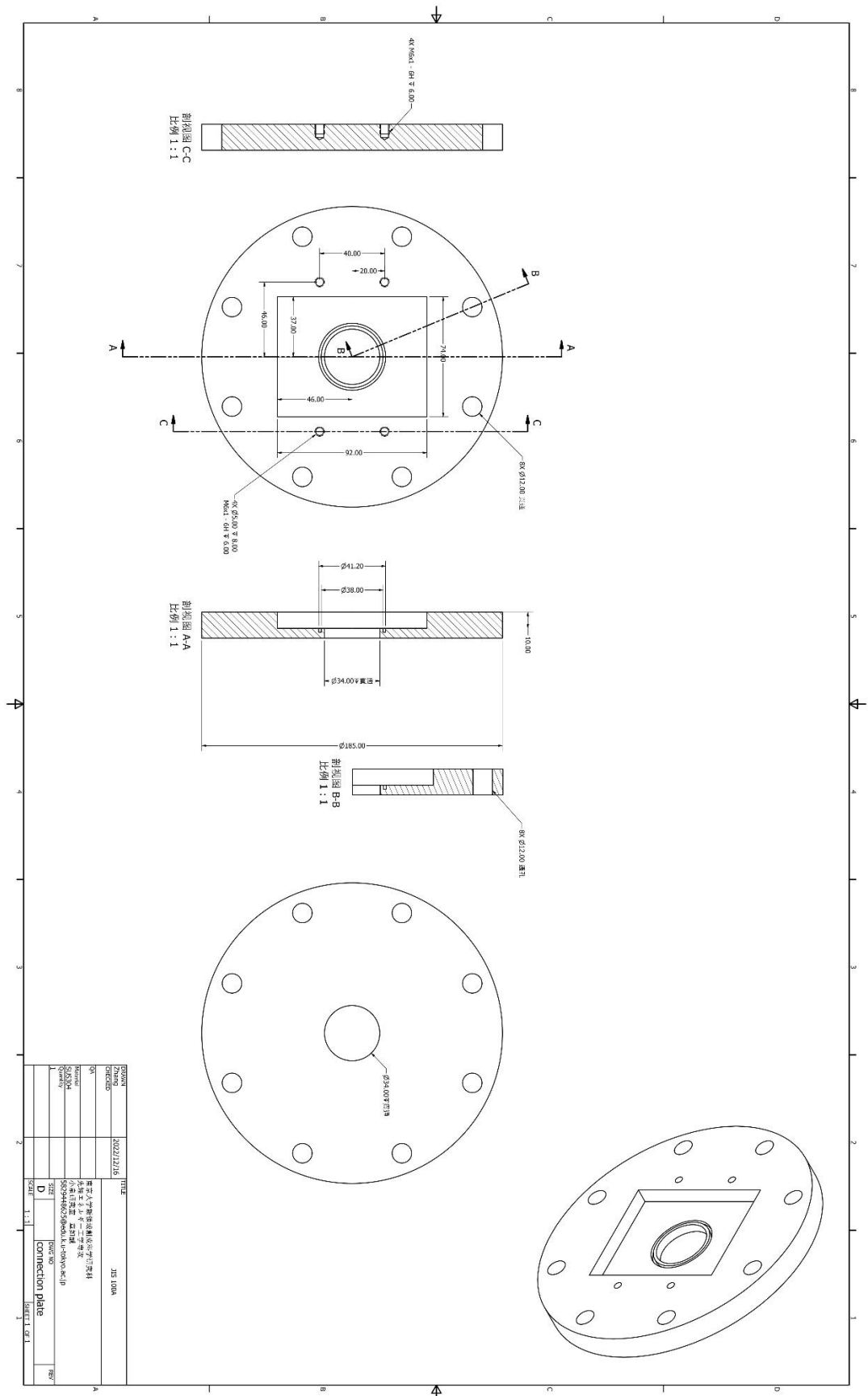
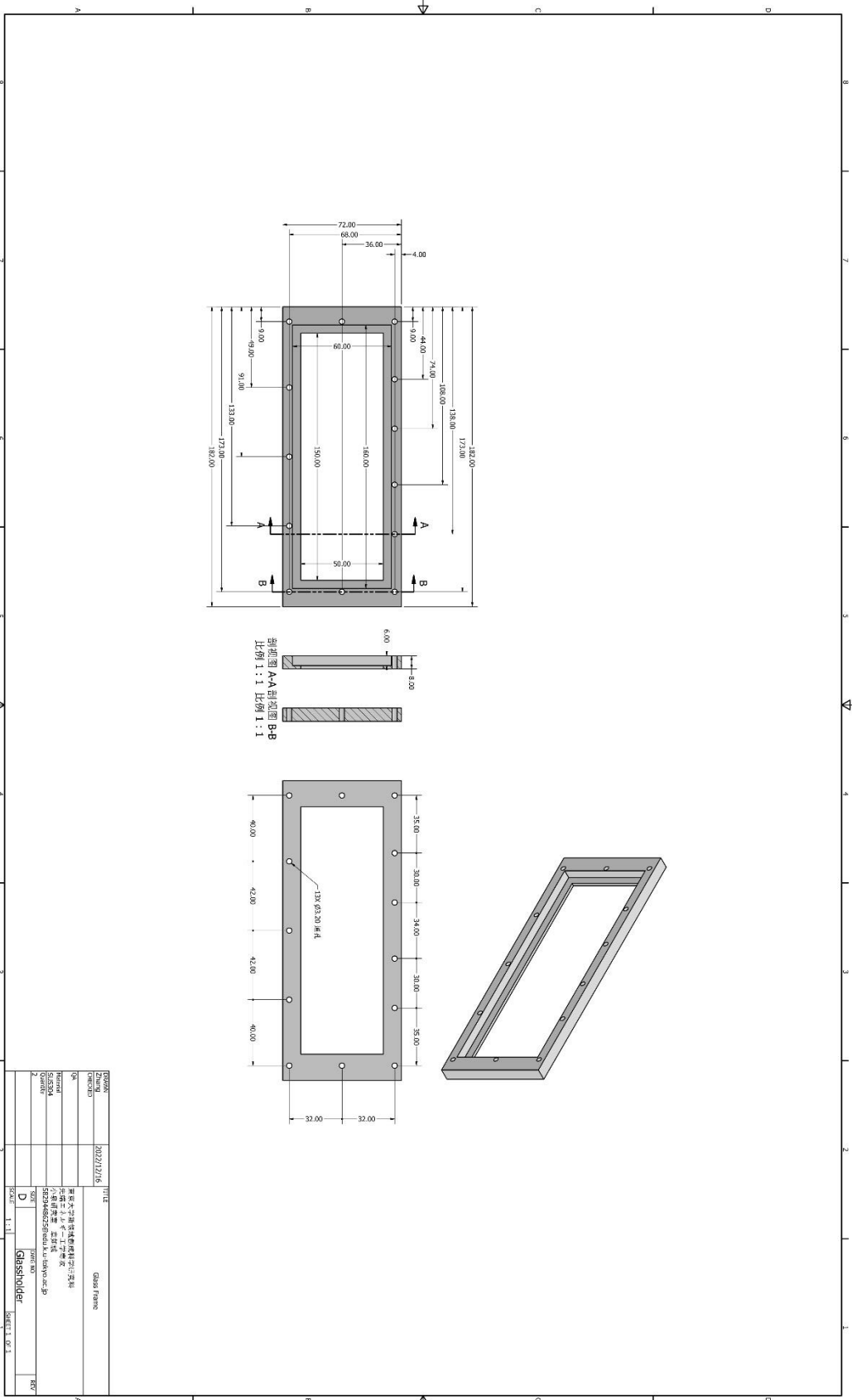
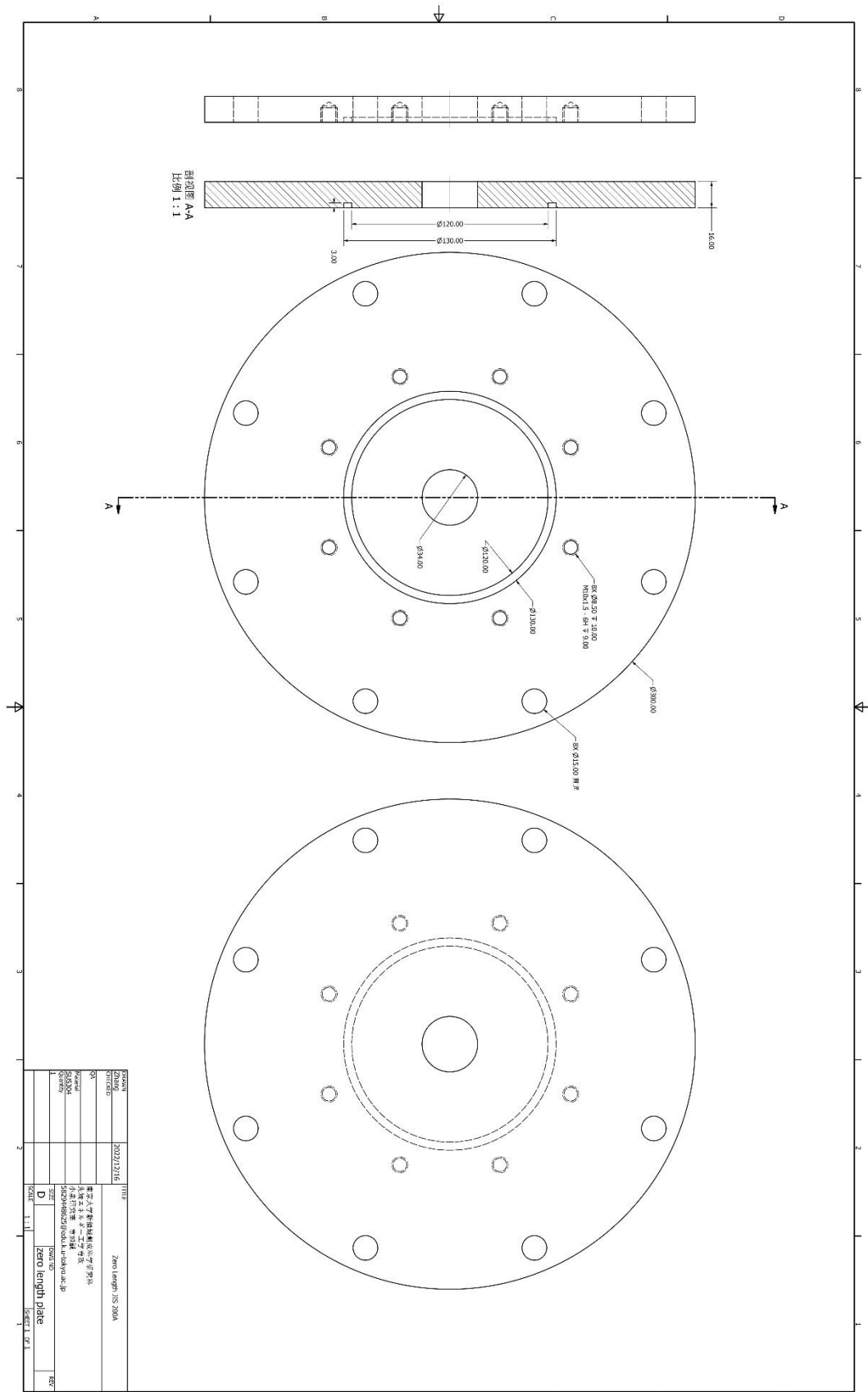


FIGURE		20231215	1 of 1
Title		COMBUSTION CHAMBER	
Author		COMBUSTION CHAMBER	
Date		20231215	
Version		1.0	
F		COMBUSTION CHAMBER	
Scale		1:1	
Sheet		1 of 1	



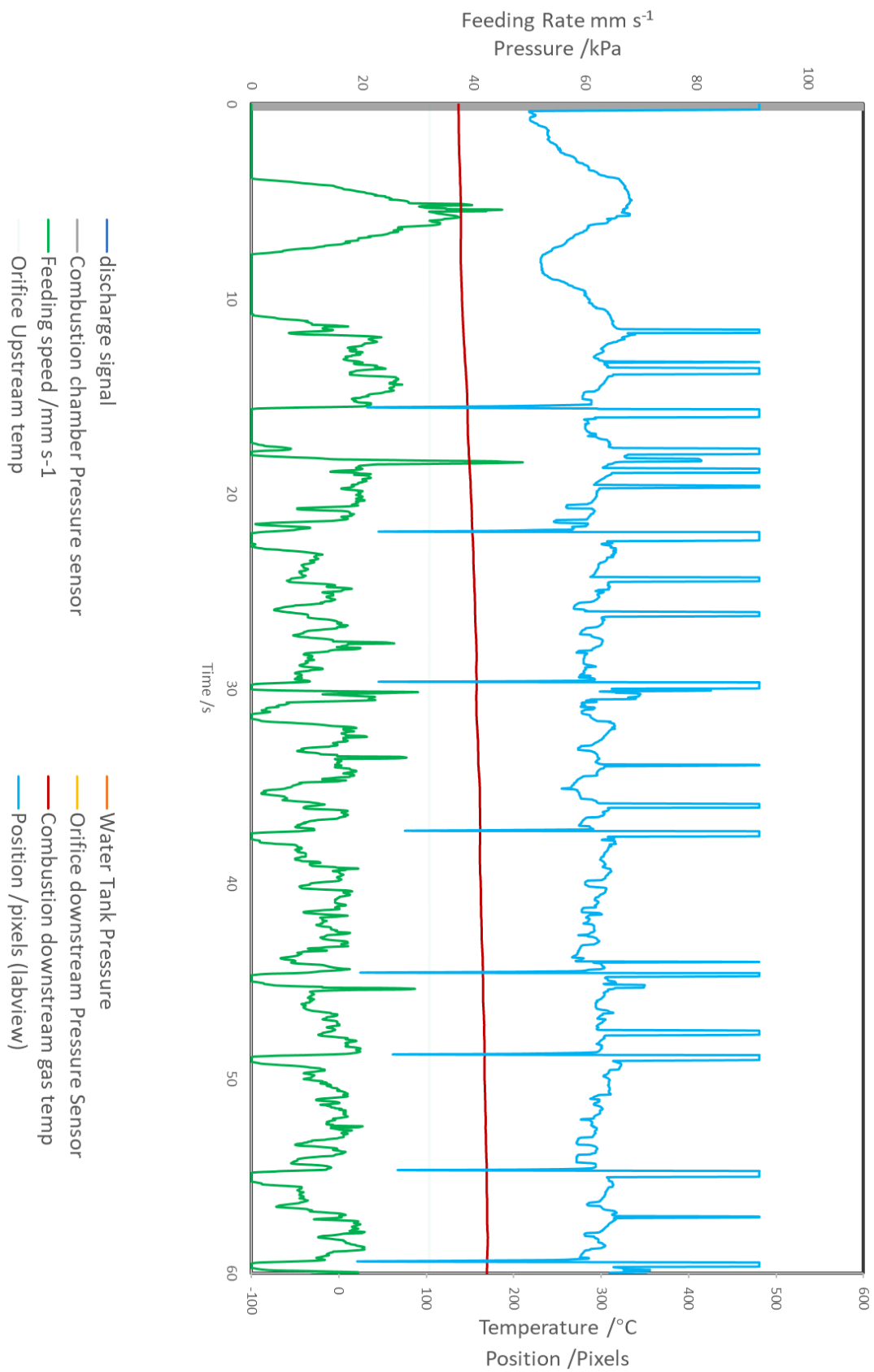


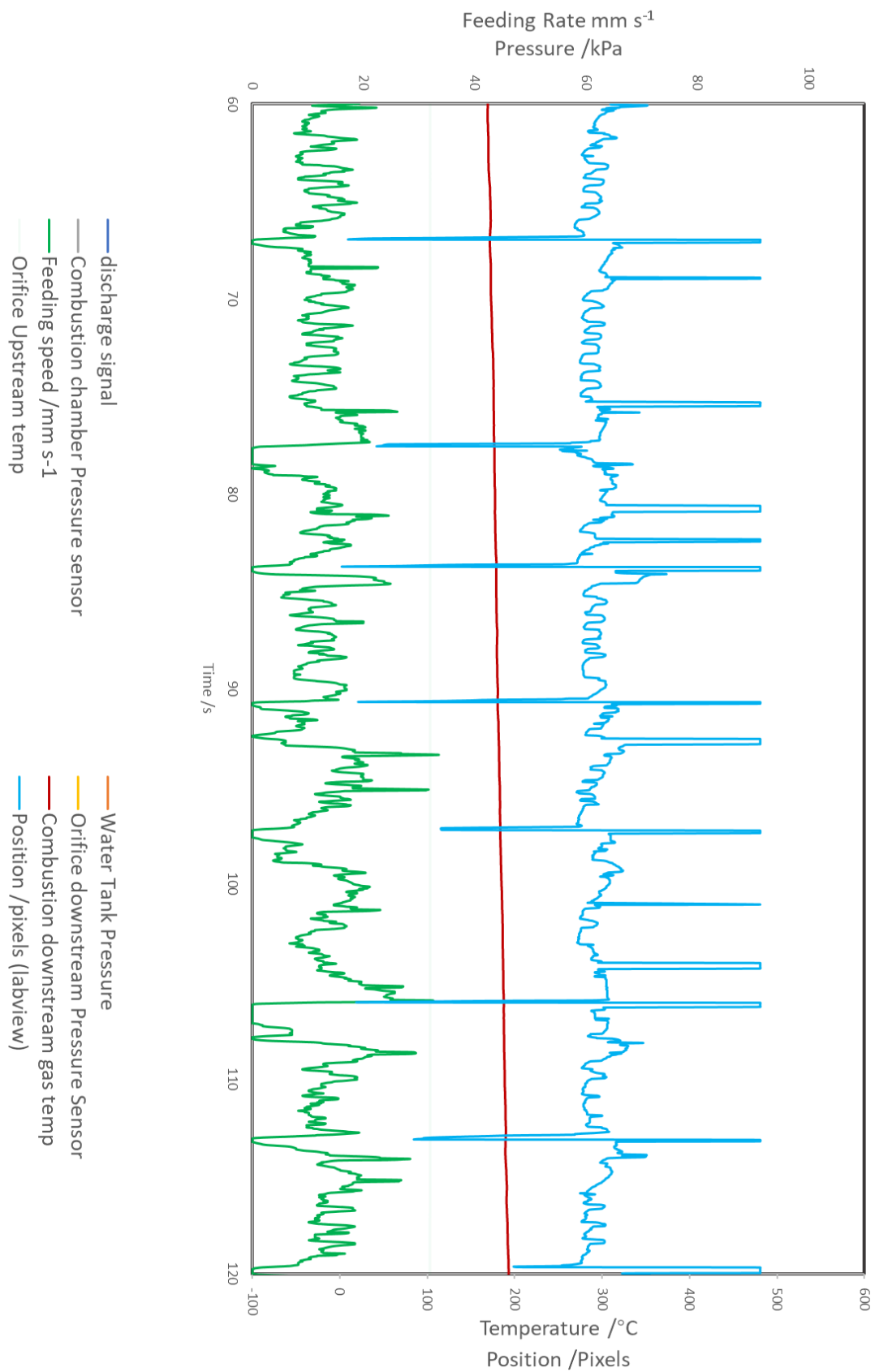


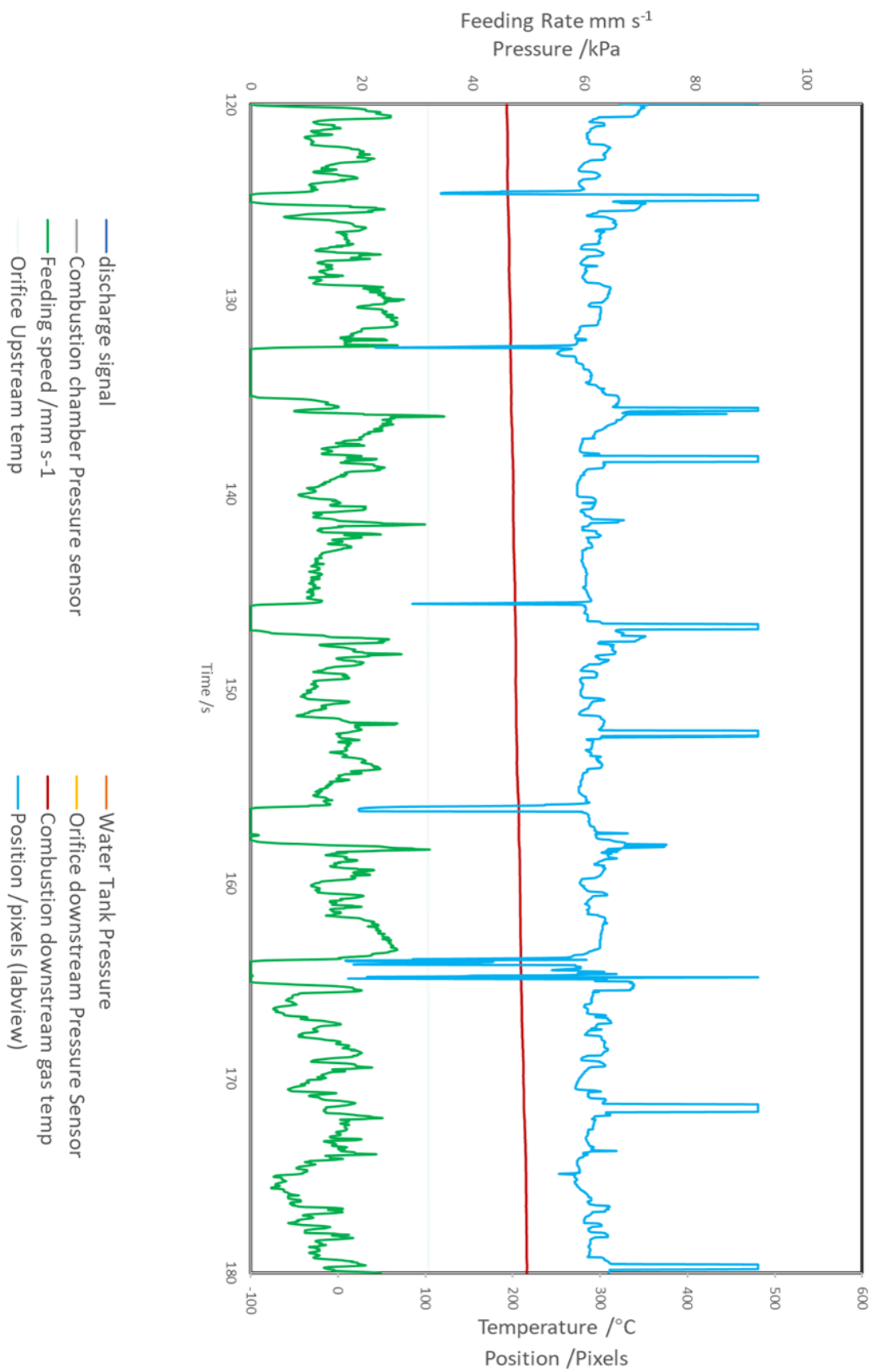
Appendix B

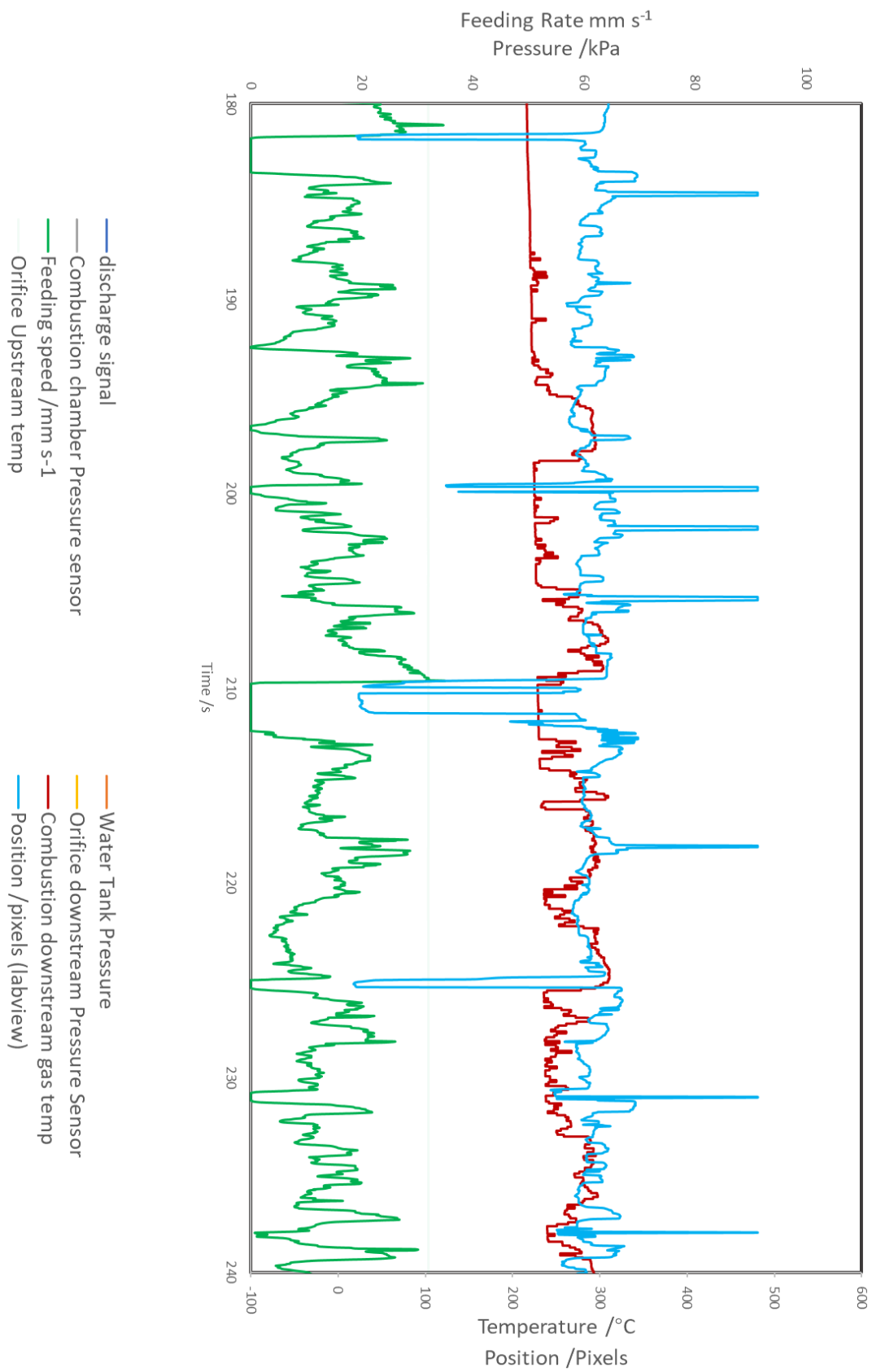
Combustion data of 280 second combustion

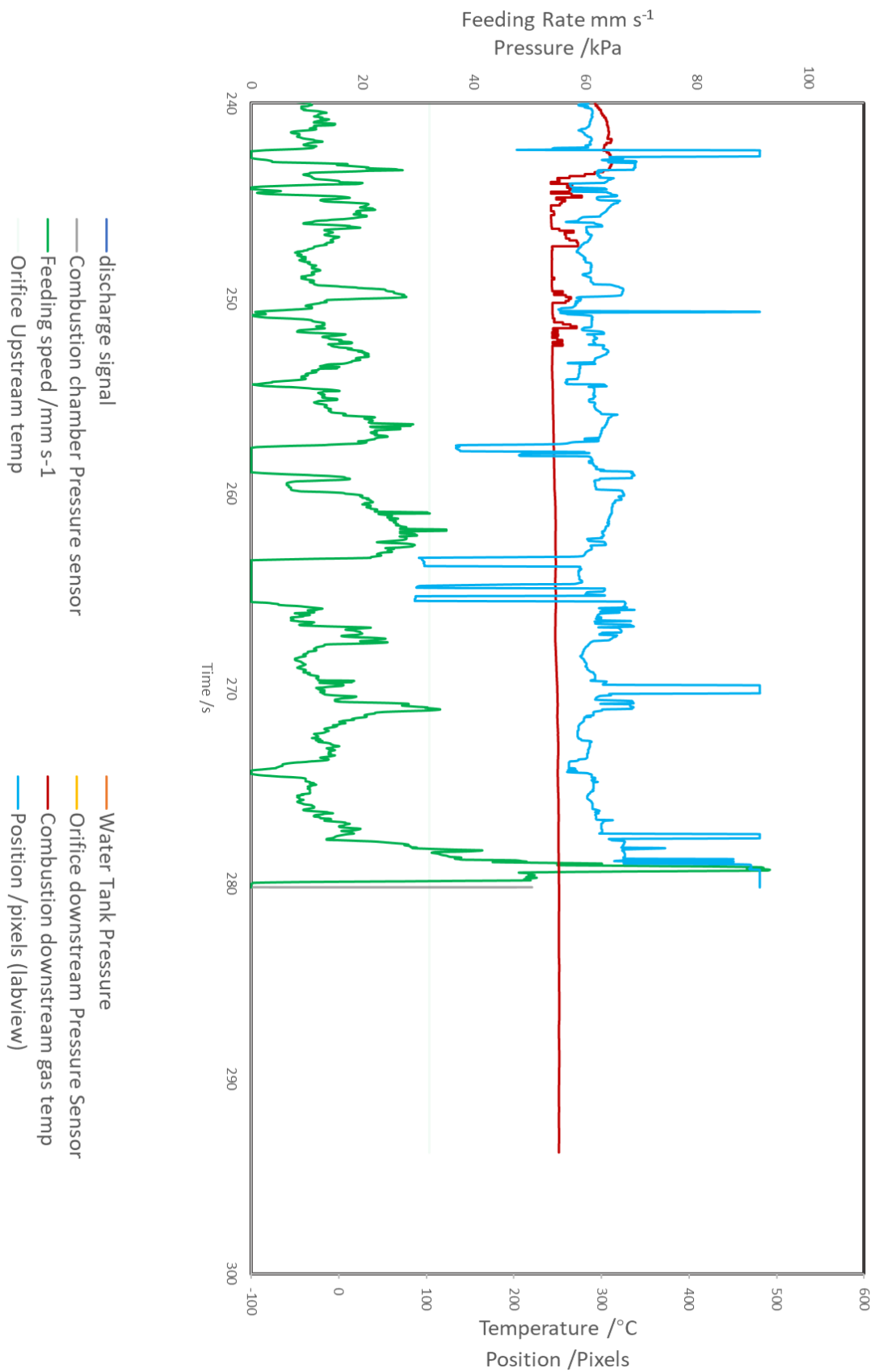
Interval of 60 seconds





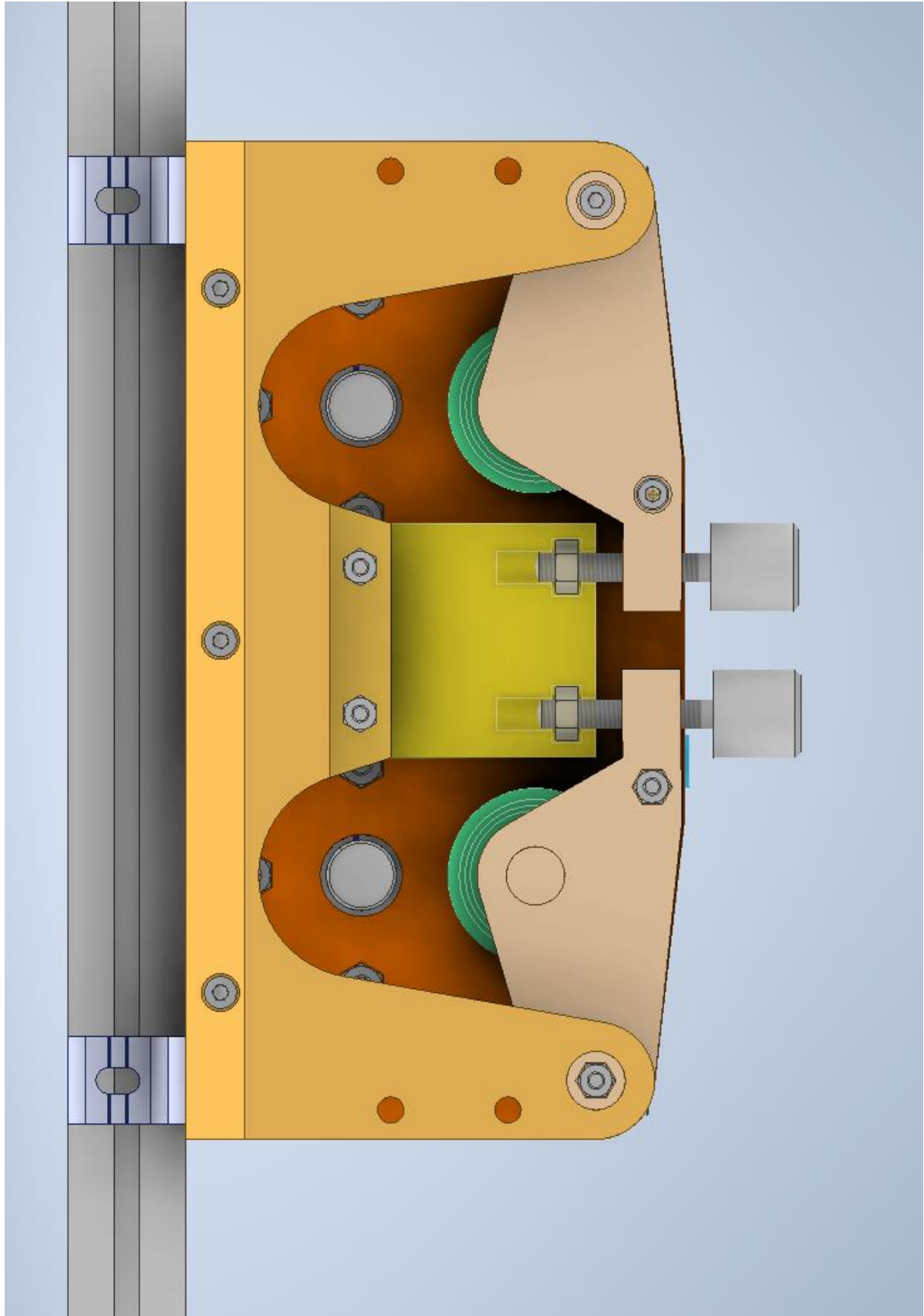






Appendix C

Wire feeder



Conference

第 66 回宇宙科学技術連合講演会 Poster session

章如誠，秋山茉莉子，小泉宏之，小紫公也

Propellant-efficient combustion parameters and oxidizer/fuel ratio in a water/metal hybrid thruster and their limits.

Bibliography

- ¹ Thyrso Villela, Cesar A. Costa, Alessandra M. Brandão, Fernando T. Bueno, Rodrigo Leonardi, "Towards the Thousandth CubeSat: A Statistical Overview", *International Journal of Aerospace Engineering*, vol. 2019, Article ID 5063145, 13 pages, 2019.
<https://doi.org/10.1155/2019/5063145>
- ² Pang, Weijian & Bo, B & Meng, X & Yu, X & Guo, Jian & Zhou, J. (2016). BOOM OF THE CUBESAT: A STATISTIC SURVEY OF CUBSATS LAUNCH IN 2003-2015.
- ³ Jonathan O. Murcia Piñeros, Walter Abrahão dos Santos, Antônio F.B.A. Prado, Analysis of the orbit lifetime of CubeSats in low Earth orbits including periodic variation in drag due to attitude motion, *Advances in Space Research*, Volume 67, Issue 2, 2021, Pages 902-918, ISSN 0273-1177,
- ⁴ M. Swartwout, "A statistical survey of rideshares (and attack of the CubeSats, part deux)," 2012 IEEE Aerospace Conference, Big Sky, MT, USA, 2012, pp. 1-7, doi: 10.1109/AERO.2012.6187008.
- ⁵ M. Swartwout, "Cubesats/Smallsats/Nanosats/Picosats/Rideshare(sats) in 2022: Making Sense of the Numbers," 2022 IEEE Aerospace Conference (AERO), Big Sky, MT, USA, 2022, pp. 1-10, doi: 10.1109/AERO53065.2022.9843832.
- ⁶ R. Funase et al., "Mission to Earth–Moon Lagrange Point by a 6U CubeSat: EQUULEUS," in *IEEE Aerospace and Electronic Systems Magazine*, vol. 35, no. 3, pp. 30-44, 1 March 2020, doi: 10.1109/MAES.2019.2955577.
- ⁷ O'Reilly, Dillon & Herdrich, Georg & Kavanagh, D.. (2021). Electric Propulsion Methods for Small Satellites: A Review. *Aerospace*. 8. 22. 10.3390/aerospace8010022.
- ⁸ Alexander Schwertheim, Aaron Knoll, Experimental investigation of a water electrolysis Hall effect thruster, *Acta Astronautica*, Volume 193, 2022, Pages 607-618, ISSN 0094-5765,
<https://doi.org/10.1016/j.actaastro.2021.11.002>.

⁹ Nakagawa, Yuichi & Koizumi, Hiroyuki & Naito, Yuki. (2020). Water and xenon ECR ion thruster - comparison in global model and experiment. Plasma Sources Science and Technology. 29. 10.1088/1361-6595/aba2ac.

¹⁰ Yuichi NAKAGAWA, Daiki TOMITA, Hiroyuki KOIZUMI, Kimiya KOMURASAKI, Design and Test of a 100 μ N-class Thrust Stand for a Miniature Water Ion Thruster with CubeSat, TRANSACTIONS OF THE JAPAN SOCIETY FOR AERONAUTICAL AND SPACE SCIENCES, AEROSPACE TECHNOLOGY JAPAN, 2018, Volume 16, Issue 7, Pages 673-678, Released on J-STAGE November 04, 2018, Online ISSN 1884-0485, <https://doi.org/10.2322/tastj.16.673>, https://www.jstage.jst.go.jp/article/tastj/16/7/16_673/_article/-char/en,

¹¹ HYPERGOLIC PROPELLANTS: THE HANDLING HAZARDS AND LESSONS LEARNED FROM USE, B. Nufer NASA Kennedy Space Center, Engineering Directorate, Fluids Division, Hypergolic and Hydraulic Systems Branch, NASA

¹² Akiyama, Mariko & Nishii, Keita & MANNAMI, Yoshihito & Murohara, Masaya & KOIZUMI, Hiroyuki. (2021). Feasibility Study of a Hybrid Thruster using Wire-Shaped Magnesium and Water for Application to Small Spacecraft. TRANSACTIONS OF THE JAPAN SOCIETY FOR AERONAUTICAL AND SPACE SCIENCES. 64. 223-233. 10.2322/tjsass.64.223.

¹³ Asakawa, Jun & KOIZUMI, Hiroyuki & Nishii, Keita & TAKEDA, Naoki & Murohara, Masaya & Funase, Ryu. (2018). Fundamental Ground Experiment of a Water Resistojet Propulsion System: AQUARIUS Installed on a 6U CubeSat: EQUULEUS. TRANSACTIONS OF THE JAPAN SOCIETY FOR AERONAUTICAL AND SPACE SCIENCES, AEROSPACE TECHNOLOGY JAPAN. 16. 427-431. 10.2322/tastj.16.427.

¹⁴ 酸化剤として H₂O/HNO₃ を用いたガスハイブリッドロケットの燃焼特性, 鈴木 一希, 平成 25 年度宇宙輸送シンポジウム

¹⁵ National Instruments USB-6001 Specifications, <https://www.ni.com/docs/ja-JP/bundle/usb-6001-specs/resource/374369a.pdf>